The implementation of stereotactic body radiotherapy for prostate cacner with two different approaches for sparing the rectal-wall

Mihaela Udrescu

N° d'ordre **319 - 2013** Année 2013

THESE DE L'UNIVERSITE DE LYON

Délivrée par

L'UNIVERSITE CLAUDE BERNARD LYON 1

ECOLE DOCTORALE :
ECOLE DOCTORALE INTERDISCIPLINAIRE SCIENCES-SANTE (EDISS)

DIPLOME DE DOCTORAT

(arrêté du 7 août 2006)

soutenue publiquement le 19 Décembre 2013

par

Corina Mihaela UDRESCU

TITRE :

Développement d'une technique de radiothérapie stéréotaxique des cancers de la prostate reposant sur deux concepts différents de préservation de la paroi rectale

Directeur de thèse :
Professeur Olivier CHAPET

JURY :

M.	David AZRIA	Professeur - ICM, Montpellier	Examinateur
M.	Olivier CHAPET	Professeur - CHU Lyon Sud, Pierre-Bénite	Directeur de thèse
M.	Olivier ROUVIERE	Professeur - Hôpital Edouard Herriot, Lyon	Examinateur
M.	Gilles CREHANGE	PH, HDR – Centre GF Leclerc, Dijon	Rapporteur
M.	Alain NOEL	Physicien Médical, HDR – Institut de Cancérologie de Lorraine	Rapporteur
M.	Patrice JALADE	Physicien Médical, PhD – CHU Lyon Sud, Pierre-Bénite	Co-directeur de thèse

N° d'ordre **319 - 2013** Year 2013

THESIS OF UNIVERSITY OF LYON

issued by

UNIVERSITY CLAUDE BERNARD LYON 1

ECOLE DOCTORALE :
ECOLE DOCTORALE INTERDISCIPLINAIRE SCIENCES-SANTE (EDISS)

DIPLOME DE DOCTORAT

(arrêté du 7 août 2006)

public defense the 19th of December 2013

by

Corina Mihaela UDRESCU

TITLE:

The implementation of stereotactic body radiotherapy for prostate cancer with two different approaches for sparing the rectal-wall

Thesis director:
Professor Olivier CHAPET

JURY:

Mr.	David AZRIA	Professor - ICM, Montpellier	Examiner
Mr.	Olivier CHAPET	Professor - CHU Lyon Sud, Pierre-Bénite	Thesis director
Mr.	Olivier ROUVIERE	Professor - Hôpital Edouard Herriot, Lyon	Examiner
Mr.	Gilles CREHANGE	PH, HDR – Centre GF Leclerc, Dijon	Referee
Mr.	Alain NOEL	Medical Physicist, HDR – Institut de Cancérologie de Lorraine	Referee
Mr.	Patrice JALADE	Medical Physicist, PhD – CHU Lyon Sud, Pierre-Bénite	Co-director

RESUME en français

Le présent travail de thèse décrit le développement d'un protocole d'irradiation stéréotaxique combinée à une radiothérapie conformationelle avec modulation d'intensité (RCMI). Ce projet a été initié dans le service de Radiothérapie-Oncologie du Centre Hospitalier Lyon Sud.

La première partie de ce travail fait état d'une revue de littérature sur les techniques d'irradiation du cancer de la prostate et plus spécifiquement sur l'état des connaissances en radiothérapie stéréotaxique. De cette analyse découle la justification des différents travaux réalisés dans le cadre de cette thèse.

Trois grands thèmes de recherche ont été identifiés et développés :

Un premier thème portant sur la définition optimale des volumes à irradier lors d'une irradiation stéréotaxique de la prostate : le volume cible anatomo-clinique (*clinical target volume*), le volume cible interne (*internal target volume*), le monitoring en temps réel du patient et de la cible sous l'accélérateur pour la définition de la marge correspondant aux incertitudes de réalisation du traitement (*set-up margin*) et la fiabilité d'un repérage de l'organe par des marqueurs intra-prostatiques.

La deuxième thématique de recherche était dédiée à la planification du traitement stéréotaxique de la prostate avec pour principal objectif une protection optimale de la paroi rectale avec deux approches différentes :

a) une augmentation focalisée de la dose d'irradiation uniquement sur la tumeur macroscopiquement visible, ou
b) l'utilisation d'un gel injecté entre la paroi du rectum et la prostate.

Le nombre optimal de faisceaux à utiliser ainsi que l'énergie la mieux adaptée ont été évalués dans le cadre de la première approche avec boost intégré.

La troisième thématique portait sur les contrôles qualité à réaliser dans le cadre de la mise en route de cette technique d'irradiation. Trois détecteurs dédiés aux contrôles de la distribution de dose sous l'accélérateur ont été évalués. De nouvelles recommandations concernant le contrôle qualité à appliquer en radiothérapie stéréotaxique notamment dans les cancers de prostate ont pu ainsi être élaborées.

L'ensemble de ces travaux serviront de supports à la réalisation d'une étude de phase II intégrant une irradiation stéréotaxique des cancers de la prostate avec injection de gel d'acide hyaluronique entre le rectum et la prostate.

DISCIPLINE

Recherche clinique, innovation technologique

MOTS-CLES

Cancers de la prostate, Irradiation stéréotaxique, Radiothérapie conformationelle avec modulation d'intensité, Contrôle qualité, Détecteurs 3D à diodes

INTITULE ET ADRESSE DE L'U.F.R. OU DU LABORATOIRE :

Ciblage Thérapeutique en Oncologie (Equipe 3 : ciblage par agents physiques)
UFR Faculté de Médecine Lyon-Sud-Charles Mérieux BP12
165 Chemin du Grand Revoyet, 69921 Oullins Cedex

TITLE (TITRE en anglais)

The implementation of stereotactic body radiotherapy for prostate cancer with two different approaches for sparing the rectal-wall

---

ABSTRACT (RESUME en anglais)

The current work describes the implementation of a protocol for stereotactic body radiotherapy (SBRT) combined with an intensity-modulated radiation therapy technique (IMRT). The project was initiated in the Department of Radiation-Oncology from Lyon Sud Hospital.

The first part summarizes the *state of the art* of prostate cancer with a literature review on irradiation techniques, in particular for SBRT. Based on this analysis, the justification of different works performed in this thesis is presented.

Three research themes were described and developed:

The first theme discusses the optimal definition of the volumes to be irradiated during a prostate SBRT: the clinical target volume, the internal target volume, the real-time monitoring of the patient and of the target for the definition of set-up margins and the accuracy of the target localization using intraprostatic markers.

The second theme of research describes the treatment planning for prostate SBRT having as main purpose an optimal protection of the rectal-wall with two different approaches:

a) an augmentation of the dose with a simultaneous integrated boost only into the visible macroscopic tumor, or
b) the use of a gel injected between the rectal-wall and the prostate.

The optimal number of fields, as well as the most favorable energy, was evaluated in the context of the first approach with a simultaneous integrated boost.

The third theme discusses the quality assurance (QA) that needs to be performed for an IMRT-SBRT technique. Three detectors that are dedicated to the QA of dose distribution under accelerator were evaluated. New recommendations regarding especially the QA for prostate IMRT-SBRT were assessed.

The results of all these studies will be used for the implementation of a phase II study for prostate SBRT with an injection of hyaluronic acid between the rectum and the prostate.

SUBJECT

Clinical research, technological innovation

KEYWORDS

Prostate Cancer, Stereotactic body radiotherapy, Intensity-modulated radiotherapy, Quality assurance, 3D diode arrays

Je dédie cette thèse…

…à ma maman, Mme Mariana Udrescu,

avec beaucoup d'amour et de reconnaissance

pour tout ce que tu as fait pour nous.

Je suis extrêmement fière de l'éducation que tu nous as donnée

et des valeurs solides que tu as pu nous transmettre.

A mon directeur de thèse, **Monsieur le Professeur Olivier Chapet**, Chef du service de Radiothérapie-Oncologie au Centre Hospitalier Lyon Sud.

Vous avez conçu la trame de ce travail et je vous remercie de m'avoir fait confiance en me proposant ce sujet de thèse. Je vous remercie aussi pour la liberté que vous m'avez laissée dans ce travail, pour votre grande disponibilité et pour votre rigueur.

J'ai beaucoup de considération pour votre vision originale des problématiques de recherche-développement et de leur application clinique.

J'ai beaucoup appris à vos cotes et je vous remercie pour votre soutien et pour votre encadrement quotidien. Veuillez trouver dans l'accomplissement de ce travail, toute l'estime et le respect que je vous porte.

A **Monsieur Patrice Jalade**, Chef du service de Physique Médicale au Centre Hospitalier Lyon Sud, pour avoir accepté de co-diriger ce travail. Je vous remercie pour votre aide constante, votre disponibilité et pour la pertinence de vos réflexions en radiophysique pendant ces années de thèse.

A **Monsieur le Professeur David Azria**, Chef de service de Radiothérapie-Oncologie de l'Institut Régional du Cancer Montpellier. Vous m'avez fait l'honneur de présider le jury de cette thèse, nonobstant vos nombreuses sollicitations. Je suis très heureuse de nos collaborations dans l'évaluation et la recherche en radiothérapie.

A **Monsieur le Professeur Olivier Rouvière**, Chef de service d'Imagerie Urinaire et Vasculaire de l'Hôpital Edouard Herriot.Vos connaissances vastes en particulier dans l'imagerie du cancer de la prostate, m'ont été d'une grande aide tout au long de ma thèse. Je suis honorée d'avoir eu la possibilité de collaborer avec vous sur de nombreux travaux et que vous ayez accepté d'être membre de mon jury de thèse. Soyez assuré de ma plus profonde reconnaissance.

A **Monsieur le Docteur Gilles Crehange**, Oncologue-Radiothérapeute au Centre Georges François Leclerc et à **Monsieur Alain Noel**, physicien médical a l'Institut de Cancérologie de Lorraine Alexis Vautrin. Vous avez acceptés d'être les rapporteurs de mon travail. Je vous remercie beaucoup pour vos suggestions et veuillez trouver ici l'assurance de mon profond respect.

Remerciements

Ce travail a été élaboré dans le cadre d'un contrat de collaboration entre l'entreprise General Electric Healthcare, le Service de Radiothérapie-Oncologie et la Délégation à la Recherche Clinique et à l'Innovation des Hospices Civils de Lyon. Je voudrais remercie en particulier **Monsieur Michel Bleuze** de General Electric pour m'avoir soutenu pendant toutes ces années. Notre collaboration a été et continu d'être très importante pour nous. Soyez assuré de notre profond respect et de notre reconnaissance.

Egalement, un grand merci à : Monsieur Thierry Capdeboscq, Monsieur Antoine Jerome, Monsieur Didier Raynaud, Monsieur Luc Posocco et à l'ensemble de l'équipe GE avec laquelle j'ai eu l'occasion et la chance d'interagir.

A **Madame le Professeur Françoise Mornex**, Radiothérapeute-Oncologue au Service de Radiothérapie-Oncologie du Centre Hospitalier Lyon Sud pour m'avoir fait l'honneur de m'impliquer dans vos travaux sur les cancers bronchiques et hépatiques. Soyez assurée de mon plus grand respect.

Je tiens à exprimer ma profonde reconnaissance à **Monsieur Irénée Sentenac**, Physicien Médical, pour avoir eu la gentillesse de m'accueillir dans son service durant mon stage Erasmus, pour son encadrement et sa confiance. Que vous soyez assuré de mon profond respect.

A **Madame le Docteur Pascale Romestaing,** Oncologue-Radiothérapeute à l'Hôpital Jean Mermoz pour votre soutien a mon arrivé dans le service et au début de ma thèse.

A **Monsieur Pascal Fenoglietto**, Physicien Médical, responsable adjoint de l'Unité de Physique de l'Institut régional du Cancer Montpellier, et à **Monsieur Robin Garcia**, Chef du Service de Physique Médicale de l'Institut Sainte Catherine Avignon, pour avoir acceptés de partager avec moi leurs connaissances scientifiques et leurs précieux conseils au début de ma thèse.

A l'ensemble du **personnel du Service de Radiothérapie-Oncologie** de Lyon Sud:

l'équipe médicale (particulièrement à **Dr. Anne D'Hombres, Dr. Véronique Favrel, Dr. Ciprian Enachescu, Dr. Fabrice Lorchel, Dr. Jean-Michel Ardiet** pour leur collaboration aux publications),

les manipulateurs (je vous dois mes premiers cours de français !),

les physiciens médicaux (notamment **Marie-Pierre Sotton, Géraldine Michel-Amadry et Gaëlle Kerneur**), les dosimétristes et les secrétaires (pour avoir supporté mes demandes perpétuelles de rendez-vous !).

Je vous remercie tous pour votre gentillesse, votre disponibilité et votre soutien continu!

Aux personnes qui me sont très chères :

A ma famille : ma maman, Mariana, ma sœur, Luciana, et mon frère, Lucian, pour leur immense amour, soutien et pour leurs encouragements durant ces années !

Julien pour ton appui inconditionnel depuis notre rencontre et pour avoir été présent à mes côtés tout au long de ce travail, dans les bons moments comme dans les moments plus difficiles.

Je remercie avec beaucoup de considération **Catherine Revault et Dr. Sylvie Mengue** pour leur accueil chaleureux à mon arrivée à Lyon et pour leur amitié! J'ai une immense pensée pour notre cher ami, le **Docteur Abdul Kubas** qui nous a quittés beaucoup trop tôt…

Ronan Tanguy, de notre première collaboration sur l'ExacTrac à la relecture de ces remerciements, tes connaissances en statistique et ton aide auront été enrichissants ! On a partagé un bon nombre de vues sur la recherche et discuter avec toi, pas seulement sur les statistiques, est toujours un plaisir !

Je remercie **Alexandra Avram** et **Rafaelle Branca** pour leur grande amitié ! Alexandra, je te remercie beaucoup pour les révisions d'anglais de ma thèse et des publications!

Au cours de mes années de thèse j'ai eu l'occasion de rencontrer beaucoup de personnes extraordinaires. Je remercie ainsi les médecins, les étudiants en DQPRM (aujourd'hui devenus physiciens), les stagiaires et les internes du Service de Radiothérapie-Oncologie de l'Hôpital Lyon Sud : **Cristina Sporea Barca, Ionela Caraivan, Shakir Shakir, Berardino de Bari, Ariane Lapierre, Tarik Chekrine, Amine Benhmidoune, Najib Derhem, Mohamed Ait Erraisse, Youssef Elkholti, Nabil Douar, Selma Mehiri, Naoual Oulmoudne, Myriam Hatime, Maud Le Grévellec, Mazen Moussallem, Maher Fawzi, Pauline Comte, Benjamin Pignata, Marion Vincent, Nabil Zahra, Christophe Mazzara**. Vous faites partie de mes plus belles rencontres et amitiés qui m'ont accompagné durant ces années. Encore, vos connaissances ont été toujours pour moi une source d'enrichissement.

J'ai une grande pensée pour mes amis et collègues physiciens avec lesquelles j'ai passée une belle année aux Etats Unis et je les remercie pour m'avoir initiée dans le métier de physicien médical: **Stefan Both, Rodica Alecu, Marius Alecu, Andrada Stan, Andrei Ciura, Gheorghe Abusan, Sanda Abusan, Serban Morcovescu.** Un grand merci à **Anca Morcovescu** et **Dr. Roxana Draghici** pour leur amitié !

Plusieurs personnes ont également joué un rôle important dans mes travaux de thèse, notamment pour le prêt du matériel (fantômes ou grains d'or), et je tiens à leur remercie : **Madame Françoise Chanlon (Bebig), Monsieur Denis Breugnot (Bebig), Monsieur Anders Adolfson (ScandiDos), Madame Cecile Birbeau (CIVCO), Madame Géraldine Le Breton et Monsieur Eric Guillet (SEEmed / Sun Nuclear)**.

A la mémoire de mes amis…

Dr. A. Kubas, M.D., PhD

Daniela Bulcu, PhD

Marcela Bulcu

TABLE OF CONTENTS

ABBREVIATIONS

2D	Two-Dimensional
3D	Three-Dimensional
3DCRT	Three-Dimensional Conformal Radiation Therapy
4DCT	Four-Dimensional Computed Tomography
6D	Six-Dimensional
α/β	Alpha/Beta ratio
AAPM	American Association of Physicists in Medicine
ADC	Apparent Diffusion Coefficient
AP	Anterior-Posterior
ASTRO	American Society for Radiation Oncology
bRFS	Biochemical Relapse-free Survival
BED	Biological Effective Dose
BPH	Benign Prostatic Hyperplasia
CBCT	Cone-Beam Computed Tomography
CC	Cranial-Caudal
CI	Conformity Index
CT	Computed Tomography
CTV	Clinical Target Volume
CZ	Central Zone
DCE	Dynamic Contrast-enhanced
DIL	Dominant Intraprostatic Lesion
DRE	Digital Rectal Examination
DRR	Digitally Reconstructed Radiograph
DTA	Distance-To-Agreement
DWI	Diffusion-weighted Imaging
EBRT	External Beam Radiation Therapy
EPID	Electronic Portal Imaging Device
ERB	Endorectal Balloon
ESTRO	European Society for Radiotherapy and Oncology

FFBF	Free From Biochemical Failure
GI	Gastrointestinal
GI	Gradient Index
GTV	Gross Tumor Volume
GU	Genitourinary
Gy	Gray
HA	Hyaluronic Acid
HI	Homogeneity Index
HRT	Hypofractionated Radiotherapy
IAEA	International Atomic Energy Agency
ICRU	International Commission on Radiation Units
IGRT	Image-Guided Radiation Therapy
IM	Internal Margin
IMRT	Intensity-Modulated Radiation Therapy
ITV	Internal Target Volume
kV	Kilovoltage
kVD	Kilovoltage Detector
kVS	Kilovoltage Source
LQ	Linear-Quadratic
LR	Left-Right
MLC	Multi-leaf Collimator
MRI	Magnetic Resonance Imaging
MV	Megavoltage
NTCP	Normal Tissue Complication Probability
OAR	Organ At Risk
OBI	On-Board Imager
PD	Prescription Dose
PET	Positron Emission Tomography
PIV	Prescription Isodose Volume
PMMA	Polymethylmethacrylate
PRS	Prostate-Rectum Separation

PSA	Prostate Specific Antigen
PTV	Planning Target Volume
QA	Quality Assurance
RI	Reference Isodose
RT	Radiation Therapy (or Radiotherapy)
SBRT	Stereotactic Body Radiation Therapy
SFPM	Société Française de Physique Médicale
SI	Superior-Inferior
SIB	Simultaneous Integrated Boost
SM	Set-up Margins
SV	Snap Verification
TCP	Tumor Control Probability
TH	Threshold
TPS	Treatment Planning System
TRUS	Transrectal Ultrasonography
TV	Target Volume
TZ	Transition Zone
VMAT	Volumetric-Modulated Arc Therapy

LIST OF TABLES

LIST OF FIGURES

I. STATE OF THE ART

1.1. Prostate cancer

1.1.1. The anatomy of the prostate gland

The prostate gland is located under the urinary bladder, anterior to the rectum wall, behind the *pubic bone (pubis symphysis)* and it surrounds the urethra just below the bladder neck (Figure 1.1). It is made up of glandular and muscular tissues, with ejaculatory ducts that empty into the urethra. The prostate is part of the male reproductive system and is responsible for the production of a clear liquid which makes almost a third of the seminal fluid used to carry and protect the male sperm. The transverse diameter of the prostate's posterior extremities is about four centimeters, the vertical diameter is about three centimeters and the antero-posterior diameter is about three centimeters. So the young adults' prostate gland has the size of a walnut.

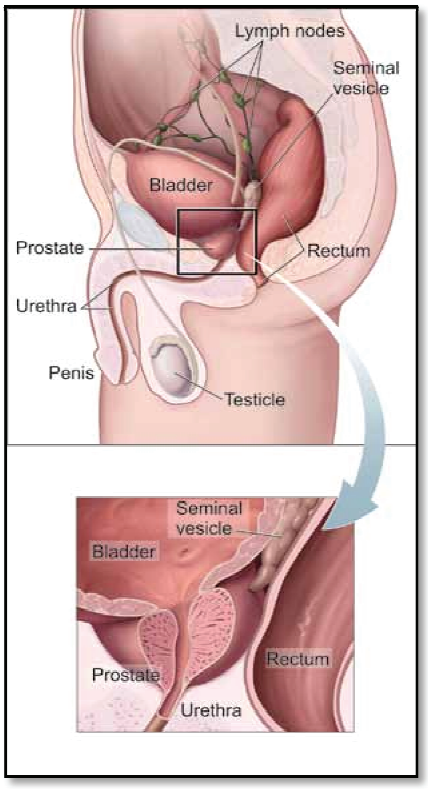

Figure 1.1. Prostate illustration (created by and property of US government agency National Cancer Institute [1]).

The notion of prostatic anatomy is derived from McNeal's description of the zonal anatomy of the prostate [2]. McNeal described four basic anatomic regions of the prostate: (1)

peripheral zone, (2) central zone, (3) preprostatic region, and (4) anterior fibromuscular stroma. Below, a short description of McNeal's concept on the prostate anatomic regions:

a.) *Transition zone (TZ):* before the development of the benign prostatic hyperplasia (BPH), the transition zone corresponds to only 5% of the glandular prostatic volume. It is composed of two lobes that surround the proximal urethra and by the smooth muscle of the internal sphincter. McNeal *et al.* refer to this zone as the *preprostatic region*. Although this zone accounts for a small percentage of the glandular tissue in young men, it shows major increase with age, because the transition zone is the site of development of benign prostatic hyperplasia (BPH) and also of a minority of prostatic carcinomas (10-20% of cancers).

b.) *Central zone (CZ):* represents 20% to 25% of the glandular volume in young man and is composed entirely of acinar tissue. It forms the central portion of the prostate and it extends proximally (to surround the paired ejaculatory ducts) and from the base of the prostate to the level of the verumontanum distally. It represents 10% of cancers.

c.) *Peripheral zone:* has a postero-lateral position, surrounding the central zone and extending to the apex, as described by McNeal. It represents 70% to 75% of the prostate volume in the normal postpubescent prostate and the majority of prostatitis and prostatic carcinomas (70-80%) are most probable to develop.

d.) *Fibromuscular stroma:* is situated on the anterior part of the prostate (from the bladder's neck to the apex) and thins posteriorly and laterally to form the capsule of the prostate. This zone of the prostate comprises approximately one third of the size of prostatic tissue, before the development of BPH.

A detailed and complete description of the prostate anatomy and imaging can be found in the literature [3].

1.1.2. Imaging of the prostate and disease

The main purposes for the imaging methods are to determine the prostate size, to localize the gland, to distinguish the benign prostatic lesions from the prostate cancer [4], to detect the isolated lymph nodes [5] or bone metastases [6].

Imaging of the prostate can be performed using several imaging techniques:

- *Diagnostic modalities* such as transrectal ultrasound (TRUS);
- *Morphological imaging*: computed tomography (CT), magnetic resonance imaging (MRI);

- *Molecular imaging combined with morphological imaging* techniques, such as whole-body positron emission tomography/computed tomography (PET/CT).

1.1.2.1. Transrectal ultrasound (TRUS)

Ultrasound provides guidance for transrectal prostate biopsy, when elevate prostatic specific antigen (PSA) is found for prostate patients. It offers an image of internal prostate anatomy and accurately estimates the volume of the prostate.

1.1.2.2. Magnetic Resonance Imaging (MRI) of the prostate

MRI is an excellent technique for imaging the pelvic organs, including the prostate [7-9] and it is the most accurate modality, compared to CT and ultrasound, with a great resolution and the facility to image the prostate in multiple planes. It precisely describes the internal prostatic zonal anatomy, displays the physiologic complexity of the gland [10] and anatomic and volumetric determination of the prostate gland can also be done [9].

The normal prostate of the *young adult male* appears relatively homogeneous on MRI [8, 9], especially on the T1-weighted images, because the internal anatomy of the gland is not visible on such imaging sequences [10-12]. On the other hand, the T1 images are able to distinguish between the prostatic parenchyma, the surrounding periprostatic fat, and vascular plexus [10]. The T2-weighted images provide better tissue differentiation than the T1 images and clearly describe the zonal anatomy of the prostate. The clarity of the T2 signal depends on the strength of the magnet [10]. The peripheral zone is hyperintense on T2 images, whereas the central and transition zones show similar MR imaging characteristics with lower signal intensity than the peripheral zone [10, 11].

A clear definition of the prostate on MR images is obtained from *older patients* [7]. With age, the signal intensity increases in the peripheral and central glands MRI images and gives better tissue discrimination [7]. Differences in signal intensity become more pronounced as the size of the prostate increases. The central zone intensity increases by an average of 175%, compared to the peripheral zone, which increases by 67%. The consequence is that the MRI is able to distinguish the peripheral zone from the central one, in older patient [7].

The changes that have been related to BPH are most clearly seen on the T2-weighted images. If BPH appears in the central gland of the prostate (transition zone), 70-80% of prostate cancer usually occurs in the peripheral gland [2]. It is possible that the MR imaging is able to distinguish the BPH from prostate cancer, based on localization. But sometimes, the prostate cancer may occur in the transition zone (about 10-20% of prostate cancer), or involve

both the transition and the peripheral zone. In this case, the MRI cannot reliably distinguish between BPH and prostate cancer. This is because changes in the MRI signal intensity that occur in patients with BPH are similar to those that occur in patients with prostate cancer, as described by several teams [8, 12, 13].

1.1.2.3. Prostate gland on the CT scan

When compared with TRUS and MRI, the CT scan has a limited accuracy to define the intraprostatic zonal anatomy [9, 10, 14-16] and therefore, it presents a limitation in the diagnosis and in the management of the prostate cancer patients. In addition, as a consequence of the high interobserver variations on the CT scan, prostate delineation on these images involves subjective evaluation of prostate margins [15, 17, 18]. However, the CT scan can give the relationship between the prostate and other pelvic organs and is a useful exam for the localization of the prostate and for the treatment planning.

1.1.2.4. Choline PET/CT for imaging prostate cancer

The PET/CT with [^{11}C]- and [^{18}F]-labeled choline derivates is a recent molecular imaging modality for the evaluation of the prostate cancer. Because of the low spatial resolution or the partial volume effect of PET imaging, this technique has a limited utility for the primary staging of the prostate cancer and for the detection of small lesions (tumors or lymph nodes). However, PET/CT imaging with ^{11}C- and ^{18}F-choline is generally used for the restaging prostate cancer patients with biochemical recurrence of prostate cancer or metastatic disease. Several publications offer a complete review of different aspects and clinical role of the ^{11}C- and ^{18}F-choline PET/CT for prostate cancer, with their importance and limitations [5, 6, 19-21].

1.1.3. Incidence of the prostate cancer and statistics

The prostate cancer is an important health concern and the first cancer in men, with more than 70 000 new cases in 2011 in France (more than 8000 deaths) [22] and approximately 200 000 new cases in United States [23, 24]. The actual diagnostic methods permit a fast localization of the disease and, in consequence, the curing. The screening - with the prostate specific antigen (PSA) blood test alone or with both, the PSA and the digital rectal examination (DRE) - should detect cancer at an earlier stage than if no screening is performed [25]. In the last years, a decrease of the prostate cancer mortality seems to be present, even if the number of new prostate cancer cases is in continuously augmentation [25,

26]. In the majority of the cases (85%), the prostatic cancer is an adenocarcinoma. It is initially microscopic (and non-detectable by the actual exams and techniques), and that changes afterward to a stage of localized cancer. Thus, it is limited to the prostate only and becomes detectable by DRE or by blood dosage of the PSA. Abnormal results from screening with the PSA or the DRE require prostate biopsies in order to determine whether the abnormal findings are cancer. If the cancer exceeds prostate limits, it can extend to the neighbor organs: seminal vesicles, bladder, etc.

1.1.4. The D'Amico classification for prostate cancer

Three risk groups were validated by D'Amico *et al.* (Table 1.1) for patients with clinically localized prostate cancer, to estimate the PSA control after radical prostatectomy, external beam radiotherapy, or brachytherapy with or without neoadjuvant androgen deprivation [27].

Table 1.1. The D'Amico classification for prostate cancer.

Risk	TNM Stage	Gleason Score	PSA (ng/ml)
Low	≤ T2a (and)	≤ 6 (and)	≤ 10
Intermediate	T2b (or)	7 (or)	10-20
High	≥ T2c (or)	≥ 8 (or)	> 20

1.1.5. The treatment possibilities for prostate cancer

The different treatment possibilities for prostate cancer are:

- *the surgery*: which consists in a radical prostatectomy and the removal of the seminal vesicles, more or less the lymph nodes, if the cancer is advanced;
- *the external beam radiation therapy*: alone or in combination with the surgery and/or the brachytherapy is a localized conformal technique of treatment. The RT requires a dose prescription to the target (prostate only, prostate and seminal vesicles, etc.) and the dose control to the surrounding tissues;
- *the brachytherapy*: consists in the implantation of radioactive seeds (Iodine-125) into the prostate, in a certain number and configuration in order to obtain the required dose coverage;
- *the hormone therapy*: in combination with the RT, is administrated mainly for the high-risk prostate cancer;

- *the chemotherapy* (less frequently);
- or a combination of these treatments.

The choice of the treatment(s) depends on the stage of the cancer, the patient's general condition and his comorbidity at that time. Given the early screening with PSA testing, the majority of patients present localized prostate cancer mainly clinical stage T1-T2. In this case, standard treatment options are radical prostatectomy, brachytherapy or external beam radiation therapy (EBRT). Patients who benefit of EBRT are treated with conventionally fractionated radiation therapy with 1.8-2.0 Gy per fraction to a total dose of 74-80 Gy.

1.1.6. The radiotherapy of prostate cancer

1.1.6.1. Irradiation technique

The radiotherapy for the prostate cancer has been improved as a consequence of the novel and advanced techniques that are used: accelerators with integrated image-guided, dynamic multileaf collimator, three-dimensional (3D) CT scan and multimodality image registration. Within the past 20 years in France, the standard of care for the prostate cancer was the 3D conformal radiation therapy (3DCRT), that was delivered most commonly using a 4- to 6-field irradiation technique. Recently, the intensity-modulated radiation therapy (IMRT) has become the most frequently used irradiation method in United States with at least a 5-field conformation technique. As well, volumetric modulated arc therapy (VMAT) with one or two dynamic arcs, helical irradiation or 6D-robotic delivery are used for the prostate irradiation.

1.1.6.2. Dose prescription

The 3DCRT technique already demonstrated its efficacy for low- and intermediate-risk prostate cancer with standard irradiation doses of 1.8 to 2 Gy per fraction. At least seven randomized studies proved a biological control improvement at 5 years when the irradiation dose is between 70-80 Gy [28-34]. For instance, the estimated 5-year FFBF rate for intermediate-risk patients treated with radiotherapy alone to 76 Gy at 2 Gy per fraction is 70% [35, 36] and the 5-year FFBF rate for high-risk patients treated with 76 Gy plus 2 years of androgen deprivation is also estimated to be about 70% [37]. However, this represents a total of 2 months treatment time for the patients, with 35 to 40 fractions, 5 times per week.

Other studies reported that a dose escalation up to 80 Gy is feasible when image-guided IMRT is available [29, 38-42]. This improvement in the dose optimization and the target conformation and localization allowed a reduction of late toxicities compared to 3DCRT and an increase of the dose to the tumor without significantly increase the toxicities. However, the treatment duration remains time-consuming for patients (approximately 8 weeks) and cost-effective.

1.2. Radiobiology of prostate cancer: low α/β ratio

1.2.1. Radiobiology - early versus late effects and the alpha/beta ratio

It is important to understand the radiobiological notions of radiotherapy as they support the interest and the progress of this type of treatment. Some of these radiobiological concepts are: total dose and treatment duration, number of fractions, tumor control probability (TCP), normal tissue complication probability (NTCP), radiobiological models, the 4Rs of radiotherapy (Reoxygenation, Redistribution, Repair, Repopulation), etc.

The most used radiobiological model is the linear-quadratic (LQ) model [43-48]. For example, for the cell survival, the curve for a *single* dose-response can be described by the LQ model [49] using:

$$S = e^{-(\alpha d+\beta d^2)},$$

where *d* is the dose per fraction.

We can than express the surviving fraction for a *multifraction* regimen by the formula:

$$S_n = [e^{-(\alpha d+\beta d^2)}]^n \text{or}$$

$$S_n = e^{-\alpha D-\beta dD},$$

where

D= (n*d) and is the total dose;

n= number of fractions;

d= dose per fraction.

The sensitivity of tissue to fractionation can be expressed as the *alpha/beta (α/β) ratio.* It is the dose where the linear-α component is equal to the quadratic-β component. In the LQ model, alpha determines initial slope and beta determines curvature. *The alpha (α) coefficient* corresponds to the linear model and is the non-repair component of the survival curve. *The beta (β) coefficient* corresponds to the quadratic model and represents the repair as well as mis-repair component of cell killing.

The LQ model takes into consideration the α/β ratio and the total dose, and is given by the relationship:

$$BED = n_1 d_1 + \frac{n_1 d_1^2}{(\alpha/\beta)} = n_2 d_2 + \frac{n_2 d_2^2}{(\alpha/\beta)}$$

A tissue sensitive to the dose-fractionation will have a small α/β ratio (≤ 4 Gy), and will be more "late-responding" (sequelae of treatment are generally seen years following treatment) than a tissue with large α/β ratio (> 8 Gy). The tissues with large α/β ratios are less sensitive to the effects of the dose-fractionation and we say that they are "early-responding" tissues. In other words, if this ratio is close to 0, the cancer cells are sensitive to fractionation, but if this ratio is high (i.e., ≥10), than the impact of the fractionation is very low.

In the LQ model, a smaller fraction size will have a relatively small benefit in reducing the acute effects, while a smaller fraction size gives also a component of tumor sparing. On the other hand, for late-effects, smaller radiation doses per fraction result in comparatively greater tissue sparing.

The benefit of the fractionating radiotherapy is to increase the therapeutic ratio (tumor control/complications) by reducing the late effects in normal tissue. Thus, fraction size is the dominant factor in determining normal tissue late effects.

1.2.2. Radiobiology of prostate cancer: low α/β ratio

The conventional prostate radiotherapy is delivered in fraction sizes of 1.8 to 2.0 Gy. This scheme of small fractionations was issued from studies where good local control was reached with reduced late-complication of the surrounding normal tissues such as rectum and bladder. In 1999, Brenner and Hall [50] calculated the α/β ratio for prostate cancer around 1.5 Gy (95 percent confidence interval: 0.8-2.2 Gy) by using clinical data to assume the linear and quadratic components of cell killing. They used data from men treated by external beam radiotherapy (1.8-2.0 Gy per fraction) and by brachytherapy seed implant with 125-I.

During the last years, many low dose-rate brachytherapy and external beam radiotherapy studies demonstrated the low α/β ratio for prostate cancer (perhaps between 1 and 4 Gy) [48, 51-62] and supported the hypothesis of Brenner and Hall [63, 64]. Fowler *et al.* have modeled various hypofractionation regimens using the linear quadratic model with the assumptions that the alpha/beta ratio for the prostate tumors is in the range of 1 to 2 Gy, and have warned against the use of too few fractions (<5) because this may limit the

possibility of reoxygenation or redistribution of tumor cells into more sensitive phases of the cell cycle [65].

Thus, decreasing the number of fractions up to 5 should have a good impact on the tumor, with the risk of increasing the late side effects, from the radiobiological view.

1.2.3. The α/β ratio for the rectum

If a hypofractionation regimen is demonstrated to be favorable for the prostate cancer, it is very important to know the α/β ratio of the rectum. Unfortunately, the α/β ratio of the rectum is not precisely known. The common value used for late-responding rectum tissue is 3 Gy, but several studies described a value ≥4 for late effects [64, 66-68]. Reports of various trials for late rectal damage showed different values: Terry and Denekamp reported 3.1 to 5.1 Gy [69], Van der Kogel *et al.* established a value of 4.1 Gy [70], Dewit *et al.* found 4.4 Gy [71], Dubray *et al.* found a range of 2.7 Gy to 6.7 Gy [67] and Brenner *et al.* found a value of 4.6 Gy [72].

Two situations may be then possible: (a) if the α/β ratio for the rectal damage is greater than the α/β ratio of the prostate, then large hypofractionated doses could give larger clinical gains for the same late complication rates [65], and (b) if the α/β ratio of late-rectal reaction is smaller than the α/β ratio of the prostate, than the rate of complications will rise.

1.3. Rationale for hypofractionated radiotherapy of prostate cancer

The hypofractionated radiotherapy (HRT) is the escalation of the irradiation dose per fraction with a decrease of the fraction number, compared to the standard fractionation of 2 Gy per day fraction [73-81]. If the α/β ratio for the prostate cancer and rectum are of 1.5 Gy and 3 Gy, respectively, then the hypofractionation presents several potential benefits and two circumstances are feasible: the tumor control may be increased for a certain level of late complications, or the late toxicities may be reduced for a certain level of tumor control.

Several reasons justify the development of the HRT for prostate cancer:

- The prostate cancer has a particular *sensitivity to the delivered dose per fraction* as presented above. Some of the studies demonstrated that this α/β ratio is between 1.5 and 3 Gy for prostate cancers. Consequently, *by increasing the delivered dose per fraction we can have an increase of the irradiation efficacy to the tumor*;
- The standard external beam radiotherapy for the prostate cancer needs between 35 and 40 irradiation fractions, equal to 8 treatment weeks, with a standard dose of 2 Gy per

fraction. *A reduction of the treatment time represents an amelioration of quality of life for patients treated of prostate cancer*;

- The number of patients treated with radiotherapy increase every year, causing an augmentation of the costs for the Health Insurance institution (treatment and patient's transportation). A reduction of the weeks of radiotherapy treatment could permit a *significant cost reduction*;
- A diminution of the accelerator occupancy time represents an *advance of the treatment accessibility for other patients*, in the radiotherapy department.

Hence, **two approaches** could be considered for the HRT:

1. The first one is a "moderate" HRT with an increase dose per fraction from 2 Gy to 2.5-3.3 Gy. It's then recommended to use conformity radiotherapy with intensity modulated radiotherapy (IMRT). The total treatment fraction is reduced by 30 to 50% (depending of the dose per fraction used) with the same biological effect as when using 35-40 fractions of 2 Gy.
2. The second approach is a "high" HRT with doses between 6 Gy and 10 Gy per fraction and a number of 4 to 5 fractions. We can talk then of stereotactic body radiotherapy for prostate cancer. The high-doses per fraction used for this technique require even more accurate prostate localization and repositioning equipment, treatment planning systems and irradiation devices of a very high precision. Indeed, the security margins around the prostate should be reduced to a few millimeters in order to allow an optimal sparing of the healthy tissues. The latter is an important condition in order to realize such a treatment.

The advantages of the hypofractionation radiotherapy attracted significant attention within the past years. However, the several randomized and non-randomized hypofractionation clinical trials found in the literature, started with modest increased doses per fraction, having as main concern the possibility of augmented rectal toxicity. Some of the hypofractionated studies are detailed in Appendix 1, with a description of the irradiation technique and the first clinical results.

1.4. Rationale for SBRT of prostate cancer

1.4.1. Stereotactic body radiation therapy (SBRT)

The term *stereotactic* refers to a precise positioning of the target volume within three-dimensional (3D) space, using a frame of reference that can be related to the treatment machine. The term *body* is used to distinguish the technique from the current terminology of stereotactic radiosurgery [82] used for the radiation treatment of the lesions of the central nervous system with a full course of therapy consisting of five or fewer treatment fractions. Stereotactic body radiotherapy (SBRT) refers to the delivery of a high dose of radiation to the target, either in a single dose or a small number of fractions (less or equal to 5) with a high level of precision within the body. The basis aspects for the development of SBRT are: a) the ability to deliver a single or few fractions of high-dose radiation with high targeting accuracy; b) the dose falls off rapidly with distance from the target within the patient and c) the consequences of a high biological effective dose (BED). Anatomical and radiobiological concerns of the normal tissue tolerance limit SBRT to those targets no larger than 3 to 4 cm in any dimension.

Patient immobilization devices and tumor motion tracking allowed to reduce the treatment margins required to account for the geometric uncertainty in the tumor position and to avoid local recurrence from target miss of the radiation. Appropriate accounting of internal organ motion may be necessary, depending on the body site under treatment (patient motion, respiratory and cardiac motion, bladder and rectum filling, soft tissue deformation, etc.). The results obtained in terms of local control for such metastasis and the new technologies in the spatial localization or repositioning, allowed the development of this irradiation technique for the extra-cranial tumors.

Several guidelines and recommendations already described the practical implementation of SBRT for different localizations (lung, non-small cell lung cancer, primary liver tumors, lung and liver metastases, pancreas, spine, kidney and prostate) [83-91]. The first cases of SBRT for extracranial sites were reported in 1994 by Lax *et al*. using an external body frame and a respiratory motion device [92]. Hamilton *et al.* developed in 1995 a rigid spinal immobilization system that is surgically locked to the spinous processes for spinal radiosurgery [93]. The first experience with lung SBRT was reported by Uematsu *et al.* in 1998 [94], followed by the one of Timmerman *et al.* [95]. The first prospective phase I/II

single-fraction liver SBRT was described in 2001 by Herfarth *et al.* [96]. Other different experiences with SBRT are moreover described in a very recent review [97].

1.4.2. Prostate SBRT: results for local control and toxicities

The few experiences of different radiotherapy centers that developed prostate SBRT in 5 fractions were reported [98-105]. At Seattle department, 40 patients were included in a phase I/II study and treated with dose of 33.5 Gy in 5 fractions of 6.7 Gy, which is equivalent to 78 Gy with a standard 2 Gy dose/fraction [98]. After a mean of 41 months of follow-up, only a Grade 3 urinary toxicity was reported. The actuarial rate of survival without biological relapse was 90% at 48 months, using Phoenix definition for local relapse. A repositioning based on the intraprostatic implants was used before each fraction. The dose was delivered with a linear accelerator [98]. At Stanford University, 41 patients included in a phase I/II study received a dose of 36.25 Gy in 5 fractions of 7.25 Gy [101]. With a mean follow-up of 33 months, no toxicity of grade 4 or more was observed. Two urinary toxicities of grade 3 were observed, but no grade 3 rectal toxicity. At the time of publication, no patient presented any local relapse [101]. In Toronto, Tang *et al.* treated 30 patients with doses of 35 Gy in 5 fractions of 7 Gy with an intensity modulated radiotherapy (IMRT) technique [99]. After six months, no toxicity superior to grade 2 was observed in the whole group of patients [99]. In Naples department, 112 patients having a low risk prostate cancer were treated with doses of 35-36 Gy in 5 fractions [104]. With a median follow-up of 24 months, 2 patients presented a local relapse that was histological proved and only one patient presented a rectal toxicity of grade 3 [104]. Finally, at the ASTRO 2009 meeting, Boike *et al.* presented the results from the Dallas team of a phase I study with a dose escalation for three arms: 45 Gy, 47.5 Gy and 50 Gy in 5 fractions [100]. Fifteen patients were included in each arm. After 11 months, only 2.5% of patients presented a rectal toxicity of grade 2 and no grade 3 toxicity was found. The PSA control was 100%. The SBRT studies for prostate cancer are detailed in Appendix 2, with a description of the irradiation technique and the initial clinical results.

Preliminary experiences from these SBRT reports let us note important information:

1) The stereotactic radiotherapy is technically feasible for prostate cancers;
2) Little reported acute morbidity: the urinary and rectal toxicities of grade 3 or more are not frequent;
3) The local control is excellent (between 90% and 100%) with a PSA response of an importance comparable to that seen with conventionally fractionated radiotherapy;

4) There might be a dose-effect; with a 6.7 Gy dose per fraction the biological control rate is 90% in the study of Madsen *et al.*, but in Naples study this rate is of 98% with doses of 7 Gy and 7.2 Gy. In the report of King *et al.* (7.5 Gy per fraction) and Boike *et al.* (9 to 10 Gy per fraction) this biological control rate is 100%.

1.5. Concepts for rectal-wall protection

1.5.1. Simultaneous-integrated boost

The cancer can be multifocal with the presence of one or more main tumors, clinically detectable on MRI, and of secondary tumors that might not be detectable by using the actual imaging methods. A global treatment of the whole prostate seems more reasonable. The control of the microscopic cancer cells might require smaller irradiation doses than the control of the macroscopic tumor. Hence, the issue of a bifocal irradiation appears interesting to develop. However, only a few studies were reported. Miralbell *et al.* treated 50 patients using the following schema: 64Gy in 32 fractions to the whole prostate, followed by a focal irradiation of two SBRT fractions of 5 to 8 Gy [106]. The survival rates without any biological relapse are of 98% at 5 years with acceptable long-term rectal and urinary toxicities. There were two patients that presented Grade 3 acute urinary toxicity and the 5-year probabilities of ≥Grade 2 late urinary and late low gastrointestinal toxicity–free survivals were 82.2%±7.4% and 72.2%±7.6%, respectively [106]. At ASTRO 2009 meeting, Willoughby *et al.* reported the results of a series of 31 patients treated using a hypofractionation schema of 70 Gy in 28 fractions of 2.5 Gy to the whole prostate with a dose per fraction augmentation to 2.86 Gy to the tumor region [107]. At 70 months, the rectal and urinary toxicity rates of grade 2 or more were respectively 11% and 3%. Until now, this concept was never evaluated for SBRT of prostate cancer, but it should be developed.

1.5.2. Rationale of a simultaneous-integrated boost in SBRT

In fact, the 10 Gy dose per fraction proposed by Boike *et al.* probably permits an optimal biological control, but could be excessive for the healthy tissues (this was tested only in phase I). The dose proposed by Seattle, of 5 x 6.7 Gy, is probably sufficient for an intraprostatic microscopic control, considering the biological equivalent dose of 78 Gy of 2 Gy per fraction, with a α/β=1.5 Gy. But the biological relapse rates of 10% let us think that it's maybe not always sufficient to also control the macroscopic tumor. It seems that:

- the optimal dose to control the macroscopic disease, always limiting the toxicities risks, it's between 5 x 6.7 Gy (Seattle) and 5 x 10 Gy (Dallas).
- it's perhaps not necessary to deliver this dose to the whole prostate, but more using a focalization technique to this macroscopic tumor.

In 2013, King *et al.* presented a pooled analysis from a multi-institutional consortium of prospective phase II trials for SBRT of localized prostate cancer [108]. They stated that a dose-response within the range of 35-40 Gy in 5 fractions has not been observed and therefore escalation beyond 40 Gy is not warranted at this time, especially for low- and intermediate-risk patients [108]. Moreover, potential higher rates of grade 3 GI and GU toxicities could be observed for SBRT at 50 Gy in 5 fractions, as previously presented by Boike *et al*.

Consequently, combining a "moderate" irradiation of 6.7 Gy per fraction to the whole prostate (in order to limit the dose to the healthy tissues, but also treating the microscopic disease) with a higher dose to the macroscopic disease could be an optimal solution. A dose of 5 x 8.5 Gy could have the advantage of:

- Being feasible, because it's inferior to 5 x 10 Gy, as it was used in the phase I study of Boike *et al.* and that was delivered to the whole prostate.
- Representing an equivalent biological dose of 110 Gy (with a α/β=1.5Gy), which is sufficient to control a macroscopic disease.
- Offering a macroscopic disease control probability close or equal to 5 x 10 Gy, always avoiding the toxicities risk.

1.5.3. Prostate-rectum separation

A prostate-rectum separation has been proposed in the past years, with the intention of possibly improving the quality of life for prostate cancer patients. This approach was previously described by Prada *et al.* for brachytherapy treatments and for external beam radiotherapy, using an injection of hyaluronic acid [109, 110].

1.5.4. Study justification

The SBRT seems to be safe, but with a "narrow-border" between tolerance and toxicity. If the first results for prostate SBRT from some expert centers are promising in terms of rectal and urinary toxicities, probably the risk of toxicity increases with any positioning error. Therefore, an optimal protection of the rectal-wall could be obtained using three different methods:

1) With an exclusive SBRT integrated boost into the tumor – but it's not a reasonable method for multiples tumors;
2) With a SBRT technique to the entire prostate and a simultaneous SBRT integrated boost into the macroscopic tumor – it gives a sufficient dose to the microscopic tumors into the prostate, increases the dose to the macroscopic tumor and the rectum is spared from the high doses;
3) With a prostate-rectum separation – for example, an injection of hyaluronic acid in the perirectal fat.

Following these conclusions and based on methods (2) and (3), a study was initiated for the implementation of prostate SBRT in the Department of Radiotherapy-Oncology from Lyon Sud Hospital (France). The present work evaluates all the critical aspects (target definition, treatment planning, healthy-organ sparing and quality assurance of the treatment) for the development of a SBRT approach with an integrated boost into the prostate and an injection of hyaluronic acid for rectum sparing.

1.6. Bibliography – section I

[1]http://www.cancer.gov/cancertopics/wyntk/prostate/allpages#ab3d4f20-6ab9-4428-9717-067035d2e691.

[2] McNeal JE. The zonal anatomy of the prostate. *Prostate* 1981; 2(1):35-49.

[3] Cornud F, *et al.* Imagerie de la prostate. 1er éd. Montpellier: Sauramps Médical, 2004, 292p.

[4] Grossfeld GD, Coakley FV. Benign Prostatic Hyperplasia: Clinical overview and value of diagnostic imaging. *Radiologic Clinics of North America* 2000;38:31-47.

[5] Kwee SA, Coel MN, Lim J. Detection of recurrent prostate cancer with 18F-fluorocholine PET/CT in relation to PSA level at the time of imaging. *Ann Nucl Med* 2012;26(6)501-507.

[6] Schwarzenböck S, Souvatzoglou M, Krause BJ. Choline PET and PET/CT in Primary Diagnosis and Staging of Prostate Cancer. *Theranostics* 2012;2(3):318-330.

[7] Allen KS, Kressel HY, Arger PH, *et al.* Age-related changes of the prostate: Evaluation by MR imaging. *AJR Am J Roentgenol* 1989;152:77.

[8] Bryan PJ, Butler HE, Nelson AD, *et al.* Magnetic resonance imaging of the prostate. *AJR Am J Roentgenol* 1986;146:543.

[9] Hricak H, Williams RD, Spring DB, *et al.* Anatomy and pathology of the male pelvis by magnetic resonance imaging. *AJR Am J Roentgenol* 1983;141:1101.

[10] Pollack HM. Imaging of the prostate gland. *Eur Urol* 1991;20:50.

[11] Carrol CL, Sommer FG, McNeal JE, *et al.* The abnormal prostate: MR imaging at 1,5 T with histopathologic correlation. *Radiology* 1987;163:521.

[12] Ling D, Lee JK, Heiken JP, *et al.* Prostatic carcinoma and benign prostatic hyperplasia: Inability of MR imaging to distinguish between the two diseases. *Radiology* 1986;158:103.

[13] Poon PY, McCallum RW, Henkelman MM, *et al.* Magnetic resonance imaging of the prostate. *Radiology* 1985; 154:143.

[14] Scheckowitz EM, Resnick MI. Imaging of the prostate. Benign Prostatic hyperplasia. *Urol Clin North Am* 1995;22:321.

[15] Debois M, Oyen R, Maes F, *et al.* The contribution of magnetic resonance imaging to the three-dimensional treatment planning of localized prostate cancer. *Int J Radiat Oncol Biol Phys* 1999;45(4):857–865.

[16] Zhou SM, Bentel GC, Lee CG, Anscher MS. Differences in gross target volumes on contrast vs. noncontrast CT scans utilized for conformal radiation therapy treatment planning for prostate carcinoma. *Int J Radiat Oncol Biol Phys* 1998;42(1):73–78.

[17] Cazzaniga LF, Marinoni MA, Bossi A, *et al.* Interphysician variability in defining the planning target volume in the irradiation of prostate and seminal vesicles. *Radiother Oncol* 1998;47(3):293–296.

[18] Fiorino C, Reni M, Bolognesi A, Cattaneo GM, Calandrino R. Intra- and inter-observer variability in contouring prostate and seminal vesicles: implications for conformal treatment planning. *Radiother Oncol* 1998;47(3):285–292.

[19] Farsad M, Schwarzenböck S, Krause BJ. PET/CT and choline: diagnosis and staging. *J Nucl Med Mol Imaging* 2012;56(4):343-353.

[20] Kitajima K, Murphy RC, Nathan MA. Choline PET/CT for imaging prostate cancer: an update. *Ann Nucl Med* 2013;27(7) :581-591.

[21] Umbehr MH, Muntener M, Hany T, Sulser T, Bachmann LM. The Role of 11C-Choline and 18F-Fluorocholine Positron Emission Tomography (PET) and PET/CT in Prostate Cancer: A Systematic Review and Meta-analysis. *Eur Urol* 2013;64(1):106-117.

[22] Recommandation en santé publique HAS, février 2012: (http://www.has-sante.fr/portail/jcms/c_1197959/has-dernieres-publications-fevrier-2012).

[23] Jemal A, Siegel R, Ward E. *et al*. Cancer statistics, 2009. *CA Cancer J Clin.*2009;59:225-49.

[24] Smith RA, Cokkinides V, Eyre HJ. Cancer screening in the United States, 2007: a review of current guidelines, practices, and prospects. *CA Cancer J Clin* 2007;57:90-104.

[25] Comité de Cancérologie de l'Association Française d'Urologie. Progrès en Urologie : Recommandations 2010-2013 en onco-urologie. Volume 20, Novembre 2010 – Supplément 4. Ed. Elsevier Masson SAS.

[26] Schroder FH, Hugosson J, Roobol MJ, *et al.* Screening and prostate-cancer mortality in a randomized European study. *N Engl J Med* 2009;360:1320-1328.

[27] D'Amico AV, Whittington R, Malkowicz SB, *et al.* Biochemical outcome after radical prostatectomy, external beam radiation therapy, or interstitial radiation therapy for clinically localized prostate cancer. *JAMA* 1998;280(11):969-974.

[28] Dearnaley DP, Sydes MR, Graham JD, *et al.* Escalated-dose versus standard-dose conformal radiotherapy in prostate cancer: first results from the MRC RT01 randomized controlled trial. *Lancet Oncol* 2007;8(6):475–87.

[29] Peeters STH, Heemsbergen WD, Koper PCM, *et al.* Dose–response in radiotherapy for localized prostate cancer: results of the Dutch multicenter randomized phase III trial comparing 68 Gy of radiotherapy with 78 Gy. *J Clin Oncol* 2006;24:1990–6.

[30] Zietman AL, DeSilvio ML, Slater JD, *et al.* Comparison of conventional-dose vs high-dose conformal radiation therapy in clinically localized adenocarcinoma of the prostate: a randomized controlled trial. *JAMA* 2005;294:1233–9.

[31] Kuban DA, Tucker SL, Dong L, *et al.* Long-term results of the M.D. Anderson randomized dose-escalation trial for prostate cancer. *Int J Radiat Oncol Biol Phys* 2008;70(1):67–74.

[32] Sathya JR, Davis IR, Julian JA, Guo Q, *et al.* Randomized trial comparing iridium implant plus external-beam radiation therapy with external-beam radiation therapy alone in node-negative locally advanced cancer of the prostate. *J Clin Oncol* 2005;23(6):1192-9.

[33] Shipley WU, Verhey LJ, Munzenrider JE, *et al.* Advanced prostate cancer: the results of a randomized comparative trial of high dose irradiation boosting with conformal protons compared with conventional dose irradiation using photons alone. *Int J Radiat Oncol Biol Phys* 1995;32(1):3-12.

[34] Beckendorf V, Guérif S, Le Prisé E, *et al.* The GETUG 70 Gy vs. 80 Gy randomized trial for localized prostate cancer: feasibility and acute toxicity. *Int J Radiat Oncol Biol Phys* 2004;60(4):1056-65.

[35] Pollack A, Zagars GK, Starkschall G, *et al.* Prostate cancer radiation dose response: Results of the M. D. Anderson phase III randomized trial. *Int J Radiat Oncol Biol Phys* 2002;53:1097–1105.

[36] Pollack A, Hanlon AL, Horwitz EM, *et al.* Prostate cancer radiotherapy dose response: An update of the Fox Chase experience. *J Urol* 2004;171:1132–1136.

[37] Pollack A, Kuban DA, Zagars GK. Impact of androgen deprivation therapy on survival in men treated with radiation for prostate cancer. *Urology* 2002;60:22–30.

[38] Dolezel M, Odrazka K, Vaculikova M, *et al.* Dose escalation in prostate radiotherapy up to 82 Gy using simultaneous integrated boost: direct comparison of acute and late toxicity with 3D-CRT 74 Gy and IMRT 78 Gy. *Strahlenther Onkol* 2010;186:197–202.

[39] Peeters ST, Heemsbergen WD, van Putten WL, *et al.* Acute and late complications after radiotherapy for prostate cancer: results of a multicenter randomized trial comparing 68 Gy to 78 Gy. *Int J Radiat Oncol Biol Phys* 2005;61:1019–34.

[40] Zelefsky MJ, Fuks Z, Hunt M, *et al.* High-dose intensity modulated radiation therapy for prostate cancer: early toxicity and biochemical outcome in 772 patients. *Int J Radiat Oncol Biol Phys* 2002;53:1111–1116.

[41] Zietman AL, Bae K, Slater JD, *et al.* Randomized trial comparing conventional-dose with high-dose conformal radiation therapy in early-stage adenocarcinoma of the prostate: long-term results from proton Radiation Oncology Group/American College of Radiology 95-09. *J Clin Oncol* 2010;28:1106–1111.

[42] Azria D, Charissoux M, Rebillard X, *et al.* Updated results of the Montpellier IMRT prostate cancer cohort: Focus on elderly patients [Abstract]. *Int J Radiat Oncol Biol Phys* 2012;84(Suppl):S407-8.

[43] Thames HD, Kuban D, Levy LB, *et al.* The role of overall treatment time in the outcome of radiotherapy of prostate cancer: an analysis of biochemical failure in 4839 men treated between 1987 and 1995. *Radiother Oncol* 2010;96:6-12.

[44] Withers HR. Biologic basis for altered fractionation schemes. *Cancer* 1985;55:2086–2095.

[45] Withers HR, Thames Jr. HD and Peters LJ. A new isoeffect curve for change in dose per fraction. *Radiother Oncol* 1983;1:187–191.

[46] Fowler JF, Ritter MA. A rationale for fractionation for slowly proliferating tumors such as prostatic adenocarcinoma. *Int J Radiat Oncol Biol Phys* 1995;32:521-529.

[47] Fowler JF. The radiobiology of prostate cancer including new aspects of fractionated radiotherapy. *Acta Oncol* 2005;44:265–76.

[48] Fowler J, Chappell R, Ritter M. Is alpha/beta for prostate tumors really low? *Int J Radiat Oncol Biol Phys* 2001;50(4):1021–1031.

[49] Hall EJ. Radiobiology for the Radiologist. 4th Edition, Philadelphia, JB Lippincott 1994.

[50] Brenner DJ, Hall EJ. Fractionation and protraction for radiotherapy of prostate carcinoma. *Int J Radiat Oncol Biol Phys* 1999;43:1095–1101.

[51] Brenner DJ. Toward optimal external-beam fractionation for prostate cancer. *Int J Radiat Oncol Biol Phys* 2000;48:315–316.

[52] Stock RG, Stone NN, Tabert A, *et al.* A dose-response study for I-125 prostate implants. *Int J Radiat Oncol Biol Phys* 1998;41:101–108.

[53] Hanks GE, Schultheiss TE, Hanlon AL, *et al.* Optimization of conformal radiation treatment of prostate cancer: Report of a dose escalation study. *Int J Radiat Oncol Biol Phys* 1997;37:543–550.

[54] Duchesne GM, Peters LJ. What is the alpha/beta ratio for prostate cancer? Rationale for hypofractionated high-dose-rate brachytherapy. *Int J Radiat Oncol Biol Phys* 1999;44:747–748.

[55] King CR, Mayo CS. Is the prostrate alpha/beta ratio of 1.5 from Brenner&Hall a modeling artifact. *Int J Radiat Oncol Biol Phys* 2000;47:536–539.

[56] D'Souza WD, Thames HD. Is the alpha/beta ratio for prostate cancer low? *Int J Radiat Oncol Biol Phys* 2001;51:1–3.

[57] King CR, Fowler JF. A simple analytic derivation suggests that prostate cancer alpha/beta ratio is low. *Int J Radiat Oncol Biol Phys*2001;51:213–214.

[58] Logue JP, Cowan RA, Hendry JH. Hypofractionation for prostate cancer. *Int J Radiat Oncol Biol Phys* 2001;49:1522–1523.

[59] Amer AM, Mott J, Mackay RI, *et al.* Prediction of the benefits from dose-escalated hypofractionated intensity-modulated radiotherapy for prostate cancer. *Int J Radiat Oncol Biol Phys* 2003;56:199–207.

[60] Kal HB, Van Gellekom MP. How low is the alpha/beta ratio for prostate cancer? *Int J Radiat Oncol Biol Phys* 2003;57:1116–1121.

[61] Lindsay PE, Moiseenko VV, Van Dyk J, *et al.* The influence of brachytherapy dose heterogeneity on estimates of alpha/beta for prostate cancer. *Phys Med Biol* 2003;48:507–522.

[62] Wang JZ, Guerrero M, Li XA. How low is the alpha/beta ratio for prostate cancer? *Int J Radiat Oncol Biol Phys* 2003;55:194–203.

[63] Brenner DJ. Hypofractionation for prostate cancer radiotherapy—what are the issues? *Int J Radiat Oncol Biol Phys* 2003;57:912–914.

[64] Brenner DJ. Fractionation and late rectal toxicity. *Int J Radiat Oncol Biol Phys* 2004;60:1013–1015.

[65] Fowler JF, Ritter MA, Chappell RJ, *et al.* What hypofractionated protocols should be tested for prostate cancer? *Int J Radiat Oncol Biol Phys* 2003;56:1093–1104.

[66] Deore SM, Shrivastava SK, Supe SJ, *et al.* Alpha/beta value and importance of dose per fraction for the late rectal and recto-sigmoid complications. *Strahlenther Onkol* 1993;169:521–526.

[67] Dubray BM, Thames HD. Chronic radiation damage in the rat rectum: An analysis of the influences of fractionation, time and volume. *Radiother Oncol* 1994;33:41– 47.

[68] Gasinska A, Dubray B, Hill SA, *et al.* Early and late injuries in mouse rectum after fractionated X-ray and neutron irradiation. *Radiother Oncol* 1993;26:244 –253.

[69] Terry NH, Denekamp J. RBE values and repair characteristics for colo-rectal injury after caesium 137 gamma-ray and neutron irradiation. II. Fractionation up to ten doses. *Br J Radiol* 1984;57:617–629.

[70] van der Kogel AJ, Jarrett KA, Paciotti MA, *et al.* Radiation tolerance of the rat rectum to fractionated X-rays and pimesons. *Radiother Oncol* 1988;12:225–232.

[71] Dewit L, Oussoren Y, Bartelink H, *et al.* The effect of cis-diamminedichloroplatinum(II) on radiation damage in mouse rectum after fractionated irradiation. *Radiother Oncol* 1989;16:121–128.

[72] Brenner D, Armour E, Corry P, *et al.* Sublethal damage repair times for a late-responding tissue relevant to brachytherapy (and external-beam radiotherapy): Implications for new brachytherapy protocols. *Int J Radiat Oncol Biol Phys* 1998;41:135–138.

[73] Arcangeli G, Saracino B, Gomellini S, *et al.* A prospective phase III randomized trial of hypofractionation versus conventional fractionation in patients with high-risk prostate cancer. *Int J Radiat Oncol Biol Phys* 2010;78(1):11–8.

[74] Arcangeli G, Fowler J, Gomellini S, *et al.* Acute and late toxicity in a randomized trial of conventional versus hypofractionated three-dimensional conformal radiotherapy for prostate cancer. *Int J Radiat Oncol Biol Phys* 2011;79(4):1013–21.

[75] Arcangeli S, Strigari L, Gomellini S, *et al.* Updated results and patterns of failure in a randomized hypofractionation trial for high-risk prostate cancer. *Int J Radiat Oncol Biol Phys* 2012;84(5):1172-1178.

[76] Lukka H, Hayter C, Julian JA, *et al.* Randomized trial comparing two fractionation schedules for patients with localized prostate cancer. *J Clin Oncol* 2005;23(25):6132–8.

[77] Pollack A, Hanlon AL, Horwitz EM, *et al.* Dosimetry and preliminary acute toxicity in the first 100 men treated for prostate cancer on a randomized hypofractionation dose escalation trial. *Int J Radiat Oncol Biol Phys* 2006;64(2):518–26.

[78] Pollack A, Walker G, Buyyounouski M, *et al.* Five year results of a randomized external beam radiotherapy hypofractionation trial for prostate cancer. *Int J Radiat Oncol Biol Phys* 2011;81(2):S1.

[79] Yeoh EE, Botten RJ, Butters J, Di Matteo AC, Holloway RH, Fowler J. Hypofractionated versus conventionally fractionated radiotherapy for prostate carcinoma: final results of phase III randomized trial. *Int J Radiat Oncol Biol Phys* 2011;81(5):1271–8.

[80] Yeoh EE, Holloway RH, Fraser RJ, *et al.* Hypofractionated versus conventionally fractionated radiation therapy for prostate carcinoma: updated results of a phase III randomized trial. *Int J Radiat Oncol Biol Phys* 2006;66(4):1072–83.

[81] Kuban DA, Nogueras-Gonzalez GM, Hamblin L, *et al.* Preliminary report of a randomized dose escalation trial for prostate cancer using hypofractionation. *Int J Radiat Oncol Biol Phys* 2010;78(3):S58–9.

[82] Leksell L. The stereotactic method and radiosurgery of the brain. *Acta Chirurg Scand* 1951;102:316-319.

[83] Luxton G, Petrovich Z, Jozsef G, Nedzi LA, Apuzzo MLJ. Stereotactic radiosurgery: principles and comparison of treatment methods. *Neurosurgery* 1993;32:241-258.

[84] Okunieff P. Design of multi-institutional and cooperative group studies of SBRT. *Acta Oncol* 2006;45:775-778.

[85] Read PW. Stereotactic body radiation therapy: 2007 update. *Community Oncology* 2007;4:616-620.

[86] American College of Radiology (ACR). Practice guideline for the performance of stereotactic body radiation therapy. *ACR* 2004; p. 995-1002.

[87] Timmerman R, Galvin J, Michalski J, *et al.* Accreditation and quality assurance for Radiation Therapy Oncology Group: Multicenter clinical trials using stereotactic body radiation therapy in lung cancer. *Acta Oncol* 2006;45:779-786.

[88] Timmerman R, McGarry R, Yiannoutsos C, *et al.* Excessive toxicity when treating central tumors in a phase II study of stereotactic body radiation therapy for medically inoperable early-stage lung cancer. *J Clin Oncol* 2006;24:4833-4839.

[89] Dahele M, Pearson S, Purdie T, *et al.* Practical considerations arising from the implementation of lung stereotactic body radiation therapy (SBRT) at a comprehensive cancer center. *J Thorac Oncol* 2008;3(11):1332-1341.

[90] Hurkmans CW, Cuijpers JP, Lagerwaard FJ, *et al.* Recommendations for implementing stereotactic radiotherapy in peripheral stage IA non-small cell lung cancer: report from the Quality Assurance Working Party of the randomized phase III ROSEL study. *Radiat Oncol* 2009;4:1.

[91] Benedict SH, Yenice KM, Followill D, *et al.* Stereotactic body radiation therapy: The report of AAPM Task Group 101. *Med Phys* 2010;37(8):4078-4101.

[92] Lax I, Blomgren H, Naslund I, *et al*. Stereotactic radiotherapy of extracranial targets. *Z Med Phys* 1994;4:112-113.

[93] Hamilton A, Lulu B, Fosmine H, *et al*. Preliminary clinical experience with linear accelerator-based spinal stereotactic radiosurgery. *Neurosurgery* 1995;36:311-319.

[94] Uematsu M, Shioda A, Tahara K, *et al*. Focal, high dose, and fractionated modified stereotactic radiation therapy for lung carcinoma patients: a preliminary experience. *Cancer* 1998;82:1062-1070.

[95] Timmerman R, Papiez L, McGarry R, *et al.* Extracranial stereotactic radioablation: results of a phase I study in medically inoperable stage I non-small cell lung cancer. *Chest* 2003;124:1946-1955.

[96] Herfarth K, Debus J, Lohr F, *et al*. Stereotactic single-dose radiation therapy of liver tumors: results of a phase I/II trial. *J Clin Oncol* 2001;117:164-170.

[97] Martin A, Gaya A. Stereotactic body radiotherapy: A Review. *Clin Oncol* 2010;22:157-172.

[98] Madsen BL, Hsi RA, Pham HT, *et al.* Stereotactic hypofractionated accurate radiotherapy of the prostate (SHARP), 33.5 Gy in five fractions for localized prostate disease: First clinical trial results. *Int J Radiat Oncol Biol Phys* 2007;67:1099–1105.

[99] Tang CI, Loblaw DA, Cheung P, *et al.* Phase I/II study of a five-fraction hypofractionated accelerated radiotherapy treatment for low-risk localized prostate cancer: early results of pHART3. *Clinic Oncol* 2008;20:729-737.

[100] Boike TP, Lotan Y, Cho LC, *et al.* Phase I dose-escalation study of stereotactic radiation therapy for low- and intermediate-risk prostate cancer. *J Clin Oncol* 2011;29:2020-2026.

[101] King CR, Brooks JD, Gill H, *et al.* Stereotactic body radiotherapy for localized prostate cancer: Interim results of a prospective phase II clinical trial. *Int J Radiat Oncol Biol Phys* 2009;73:1043–1048.

[102] King CR, Brooks JD, Gill H, Presti JC. Long-term outcomes from a prospective trial of stereotactic body radiotherapy for low-risk prostate cancer. *Int J Radiat Oncol Biol Phys* 2012;82:877-882.

[103] Bolzicco G, Favretto MS, Scremin E, *et al.* Image-guided stereotactic body radiation therapy for clinically localized prostate cancer: preliminary clinical results. *Technol Cancer Res Treat* 2010;9:473-477.

[104] Friedland JL, Freeman DE, Masterson-McGary ME, Spellberg DM. Stereotactic body radiotherapy: An emerging treatment approach for localized prostate cancer. *Technol Cancer Res Treat* 2009;8:387-392.

[105] Lukka H. RTOG 0938: A Randomized Phase II Trial Of Hypofractionated Radiotherapy For Favorable Risk Prostate Cancer-RTOG CCOP Study. 2011. (http://www.rtog.org/ClinicalTrials/ProtocolTable/StudyDetails.aspx?study=0938).

[106] Miralbell R, Mollà M, Rouzaud M, *et al.* Hypofractionated boost to the dominant tumor region with intensity modulated stereotactic radiotherapy for prostate cancer: a sequential dose escalation pilot study. *Int J Radiat Oncol Biol Phys* 2010;78:50-57.

[107] Willoughby T, Reddy CA, Kupelian PA. Concomitant boost of the peripheral zone with hypofractionated radiotherapy in locally advanced prostate cancer patients: Results of a Phase II protocol [Abstract]. *Int J Radiat Oncol Biol Phys* 2009;75(3):S82.

[108] King CR, Freeman D, Kaplan I, *et al.* Stereotactic body radiotherapy for localized prostate cancer: Pooled analysis from a multi-institutional consortium of prospective phase II trials. *Radiother Oncol* 2013, *in press*.

[109] Prada PJ, Fernandez J, Martinez AA, *et al.* Transperineal injection of hyaluronic acid in anterior perirectal fat to decrease rectal toxicity from radiation delivered with intensity modulated brachytherapy or EBRT for prostate cancer patients. *Int J Radiat Oncol Biol Phys* 2007;69:95-102.

[110] Prada PJ, Gonzalez H, Mene´ndez C, *et al.* Transperineal injection of hyaluronic acid in the anterior perirectal fat to decrease rectal toxicity from radiation delivered with low-dose-rate brachytherapy for prostate cancer patients. *Brachytherapy* 2009;8:210-217.

II. TARGET VOLUME DEFINITION FOR STEREOTACTIC BODY RADIOTHERAPY OF PROSTATE CANCER

2.1. Introduction to planning target volume definition

The principle of escalating the dose to the prostate tumor while sparing the normal tissues (e.g. rectum and bladder) increases the probability of the tumor control and decreases the probability of the normal tissues toxicity. Stereotactic body radiation therapy (SBRT) requires precise delineation of the target and of the surrounding tissues and an accurate target localization during treatment delivery. Prostate SBRT, similar to conventional radiation therapy, involves the use of two reports from the International Commission on Radiation Units (ICRU 50 and 62) [1, 2] for definitions of gross tumor volume (GTV), clinical target volume (CTV), internal target volume (ITV), set up margins (SM), planning target volume (PTV) and organ at risk (OAR) (Figure 2.1). In 2010, the last report of American Association of Physicists in Medicine (AAPM Task Group 101) for SBRT has suggested that margins should be in the order of millimeters [3].

These essential notions will be studied in this chapter for defining the final target volume for a prostate SBRT protocol.

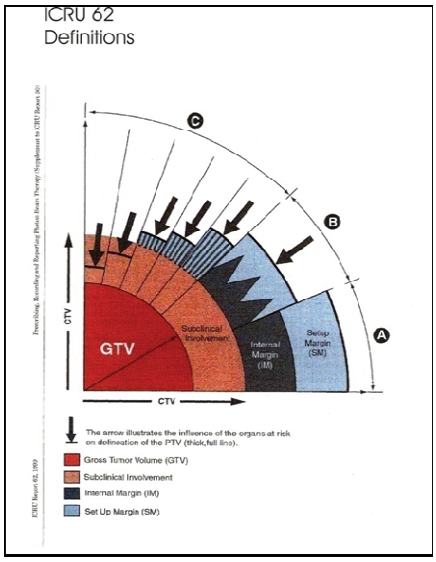

Figure 2.1. ICRU 62 - definition of target volumes [1, 2].

CTV delineation

The stereotactic body radiation therapy is a very precise technique which requires high accuracy from the very beginning of the treatment planning, in consequence, starting with the delineation of the CTV. An underestimation of the prostate organ may lead to underdosage and therefore to treatment failure. In addition, an overestimation of the target in particular for SBRT may potentially increase the acute and the late toxicities of bladder and rectum.

In general practice, the prostate is considered as the clinical tumor volume, to account for direct microscopic extension and because the macroscopic disease is not visible on the simulation CT scan. Generally, for prostate SBRT the GTV and CTV are considered to be the same.

With the progress of the MR imaging, the primary tumor becomes often visible. Then, a gross tumor volume can be delineated. Thus, CTV can be defined as the prostate and the GTV as the visible tumor with its direct extensions (prostatic capsule and seminal vesicles) that may be detectable on MRI. The improvement of the target definition with a GTV within the CTV opens the way for developing an irradiation scheme with two levels of dose. However, several aspects may influence the delineation of the GTV: the tumor characteristics, the imaging technique, the experience of the physician in delineating that region, etc.

Regardless of the stereotactic irradiation that is used, the constraint of volume limitation required by this technique imposes the most precise definition of the prostate on the CT/MRI fusion. Then, one major question is if the prostate contour can be performed by a radiation oncologist alone, or with the help of a radiologist, especially if the radiation oncologist is not a “great” expert in prostate cancer. Therefore, in section 2.2 is reported a study that evaluates if a radiologist could improve the prostate delineation of radiation oncologists, non-experts in prostate cancer, using a CT-MRI registration.

ITV delineation

The internal target volume depends mainly on the respiratory motion. Subsequently, it is possible that prostate changes its position during free breathing. The purpose of the second study (section 2.3) was to verify the respiratory-induced prostate motion using a four-dimensional computed tomography scan (4DCT).

SM definition

To guarantee that the CTV receives an adequate radiation dose, an appropriate planning target volume (PTV) margin should be added. The CTV to PTV margins are based

on random and systematic errors that represent the setup margin (SM). Setup margin exactness depends on the uncertainties related to the equipment (e.g., mechanical uncertainties of the devices or technical restrictions of the accelerator, beam penumbra) and is related to patient and target position (intrafraction and interfraction motion). Thus, SM take into consideration all possible geometrical deviations and inaccuracies.

Systematic errors are due to the treatment preparation (setup errors, variations in patient positioning, etc.) and may occur during all fractions, while random errors may arise during only one fraction.

One approach to limit the SM for SBRT is the use of three to four markers into the prostate as surrogates in localizing the target. The markers became a gold standard in monitoring and correcting the intrafraction and interfraction motion of the prostate. This method was implemented at Lyon Sud Hospital in 2009 and three gold markers are used in routine for radiotherapy treatment of prostate cancer. The accuracy of the prostate localization at each treatment fraction could allow to greatly reduce the PTV margins. However, before limiting the SM for SBRT, it was indicated to verify that the markers didn't migrate during the treatment. Their stability was studied in a series of patients treated with image-guided intensity-modulated radiotherapy and with three gold markers, as described in section 2.4.

A second approach to limit the SM for SBRT is to be able to control the prostate position throughout irradiation. The ExacTrac® system (BrainLab), available on the Novalis stereotactic-dedicated accelerator, presents the Snap Verification® (SV) tool. It acquires instant images before or during the irradiation and allows the verification of the patient's position or of the target, using bony landmarks or implanted markers, respectively. In section 2.5, the Snap Verification (SV) tool from the ExacTrac® system was evaluated.

2.2. Clinical target volume delineation

Computed tomography has been shown to considerably overestimate the volume of the prostate [4, 5]. Three factors contribute considerably to the CT contour variation in prostate cancer patients:

- poor distinction of the prostate from important adjacent structures on CT;
- large variation in anatomic position of the prostate compared with the pelvic bones and other structures, and
- difference in the shape of the prostate because of cancer stage or initial treatment choice (e.g. hormone therapy).

The reduced distinction of the prostate from adjacent structures on CT was demonstrated with underestimation in the posterior prostate (at the prostate and rectal interface) [6]. Moreover, intraobserver and intramodality variations occur when this imaging technique is used. In consequence, delineation suggestions were recently proposed for CT [7] and MRI contouring [8] in order to possibly improve the prostate delineation for radiation oncologists.

If the delineation of the target only using the CT scan seems to be sufficient for three-dimensional conformal radiotherapy, in the last report of AAPM (TG101) multimodality imaging is highly recommended for prostate SBRT treatment planning [3].

Magnetic resonance imaging can offer superior definition of the prostate gland with respect to the surrounding tissue, providing excellent soft tissue contrast on T2-weighted images and allowing image acquisition of multiple planes with good spatial resolution [9]. Several studies demonstrate the difference between CT- and MRI-delineated prostate contours and therefore, the interest in using registrations between these two exams [10-12].

Nowadays, image registration for prostate cancer between CT scan and MRI acquisition is recommended for visualization of target and organs and is increasingly used for IMRT and SBRT techniques. In Table 2.1 are summarized several SBRT studies with the delineation technique, as well as the PTV margins used for the treatment planning.

Table 2.1. Prostate SBRT studies and IGRT method used for treatment.

Study (dose prescription)	**CT/MRI fusion**	**Repositioning system**	**No of fiducials**	**PTV margins**
Madsen *et al*., 2007 (33.5Gy=5 x 6.7Gy)	Yes	EPI	3	●4-5 mm margin from the prostate to the block edge
Tang *et al*., 2008 (35Gy =5 x 7Gy)	*NA*	EPID	3	●prostate with a 4-mm uniform expansion
King *et al*., 2012 (36.25Gy=5x7.25Gy)	*NA*	CyberKnife	3	●prostate with a 5-mm volumetric expansion, reduced to 3 mm toward the rectum
Bolzicco *et al*., 2010 (35Gy = 5 x 7Gy)	*NA*	CyberKnife	4	●prostate with a 5-mm volumetric expansion, reduced to 3 mm toward the rectum
Friedland *et al*., 2009 (35-36Gy=5x7-7.2Gy)	Yes	CyberKnife	4	●the prostate and the proximal 1 cm of the seminal vesicles expanded by 5 mm in all other directions 3 mm posteriorly
Boike *et al.*, 2011 (45-50Gy in 5 x 9-10Gy)	Yes	MV/kV-IGRT or Calypso	Yes	●prostate with a 3-mm uniform expansion
Jabbari *et al.*, 2012 (38 Gy = 4 x 9.5 Gy)	Yes	CyberKnife	3	●Prostate ± seminal vesicles with: 0-mm expansion (for 15 patients) 2-mm uniform expansion (23 patients)
Lee *et al*., 2012 (36 Gy = 5 x 7.2 Gy)	*NA*	CyberKnife	3-4	●5 mm, with a reduction to 2-3 mm in the posterior direction

If SBRT demands increased precision in delineation of the prostate, a high level of expertise for the radiation oncologist is required. With the development of prostate SBRT in large number of radiotherapy departments, less expert radiation oncologists in prostate cancer could venture in the delineation of the prostate for SBRT. A major issue is to define if these physicians can use CT/MRI registrations alone or if they should be helped by a radiologist in the delineation of the prostate.

2.2.1. Publication

In collaboration with the Radiology Department from Lyon Sud Hospital we created in 2009 a protocol for pelvic MRI acquisitions that is additionally described below. This protocol is used in routine for prostate delineation on CT/MRI registrations. We subsequently initiated a study in order to evaluate the contribution of CT/MRI registrations without and with the prostate delineated by a radiologist on the MRI exam to improve the CTV definition for prostate SBRT. This work includes the evaluations of the prostate contour made by five non-expert radiation oncologists on three different imaging modalities: only on the planning CT scan, on the CT/MRI registration and on the registration with the contour of a radiologist available on the MRI. The initial results were accepted as a poster at the ESTRO 29 meeting (September 12-16, 2010) in Barcelona (Appendix 3, *abstract number 1186*) [13]. The study is presented below as an article.

Does Image Registration between the Computed Tomography Scan and the Magnetic Resonance Imaging Improve the Clinical Target Volume Delineation When We Are Not Specialists in Prostate Cancer?

Corina UDRESCU, M.S.[1-2], Ronan TANGUY, M.D.[1], Fabrice LORCHEL, M.D., PH.D.[1], Olivier ROUVIERE, M.D., PH.D.[3], Berardino DE BARI, M.D.[1], Sylvie MENGUE, M.D.[1], Tarik CHEKRINE, M.D.[1], Anne D'HOMBRES, M.D.[1], Nicolas GIROUIN, M.D.[3], Juliette BOUFFARD-VERCELLI, M.D.[4], Olivier CHAPET, M.D., PH.D.[1]

[1]Department of Radiation Oncology, Centre Hospitalier Lyon Sud, EA-3738, Lyon-Pierre Benite, France;

[2]Department of Medical Physics, Centre Hospitalier Lyon Sud, Lyon-Pierre Benite, France;

[3]Department of Urologic Radiology, HopitalEdouard Herriot, Lyon, France;

[4]Department of Radiology, Centre Hospitalier Lyon Sud, Lyon-Pierre Benite, France

Corresponding author:

Pr. Olivier CHAPET
Département de Radiothérapie - Oncologie
Centre Hospitalier Lyon Sud
Chemin du Grand Révoyet
69495, PIERRE BENITE Cedex
FRANCE
Tel 00 33 4 78 86 42 60
Fax 00 33 4 78 86 42 65
E-mail: olivier.chapet@chu-lyon.fr

Running title: Image registration for prostate delineation

Conflict of Interest Notification: none.

Summary:

The aim of this study was to evaluate if a CT/MRI registration, integrating the prostate contour made by a radiologist on the T2-MRI exam, could reduce the interobserver variations and improve the prostate delineation of the radiation oncologists who are not experts in prostate cancer. Alone, a CT/T2-MRI fusion didn't improve the contouring variability among the radiation oncologists (p=0.12). But a CT/T2-MRI fusion with a radiologist contour decreased significantly the volume variation between radiation oncologists (p=0.0002).

Abstract

Purpose

The objective of this study was to evaluate if an image registration between the dosimetric computed-tomography (CT) scan and the magnetic resonance imaging (MRI) decreases the variation in contouring between radiation oncologists non-experts in prostate cancer.

Methods and Materials

Five prostate cancer patients had a CT/T2-MRI image registration (AdvantageFusion® software, General Electric Medical Systems) based on three gold markers. The prostate was delineated on the T2-MRI exam by one radiologist, specialist in prostate cancer. Five radiation oncologists (RO) not specialized in prostate cancer delineated three contours on each CT scanin the following order: 1) without the MRI (CT), 2) with the CT/T2-MRI registration available (CT/T2-MRI) and 3) with the CT/T2-MRI registration and the radiologist's prostate delineation available on the T2-MRI (CT/T2-MRI+CR). The volume variation and the contouring variability were evaluated for each RO and modality using the CRCV ratio (the contour of the RO divided by the common volume for a modality), the Jaccard index, the uncertainty ratio (inverse of Jaccard) and measures for directional variability.

Results

The results for prostate delineations for all the patients showed a volume variation (CRCV ratio) of 1.46±0.19, 1.58±0.38 and 1.25±0.13 (mean±SD) for CT, CT/T2-MRI and CT/T2-MRI+CR, respectively. There was a significant difference between CT and CT/T2-MRI+CR (p=0.0003) and between CT/T2-MRI and CT/T2-MRI+CR (p=0.0002) but no difference between CT and CT/T2-MRI (p=0.12).

The overall Jaccard index, (mean±SD) was of 0.51±0.04, 0.46±0.09 and 0.65±0.05 for CT, CT/T2-MRIand CT/T2-MRI+CR, respectively. There was a significant difference for CT

vs CT/T2-MRI+CR (p=0.03) and for CT/T2-MRI vs CT/T2-MRI+CR (p=0.02) and no difference between CT and CT/T2-MRI (p=0.34). Similar results were obtained using the ratio of uncertainty.

Evaluating the impact of the radiologist contours for different directions, it improved the prostate contouring especially at the apex: in the anterior part of the organ (p=0.02) and in the caudal direction (p=0.02).

Conclusions

A CT/T2-MRI fusion didn't improve the volume variation among the radiation oncologists, non-experts in prostate cancer. Only a CT/T2-MRI image registration with the contour of the prostate delineated by a radiologist improved the delineation of the RO. The variation between radiotherapists decreased significantly when this method was used.

Keywords: Prostate delineation, radiotherapy, CT-MRI, image registration

Introduction

According to the International Commission on Radiation Units (ICRU, reports 50 and 62) it is recommended to accurately delineate the target [1, 2]. The recent irradiation techniques for prostate cancer, such as intensity-modulated radiation therapy and stereotactic body radiation therapy, require a higher level of precision at any step of the treatment. Therefore, the definition of the prostate becomes essential.

Prostate definition on the CT scan is associated with high interphysician and interscan variations [3-7] and an overestimation of the clinical target volume (CTV) with CT images was confirmed [8]. However, these differences are significantly reduced when a magnetic resonance imaging (MRI) is used [9-12].

The importance of using a CT/MRI image registration or a MRI exam for prostate delineation in radiotherapy was already demonstrated for: a) apex and base definition [13], b) reducing the dose to the rectum, penile bulb and the erectile arteries in order to improve the patients post-therapy sexual functioning and quality of life [14, 15], c) precision in prostate delineation for patients with bilateral hip prostheses [16], d) postimplant dosimetry for prostate brachytherapy [17] or permanent implantation [18] and e) tumor validation and localization into the prostate using different MRI sequences [19-21].

However, the interpretation of a pelvic MRI may be difficult and its usefulness for prostate contouring could be complex. Therefore, it's reasonable to verify if the CT/MRI image registration could improve the prostate contouring or it could be a source of error for a radiation oncologist who treats less frequent prostate cancer patients.

The aim of this study was to evaluate if a CT/MRI registration, with and without the prostate contour made by a radiologist on the T2-MRI exam, could reduce the interobserver variations and could improve the prostate delineation of the radiation oncologists who are not specialized in prostate cancer, compared to a CT/MRI registration alone.

Methods and Materials

Patients

Five patients with prostate cancer were treated by an exclusive IMRT irradiation technique, with total dose of 74 Gy to 76 Gy (2 Gy daily fractions). They underwent three gold markers implantation with a transrectal ultrasound-guided technique.

Image acquisition and registration

In 2009, a protocol was established in our radiotherapy department for low- and intermediate-risk prostate cancer patients for prostate tumor delineation. This protocol was furthermore used for the present study. Each patient had two image sets acquired with the patient in supine position:

- a CT scan (GE LightSpeed16®) used for treatment planning purpose and acquired in helical mode with image slice thickness of 2.5 mm;

- an axial T2-MRI pelvic acquisition made using Achieva® 1,5 Tesla system (Philips). In collaboration with the Radiology Department the parameters of the T2-MRI exam were defined in order to optimize the visualization of the markers and the definition of the prostate: turbo spin echo images (TSE) (TR=7449 ms, TE=135 ms) with an axial slice thickness of 3 mm and no space between the slices (gap = 0 mm), the images were acquired using a Sense body coil 4 elements (a phased array coil for increased signal-to-noise ration and high-resolution body imaging), with a 332 x 243 matrix, a TSE factor of 19 and a field of view (FOV) of 200 x 200 mm.

The MRI images were registered with the CT images using the Advantage Fusion® software (General Electric Medical Systems) and the fusion was based on the three gold markers visible on both acquisitions. The registrations were constantly made and approved by the same radiation physician (OC), specialist in prostate cancer.

Prostate delineation

Initially, the prostate was delineated on T2-MRI exam by one radiologist (Rad), specialist in prostate imaging. Subsequently, 5 radiation oncologists (RO) were asked to independently contour the prostate on the available images. They weren't specialized in prostate cancer, but they were in charge of different tumor localizations (head and neck, lung, etc). All RO completed three contours for each patient, in the following order:

Step 1) using only the CT scan (CT);

Step 2) having available the CT/T2-MRI fusion (CT/T2-MRI);

Step 3) having available the CT/T2-MRI fusion with the projection of the prostate outlined constantly by the same radiologist (OR) on the T2-MRI exam (CT/T2-MRI+CR).

During contouring, the physicians were blinded to the others and no repeated delineations to study the intraobserver variation were performed.

Contour evaluation

The volume in cubic centimeters (cc) of each contour was measured using the treatment planning system (Eclipse®TPS, Varian). A common volume (CV) and a union volume (UV) were created using the Boolean operators. The common volume is the volume common to all radiation oncologists in one modality. The union volume is the volume that encompasses all the volumes defined by the radiation oncologists in one modality.

The volume variation was calculated as the ratio between the contour of the radiation oncologist and the common volume on each modality (CT, CT/T2-MRI and CT/T2-MRI+CR). This volume variation will be furthermore called CRCV (the contour of the radiation oncologist divided by the common volume for a modality).

The contouring variability was calculated:

a) with the Jaccard index (the ration between the CV and the UV), as recently published by Usmani *et al.* [12].

b) with the ratio between the UV and the CV [10, 22]. This ratio of uncertainty is the inverse of the Jaccard index thus we calculate them both, allowing a comparison of our results with the ones of Rasch and Usmani.

c) for different directions - In order to see where the contouring variability was present in a particular modality, measures were taken on the axial view between the CV and the UV on the same central axis, in the anterior (A), posterior (P), right (R) and left (L) directions. This analysis was made at different levels through the prostate (following the representation of Kagawa *et al.* [23]:

- at the base, 5, 10, 15 and 20 mm superior to the geometrical isocenter of the prostate defined on CT (noted "(+)5mm", "(+)10mm","(+)15mm" and "(+)20mm");
- at the isocenter of the prostate (noted "0 mm") and
- at the apex, 5, 10, 15 and 20 mm inferior to the isocenter of the prostate (noted "(-)5mm", "(-)10mm","(-)15mm" and "(-)20mm").

For the cranial-caudal direction (CC), the measures were taken on the coronal view.

Statistical method

The CRCV was calculated for each modality by obtaining the average, the standard deviation (SD), the median and the range values for each physician and among all patients.

The overall interobserver contouring variability for a particular imaging modality was assessed using the Jaccard index and the ratio of uncertainty, by obtaining the mean and the standard deviations in the entire patient population.

The Wilcoxon matched-pairs test was used to analyze the overall contouring variability between two modalities.

Subsequently, the contouring variability (in millimeters) for each level of the prostate in the A, P, R and L directions and for the CC direction was compared between imaging modalities using a repeated measures Friedman test.

All tests were bilateral with a significant threshold set at $p<0.05$ and were made using GraphPad Prism V5.0 (GraphPad Software Inc., La Jolla, CA).

Results

General evaluation

The average clinical prostate volume was 63.2 cc (range 44.7–100.4 cc). The average delineated prostate volumes for all patients and all radiation oncologists were 74.1 cc (range 45–134.6 cc), 62.6 cc (range 30.7–129.5 cc) and 69.3 cc (range 39.8–141.2 cc) for CT, CT/T2-MRI and CT/T2-MRI+CR, respectively. The average prostate volume delineated by the radiologist on T2-MRI was 60.7 cc (range 39.9-124.3 cc). The average±SD, median and range values of the prostate are presented for each physician in Table 1.

CRCV

The overall volume variation between each modality (CRCV) is presented in Figure 1. The mean±SD was of 1.46±0.19, 1.58±0.38 and 1.25±0.13 for CT, CT/T2-MRI and CT/T2-MRI+CR, respectively. There wasn't any statistical difference between CT vs CT/T2-MRI ($p=0.12$), but a significant difference was found for CT vs CT/T2-MRI+CR ($p=0.0003$) and for CT/T2-MRI vs CT/T2-MRI+CR ($p=0.0002$). The average results for volume variation in terms of CRCV for each radiation oncologist on each modality are detailed in Table 1.

Interobserver contouring variability

The average overall contouring variability (the Jaccard index) for each modality is presented in Figure 2 (left). For the overall Jaccard index, the mean±SD was of 0.51±0.04, 0.46±0.09 and 0.65±0.05 for CT, CT/T2-MRI and CT/T2-MRI+CR, respectively. There wasn't any significant difference between CT and CT/T2-MRI ($p=0.34$), but a significant difference was found for CT vs CT/T2-MRI+CR ($p=0.03$) and for CT/T2-MRI vs CT/T2-MRI+CR ($p=0.02$).

The average ratio of uncertainty (inverse of Jaccard index) between each modality is illustrated in Figure 2 (right). For the ratio of uncertainty, the mean±SD was of 1.99±0.19, 2.23±0.48 and 1.55±0.14 for CT, CT/T2-MRI and CT/T2-MRI+CR, respectively. There

wasn't any significant difference for CT vs CT/T2-MRI (p=0.31), but a significant difference was found for CT vs CT/T2-MRI+CR (p=0.03) and for CT/T2-MRI vs CT/T2-MRI+CR (p=0.03).

Contouring variability through the prostate

The average contouring variability (in mm) for each modality is showed in Figure 3 for the anterior, posterior and right-left directions for the different regions of the prostate. In the anterior direction, there was a significant difference between the 3 modalities for "+15mm" (p=0.02), "-10mm" (p=0.008), "-15mm" (p=0.02) and "-20mm" (p=0.02). The contouring variability (in mm) between the three modalities in the cranial-caudal direction is illustrated in Figure 4. There wasn't any significant difference between modalities at the base of the prostate (p=0.09), but a significant difference was found at prostate's apex (p=0.02).

Discussion

The overestimation of the target may contribute to higher acute and late toxicities. On the other hand, the underestimation of the prostate contour may have an implication on the local control.

Gao *et al.* have demonstrated that the prostate volume delineated on CT was overestimated by an average of 30% of the real prostate volume (available from anatomical photographic digital images of pelvic region) and that included only 84% of the existent prostate volume [5]. For 8 patients, Sannazzari *et al*. reported a mean overestimation of the CTV of 34% with CT compared with MRI [8]. Along the anterior-posterior and superior-inferior direction the authors found that CTV was a mean 5 mm larger with CT scans compared with MRI acquisitions.

In 2003, Parker *et al*. assessed the feasibility of using intra-prostatic gold markers for the registration of CT and MR images. Overall, the magnitude of the prostate volume contoured on CT did not differ significantly from that contoured on MR images (p=0.20) [22]. Their results are similar to the ones found in the present study for the comparison of the CT versus CT/T2-MRI (p=0.25). Moreover, the authors showed that prostate contouring on MR is associated with less inter-observer variation than on CT (p=0.036) [22]. They obtained an average ratio of uncertainty in delineating the prostate of 1.58 for CT scans and of 1.37 for MRI scans [22].

In 1999, Rasch *et al.* calculated the mean ratio between the scan encompassing and scan common volume for several scans, including CT and axial MRI. They found that the

mean ratio±SD was of 1.5±0.4 and of 1.5±0.2 for CT and axial MRI, respectively. Their results indicated that the variation between the observers was similar in each modality [10].

Recently, Usmani *et al.* demonstrated that MRI decreased the contouring variability of the prostate compared with CT. They observed that the Jaccard index for the whole prostate becomes >0.8 when an MRI is used. However, the radiation oncologists attended a contouring workshop with a radiologist experienced in prostate MRI, or they completed the prostate atlas and contouring modules [12].

The first intend of the present study was to evaluate the use of CT/MRI registrations for radiation oncologists who were in charge of different tumor localizations, but not specialized in prostate cancer. They didn't attend any workshop for prostate contouring on T2-MRI. This absence of expertise may explain the low Jaccard index for CT/T2-MRI image registration and the high ratio of uncertainty whatever the modality used (1.99±0.19 with CT and 2.23±0.48 with CT/T2-MRI registration).

The second intend of the study was to evaluate if an additional prostate delineation contoured by a radiologist on the T2-MRI (CT/T2-MRI+CR) may reduce the interobservers variability in this group of RO non-experts in prostate cancer. The results show an increase of the Jaccard index from 0.46±0.09 for CT/T2-MRI to 0.65±0.05 for CT/T2-MRI+CR (Figure 2, left). The variation in contouring between all radiotherapists was significantly reduced ($p=0.02$) when the prostate contour of the radiologist was available. A more precise analysis revealed that the radiologist's delineation improved the prostate contouring in all directions, but more specifically at the apex in the anterior part ($p=0.02$) (Figure 3) and in the caudal direction ($p=0.02$) of the organ (Figure 4).

In the past years, guides for prostate contouring were suggested when using only the CT scan [24] or the MRI data [25]. These may be an option for prostate delineation and should be furthermore studied. In the current work, we present another method in order to possibly improve prostate definition for standard image registration using the prostate contour made by a radiologist on the MR images.

Conclusion

A CT/T2-MRI fusion didn't improve the volume variation among the radiation oncologists who were not specialists in prostate cancer. The prostate contouring on a CT/T2-MRI fusion with a radiologist contour is associated with less inter-observer variation than on CT or CT/T2-MRI for physicians that are not familiar with MR imaging of prostate cancer. This seems to be even more relevant in defining the apex and the anterior region of the

prostate volume. These results may suggest that a CT/T2-MRI registration should not be used by RO who are not experts in prostate cancer unless a prostate delineation on MRI performed by a radiologist is available. The level of expertise of the radiologist was not evaluated in this study but could impact on the accuracy of the final CTV definition.

Bibliography

[1] ICRU, “Prescribing, recording, and reporting photon beam therapy”, ICRU Report No. 50, 1993.

[2] ICRU, “Prescribing, recording, and reporting photon beam therapy (supplement to ICRU Report No. 50)”, ICRU Report No. 62, 1999.

[3] Mitchell DM, Perry L, Smith S, *et al.* Assessing the effect of a contouring protocol on post prostatectomy radiotherapy clinical target volumes and interphysician variation. *Int J Radiat Oncol Biol Phys* 2009;75:990-993.

[4] Valicenti RK, Sweet JW, Hauck WW, *et al.* Variation of clinical target volume definition in three-dimensional conformal radiation therapy for prostate cancer. *Int J Radiat Oncol Biol Phys* 1999;44:931-935.

[5] Gao Z, Wilkins D, Eapen L, *et al.* A study of prostate delineation referenced against a gold standard created from the visible human data. *Radiother Oncol* 2007;85:239–246.

[6] Fiorno C, Reni M, Bolgnesi A, *et al.* Intra- and inter-observer variability in contouring prostate and seminal vesicles: Implications for conformal treatment planning. *Radiother Oncol* 1998;47:285–292.

[7] Cazzaniga LF, Mariononi MA, Bossi A, *et al.* Interphysician variability in defining the planning target volume in the irradiation of prostate and seminal vesicles. *Radiother Oncol* 1998;47:293–296.

[8] Sannazzari GL, Ragona R, RuoRedda MG, Giglioli FR, Isolato G, Guarneri A. CT-MRI image fusion for delineation of volumes in three-dimensional conformal radiation therapy in the treatment of localized prostate cancer. *Br J Radiol* 2002;75:603-607.

[9] Smith WL, Lewis C, Bauman G, *et al.* Prostate volume contouring: A 3D analysis of segmentation using 3DTRUS, CT, and MR. *Int J Radiat Oncol Biol Phys* 2007;67:1238-1247.

[10] Rasch C, Barillot I, Remeijer P, *et al.* Definition of the prostate in CT and MRI: A multi-observer study. *Int J Radiat Oncol Biol Phys* 1999;43:57–66.

[11] RoachMIII, Faillace-Akazawa P, Malfatti C, *et al.* Prostate volumes delineated by magnetic resonance imaging and computerized tomographic scans for three-dimensional conformal radiotherapy. *Int J Radiat Oncol Biol Phys* 1996;35:1011–1018.

[12] Usmani N, Sloboda R, Kamal W, *et al.* Can images obtained with high field strength magnetic resonance imaging reduce contouring variability of the prostate? *Int J Radiat Oncol Biol Phys* 2011;80:728-734.

[13] Milosevic M, Voruganti S, Blend R, *et al.* Magnetic resonance imaging (MRI) for localization of the prostate apex: Comparison to computed tomography (CT) and urethrography. *Radiother Oncol* 1998;47:277–284.

[14] Perna L, Fiorino C, Cozzarini C, *et al.* Sparing the penile bulb in the radical irradiation of clinically localised prostate carcinoma: A comparison between MRI and CT prostatic apex definition in 3DCRT, Linac-IMRT and Helical Tomotherapy. *Radiother Oncol* 2009;93:57-63.

[15] Steenbakkers RJHM, Deurloo KEI, Nowak PJCM, *et al.* Reduction of dose delivered to the rectum and bulb of the penis using MRI delineation for radiotherapy of the prostate. *Int J Radiat Oncol Biol Phys* 2003;57:1269-1279.

[16] Rosewall T, Kong V, Vesprini D, *et al.* Prostate delineation using CT and MRI for radiotherapy patients with bilateral hip prostheses. *Radiother Oncol* 2009;90:325-330.

[17] Tanaka O, Hayashi S, Sakurai K, *et al.* Importance of the CT/MRI fusion method as a learning tool for CT-based postimplant dosimetry in prostate brachytherapy. *Radiother Oncol* 2006;81:303-308.

[18] McLaughlin PW, Narayana V, Drake DG, *et al.* Comparison of MRI pulse sequences in defining prostate volume after permanent implantation. *Int J Radiat Oncol Biol Phys* 2002;54:703-711.

[19] Groenendaal G, Moman MR, Korporaal JG, *et al.* Validation of functional imaging with pathology for tumor delineation in the prostate. *Radiother Oncol* 2010;94:145-150.

[20] Franiel T, Ludemann L, Taupitz M, Bohmer D, Beyersdorff D. MRI before and after external beam intensity-modulated radiotherapy of patients with prostate cancer: The feasibility of monitoring of radiation-induced tissue changes using a dynamic contrast-

enhanced inversion-prepared dual-contrast gradient echo sequence. *Radiother Oncol* 2009;93:241-245.

[21] Kajihara H, Hayashida Y, Murakami R, *et al.* Usefulness of diffusion-weighted imaging in the localization of prostate cancer. *Int J Radiat Oncol Biol Phys* 2009;74:399-403.

[22] Parker CC, Damyonovich T, Haycocks M, *et al.* Magnetic resonance imaging in radiation treatment planning of localized prostate cancer using intra-prostatic fiducial markers for computed tomography co-registration. *Radiother Oncol* 2003;66:217–224.

[23] Kagawa K, Lee WR, Schultheiss TE, Hunt MA, Shaer AH, Hanks GE. Initial clinical assessment of CT-MRI image fusion software in localization of the prostate for 3D conformal radiation therapy. *Int J Radiat Oncol Biol Phys* 1997;38:319-325.

[24] McLaughlin PW, Evans C, Feng M, Narayana V. Radiographic and anatomic basis for prostate contouring errors and methods to improve prostate contouring accuracy. *Int J Radiat Oncol Biol Phys* 2010;76:369-378.

[25] Villeirs GM, Verstraete KL, De Neve WJ, De Meerleer GO. Magnetic resonance imaging anatomy of the prostate and periprostatic area: a guide for radiotherapists. *Radiother Oncol* 2005;76:99-106.

Table 1. Mean, standard deviation (SD) and median (range) of two variables (prostate volume and CRCV) for the five radiation oncologists.

Variable		R1	R2	R3	R4	R5
Prostate volume (cc)						
CT	Mean ± SD	75.3±30.5	70.7±27.3	79.3±29.4	68.8±28.9	76.3±34.8
	Median (range)	68.4 (54.4-128.3)	56 (50.8-116.4)	70.7 (59.9-130.6)	55.4 (51.5-119.7)	73.4 (45-134.6)
CT/T2-MRI	Mean ± SD	62±30.9	48.4±25.4	70.5±33.3	68.4±23.6	63.7±25.1
	Median (range)	51.1 (39.8-116.2)	42.6 (30.7-92.3)	55.3 (52-129.5)	59.9 (51.7-109)	55.3 (44.8-107.8)
CT/T2-MRI+CR	Mean ± SD	67.1±32.9	66±32.2	77.8±36.2	72±33.6	63.8±32.2
	Median (range)	48.4 (46.1-123.5)	48.8 (46.1-121.8)	59.9 (56.8-141.2)	57.9 (48.4-130)	49.6 (39.8-119.6)
CRCV Ratio						
CT	Mean ± SD	1.48±0.12	1.41±0.26	1.57±0.12	1.35±0.13	1.48±0.24
	Median (range)	1.44 (1.35-1.66)	1.28 (1.21-1.84)	1.6 (1.44-1.72)	1.32 (1.22-1.55)	1.48 (1.19-1.79)
CT/T2-MRI	Mean ± SD	1.55±0.34	1.17±0.12	1.77±0.35	1.79±0.5	1.61±0.19
	Median (range)	1.41 (1.21-1.92)	1.14 (1.06-1.37)	1.68 (1.45-2.35)	1.61 (1.32-2.55)	1.66 (1.3-1.81)
CT/T2-MRI+CR	Mean ± SD	1.21±0.03	1.19±0.07	1.41±0.1	1.31±0.15	1.14±0.07
	Median (range)	1.21 (1.16-1.24)	1.16 (1.14-1.32)	1.42 (1.29-1.53)	1.26 (1.2-1.56)	1.12 (1.07-1.23)

Abbreviation: CRCV = the contour of the radiation oncologist divided by the common volume for a modality

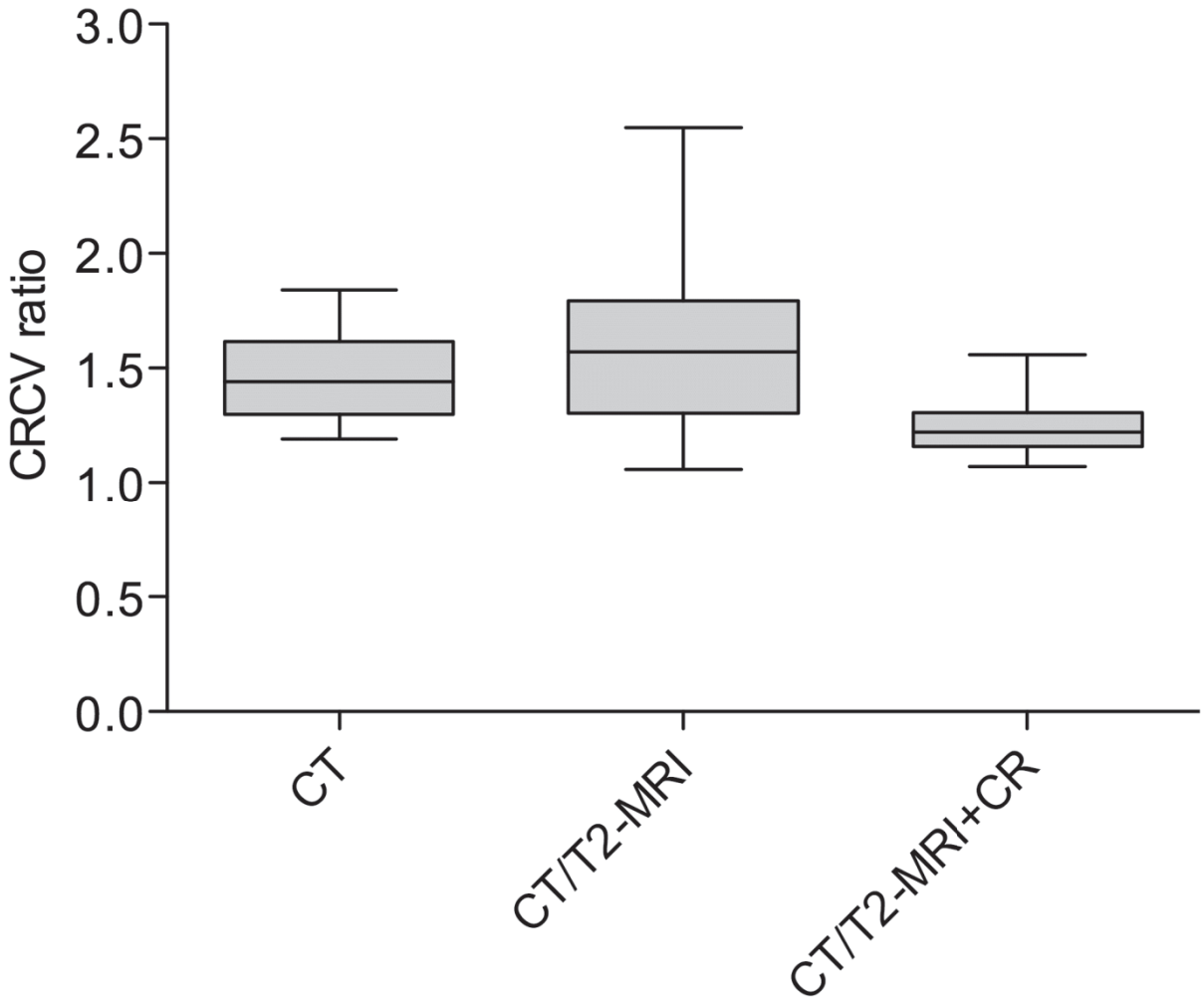

Figure 1. Overall volume variation between each modality (CRCV).

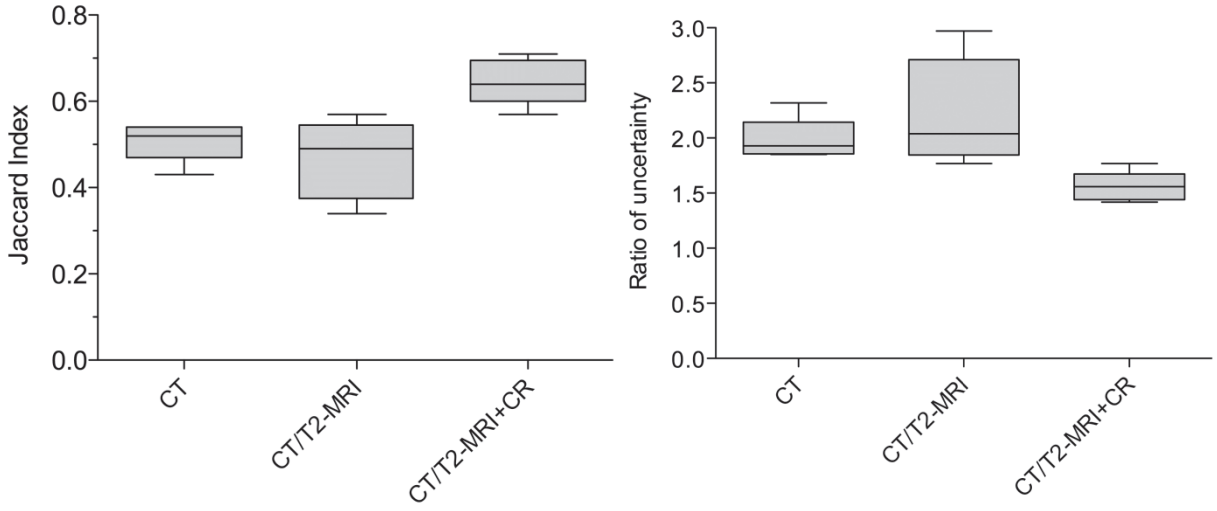

Figure 2. The average overall contouring variability (the Jaccard index) (left) and the average ratio of uncertainty (inverse of Jaccard index) (right) between each modality.

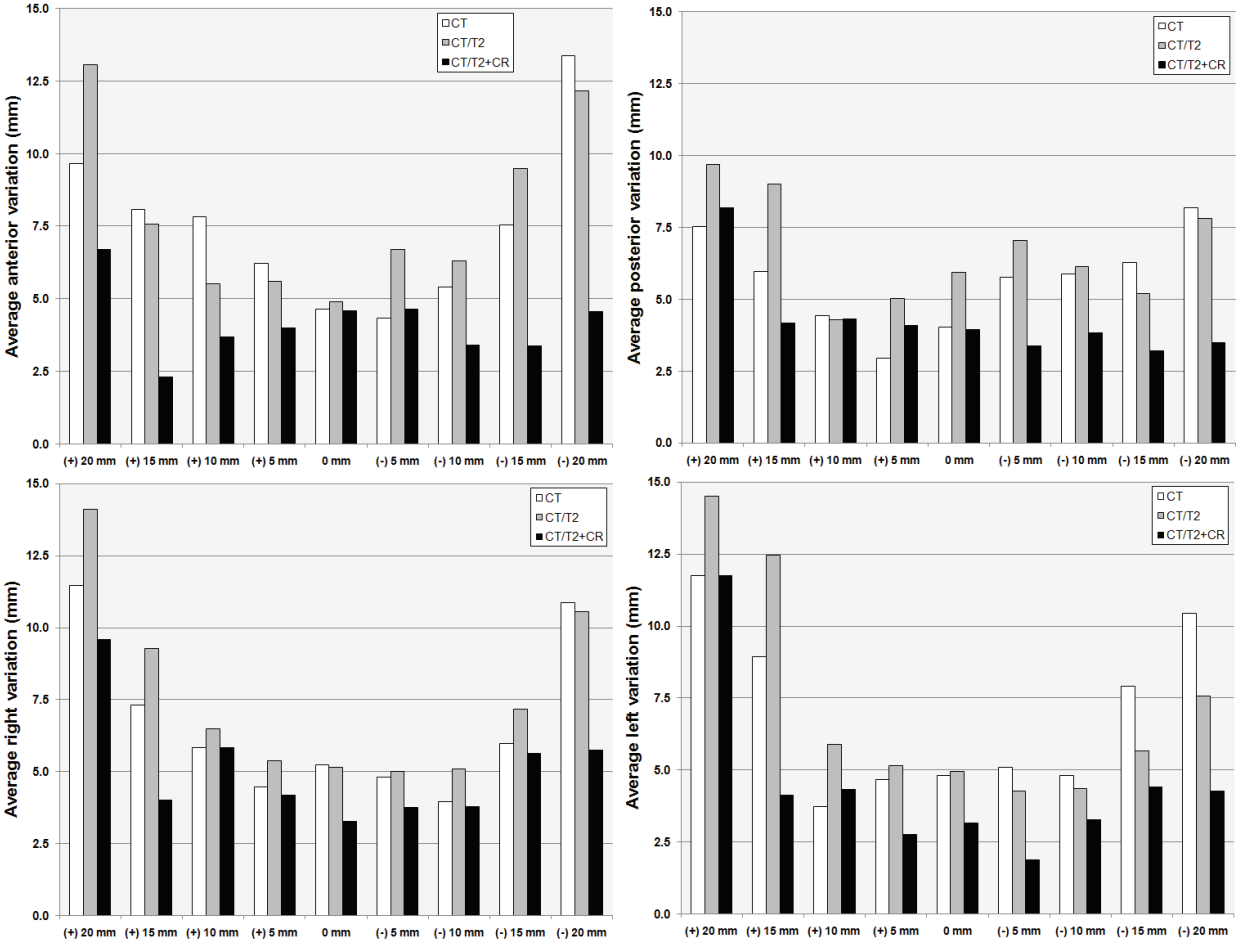

Figure 3. The average contouring variability (in mm) for each modality and for: anterior, posterior and right-left directions for the different regions of the prostate.

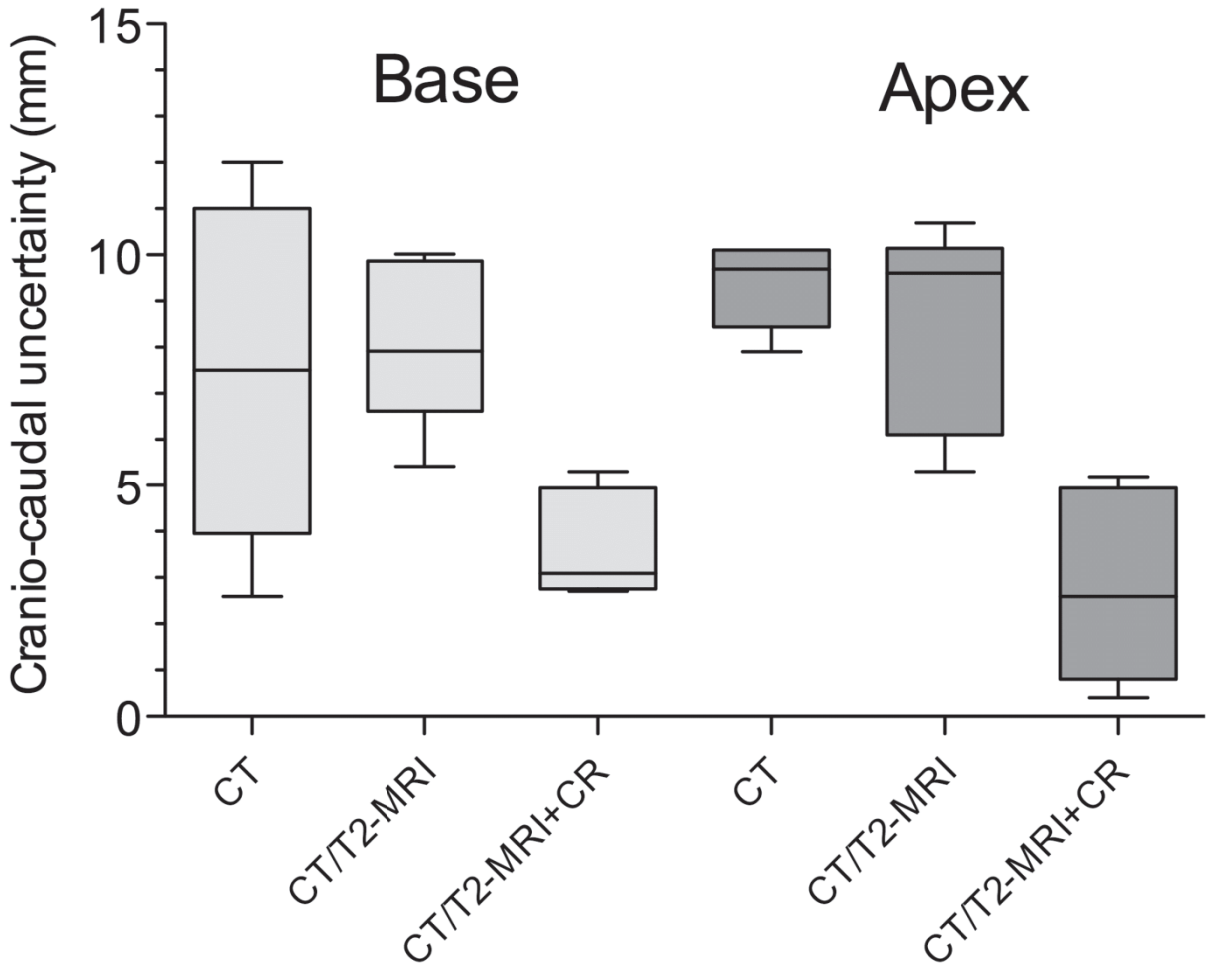

Figure 4. The contouring variability (in mm) between the three modalities in the cranial-caudal direction.

2.2.2. Conclusion

The variation of the inter-observers in the delineation of the prostate on CT is high when the radiation oncologists are not experts in the prostate cancer. Sole the CT/MRI registration could increase this variation by the difficulties meet to correctly read the MRI. Hence, the help of a radiologist is highly recommended when a SBRT treatment is planned.

2.3. Internal target volume definition

Both, intrafraction (organ motion) and interfraction (patient movement and patient setup) contribute to increased uncertainty in defining the PTV margins. The magnitude of this uncertainty is summarized in a review of the prostate motion by Langen and Jones [14]. It has been demonstrated that the intrafraction prostate motion is less than the interfraction prostate motion [15-22]. But quantifying all these motions is crucial in order to create adequate smaller PTV margins minimizing these uncertainties that become important particularly when techniques like SBRT are considered [23, 24].

There are two types of intrafraction prostate motion:

1) random motion of the organ (e.g. because of adjacent organ condition – rectum and bladder repletion);
2) respiration-induced organ motion (e.g. abdominal pressure).

The *random prostate motion* will be discussed in section 2.5, as it's directly linked to the definition of the setup margins.

2.3.1. Respiratory-induced prostate motion

Internal margin (IM), or ITV, is part of the PTV margin design and may cause a problem for high-dose escalation irradiation. Usually, for the SBRT of the thoracic and abdomen localizations, the ITV accounts for in the delineation of the PTV margins. This is generally true because of the important target motion during free breathing. Such motion can be verified and comprised in the treatment planning using four-dimensional CT (4DCT) scans [25-27]. In our department, the 4DCT scan (LightSpeed16®, General Electric Medical Systems) is used in routine for the thoracic and abdomen irradiations.

2.3.2. Publication

In 2009, we performed a study in order to verify if prostate motion could occur during free breathing. If important displacements exist, they should be taken into consideration for SBRT irradiation, as the reduction in PTV margin is required. The initial results were presented at the ESTRO 29 meeting (September 12–16, 2010) in Barcelona (Appendix 3, *abstract number 1191*) [28] and the study was accepted for publication in 2012 in the *Radiotherapy Oncology* journal [29].

Radiotherapy and Oncology 103 (2012) 266–269

Contents lists available at SciVerse ScienceDirect

Radiotherapy and Oncology

journal homepage: www.thegreenjournal.com

Prostate treatment planning

Evaluation of the respiratory prostate motion with four-dimensional computed tomography scan acquisitions using three implanted markers

Corina Udrescu [a,b], Patrice Jalade [b], Berardino de Bari [a], Géraldine Michel-Amadry [b], Olivier Chapet [a,*]

[a] Department of Radiation Oncology; [b] Department of Medical Physics, Centre Hospitalier Lyon Sud, Pierre Benite, France

ARTICLE INFO

Article history:
Received 24 June 2011
Received in revised form 15 March 2012
Accepted 20 March 2012
Available online 20 April 2012

Keywords:
Respiratory-induced
Prostate motion
4D
Gold markers

ABSTRACT

Background and purpose: During the irradiation of the prostate cancer, it is crucial to take into account the possible displacements in defining the planning target volume. The objective of this study was to specifically analyze the respiratory-induced prostate motion using a four-dimensional CT scan (4DCT).
Materials and methods: Ten patients have been treated for prostate cancer in the supine position and with three implanted gold markers; they underwent a 4DCT using a GE LightSpeed16® CT scan (slice thickness 2.5 mm). This acquisition was divided into 10 phases over the respiratory cycle using the Advantage4D software. For each phase, digitally-reconstructed radiographs (DRRs) were created at 0° and 90° with the view of the markers. The coordinates of each marker center were generated from the scan isocenter. The motion amplitude was: visually analyzed on the dynamic 4DCT sequences and then more precisely calculated by comparing the marker coordinates on the 10 scans.
Results: There was not any difficulty in defining the coordinates of the markers on each series. No prostate motion was observed on a simple visual analysis of the dynamic 4DCT sequences. After a more specific analysis, using the coordinates of the fiducials on the 10 phases, the prostate motion remained below 1 mm in all directions, except for the cranio-caudal, where it was undetectable (thereby below the slice thickness of 2.5 mm).
Conclusions: To our knowledge, this is the first study that evaluates the respiratory-induced prostate motion, using a 4DCT scan. Even if important prostate displacement can occur during the prostate treatment, because of the bladder or rectum filling, in the present study no respiratory-induced prostate motion was observed.

The prostate motion is an important issue to define the internal target volume (ITV) and the planning target volume (PTV) margins around the organ. The subject becomes crucial when a hypofractionated intensity modulated radiotherapy (HIMRT) [1–9] or stereotactic body radiation therapy (SBRT) [10–14] approach is scheduled, with limited PTV margins and high doses per fraction. An inadequate definition of the PTV could result in an underdosage for the target and/or an overdosage for the rectum and/or bladder.

The prostate intrafraction movement was already analyzed using fluoroscopic [15–22], electronic portal [23] or kV [24] images and intraprostatic gold markers; radiofrequency transponders with the Calypso system [25–27], or using dynamic MRI [28–30] but never with a four dimensional (4D) CT scan. The patient position (prone vs. supine) was specially considered and substantial reductions in the prostate motion were seen for the supine position compared with the prone position [19,20,31,32]. The 4DCT technique is the most efficient one for detecting the motion of the thoracic and abdominal organs (lungs, liver, kidneys, etc.) and has been routinely used by our department team for ITV delineation, for more than three years. Due to its image quality, the 4DCT scan offers a precise analysis of the prostate and of the intraprostatic gold markers motion during normal breathing. The aim of the present study was to analyze the potential respiratory-induced prostate motion on patients who underwent a 4DCT scan, in the supine position, after the implantation of three gold markers.

Materials and methods

Patients

In our department, patients are often treated for low- and intermediate-risk prostate cancer with an intensity modulated radiotherapy (IMRT) technique and three gold markers implanted by a urologist surgeon or a radiologist. The markers are 3 mm long and 1.2 mm thick and are implanted in triangle: one at the base on the right side of the urethra, one at the middle left laterally and the third one at the apex, on the right side of the urethra. The three

* Corresponding author. Address: Département de Radiothérapie – Oncologie, Centre Hospitalier Lyon Sud, Chemin du Grand Révoyet, 69495 Pierre Benite Cedex, France.
E-mail address: olivier.chapet@chu-lyon.fr (O. Chapet).

0167-8140/$ - see front matter © 2012 Published by Elsevier Ireland Ltd.
http://dx.doi.org/10.1016/j.radonc.2012.03.016

gold markers are used for: (1) better delineation of the prostate on an image fusion between the dosimetric CT scan and the T2-MRI series, (2) the daily kV/kV prostate repositioning under the accelerator. All the patients are treated supine, using specific knee cushion and leg immobilization (Civco Medical Solutions).

The 4D acquisition technique

Ten patients underwent a dosimetric scan (in helical mode), for the treatment planning, followed by a 4D acquisition (in cine clusters with multiple acquisitions along the *Z*-axis), using the GE LightSpeed16® CT scan. The 4D acquisition was made 2 cm above the prostate to 2 cm below during normal breathing. The dose delivered to one patient for a GE 4DCT scan acquisition was 20–23 mSv. The 4D cine acquisition protocol used for these patients is presented in Table 1.

The respiratory-induced motion was recorded via an external gating system, Real-Time Position Management (RPM) from Varian. Both, the 4DCT exam and the respiratory motion data file were transferred to the Advantage4D® software (General Electric Medical Systems), where the respiratory phase was correlated with the acquired image. Ten CT scan phases were created for each respiratory cycle, all with the same isocenter.

Prostate movement analysis

The prostate motion was first evaluated by a simple visual analysis of the dynamic 4DCT scan sequences and then more precisely measured on each phase of the respiratory cycle, according to the following procedure:

– for each patient and for each CT scan phase, two digitally reconstructed radiographs (DRRs) were created at 0° (anterior) and 90° (left lateral) with a view of the markers (image pixel size = 0.02 cm). On these two DRRs, the coordinates (*x*, *y* and *z*) of the middle of the three markers were generated from the isocenter of the CT scans, taken as a reference (coordinates: 0,0,0). The amplitude of the prostate motion was calculated by comparing the coordinates of the markers on the 10 scans. All the values in millimeters were analyzed in order to observe a possible movement of the prostate during respiration.

Results

The 4D acquisitions were performed on an average of 10 respiratory cycles [7–14], with an average of 4 s per breathing cycle. The average time for a cine acquisition was of approximately 2 min. No prostate motion was observed on a simple visual analysis of the 10 dynamic 4DCT scan sequences.

There was not any difficulty in defining the coordinates of the markers on each CT scan series. After a more specific analysis on the DRRs, using the coordinates of the seeds on each of the 10 respiratory phases, the prostate motion remained below 1 mm with an average of 0.27 mm in both left–right (LR) and anterior–posterior (AP) directions. The maximum values and the averages ± standard deviations (SD) of the movement amplitudes for every direction and each patient are presented in Table 2. In the cranio-caudal (CC) direction, the prostate motion remained undetectable according to the slice thickness and thereby below 2.5 mm. Smaller slice thicknesses were not used in order to avoid an increasing dose to the pelvis, for the 4D acquisition.

Table 1
4D-Cine Protocol that was used for the acquisitions of the prostate cancer patients.

Scan parameters	• kV = 120 • mA for abdomen = 160–175 • Time = 0.5–1 s for Cine full, cine duration was 6
Scan type	• Scan Type = Cine • Rotation time = 0.5–1.0 s • Rotation length = Full
Scan range	• 2 cm around the prostate, in the cranio-caudal axis
Cine duration	• Cine duration = breathing cycle + scan rotation
Slice parameters	• Detector row = 16 • Axial thickness = 2.5 mm • Number of images per rotation = 4i • Cine time between images = breathing cycle/10

Discussion

Ventilatory prostate motion in the supine vs. prone position

The respiratory-induced prostate organ motion with particular regard to the patient's position (supine or prone) was previously studied using three gold markers and fluoroscopic images [21,33]. When using, or not, an immobilization device, the results are not always similar. Malone et al. [21] evaluated images from 20 patients (prone with and without thermoplastic shells and supine without their shells) and measured the prostate position during quiet respiration over 20-s fluoroscopy time interval. When the patients were immobilized prone in thermoplastic shells, the prostate moved synchronously with the respiration. In their study, the prostate was displaced at a mean distance of 3.3 ± 1.8 (SD) mm (range, 1–10.2 mm), with 23% of the displacements being 4 mm or greater due to the intra-abdominal pressure. The respiration-associated prostate movement decreased significantly in supine without thermoplastic shells.

A comparison of the prostate motion in four different treatment positions was made on four patients and using fluoroscopic images by Dawson et al. [19]: prone in an alpha cradle, prone with an aquaplast custom mold, supine on a flat table and supine with a false table top under the buttocks. The fluoroscopic observation times were of 10–30 s (2–6 breathing cycles). They noticed that the largest prostate ventilatory movement was in the CC direction. When the patient had *a normal breathing*, the prostate movement remained below 1 mm in all directions for the supine position, whereas, in the prone position the CC movements ranged from 0.9 to 5.1 mm, i.e. results comparable with the present study. When the patient had *a deep breathing*, the CC movements were of: 3.8–10.5 mm in the prone position (with and without an aquaplast mold), 2.0–7.3 mm in the supine position and 0.5–2.1 mm in the supine position with a false table top. They concluded that the ventilatory movement of the prostate was substantial in the prone position and was reduced in the supine position.

In 2002, Kitamura et al. [20] found similar results in the study of 10 patients, using two sets of real-time fluoroscopic images and no immobilization. The coordinates of only one marker were recorded automatically and analyzed in terms of 3D trajectories and

Table 2
The maximum (max), average (mean) and standard deviation (SD) values in millimeters, representing the movement amplitudes for every direction and each patient.

Patient No.	LR (*x* axis)		AP (*y* axis)		CC (*z* axis)
	Max	Mean ± SD	Max	Mean ± SD	Max (mm)
1	0.7	0.4 ± 0.2	0.8	0.5 ± 0.1	<2.5
2	0.3	0.1 ± 0.1	0.4	0.1 ± 0.1	<2.5
3	0.4	0.2 ± 0.1	0.6	0.3 ± 0.2	<2.5
4	0.6	0.2 ± 0.2	0.2	0.1 ± 0.1	<2.5
5	0.2	0.1 ± 0.1	0.3	0.1 ± 0.1	<2.5
6	0.1	0.1 ± 0.1	0.3	0.1 ± 0.1	<2.5
7	0.4	0.2 ± 0.1	0.4	0.2 ± 0.1	<2.5
8	0.1	0.1 ± 0.1	0.3	0.1 ± 0.1	<2.5
9	0.5	0.1 ± 0.1	0.5	0.2 ± 0.1	<2.5
10	0.2	0.1 ± 0.1	0.6	0.2 ± 0.2	<2.5

movement frequency. The average amplitude in the supine position was 0.1 ± 0.1, 0.3 ± 0.2 and 0.3 ± 0.4 mm vs. 0.5 ± 0.4, 1.4 ± 0.5 and 1.6 ± 0.4 mm in the prone position, in respectively L–R, CC and AP directions. The supine position amplitude was statistically smaller in all directions than in the prone position. The authors agreed that with the limitation of their method, tracking a single marker in the prostate might not reflect the movement of the entire prostate gland.

Normal breathing vs. deep inspiration

A study was conducted in 2004 [18] to quantify the intrafraction motion of the prostate using digital fluoroscopy and gold seeds. Thirty-two patients were instructed to breathe normally and then to provide a deep inspiration in order to observe its effects. Means and standard deviations for superior–inferior, lateral and anterior-posterior prostate motions were 0.5 ± 0.2, 0 ± 0.1 and 0.2 ± 0.2 mm, respectively, during quiet respiration. Results for deep inspiration for the same three directions were 2.1 ± 1.6, 0.6 ± 0.6 and 1.7 ± 0.5 mm, respectively, with observed extremes of motion in the superior–inferior direction of 6.3, 2.5 mm in the lateral direction and 6.5 mm in the anterior–posterior direction.

Recently, a total of 43 patients and eight healthy volunteers were examined with dynamic MRI [30]. Images during deep respiration and during the contraction of abdominal musculature (via a coughing maneuver) were obtained with dynamic two-dimensional (2D) balanced SSFP; 3 frames/s were obtained over an acquisition time of 15 s. Images were acquired in the sagittal orientation to evaluate motion along both the craniocaudal (cc)-axis and anteroposterior (ap)-axis. The prostate motion was quantified semi-automatically using dedicated software tools. The respiratory-induced mean cc-axis displacement of the prostate was 2.7 ± 1.9 (SD) mm (range, 0.5–10.6 mm) and the mean ap-axis displacement 1.8 ± 1.0 (SD) mm (range, 0.3–10 mm). In 69% of the subjects, breathing-related prostate movements were found to be negligible (<3 mm). The prostate displacement for abdominal contraction was significantly higher.

In the current study, displacements inferior to 1 mm were found in all directions, except in the CC direction where they were undetectable. The results are comparable to those of Dawson et al. [19]. Similar results were also found in the study of Kitamura et al. [20] for the supine position. To our knowledge, the present study is the first to corroborate the previous results on the respiratory prostate motion in the supine position, using a recent 4DCT scan technique and three intraprostatic gold markers, intended for normal breathing respiration. The 4D scan is a continuous acquisition during the entire breathing cycle and consequently allows an accurate visualization of any motion of the pelvic organs (prostate, bladder, etc.) induced by respiration. With an acquisition time of 2 min and a breathing cycle around 3–4 s, any prostate motion could be well monitored and the effect of respiration well observed.

Conclusions

Although an important prostate displacement can occur during the prostate treatment, because of the bladder or rectum filling, in our study we did not observe any motion of the prostate, linked to normal breathing. Taking into consideration the slice thickness of the CT scan (2.5 mm), our study shows that the prostate motion with respiration, if present, remains always below 1 mm in AP and LR directions and below 2.5 mm in the CC direction, a very important aspect for the reductions of the PTV margins for the 3D-conformal radiotherapy and especially for hypofractionated IMRT and/or SBRT irradiation techniques.

Conflict of interest statement

None.

References

[1] Coote JH, Wylie JP, Cowan RA, et al. Hypofractionated intensity-modulated radiotherapy for carcinoma of the prostate: analysis of toxicity. Int J Radiat Oncol Biol Phys 2009;74:1121–7.
[2] Kupelian PA, Willoughby TR, Reddy CA, et al. Hypofractionated intensity-modulated radiotherapy (70 Gy at 2.5 Gy per fraction) for localized prostate cancer: Cleveland clinic experience. Int J Radiat Oncol Biol Phys 2007;68:1424–30.
[3] Faria SL, Souhami L, Joshua B, et al. Reporting late rectal toxicity in prostate cancer patients treated with curative radiation treatment. Int J Radiat Oncol Biol Phys 2008;72:777–81.
[4] Ritter MA, Forman JD, Kupelian PA, et al. A phase I/II trial of increasingly hypofractionated radiation therapy for prostate cancer [Abstract]. Int J Radiat Oncol Biol Phys 2009;75:S80.
[5] Miralbell R, Roberts SA, Zubizarreta E, et al. Dose- fractionation sensitivities of low/middle/high-risk prostate cancer deduced from seven international primary institutional datasets [Abstract]. Int J Radiat Oncol Biol Phys 2009;75:S81.
[6] Pollack A, Buyyounouski M, Horwitz E, et al. Hypofractionation for prostate cancer: interim results of a randomized trial [Abstract]. Int J Radiat Oncol Biol Phys 2009;75:S81.
[7] Martin JM, Rosewall T, Bayley A, et al. Phase II trial of hypofractionated image-guided intensity-modulated radiotherapy for localized prostate adenocarcinoma. Int J Radiat Oncol Biol Phys 2007;69:1084–9.
[8] Ritter MA, Forman JD, Petereit DG, et al. Dose-per-fraction escalation for localized prostate cancer- a multi-institutional phase I/II trial [Abstract]. Int J Radiat Oncol Biol Phys 2006;66:S11.
[9] Yeoh EEK, Fraser RJ, McGowan RE, et al. Evidence for efficacy without increased toxicity of hypofractionated radiotherapy for prostate carcinoma: early results of a phase III randomized trial. Int J Radiat Oncol Biol Phys 2003;55:943–55.
[10] Boike TP, Cho L, Lotan Y, et al. A phase I dose escalation study of stereotactic body radiation therapy (SBRT) for low- and intermediate risk prostate cancer [Abstract]. Int J Radiat Oncol Biol Phys 2009;75:S80.
[11] Miralbell R, Mollà M, Rouzaud M, et al. Hypofractionated boost to the dominant tumor region with intensity modulated stereotactic radiotherapy for prostate cancer: a sequential dose escalation pilot study. Int J Radiat Oncol Biol Phys 2010;78:50–7.
[12] Wulf J, Hadinger U, Oppitz U, et al. Stereotactic boost irradiation for targets in the abdomen and pelvis. Radiother Oncol 2004;70:31–6.
[13] King CR, Brooks JD, Gill H, et al. Stereotactic body radiotherapy for localized prostate cancer: interim results of a prospective phase II clinical trial. Int J Radiat Oncol Biol Phys 2008:1–6.
[14] Tang CI, Loblaw DA, Cheung P, et al. Phase I/II study of a five-fraction hypofractionated accelerated radiotherapy treatment for low-risk localized prostate cancer: early results of pHART3. Clin Oncol 2008;20:729–37.
[15] Scarbrough TJ, Golden NM, Ting JY, et al. Comparison of ultrasound and implanted seed marker prostate localization methods: implications for image-guided radiotherapy. Int J Radiat Oncol Biol Phys 2006;65:378–87.
[16] Shirato H, Shimizu S, Shimizu T, et al. Real-time tumour-tracking radiotherapy. Lancet 1999;353:1331–2.
[17] Shimizu S, Shirato H, Kitamura K, et al. Use of implanted marker and real-time imaging for the positioning of prostate and bladder cancers. Int J Radiat Oncol Biol Phys 2000;48:1591–7.
[18] Tirona R, Sixel K, Cheung P. Measurement of respiratory induced motion of implanted gold seeds in the prostate using digital fluoroscopy [Abstract]. Radiother Oncol 2004;72:S55.
[19] Dawson L, Litzenberg D, Brock Kristy, et al. A comparison of ventilatory prostate movement in four treatment positions. Int J Radiat Oncol Biol Phys 2000;48:319–23.
[20] Kitamura K, Shirato H, Seppenwoolde Y, et al. Three-dimensional intrafractional movement of prostate measured during real-time tumor-tracking radiotherapy in supine and prone treatment positions. Int J Radiat Oncol Biol Phys 2002;53:1117–23.
[21] Malone S, Crook JM, Kendal W, et al. Respiratory-induced prostate motion: quantification and characterization. Int J Radiat Oncol Biol Phys 2000;48:105–9.
[22] Nederveen AJ, van der Heide UA, Dehnad H, van Moorselaar RJ, Hofman P, Lagendijk JJ. Measurements and clinical consequences of prostate motion during a radiotherapy fraction. Int J Radiat Oncol Biol Phys 2002;53:206–14.
[23] Rosewall T, Chung P, Bayley A, et al. A randomized comparison of interfraction and intrafraction prostate motion with and without abdominal compression. Radiother Oncol 2008;88:88–94.
[24] Budiharto T, Slagmolen P, Haustermans K, et al. Intrafractional prostate motion during online image guided intensity-modulated radiotherapy for prostate cancer. Radiother Oncol 2011;98:181–6.
[25] Kupelian P, Willoughby T, Mahadevan A, et al. Multi-institutional clinical experience with the Calypso system in localization and continuous, real-time monitoring of the prostate gland during external radiotherapy. Int J Radiat Oncol Biol Phys 2007;67:1088–98.

[26] Su Z, Zhang L, Murphy M, et al. Analysis of prostate patient setup and tracking data: potential intervention strategies. Int J Radiat Oncol Biol Phys 2011;81:880–7.
[27] Shah AP, Kupelian PA, Willoughby TR, Langen KM, Meeks SL. An evaluation of intrafraction motion of the prostate in the prone and supine positions using electromagnetic tracking. Radiother Oncol 2011;99:37–43.
[28] Khoo VS, Bedford JL, Padhani AR, Leach MO, Husband JE, Dearnaley DP. Prostate and rectal deformation assessed using cine magnetic resonance imaging (MRI) during a course of radical prostate radiotherapy. Radiother Oncol 2002;64:285.
[29] Ghilezan MJ, Jaffray DA, Siewerdsen JH, et al. Prostate gland motion assessed with cine-magnetic resonance imaging (cine-MRI). Int J Radiat Oncol Biol Phys 2005;62:406–17.
[30] Dinkel J, Thieke C, Plathow C, et al. Respiratory-induced prostate motion. Strahlenther Onkol 2011;187:426–32.
[31] Weber DC, Nouet P, Rouzaud M, et al. Patient positioning in prostate radiotherapy: is prone better than supine? Int J Radiat Oncol Biol Phys 2000;47:365–71.
[32] Awunor OA, Lovelock MD, Ashman JB, Mageras GS, Zelefsky MJ. Measurement of respiratory motion of the prostate in the prone and supine orientations using respiratory correlated computed tomography [Abstract]. Int J Radiat Oncol Biol Phys 2005;63:S492.
[33] Szanto J, Gerig L, Crook J, et al. Respiratory variation in prostate position: considerations for conformal radiotherapy treatment planning [Abstract]. Int J Radiat Oncol Biol Phys 1998;42:367.

2.3.3. Conclusion

In conclusion, the prostate doesn't move during free-breathing and should not be an issue throughout a stereotactic irradiation.

2.4. Setup margin definition: Reliability of the implanted fiducial markers

If no intrafraction prostate motion during free-breathing were noticed in the previous study [29], other important prostate displacements can occur during irradiation because of the bladder or rectum filling. This *intrafraction* prostate motion (as a result of organ repletion) and the *interfraction* prostate motion (primarily related to changes inpatient localization) continue, in consequence, to account for in the definition of prostate setup margins. Image-guided radiation therapy (IGRT) can be used to determine and correct positional errors for patient/target and critical structures, before or during irradiation. Gold markers are commonly used for the localization of the prostate before the irradiation and the intra-fraction control.

2.4.1. Prostate localization and patient setup using fiducial markers

A number of studies have been published analyzing PTV margins required for prostate radiotherapy based on setup errors (interfractional movement) and internal margin (intrafractional movement) for different repositioning techniques and using implanted markers.

There were two studies that reported up to 50% PTV margins reduction when implanted markers are used. Beltran *et al.* reported PTV margins for pelvic bony anatomy setup of 4.3 mm, 9.8 mm and 11.5 mm in the left-right (LR), superior-inferior (SI) and anterior-posterior (AP) directions, respectively. When they used fiducials and EPID instead of kV imaging, they found margins of 4.8 mm, 5.4 mm and 5.2 mm for LR, SI and AP, respectively (using 5-mm action threshold), and 4.3 mm, 4.9 mm and 4.8 mm for LR, SI and AP, respectively (with no-threshold method) [18]. Moseley *et al.* compared kV cone beam CT with MV portal images in terms of MS patient setup, finding no difference between systems [30]. Nederveen *et al.* presented their results with markers and provide a smaller margin for the PTV (3.2 mm, 4.3 mm and 4.4 mm in the LR, AP and SI positions, respectively). Standard deviations for systematic marker displacement were of 2.4 mm in RL direction, 4.4 mm in the AP direction and 3.7 mm in the caudal-cranial direction (CC) [31]. Huang *et al.* studied 400 alignment procedures with US for 20 patients and reported a small intrafraction movement of the prostate. The mean magnitude of shifts (±SD) was 0.2 ±1.3 mm, 0.1±1.0 mm, and 0.01 ± 0.4 mm, in the anterior, superior and left directions, respectively. The maximal range of motion occurred in the AP dimension, from 6.8 mm anterior to 4.6 mm posterior [15].

Cheung *et al.* used EPID and fiducial markers with 33 patients and a total of 297 images. The average PTV margin used during the hypofractionated IMRT boost was of 3 mm in the LR direction, 3 mm in the SI direction, and 4 mm in the AP direction [32]. Vigneault *et al.* also studied the intrafraction motion with implanted markers using EPID. The displacements of the marker up to 1.6 cm were measured within 2 consecutive days of treatment, but they didn't find any intrafraction motion [33]. Nederveen *et al.* reported the intrafraction motion of the prostate for 10 patients using an a-Si flat-panel imager. The detection of a marker displacement as large as 9.5 mm was possible and the authors affirmed that the prostate motion is typically in the posterior direction when patients are treated supine. Within 2 to 3 minutes, the average deviations from the initial marker position were 0.3 mm ± 0.5 mm and -0.4 mm ± 0.7 mm in the AP and CC directions, respectively [34].

In conclusion, intraprostatic markers are the gold standard for the detection of the intrafraction motion and are highly recommended for the prostate image-guided SBRT. We, as other teams, have demonstrated the stability of the fiducials and the importance that should be given for PTV margins reductions up to 3 mm for SBRT.

2.4.2. Real-time tracking systems

In addition, it is highly recommended to monitor the prostate motion with real-time tracking systems.

On 11 patients, Litzenberg *et al.* assessed the impact of the intrafraction motion on the margins for prostate radiotherapy. Positioning by Calypso and three implanted transponders at the start of the treatment fraction required average margins of 1.8 mm, 5.8 mm, and 7.1 mm in the LR, AP and CC directions, respectively. Intrabeam adjustment provided margins of 1.3 mm, 1.5 mm, and 1.5 mm, respectively [35]. Kupelian *et al.* carried out a real-time monitoring of the prostate with the Calypso system and three implanted electromagnetic transponders. Displacements ≥3 and ≥5 mm for cumulative durations of at least 30 seconds were observed during 41% and 15% of sessions. They observed good agreement with the X-ray localization system [36].

Alonso-Arrizabalaga *et al.* acquired 1330 pairs of ExacTrac® kV-images of 30 patients. They suggested that the PTV margins, based on daily bony anatomy match, including intrafraction correction, would be of 4.5 mm, 13.5 mm and 11.5 mm in the LR, SI and AP directions, respectively. This margin could be additionally reduced to 4.8 mm, 8.6 mm and 8.1 mm in the same directions (including intrafraction motion) if implanted marker seeds are used. They concluded that with daily markers repositioning, the PTV margins could

be reduced to 1.9 mm, 6.2 mm and 4.7 mm in LR, SI and AP, respectively [37]. ExacTrac® seems to be an important system for target localization and combined with the Snap Verification® tool allow margin reductions below 5 mm.

2.4.3. Fiducial markers stability

If the implanted fiducials are commonly used for daily prostate localization and became the gold standard for a daily basis repositioning of the prostate before and also during the external beam radiotherapy, and more specifically for the stereotactic irradiation [38-45], the question of the potential migration of the markers within the prostate is essential. Usually, for SBRT, the CT scan is performed minimum one week after fiducial implantation, for potential stabilization of the fiducials in the prostate [39, 41-44]. However, the CT simulation and SBRT treatment might be performed immediately after fiducials implantation [40, 45].

Sometimes, the hormone therapy is administered before SBRT to downsize the prostate gland [43]. This is in agreement with the clinical observation that the prostate gland decreases in size after radiotherapy. The stability of the markers is crucial for SBRT as IGRT accuracy is < 1mm. The variations of the intermarker distance because of the prostate shrinkage or fiducials migration may affect or induce errors in prostate repositioning and can lead to overdosage or underdosage of the organs [46].

2.4.4. Publication

A study was conducted to evaluate the stability of the markers in the prostate specifically when the hormone therapy is used. We describe below our results following the assessment of the intermarker distance of three gold markers. The evaluation was made for two groups of patients who received (5 patients) or not (5 patients) a hormone therapy before prostate irradiation. This paper was presented at the 52nd Annual ASTRO Meeting (October 31 – November 4, 2010) in San Diego (Appendix 4, *abstract number 3052*) [47] and published in 2013 in *Cancer Radiothérapie* [48].

Cancer/Radiothérapie 17 (2013) 215–220

Disponible en ligne sur SciVerse ScienceDirect www.sciencedirect.com

Elsevier Masson France EM|consulte www.em-consulte.com

Original article

Does hormone therapy modify the position of the gold markers in the prostate during irradiation? A daily evaluation with kV-images

L'hormonothérapie modifie-t-elle la position des grains d'or dans la prostate en cours d'irradiation ? Évaluation journalière par images de basse énergie (kV)

C. Udrescu[a,b], B. De Bari[a,1], O. Rouvière[c], A. Ruffion[d], G. Michel-Amadry[b], P. Jalade[b], M. Devonec[d], M. Colombel[e], O. Chapet[a,*]

[a] *Department of radiation oncology, centre hospitalier Lyon-Sud, hospices civils de Lyon, 165, chemin du Grand-Revoyet, 69495 Pierre-Bénite, France*
[b] *Department of medical physics, centre hospitalier Lyon-Sud, hospices civils de Lyon, 165, chemin du Grand-Revoyet, 69495 Pierre-Bénite, France*
[c] *Department of urologic radiology, hôpital Édouard-Herriot, hospices civils de Lyon, 5, place d'Arsonval, 69003 Lyon, France*
[d] *Department of urology, centre hospitalier Lyon-Sud, hospices civils de Lyon, 165, chemin du Grand-Revoyet, 69495 Pierre-Bénite, France*
[e] *Department of urology, hôpital Édouard-Herriot, hospices civils de Lyon, 5, place d'Arsonval, 69003 Lyon, France*

ARTICLE INFO

Article history:
Received 16 October 2012
Accepted 20 January 2013

Keywords:
Gold markers
Prostate repositioning
IGRT
Hormone therapy

ABSTRACT

Purpose. – Gold markers are frequently used for a better daily repositioning of the prostate before irradiation. The purpose of this work was to analyze if the combination of an androgen deprivation with the external irradiation could modify the position of the gold markers in the prostate.
Patients and methods. – Ten patients have been treated for a prostate cancer, using three implanted gold markers. The variations of the intermarker distances in the prostate were measured and collected on daily OBI® kilovoltage images acquired at 0° and 90°. Five patients had a 6-month androgen deprivation started before the external irradiation (H group) and five did not (NH group).
Results. – A total number of 1062 distances were calculated. No distance variation greater than 3.7 mm was seen between two markers, in any of the two groups. The median standard deviations of the daily intermarker distance differences were 0.7 mm (range 0.3–1.2 mm) for the H group and 0.6 mm (range 0.2–1.2 mm) for the NH group. The intermarker distances variations were noted as greater than –2 mm, between –2 mm and 2 mm and greater than 2 mm in 16.4, 83.4 and 0.2% for the H group and 1.3, 98.5 and 0.2% for the NH group, respectively.
Conclusion. – The distance variations remained less than 4 mm in both groups and for all the measurements. In the NH group, the variation of the distance between two markers remained below 2 mm in 98.5%. In the H group, the presence of a reduction of distance above 2 mm in 16.4% of measurements could indicate the shrinkage of the prostate volume.

Mots clés :
Marqueurs d'or
Repositionnement de la prostate
Radiothérapie guidée par l'image
Hormonothérapie.

RÉSUMÉ

Objectif de l'étude. – Les grains d'or sont fréquemment utilisés pour une meilleure localisation de la prostate à chaque séance d'irradiation. L'objectif de cette étude était d'analyser si l'association d'une hormonothérapie et de la radiothérapie pouvait modifier la position des marqueurs dans la prostate en cours de traitement.
Patients et méthodes. – Les images de basse énergie (kV) de dix patients, traités par irradiation avec repositionnement sur trois grains d'or pour un cancer de la prostate, ont été analysées. Les variations de distance entre les marqueurs ont été mesurées sur les deux images de basse énergie acquises chaque jour à 0° et à 90°. Cinq patients ont reçu une hormonothérapie de six mois associée à l'irradiation (groupe H) et cinq ont reçu une radiothérapie seule (groupe NH).

* Corresponding author.
E-mail address: olivier.chapet@chu-lyon.fr (O. Chapet).
[1] B. De Bari present address: Radiation Oncology Department, Spedali Civili di Brescia, Istituto del Radio O. Alberti, University of Brescia, Piazzale Spedali Civili 1, 25123 Brescia, Italy.

1278-3218/$ – see front matter © 2013 Published by Elsevier Masson SAS on behalf of the Société française de radiothérapie oncologique (SFRO).
http://dx.doi.org/10.1016/j.canrad.2013.01.015

Résultats. – Au total, 1062 distances ont été calculées entre marqueurs. Aucune variation de distance supérieure à 3,7 mm n'a été observée en cours de traitement dans les deux groupes. Les déviations standard des variations de distance entre les marqueurs ont été 0,7 mm (0,3–1,2 mm) en cas d'hormoradiothérapie et 0,6 mm (0,2–1,2 mm) en cas de radiothérapie exclusive. Les variations des variations de distance entre les marqueurs ont été notées supérieures à –2 mm, entre –2 et 2 mm et supérieures à 2 mm dans 16,4, 83,4 et 0,2 % en cas d'hormoradiothérapie et 1,3, 98,5 et 0,2 % en cas de radiothérapie exclusive.
Conclusion. – La réduction des distances restait inférieure à 4 mm dans les deux groupes pour toutes les mesures. Pour le groupe exclusivement irradié, la variation de distances entre deux marqueurs restait inférieure à 2 mm dans 98,5 %. Dans le groupe H, la présence d'une réduction de distance supérieure à 2 mm dans 16,4 % de mesures pourrait signifier une diminution du volume prostatique.

1. Introduction

The high conformity of the dose to the target volume, which is expected during the irradiation of prostate cancer, requires a great level of precision for the localization and the repositioning of this organ [1–6].

The intraprostatic gold markers are frequently implanted for a better daily repositioning of the prostate before and also during the irradiation [7–13]. They could improve the prostate localization and allow a reduction of the planning target volume (PTV) margins [14–16]. However, any reduction of the PTV could be conditioned by the risk of markers migration throughout the course of treatment. Sometimes, the patients have a hormonal therapy before or during radiotherapy [17,18]. Several studies evaluated the intraprostatic markers stability for patients receiving [19–22], or not, a hormone therapy [10,19–25]. However, none of these studies evaluated the impact of the hormone therapy on the position of the markers using daily kV-images throughout the whole course of the treatment. Hence, the purpose of this study was to assess if the variations of the intraprostate gold seeds positions could be influenced by the combination of an androgen deprivation with the irradiation.

2. Patients and methods

2.1. Patients

Ten patients have been treated by exclusive irradiation for low- or intermediate-risk prostate cancer (according to the D'Amico classification). The total dose was of 74–76 Gy (2 Gy daily fraction), delivered by image-guided irradiation. Five patients received a neoadjuvant hormone therapy (6 months of androgen deprivation), started during the week preceding the first session of radiotherapy. Details regarding the patients' stage and prostate characteristics are presented in Table 1. The daily patient repositioning was made in the supine position, using specific prostate cradle for knee and leg immobilization (Civco Medical Solutions).

2.2. Gold markers implantation technique

Three porous gold markers (Eckert and Ziegler Bebig) were implanted into the prostate by an urologist surgeon (AR and MD) or a radiologist (OR). The implantation technique was similar to biopsies, transrectally under ultrasound guidance and using three 17 G (gauge) needles. The markers were 3 mm long and 1.2 mm thick and were implanted in triangle: one at the base on the right side of the urethra (M1), one at the middle left laterally (M2) and the third one at the apex, on the right side of the urethra (M3). They were used for image fusions (between the T2-MRI exam and the dosimetric computed tomography scan) and for daily repositioning of the prostate before irradiation.

2.3. Image acquisition

The patients underwent a CT scan simulation (GE LightSpeed® RT16 CT scan) with a slice thickness of 2.5 mm. Digitally reconstructed radiographs (DRRs) were then created.

For each patient, two kV-images (pixel size of the image = 0.02 cm) were performed before each fraction at 0° (anterior) and 90° (left lateral) on an OBI® system from Varian Medical Systems, Inc. The total irradiation dose delivered to one patient by the kV-images was of 0.22 Gy.

2.4. Statistical analysis

The analysis of the seeds displacements was made by the same operator (CU) using an offline image software (Offline Review®, Varian Medical Systems, Inc.). The size and the center of each marker were precisely defined. The coordinates of the centers of two markers, M1 and M2, were measured on both kV-images (x, y and z axes) from the center of the M3 marker (coordinates: 0, 0, 0) (Figs. 1 and 2). This marker (M3) was constantly used as reference, for all kV-images. The distances between the markers were extrapolated from the coordinates of these three markers using the formula:

$$D_{ij} = \sqrt{\left(x_j - x_i\right)^2 + \left(y_j - y_i\right)^2 + \left(z_j - z_i\right)^2}$$

The values in millimeters were recorded and analyzed in order to assess the time related to any distance variation, in the whole

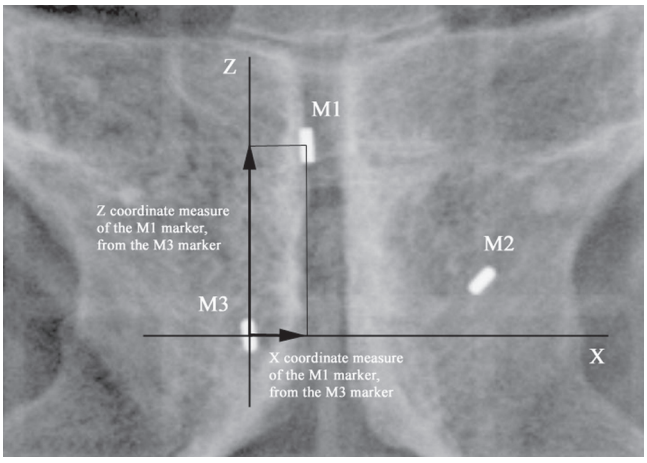

Fig. 1. Example of an anterior OBI kV-image. The M3 marker was chosen as reference $(x, y, z) = (0, 0, 0)$ for all the images. The coordinates x and z of the other two markers were measured on the anterior acquisition.
Exemple d'image de basse énergie avec l'OBI (On-Board Imager) de face. Le marqueur M3 a été choisi comme référence (x, y, z) = (0, 0, 0) pour toutes les images. Les coordonnées x et z des deux autres marqueurs ont été mesurées sur les acquisitions de face.

Table 1
Details regarding the prostate cancer stage of the patients.
Caractéristiques des tumeurs prostatiques par patient.

Patient	Hormone therapy	Gleason Score	PSA (ng/mL)	Prostate T stage	Prostate volume (cm^3)
1	No	7 (3+4)	3.5	T2a N0M0	32.3
2	No	7 (3+4) grade 4 at 20%	8.9	T1c N0M0	44.7
3	No	7 (3+4)	7.8	T1c N0M0	62.7
4	Yes	7 (4+3) grade 4 at 70%	16, 17	T1c N0M0	56.4
5	Yes	7 (4+3) grade 4 at 80% grade 3 at 20%	8	T1c N0M0	52.5
6	No	7 (3+4)		T1c N0M0	100.4
7	Yes	7 (4+3) grade 4 at 60%	4.66	T1c N0M0	51.7
8	Yes	7 (4+3) grade 4 at 70%	4.5	T1c N0M0	41.4
9	No	6 (3+3)	11.89	T1c N0M0	36.9
10	Yes	7 (3+4)	11.94	T1c N0M0	48.6

population. This analysis was made for both groups: the hormone (H) and the non-hormone (NH), as follows:

- a general analysis of all the distances between markers was made and the distance variations were presented as: significant reduction of the distances (> –2 mm), significant increase of the distances (> 2 mm) and non-significant variation of the distances (–2 mm to 2 mm). Because of the uncertainties in image definition and distance measurement, we considered that the variations less than 2 mm are not important. The results are presented in percentages;
- the intermarker distance variations throughout the treatment time were analyzed and the mean ± standard deviations were noted as well. The daily differences of the intermarker distances from the first day to the end of the treatment were calculated and plotted in a histogram, as also described earlier by Dehnad et al. [26];
- the initial distance (i_5D) value between two markers was defined as the mean distance measured from the first five kV-pairs and the final distance (f_5D) value was noted as the mean distance calculated from the last five kV-pairs. For each patient, a distance variation (D_5var) between two markers was thereby obtained by subtraction of the final mean value from the initial one ($D_5\text{var} = f_5D - i_5D$).

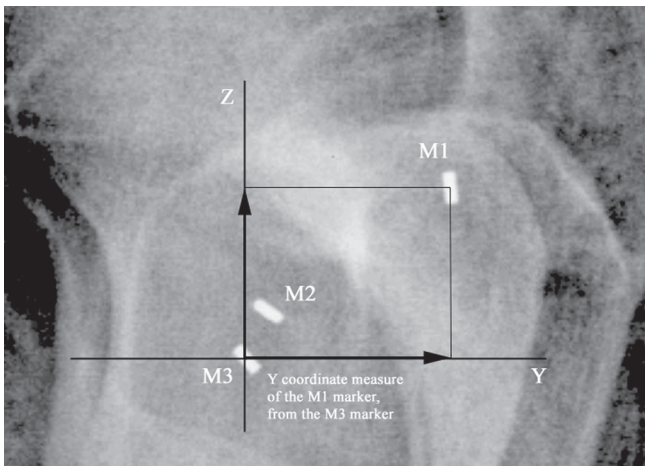

Fig. 2. Example of a left lateral OBI kV-image. The M3 marker was chosen as reference $(x, y, z) = (0, 0, 0)$ for all the images. The y coordinates of the other two markers were measured on the lateral acquisition.
Exemple d'image de basse énergie avec l'OBI (On-Board Imager) de profil. Le marqueur M3 a été choisi comme référence (x, y, z) = (0, 0, 0) pour toutes les images. Les coordonnées y des deux autres marqueurs ont été mesurées sur les acquisitions de profil.

3. Results

The implantation of the gold markers was easily made under local anesthesia. A total number of 758 images were acquired for this study and 708 out of 758 images were available for analysis, corresponding to 354 kV-pairs (0° and 90°). Fifty images couldn't be evaluated due to technical problems (for patients nº 2, 8 and 10). A total of 1062 distances were thereby calculated for all the patients and all the marker pairs. The mean number of kV-pairs available for analysis per patient was 35 (range 25–39).

3.1. General analysis of the distance variations between the markers

Among the 1032 daily variations measured, 940 (91.1%) remained less than ± 2 mm. An increase of the distance (greater than 2 mm) was observed on two (0.2%) measurements, which did not exceed 2.7 mm. A decrease of distance greater than –2 mm was noted on 90 (8.7%) measurements with a maximum value of –3.7 mm.

The daily intermarker distance variations for the two groups separately were: 507/1032 intermarker distance variations for the H group and 525 out of 1032 intermarker distance variations for the NH group. These variations were greater than –2 mm, between –2 mm and 2 mm and greater than 2 mm in 16.4, 83.4 and 0.2% for the H group and 1.3, 98.5 and 0.2% for the NH group, respectively.

3.2. Daily intermarker distance variations during the treatment and the impact of hormone therapy

The mean standard deviations of the daily intermarker distance differences were 0.7 mm (range 0.3–1.2 mm) for the hormone group and 0.6 mm (range 0.2–1.2 mm) for the non-hormone group. Performing a linear regression analysis, for the H group in all 15 intermarker distance s, the slope significantly differed from zero ($P < 0.001$) and the slope coefficient was negative for all these distances, showing a decrease of the intermarker distances during the treatment. In the NH group, 4/15 intermarker distances had a positive slope coefficient (increased distance between markers), which did not significantly differed from zero ($P = 0.308$). For the 11 remaining intermarker distance s, significant negative slope coefficient was noted ($P < 0.005$).

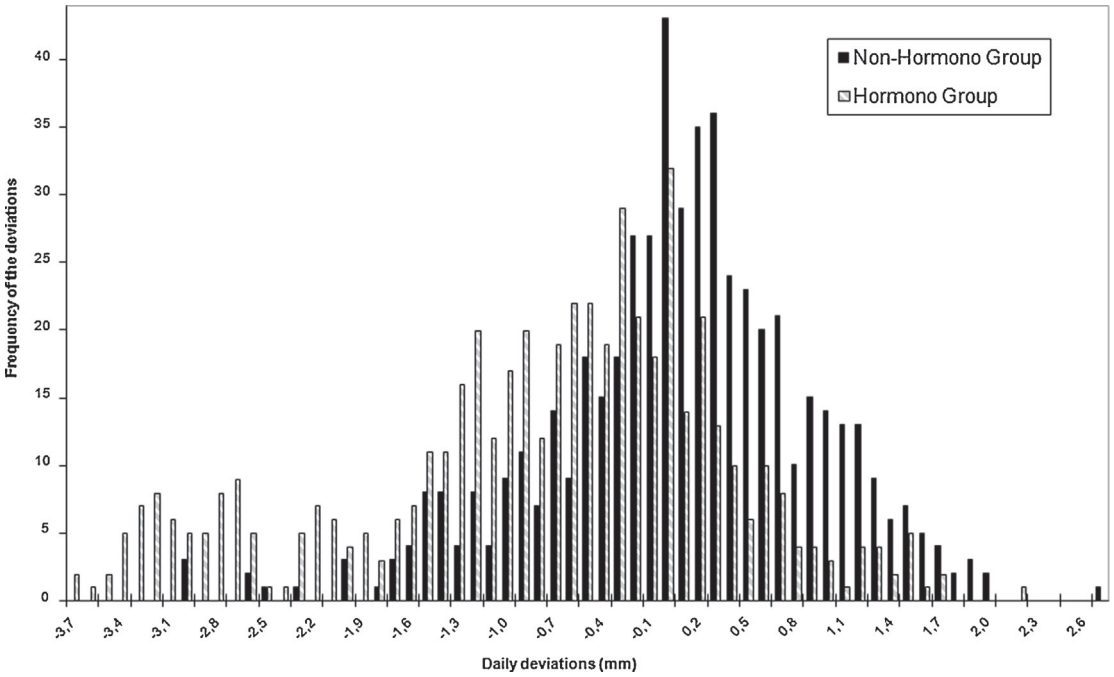

Fig. 3. Frequencies of the daily intermarker distance deviations of the hormone and no-hormone groups of patients.
Fréquence de variation journalière entre marqueurs pour les groupes de patients avec et sans hormonothérapie.

The daily intermarker distance variations were grouped as well in a histogram that shows the frequency of the deviations (Fig. 3). The distance between two markers seems to decrease more in the H group than in the NH group.

3.3. Analysis of the D5var (from the first five to the five last measurements)

The D_5var values between two seeds are presented in Table 2. For the hormone-therapy group, only reductions of the D_5var values were observed and no increase in distances was seen. The mean value of all the D_5vars for this group was –1.55 mm, with a minimum variation of –0.2 mm and a maximum of –3.1 mm. For the non-hormone group, reductions were noted, but also four non-significantly increased values. The mean value of all the D_5vars for this group was –0.76 mm, with a minimum variation of 0.9 mm and a maximum of –3.3 mm.

4. Discussion

The present study evaluates the variations of the distances between markers in two groups of patients (with and without neoadjuvant androgen deprivation) treated for a prostate cancer with exclusive irradiation. The present work used OBI® kV-images at 0° and 90° from the first to the last day of the treatment. Taking into account the pixel size of the image which is of 0.02 cm and the measurement accuracy, only the variations greater than –2 mm and greater than 2 mm were considered important.

Several studies previously analyzed the migration of the fiducials in the prostate. Among these studies, one attempted the effect of the hormone therapy on the markers position into the prostate [21]. In 2003, Pouliot et al. studied the migration of three gold markers using an a-Si electronic portal imaging device (EPID) [21]. Daily images were acquired during the first week and weekly thereafter. The average standard deviation of the distances between two markers was 1.3 mm and three out of 11 patients showed a standard deviation larger than 2 mm. All three patients had received neoadjuvant hormone therapy. The major distance reduction observed was of 6 mm over 52 days during the treatment. No significant migration was noted for all the patients but for the last three ones a correlation with shrinkage of the prostate was made. They concluded that the use of three markers is an important tool to monitor the prostate position and volume changes that can occur over time due to the hormone or radiation therapy. Further studies did not evaluate the impact of hormone therapy on markers position variations, but they all showed a negligible to minimal markers migration, using different methods of measurements [10,25].

In the present study, data were collected on the variations of intermarker distances between three implanted gold markers on a daily basis throughout the treatment. Five patients had a hormone therapy and five did not. The impact of the hormone therapy on markers variation positions was questioned and analyzed using daily intermarker distance variations. This reduction did not exceed 3.7 mm and remained below 2 mm in 83.4% of the measurements. A significant reduction of distance (> –2 mm) was more frequently observed in the H group than in the NH group (16.4% vs 1.3%, *P*-value = 0.0001). Between the first five and the last five measurements, the variation of distance between two seeds always remains below 3.3 mm, but was significant in the H group than in the NH group (*P*-value = 0.045), with an average of –1.55 mm and –0.76 mm, respectively. Helou et al. described, in a series of 138 patients, that the hormone treatment started before the radiotherapy course will reduce the prostates volume [27]. A mean of 3.8 months of hormone treatment was necessary to obtain a mean reduction of prostate volume of 20.5%. Sanguineti et al. confirmed these results and showed approximately 15% mean prostate gland reduction during the course of radiotherapy when the planning CT is performed within 3 months from neoadjuvant androgen deprivation. With longer time intervals between the neoadjuvant androgen deprivation and the planning CT, the prostate gland volume changes are less important, on average. Therefore, the authors allow 2 to 3 months between the neoadjuvant androgen deprivation and the planning CT for prostate cancer patients [22]. In the current study, when an androgen deprivation is combined with

Table 2
D_5var and statistical parameters of the daily intermarker distances, for the H and NH groups.
D_5var et paramètres statistiques des variations de distance entre les marqueurs journalières pour les groupes avec et sans hormonothérapie.

Patient	Distance	Slope coefficient	*P*	Standard deviation (mm)	D_5var (mm)
Hormone therapy					
4	M1M2	−0.0042	< 0.001	0.5	−1.5
	M2M3	−0.0093	< 0.001	1.1	−3.1
	M3M1	−0.0084	< 0.001	1.0	−2.9
5	M1M2	−0.0056	< 0.001	0.7	−1.6
	M2M3	−0.002	0.01	0.5	−0.2
	M3M1	−0.0043	< 0.001	0.6	−1.1
7	M1M2	−0.0048	< 0.001	0.6	−1.5
	M2M3	−0.0098	< 0.001	1.1	−2.9
	M3M1	−0.0108	< 0.001	1.2	−3.0
8	M1M2	−0.0032	< 0.001	0.5	−1.0
	M2M3	−0.0035	< 0.001	0.4	−1.0
	M3M1	−0.0032	< 0.001	0.5	−0.8
10	M1M2	−0.0059	0.001	0.7	−0.9
	M2M3	−0.0023	0.004	0.3	−0.4
	M3M1	−0.0063	< 0.001	0.7	−1.1
No hormone					
1	M1M2	−0.0098	< 0.001	1.2	−3.3
	M2M3	−0.0067	< 0.001	0.9	−1.9
	M3M1	−0.0031	0.001	0.6	−0.7
2	M1M2	−0.0017	0.004	0.3	−0.4
	M2M3	0.00036	0.443	0.2	0.03
	M3M1	−0.0021	0.031	0.5	−0.4
3	M1M2	−0.0045	< 0.001	0.6	−1.3
	M2M3	−0.0056	< 0.001	0.7	−1.6
	M3M1	−0.0045	< 0.001	0.6	−1.3
6	M1M2	0.0017	0.007	0.4	0.9
	M2M3	−0.001	0.011	0.3	−0.3
	M3M1	0.00055	0.411	0.4	0.5
9	M1M2	0.00094	0.371	0.6	0.2
	M2M3	−0.0028	< 0.001	0.5	−1.2
	M3M1	−0.0024	0.007	0.6	−0.7

H group: patients receiving hormone therapy; NH group: exclusive radiotherapy.

the irradiation treatment, a significant reduction of the distances between the markers is observed along the irradiation. Based on Sanguineti et al. and Helou et al. results, the present reduction may be linked to the shrinkage of the prostate volume. However, there was no difficulty in repositioning the prostate on the three gold markers.

5. Conclusion

Analysis of daily orthogonal OBI kV-images showed that the variation of the distance between two seeds remained below 3.7 mm throughout the treatment. In the hormone therapy group, the daily trend data confirmed gradual reduction of all intermarker distance s, which may be linked to a prostate shrinkage. As this reduction remained less than a few millimeters, it should not affect the prostate repositioning. In our department we will continue to use this repositioning method for the standard prostate image-guided and hypofractionated radiotherapy.

Disclosure of interest

The authors declare that they have no conflicts of interest concerning this article.

References

[1] Chiavassa S, Brunet G, Gaudaire S, Munos-Llagostera C, Delpon G, Lisbona A. Radiothérapie conformationnelle avec modulation d'intensité : analyse des résultats des contrôles précliniques, expérience du centre René-Gauducheau. Cancer Radiother 2011;15:265–9.
[2] Cazoulat G, Lesaunier M, Simon A, Haigron P, Acosta O, Louvel G, et al. De la radiothérapie guidée par l'image à la radiothérapie guidée par la dose. Cancer Radiother 2011;15:691–8.
[3] Delpon G, Llagostera C, Le Blanc M, Rio E, Supiot S, Mahé MA, et al. Quelle radiothérapie guidée par l'image pour quels patients ? Expérience concomitante de l'utilisation de trois dispositifs d'imagerie de repositionnement dans le cas du cancer de la prostate. Cancer Radiother 2009;13:399–407.
[4] Dudouet P, Boutry C, Mounié G, Latorzeff I, Thouveny F, Redon A. Système d'imagerie par tomographie conique de basse énergie (kV) de Varian : expérience de Montauban. Cancer Radiother 2009;13:375–83.
[5] Jouyaux F, de Crevoisier R, Manens J-P, Bellec J, Cazoulat G, Haigron P, et al. Haute dose dans la prostate par radiothérapie guidée par l'image : apport de l'arcthérapie avec modulation d'intensité du faisceau. Cancer Radiother 2010;14:679–89.
[6] Pommier P, Morelle M, Perrier L, de Crevoisier R, Laplanche A, Dudouet P, et al. Évaluation économique prospective de la radiothérapie guidée par l'image des cancers de la prostate dans le cadre du programme national de soutien aux thérapeutiques innovantes et coûteuses. Cancer Radiother 2012;16:444–51.
[7] van Haaren PMA, Bel A, Hofman P, van Vulpen M, Kotte ANTJ, van der Heide UA. Influence of daily setup measurements and corrections on the estimated delivered dose during IMRT treatment of prostate cancer patients. Radiother Oncol 2009;90:291–8.
[8] Kron T, Thomas J, Fox C, Thompson A, Owen R, Herschtal A, et al. Intrafraction prostate displacement in radiotherapy estimated from pre- and post-treatment imaging of patients with implanted fiducial markers. Radiother Oncol 2010;95:191–7.
[9] Kudchadker R, Lee AK, Yu ZH, Johnson JL, Zhang L, Zhang Y, et al. Effectiveness of using fewer implanted fiducial markers for prostate target alignment. Int J Radiat Oncol Biol Phys 2009;74:1283–9.
[10] Kupelian PA, Willoughby TR, Meeks SL, Forbes A, Wagner T, Maach M, et al. Intraprostatic fiducials for localization of the prostate gland: monitoring intermarker distances during radiation therapy to test for marker stability. Int J Radiat Oncol Biol Phys 2005;62:1291–6.
[11] Logadóttir A, Korreman S, Petersen PM. Comparison of the accuracy and precision of prostate localization with 2D-2D and 3D images. Radiother Oncol 2011;98:175–80.
[12] Moman MR, van der Heide UA, Kotte ANTJ, van Moorselaar RJA, Bol GH, Franken SPG, et al. Long-term experience with transrectal and transperineal implantations of fiducial gold markers in the prostate for position verification in external

beam radiotherapy; feasibility, toxicity and quality of life. Radiother Oncol 2010;96:38–42.
[13] Shirato H, Harada T, Harabayashi T, Hida K, Endo H, Kitamura K, et al. Feasibility of insertion/implantation of 2.0-mm-diameter gold internal fiducial markers for precise setup and real-time tumor tracking in radiotherapy. Int J Radiat Oncol Biol Phys 2003;56:240–7.
[14] Gauthier I, Carrier JF, Béliveau-Nadeau D, Fortin B, Taussky D. Dosimetric impact and theoretical clinical benefits of fiducial markers for dose escalated prostate cancer radiation treatment. Int J Radiat Oncol Biol Phys 2009;74:1128–33.
[15] Lerma FA, Liu SZ, Liu B, Li H, Yi B, Amin P, et al. Image guided intermediate-stage prostate cancer IMRT: minimum margins and an ideal alignment strategy [Abstract]. Int J Radiat Oncol Biol Phys 2008;72:S565.
[16] Madsen BL, Hsi RA, Pham HT, Presser J, Esagui L, Corman J, et al. Intrafractional stability of the prostate using a stereotactic radiotherapy technique. Int J Radiat Oncol Biol Phys 2003;57:1285–91.
[17] Edelman S, Liauw SL, Rossi PJ, Cooper S, Jani AB. High-dose radiotherapy with or without androgen deprivation therapy for intermediate-risk prostate cancer: cancer control and toxicity outcomes. Int J Radiat Oncol Biol Phys 2012;83:1473–9.
[18] Quon H, Cheung PCF, Loblaw DA, Morton G, Pang G, Szumacher E, et al. Hypofractionated concomitant intensity-modulated radiotherapy boost for high-risk prostate cancer: late toxicity. Int J Radiat Oncol Biol Phys 2012;82:898–905.
[19] He TT, Tanyi J, Laub W, Hung A. Effect of concurrent hormone therapy on the positional stability of electromagnetic transponders implanted in the prostate [Abstract]. Int J Radiat Oncol Biol Phys 2010;78:S700.
[20] King BL, Butler WM, Merrick GS, Kurko BS, Reed JL, Murray BC, et al. Electromagnetic transponders indicate prostate size increase followed by decrease during the course of external beam radiation therapy. Int J Radiat Oncol Biol Phys 2011;79:1350–7.
[21] Pouliot J, Aubin M, Langen KM, Liu YM, Pickett B, Shinohara K, et al. (Non)-migration of radiopaque markers used for on-line localization of the prostate with an electronic portal imaging device. Int J Radiat Oncol Biol Phys 2003;56:862–6.
[22] Sanguineti G, Marcenaro M, Franzone P, Foppiano F, Vitale V. Neoadjuvant androgen deprivation and prostate gland shrinkage during conformal radiotherapy. Radiother Oncol 2003;66:151–7.
[23] Delouya G, Carrier JF, Béliveau-Nadeau D, Donath D, Taussky D. Migration of intraprostatic fiducial markers and its influence on the matching quality in external beam radiation therapy for prostate cancer. Radiother Oncol 2010;96:43–7.
[24] Nichol AM, Brock KK, Lockwood GA, Moseley DJ, Rosewall T, Warde PR, et al. A magnetic resonance imaging study of prostate deformation relative to implanted gold fiducial markers. Int J Radiat Oncol Biol Phys 2007;67:48–56.
[25] Poggi MM, Gant DA, Sewchand W, Warlick WB. Marker seed migration in prostate localization. Int J Radiat Oncol Biol Phys 2003;56:1248–51.
[26] Dehnad H, Nederveen AJ, van der Heide UA, van Moorselaar RJA, Hofman P, Lagendijk JJW. Clinical feasibility study for the use of implanted gold seeds in the prostate as reliable positioning markers during megavoltage irradiation. Radiother Oncol 2003;67:295–302.
[27] Helou J, Nasr E, Nasr DN, Fares A, Elie N, Maroun M, et al. Réduction du volume prostatique par hormonothérapie avant radiothérapie conformationnelle pour cancer de la prostate [Abstract]. Cancer Radiother 2009;13:684.

2.4.5. Conclusion

The stability of the gold markers was demonstrated for long radiotherapy duration. The distance variations remained below 2 mm in 98.5% of measurements when radiotherapy alone was delivered and didn't reduce the repositioning accuracy. If the hormone therapy is administrated in combination with the radiotherapy, the shrinkage of the prostate might occur. However, for a short SBRT irradiation duration, these small distance variations should not affect the target repositioning.

2.5. Setup margin definition: Image-guided radiotherapy and intrafraction motion

2.5.1. IGRT for prostate SBRT

The image guidance is a prerequisite for SBRT and must be used to improve the spatial accuracy of the delivered dose. The accuracy of the currently available IGRT techniques intended for SBRT allowed a diminution of the planning margins between 0 mm and 5 mm [38-45]. The patients treated in these studies have benefited of daily repositioning with MV or kV images with proper position of the markers, or real-time tracking of implanted fiducials with automatic beam adjustment carried out by the CyberKnife® system (Table 2.1).

Moreover, various existing radiation units meet the rigorous localization requirements for SBRT. As shown in Table 2.2, the most common units have different imaging capabilities that have been used for SBRT (lung, liver, etc.). The real-time target monitoring and/or the positioning and motion correction before or during delivery are mandatory for SBRT.

Table 2.2. Characteristics of several standard radiation units appropriate for SBRT.

Radiation unit and company	**Image guidance**
CyberKnife, Accuray	Two fixed pairs x-ray source-detector; simultaneous imaging
Trilogy, Varian	Two rotating kV pairs x-ray source-detector for fixed planar views and kV-CBCT
Novalis, BrainLab	Two fixed pairs x-ray source-detector; sequential imaging, and CBCT
SynergyS, Elekta	Rotating kV x-ray for fixed planar views and kV-CBCT

CBCT = Cone Beam Computed Tomography; kV=kilovoltage

In our department, two devices are available for SBRT-IGRT: On Board Imager (OBI) from Varian and ExacTrac® (ET) system from BrainLAB. The characteristics of the two systems are illustrated in Table 2.3.

Table 2.3. Characteristics of the OBI® and the ExacTrac® systems.

	OBI® (Varian)	**ExacTrac® (BrainLAB)**
Acquisition type	2D/3D (kV image/CBCT)	2D (kV image)
Dose	≈ 3 mGy/image ≈ 20 mGy/CBCT	≈ 1-2 mGy/image
Advantage	2D and 3D modes	Image quality Real-time monitoring (Snap Verification)
Disadvantage	Real-time tracking	2D mode only

2.5.1.1. The On Board Imager® system, Varian

The OBI kV imaging system provides improved tumor targeting using high-resolution and low-dose digital images. The patient control and target movement are possible before and during the treatment with digital kilovoltage (kV) radiography and/or cone-beam CT (CBCT).

The OBI uses two robotically-controlled arms that work with three axes of motion, optimizing the positioning of the imaging system for the best possible view of the target (Figure 2.2). Thus, it consists of a kV X-ray source (kVS) and an amorphous silicon kV panel that has the role of detector (kVD). The OBI allows for simultaneous acquisitions of MV and kV radiographic pairs without gantry rotation. The therapists may acquire either a pair of radiographs (kV/kV or MV/kV pair) or a CBCT scan. The verification can be done by using bony anatomy or implanted radiopaque markers in paired images, or by visualizing soft-tissue and bony anatomy in cone-beam CT images. The OBI images can be register with the reference image depending on the verification modality (kV radiographs, DRRs, or planning CT scans). An accurate quality assurance program has to be applied for each IGRT device. Therefore, a protocol has been proposed in our department in 2008 for the quality control of the OBI. The protocol is presented in Appendix 5 and it is applied monthly or weekly as described by the SBRT recommendations.

The use of CBCT for prostate radiotherapy is important in order to locate the isocentre of the target, but also to identify the critical cases where repletion of rectum and bladder is not conforming to the initial scan. Recently, Voyant *et al.* found that CT acquisition during the treatment (scanner or CBCT) describes an increase or decrease of repletion. They recommend that if the change is out of the 95% interval, it is decided to redo the dosimetry [49]. This aspect is even critical for SBRT, for which the overdosage of the organs at risk may lead to high toxicity. Wang *et al.* compared two-dimensional (2D) orthogonal kV with three-

dimensional (3D) cone-beam CT (CBCT) for target localization and assessed intrafraction motion with kV images in patients undergoing SBRT. After the localization based on superficial markings in patients undergoing SBRT, orthogonal kV imaging detected setup variations of approximately 3 to 4 mm in each direction and subsequently, CBCT detected residual setup variations of approximately 2 to 3 mm [50].

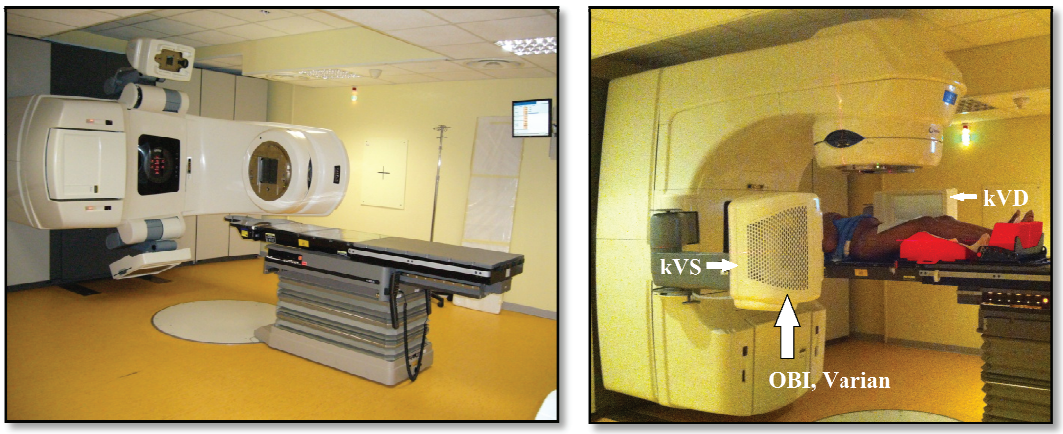

Figure 2.2. The OBI® system, Varian.

2.5.1.2. The ExacTrac® X-ray repositioning system, BrainLab

The ExacTrac® system is installed in one of our treatment rooms since 2007. Two stereoscopic images can be acquired sequentially with ET X-ray system. These images are produced by two kilovoltage X-ray tubes inserted into the floor together with two ceiling mounted amorphous silicon flat panels. The image acquisition takes a couple of seconds per tube and another 2-3 seconds to change from tube 1 to tube 2. The system software then fuses the acquired images with digitally reconstructed radiographs created from the planning CT. As a result, vertical, longitudinal, and lateral displacements of the table, as well as couch angles (table, longitudinal and lateral) are calculated by the software. Online corrections can be made, depending on the ability of the table to perform only translational movements or translational and rotational. The particularity of ExacTrac system compared to OBI is that repositioning of the target can be done using six-degrees of freedom (6D).

Two choices related to the fusion are available: fusion according to bony anatomy or fusion based on markers. It allows quantitative displacement of the CTV, relative to the planning CT, when using implanted gold markers.

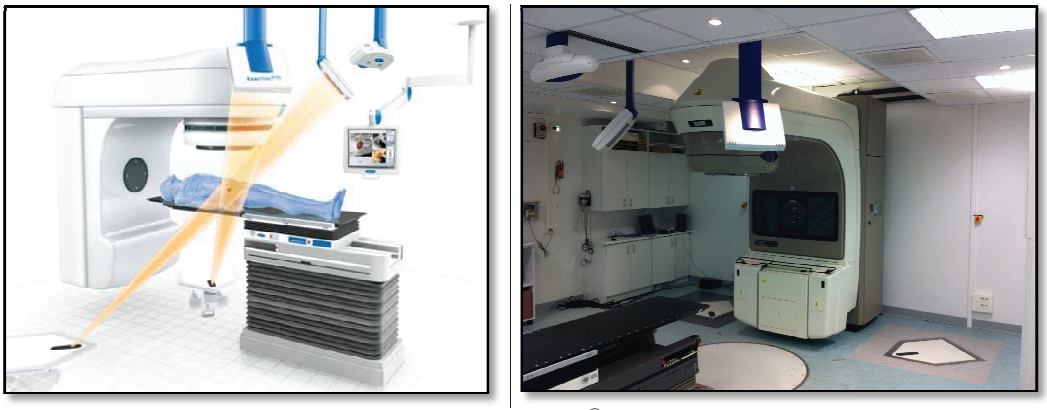

Figure 2.3. The ExacTrac® system, BrainLab.

2.5.2. Monitoring of intrafraction motion

2.5.2.1. Random prostate motion

The time between images that account for setup margins and the beginning of irradiation may be long, sometimes up to 5 minutes. Thereby intrafraction motion is one of the main issue limiting PTV margin diminution for prostate SBRT [18, 51, 52]. This time could be reduced when automatic seed matching and robotic table are used. However, during this time intrafractional motion of the prostate is essentially related to random repletion of bladder and rectum. If displacement variations are important, the patient dosimetry must be created again or corrected. The *intrafraction motion* of the prostate has already been reported by several teams [22, 34, 35]. The results of these studies described that motion of the prostate greater than 1 cm occurs at various frequencies [35, 53] and that sometimes can last more than 1 minute. This aspect may have an impact on irradiation treatment and important dosimetric consequences [17, 22, 32, 54, 55].

Indeed, a recent article was published concerning the dosimetric uncertainties related to the elasticity of bladder and rectal wall [49]. Voyant *et al*. described their experience with 54 patients treated for prostate cancer with full bladder and empty rectum. The patients had two CT scans (one for treatment simultation and the second one before treatment) and the authors showed that the bladder volume was dramatically reduced by 50% on the second CT scan. They noted that the use of the cone-beam computed tomography scan is relevant to position the isocenter of the prostate and also to identify the cases when repletion is not conforming to the initial scan [49].

Therefore, a stereotactic irradiation needs setup precision and volumetric image guidance that allow accurate localization of soft tissue targets or surrogates (e.g. fiducials). The ExacTrac® system installed in the Department of Radiation Oncology from Lyon Sud

Hospital integrates a Snap Verification® tools created to control the position of the target volume before or during irradiation.

2.5.2.2. Snap Verification®

As the position of the patient is tracked (through body markers or reference device), it's possible to generate the corresponding DRRs. Once the X-ray correction has been made, single X-ray images can be acquired. These images can be acquired at any time during the treatment in order to verify the repositioning precision at that instant. If a greater precision is needed with snap verification, then both X-ray tubes have to be used individually. The snap verification is based on a rigid 2D image fusion and provides only in-plane shift information without rotations (for both implanted and bony fusion). After the acquisition of SV, the DRRs and X-ray images are fused (could be bone or marker-based fusion) and the fusion results will define the position of the patient's isocenter. The results of the 2D fusion are an in-plane deviation in the isocenter plane (perpendicular to flat panels). For example, if the correction has been initially calculated from a fusion based on markers, a tolerance value will be indicated and we have to check that the isocenter of the accelerator and the isocenter of the target are matched exactly in the same position. As the snap verification is based only on one image, a 2D correction is available.

2.5.3. Publication

Consequently, we initiated a study to assess the efficacy of the Snap Verification tool for the real-time detection of intrafraction motion for large SBRT fractions. Our former results were obtained for lung cancer patients with repositioning on bony anatomy, as this was our first SBRT experience with this device. In our department the ET-SV system is mounted on a single energy (6MV) beam accelerator and therefore, the prostate patients are so far treated on a different linear accelerator (with OBI-IGRT verification).

The initial results for the verification of intrafraction lung motion with ET-SV were presented at the 51st Annual ASTRO Meeting (November 1-5, 2009) in Chicago (Appendix 6, *abstract number 2954*) [56]. This work was also published in 2013 in the *International Journal of Radiation Oncology Biology Physics* and is presented below [57].

International Journal of
Radiation Oncology
biology • physics

www.redjournal.org

Physics Contribution

ExacTrac Snap Verification: A New Tool for Ensuring Quality Control for Lung Stereotactic Body Radiation Therapy

Corina Udrescu, MS, Francoise Mornex, MD, PhD, Ronan Tanguy, MD, and Olivier Chapet, MD, PhD

Department of Radiation Oncology, Centre Hospitalier Lyon Sud, Pierre Benite, France

Received Nov 21, 2011, and in revised form Sep 13, 2012. Accepted for publication Sep 16, 2012

Summary

Intrafraction patient verification for lung stereotactic body radiation therapy involves precise imaging systems for tracking possible tumor motions, even during irradiation, and eventually for realigning the target throughout the treatment session, if displacements are found. A study of 20 patients showed ExacTrac X-ray 6D Snap Verification tool gives accurate targeting before and during irradiation, from the beginning to the end of each fraction. This could raise confidence to escalate the dose.

Purpose: The intrafraction verification provided by ExacTrac X-ray 6D Snap Verification (ET-SV) allows the tracking of potential isocenter displacements throughout patient position and treatment. The aims of this study were *(1)* to measure the intrafraction variations of the isocenter position (random errors); *(2)* to study the amplitude of the variation related to the fraction duration; and *(3)* to assess the impact of the table movement on positioning uncertainties.

Methods and Materials: ET-SV uses images acquired before or during treatment delivery or both to detect isocenter displacement. Twenty patients treated with stereotactic body radiation therapy (SBRT) for lung tumors underwent SV before or during each beam. Noncoplanar beams were sometimes necessary. The time between the setup of the patient and each SV was noted, and values of deviations were compiled for 3 SV time groups: SV performed at $\leq$10 min (group 1), between 11 and 20 min (group 2), and $\geq$21 min (group 3). Random errors in positioning during the use of noncoplanar fields were noted.

Results: The mean isocenter deviation $\pm$SD was 2 $\pm$ 0.5 mm (range, 1-8 mm). The average deviations $\pm$SD increased significantly from 1.6 $\pm$ 0.5 mm to 2.1 $\pm$ 0.8 mm and 2.2 $\pm$ 0.6 mm for groups 1, 2, and 3 ($P = .002$), respectively. Percentages of deviation $\geq$3 mm were 7.06%, 22.83%, and 28.07% and 1.08%, 4.15%, and 8.4% for $\geq$5 mm ($P < .0001$). For 11 patients, table rotation was necessary. The mean isocenter deviation $\pm$SD increased significantly from 1.9 $\pm$ 0.5 mm before table rotation to 2.7 $\pm$ 0.5 mm ($P = .001$) for the first beam treated after rotation.

Conclusions: SV detects isocenter deviations, which increase in amplitude and frequency with the fraction duration, and enables intrafraction verification for SBRT (taking into account clinical condition and technical issues). SV gives accurate targeting at any time during irradiation and may raise confidence to escalate the dose. SV appears to be an important tool for ensuring the quality control of SBRT.

Reprint requests to: Pr. Françoise Mornex, Département de Radiothérapie-Oncologie, Centre Hospitalier Lyon Sud, Chemin du Grand Révoyet, 69495, Pierre Benite Cedex, France. Tel: 33 4 78 86 42 53; Fax: 33 4 78 86 42 65; E-mail: francoise.mornex@chu-lyon.fr

Int J Radiation Oncol Biol Phys, Vol. 85, No. 1, pp. e89–e94, 2013
0360-3016/$ - see front matter
http://dx.doi.org/10.1016/j.ijrobp.2012.09.020

Conflict of interest: none.

Acknowledgment—The authors thank Dr Berardino de Bari for help and pertinent discussions during his residency and Geraldine Michel-Amadry, physicist in our department.

Introduction

Over the past few decades, stereotactic body radiation therapy (SBRT) has undergone considerable development for all sites, thanks to progress in dosimetric systems and image guided RT. SBRT involves precise positioning of the patient and the target volume in 3-dimensional space. External RT has an important role in curative and palliative treatment for nonoperable lung cancer patients. Improvement in local control rates of 85% to 95% has been reported when high doses in a small number of fractions have been used for stereotactic lung irradiation (1-6), with limited and low overall toxicity (6-8).

Small margins are usually required for SBRT irradiation, as recommended in 2010 by the American Association of Physicists in Medicine (9). Monitoring of patient intrafractions for SBRT needs precise imaging systems in order to track potential isocenter displacements and eventually to realign the target during the treatment session. Intrafraction motion for lung cancer patients can have an important impact on planning target volume (PTV) margins and, therefore, depends on the clinical implementation of an image-guided system.

ExacTrac X-ray 6D (ET) system (BrainLab) enables precise imaging and verification of patient intrafraction motion (10-12). Recently, Wang et al (13) calculated the margin required to account for setup errors for treating lung cancer patients using ET bony anatomy as a surrogate for the target and found values between 1.32 and 3.13 mm. An interesting work by Jin et al (14) described residual position variations by using the Novalis system. The study highlights the importance of rotational deviation for spinal radiosurgery patients, but the authors did not consider the impact of time on this deviation. In a study by Spadea et al (15), 32 lung patients were prepositioned by using an infrared system, and the couch was moved to compensate for linear shifts. Subsequently, kV images were acquired to perform automatic image fusions with 6 degrees of freedom (6D) on digitally reconstructed radiographs (DRRs) for setup refinement. In 16 patients, setup refinement was performed automatically with the aid of a robotic couch featuring 6D, and in the remaining patients, the 6D parameters estimated by x-ray image registration were performed manually (nonrobotic couch). Retrospectively, median $\pm$ quartile values of the target registration error were reduced to 2.46 ± 0.76 mm and 2.14 ± 0.95 mm for the robotic couch and nonrobotic couch patients, respectively. ET was also used to calculate and automatically adjust patient positioning in a study by Macklis et al (16). The absolute magnitude of the shifts (mean $\pm$ SD) for the targets' centers of mass was represented for lung patients in the range of 2 to 7 ± 2 mm. An extra time of less than 5 min was added to daily clinical treatment time.

Similar results were found by Li et al (17) in a study of 108 SBRT lung patients in whom intrafractional geometric accuracy of lung SBRT treated under image guidance was assessed using cone beam computed tomography (CBCT) imaging. Tumor matching was performed with the internal target volume (ITV) contour, and couch position was adjusted when positional discrepancies exceeded ± 3 mm in any direction, verified with a second CBCT. The mean time from localization to end fraction CBCT was 31 min 50 sec. After initial setup, CBCT assessment of ITV coverage showed 15% of all fractions were within ± 3 mm and 39% were within ± 5 mm. After correction of discrepancies and acquisition of CBCT verification, 88% of fractions were within ± 3 mm, and 99% were within ± 5 mm. At the end-CBCTs, 65% of fractions were maintained within ± 3 mm, and 93% were within ± 5 mm. The largest random error was 2.2 mm, observed in the superior-inferior direction.

ET Snap Verification (ET-SV) is a tool that offers easy setup control and real-time monitoring of patient position at all times during SBRT irradiation but also for conventional, 3-dimensional conformal RT (3DCRT).

The purposes of this study were *(1)* to measure the intrafraction variations of isocenter position (random errors, σ) with the use of SV; *(2)* to study the amplitude of the variation related to the fraction duration; and *(3)* to assess the impact of table movement on positioning uncertainties. To our knowledge, this is the first study that uses ET-SV for real-time tracking and monitoring of isocenter variations for lung cancer patients.

Methods and Materials

Patients

Between 2009 and 2010, 20 patients with 23 tumors (T1-T2 lung cancer or metastatic lesions) were treated with a Clinac 600CD (Varian) using the 3DCRT technique. Tumors were ≤ 4 cm in diameter and located in the right inferior lobe (3 lesions), right superior lobe (6 lesions), left inferior lobe (4 lesions), and left superior lobe (10 lesions). Thirteen patients were scanned with 4-dimensional (4D) CT (LightSpeed16; General Electric Medical Systems) for ITV delineation. All patients underwent a dosimetric CT scan with 2.5-mm-slice thickness. They were treated in the supine position using specific knee cushion and arm immobilization. Sixteen patients received stereotactic irradiation (at first we started with low doses that corresponded to 4-6 Gy per fraction), and 4 patients received a standard dose of 2 Gy per fraction.

In our department, 2 protocols are available for SBRT lung treatment. All patients undergo a 4DCT scan for ITV delineation. If the amplitude of tumor motion is considered less crucial, patients are treated as described in this paper with ET repositioning and SV monitoring. Otherwise, if important (>1 cm) amplitude of tumor motion is observed, gated treatment (SDX system; Dyn'R) is delivered using the same repositioning protocol.

ET X-ray repositioning technique

The ET system has 2 in-room-mounted orthogonal x-ray tubes and 2 detectors that can monitor the patient's anatomy in the treatment position and offers high detection and subdegree positioning accuracy for rotations, as demonstrated in a study by Gevaert et al (18). Bony landmarks or implanted markers can be tracked and matched with the DRRs generated from the dosimetric CT scan, taking into account 6D: 3 translations and 3 rotations.

Initially, the patients in the present study were positioned using tattoo marks. X-ray-based corrections of patient position were performed with the ET X-ray 6D system. For each patient, bone structures were used as references, and 2 DRRs were generated using the imported CT scan images. These DRRs were compared with the 2 noncoplanar kV images before each fraction. The amorphous silicon detectors gave high-quality digital images with a resolution of 512×512 pixels; the receptor area is 204.8×204.8 mm^2 and has an accuracy of ± 0.2 mm. The software uses

a first fusion based on 3 degrees of freedom, taking into account only the translational shifts, and then a final registration is made using 6D that takes into account both translational and rotational shifts. Thus, translational and angular rotations are automatically calculated for vertical, longitudinal, and lateral shifts.

Snap verification

Once the x-ray corrections were completed, individual x-ray images were acquired with SV, which is an ET device that uses real-time x-ray images acquired at any moment during treatment delivery or between fields. It instantly detects and visualizes the isocenter displacement (during beam-on or -off) in 2 dimensions. The displacement can be measured using the fusion of the DRRs with the bony structures or the implanted markers or both. A tolerance level (in millimeters) indicates whether a setup correction of the patient is needed. The patients presented in the current study underwent SV before or during each radiation beam. Setup verification was systematically made using the bony anatomy.

Evaluation method

The time (T) from patient setup on the treatment table to each SV was systematically noted for each beam, as was the corresponding maximum deviation (D) in 2 dimensions, as indicated by the software. Furthermore, mean deviation (D_{mean}) and daily treatment time (T_{mean}) were calculated for all patients and fractions.

SV time groups and noncoplanar group

The time (in minutes) for each SV was grouped into 3 SV time groups: SV performed at less than 10 min (group 1), between 11 and 20 min (group 2), and more than 21 min (group 3), after the setup of the patient. Mean deviations (in millimeters) per SV group and deviations greater than or equal to 3 mm and 5 mm (in percentages) were calculated for each of these 3 groups. We also noted frequencies of mean deviations between 1 mm and 5 mm and the mean deviation before and during the use of a noncoplanar field.

Statistical analyses

A descriptive analysis was made for each of the variables, and values of deviations were compiled for 3 SV time groups. Differences between the 3 SV time groups in terms of mean deviation needed for each group were tested with a nonparametric Friedman test. Differences in frequencies of deviation greater than or equal to 3 or 5 mm between each SV time group were tested by χ^2 test. Differences between the mean deviations needed before and during the use of a noncoplanar field were tested with a nonparametric Wilcoxon matched pairs test. As a final control of confounding factors, the same analyses of SV time groups were made excluding the noncoplanar beams, and differences between deviations greater than or equal to 3 and 5 mm in each SV time group between coplanar and noncoplanar beams were analyzed with a χ^2 bilateral test. All tests were bilateral, with a P value set at $<.05$, and were performed with SPSS, version 19.0, software.

Results

General evaluation

A total of 2121 beams were verified with SV, of which 585 of 2121 beams were noncoplanar, with a table rotation. Of the 2121 SVs, 211 could not be evaluated due to technical problems (error messages or images not available on the screen). Thus, 1910 SVs were analyzed with a measure of the isocenter displacement. The mean treatment field number was 8 (range, 3-14) beams. The average isocenter deviation, $D_{mean} \pm SD$, for all beams and all fractions was 2 ± 0.5 mm (range, 1-8 mm), and the total mean time, $T_{mean} \pm SD$, for 1 fraction was 26 ± 8.2 min (range, 7-70 min).

SV time groups

All displacements greater than or equal to 5 mm detected by the SV tool were systematically corrected, following the department's tolerance procedure (if SV deviation was $\geq$5 mm, then the patient was repositioned with the ET 6D system). However, only 1 SV was taken per treatment field, and the chronometer was not set back to zero.

The number of SVs that showed deviations $\geq$3 mm and $\geq$5 mm were 13 of 184, 242 of 1060, 187 of 666, and 2 of 184, 44 of 1060, and 56 of 666 for groups 1, 2, and 3, respectively. Results, expressed in percentages of deviation, were 7.06%, 22.83%, and 28.07% for $\geq$3 mm and 1.08%, 4.15%, and 8.4% for $\geq$5 mm. Frequencies of deviation of more than 3 mm and more than 5 mm were significantly different among the SV time groups ($P<.0001$) (Fig. 1).

Values of mean deviations increased among the 3 SV time groups from 1.6 ± 0.5 mm (range, 1-3.2 mm) to 2.1 ± 0.8 mm (range, 1-5 mm) and 2.2 ± 0.6 mm (range, 1.1-3.2 mm) for groups 1, 2, and 3, respectively (Fig. 2). These differences were significant from group 0 to 10 min to group 11 to 20 min and to group $\geq$21 min ($P=.002$).

Results of the same tests excluding table rotations (as possible confounding factors) were still significant (maximum P value of

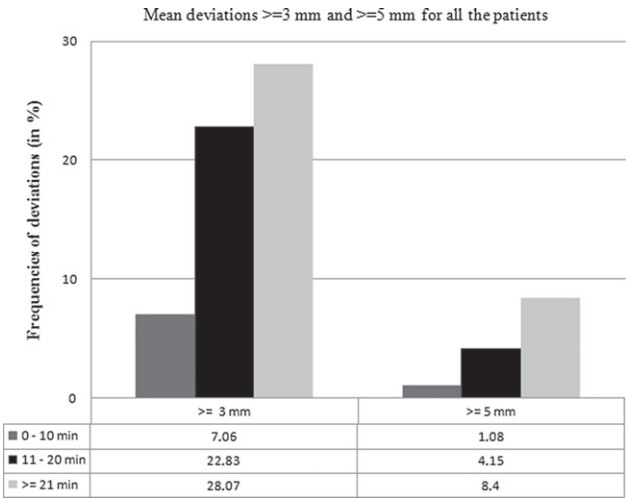

Fig. 1. Percentages of mean deviations greater than or equal to 3 mm and 5 mm.

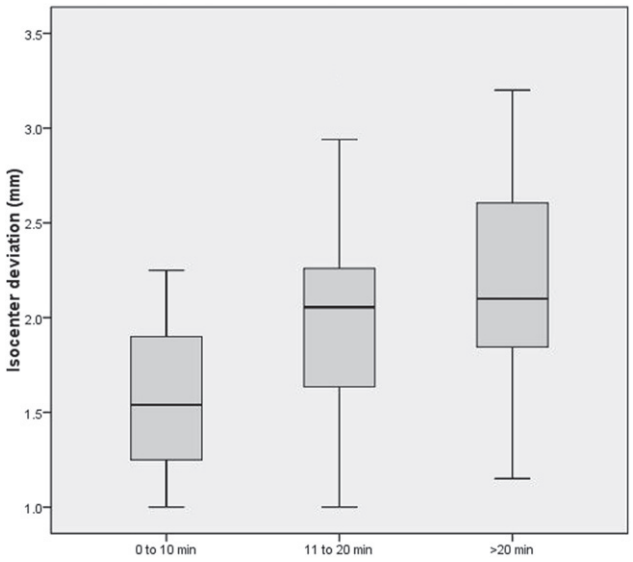

Fig. 2. Isocenter deviation (in millimeters) related to SV time groups (in minutes). For each box plot, minimal, maximal, median, and quartile values are represented.

.0087 for the analyses of the mean deviations between the 3 SV time groups).

Table rotation groups

For the treatment planning of 11 patients, a total of 585 table rotations were necessary. The mean isocenter deviation increased significantly from 1.9 ± 0.5 mm (range, 1.3-2.8 mm) before table rotation to 2.7 ± 0.5 mm (range, 1.8-3.4 mm) ($P = .001$) for the first beam treated after rotation (Fig. 3). The proportions of deviation greater than or equal to 3 mm between noncoplanar and coplanar beams in each SV time group were 16% versus 7%, 41% versus 23%, and 37% versus 28% for groups 1, 2, and 3, respectively, with a P value of .023. The proportions of deviations greater than or equal to 5 mm between noncoplanar and coplanar beams at each SV time group were 0% versus 1%, 12% versus 2.3%, and 11% versus 8.4% for groups 1, 2, and 3, respectively, with a P value $<.0001$ (Fig. 4).

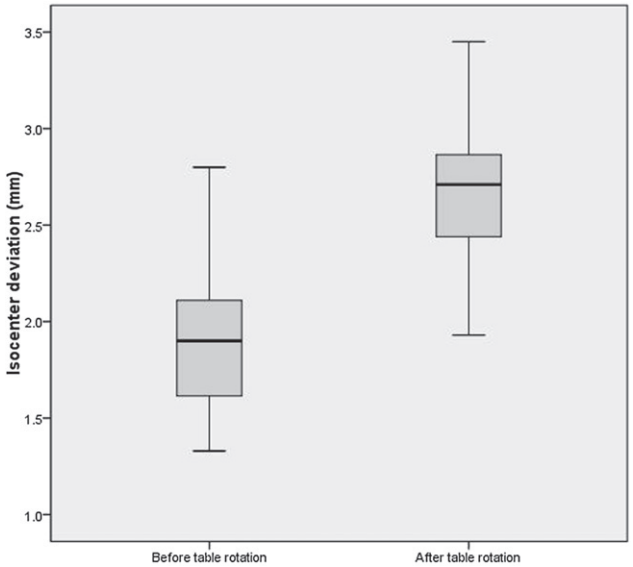

Fig. 3. Isocenter deviation (in millimeters) related to table rotation. For each box plot, minimal, maximal, median, and quartile values are represented.

Discussion

The ET system was already evaluated in the literature for lung SBRT (10), as well as for other tumor locations (16, 19), and demonstrated its feasibility for PTV margin calculation (13, 20) and localization accuracy (15). However, the present work describes the first experience with the SV tool for the study of intrafraction motion for lung cancer patients. SV allows an accurate verification of the patient position, an instant monitoring of isocenter displacements at all times (before and during the treatment beam). Consequently, a tolerance margin established by our department indicates whether the patient setup correction is needed or not during SBRT treatment. When a correction was necessary as indicated by SV (≥5 mm), a new ET 6D is performed to set the patient back to the right position, and no additional SV was acquired for that field (we always acquired 1 SV per field). The chronometer was not set back to zero, as we considered that the impact of treatment duration (that may have a link with patient condition) on isocenter deviations does not depend on those realignments.

In the present study, a total mean average isocenter displacement of 2 mm (range, 1-8 mm) was found for a mean treatment time of 26 min (range, 7-70 min). Maximum deviation observed with SV was 8 mm. We have shown here the link between time of treatment, use of noncoplanar field, and increase of random errors during treatment. SV seems to be a good tool with which to avoid unacceptable deviation during long treatments due to the relative complexity of the planned dosimetry. In some situations, patients experienced pain or fatigue, or they coughed at the end of treatment, probably because of long fractions. Although our assumption is that these reasons may explain the observed deviations, we cannot provide any statistical analysis.

Furthermore, noncoplanar beams are often necessary for better tumor coverage or sparing of normal tissue. In the current evaluation, 11 patients had a total of 585 table rotations. For each table rotation, differences between SV values were observed. These

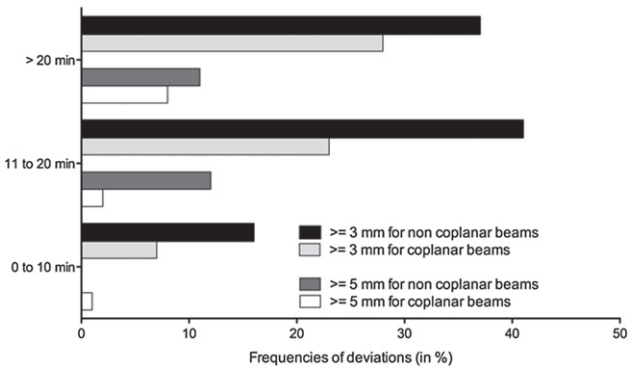

Fig. 4. Percentages of deviations greater than or equal to 3 mm and 5 mm for the coplanar and the noncoplanar beams and for the 3 SV time groups.

deviations can result from mechanical table tolerance (±2 mm) or movement of the treatment table. The impact of table rotation must be considered, as larger deviations were noted for the verification of the noncoplanar beams. An increase in mean random errors was observed from 1.9 mm before the table rotation to 2.7 mm for the first beam after table rotation. Therefore, the potential patient motion caused by table rotations may be verified using the ET-SV tool. Coplanar and noncoplanar beams are not distributed uniformly in time, as the noncoplanar beams are used at the end of each fraction. This was a potential confounding aspect. We made the same statistical analysis as above but excluded the noncoplanar beams. We still found a statistical difference between mean deviations ± SD for the 3 time groups (1.28 mm ± 0.7 mm, 2 mm ± 1 mm, and 2 mm ± 0.5 mm) with a P value of .0087 between the first and third time groups (using the Friedman test). A significant difference also was found for frequencies of deviation of more than 3 mm among the 3 time groups, with $P = .0004$, and for frequencies of deviation of more than 5 mm among the 3 time groups, with $P = .0017$ (χ^2 test). We are therefore confident that the table rotation was not a confounding parameter.

The accuracy of using the spine as a surrogate for tumor position is an essential issue when discussing the precision needed to realize SBRT for lung cancer. We acknowledge that the measurements of isocenter variations are based on bony anatomy and that the SV tool cannot give information about the changes in the actual target position. In the present work, we studied positioning uncertainties in time by using the ET system, with its strength, like the ability to verify the positioning during irradiation, and its weakness as the use of spine as a surrogate for patient positioning, and not a direct tumor positioning. We assessed tumor movement with 4DCT to determine whether the amplitude of movement needs a gated respiratory procedure, and we used the spine to determine with submillimeter precision the patient positioning related to the isocenter position.

SV based on bony markers may provide good level of confidence in PTV setup margin reductions for SBRT irradiation with permanent patient monitoring and independent treatment verification. In our department, the ET-SV repositioning and monitoring system combined with 4D delineation or gated treatment allowed a reduction of PTV margins for lung patients from 1.5 cm to 0.8 cm. However, these results are only an indication, and each RT department should choose the PTV margins according to the particular practice.

Conclusions

Treatment duration and use of noncoplanar beams are 2 factors significantly correlated to an increase in random errors (σ) in isocenter positioning, as presented in our study.

It can be concluded from the experience with the first patients that SV is an efficient tool for detecting these random errors. SV makes intrafraction verification possible for SBRT and also during irradiation, taking into account clinical condition and technical issues. With high-quality images at low x-ray doses, the SV tool gives precise verification of the patient or of the target from the beginning to the end of each fraction, raising confidence to escalate the dose. SV appears to be an important device or accessory for ensuring quality control for SBRT. Our radiation therapy department continues to use this technique for lung and cranial irradiation and treating liver metastases or hepatocellular carcinoma (21), and the combination of gated treatment and SV allows a considerable reduction in PTV margins for lung and liver SBRT.

References

1. Lagerwaad FJ, Haasbeek CJ, Smit EF, et al. Outcomes of risk-adapted fractionated stereotactic radiotherapy for stage I non-small-cell lung cancer. *Int J Radiat Oncol Biol Phys* 2008;70:685-692.
2. Nagata Y, Takayama K, Matsuo Y, et al. Clinical outcomes of a phase I/II study of 48 Gy of stereotactic body radiotherapy in 4 fractions for primary lung cancer using a stereotactic body frame. *Int J Radiat Oncol Biol Phys* 2005;63:1427-1431.
3. Inoue T, Shimizu S, Rikiya O, et al. Clinical outcomes of stereotactic body radiotherapy for small lung lesions clinically diagnosed as primary lung cancer on radiologic examination. *Int J Radiat Oncol Biol Phys* 2009;75:683-687.
4. Matsuo Y, Shibuya K, Nagata Y, et al. Prognostic factors in stereotactic body radiotherapy for non-small-cell lung cancer. *Int J Radiat Oncol Biol Phys* 2011;79:1104-1111.
5. Soliman H, Cheung P, Yeung L, et al. Accelerated hypofractionated radiotherapy for early-stage non-small-cell lung cancer: long-term results. *Int J Radiat Oncol Biol Phys* 2011;79:459-465.
6. Taremi M, Hope A, Dahele M, et al. Stereotactic body radiotherapy for medically inoperable lung cancer: prospective, single-center study of 108 consecutive patients. *Int J Radiat Oncol Biol Phys* 2012;82: 967-973.
7. Baumann P, Nyman J, Hoyer M, et al. Stereotactic body radiotherapy for medically inoperable patients with stage I nonsmall cell lung cancer: A first report of toxicity related to COPD/CVD in a non-randomized prospective phase II study. *Radiother Oncol* 2008;88:359-367.
8. Bishawi M, Kim B, Moore W, et al. Pulmonary function testing after stereotactic body radiotherapy to the lung. *Int J Radiat Oncol Biol Phys* 2012;82:e107-e110.
9. Benedict SH, Yenice KM, Followill D, et al. Stereotactic body radiation therapy: the report of AAPM Task Group 101. *Med Phys* 2010; 37:4078-4101.
10. Videtic GMM, Stephans K, Reddy C, et al. Intensity-modulated radiotherapy-based stereotactic body radiotherapy for medically inoperable early-stage lung cancer: excellent local control. *Int J Radiat Oncol Biol Phys* 2010;77:344-349.
11. Willoughby TR, Forbes AR, Buchholz D, et al. Evaluation of an infrared camera and x-ray system using implanted fiducials in patients with lung tumors for gated radiation therapy. *Int J Radiat Oncol Biol Phys* 2006;66:568-575.
12. Jin JY, Yin FF, Tenn SE, et al. Use of the BrainLAB ExacTrac X-ray 6D system in image-guided radiotherapy. *Med Dosim* 2008;33: 124-134.
13. Wang F, Badkul R, Park J. Stereotactic body radiotherapy for lung cancer using ExacTrac X-ray 6D and four-dimensional cone beam CT image guidance [abstract]. 14th World Conference on Lung Cancer *IASLC*, Amsterdam, July 3-7, 2011.
14. Jin JY, Ryu S, Rock J, et al. Evaluation of residual patient position variation for spinal radiosurgery using the Novalis image guided system. *Med Phys* 2008;35:1087-1093.
15. Spadea M, Riboldi M, Tagaste B, et al. Assessment of target registration error (TRE) in extra-cranial radiotherapy patient setup guided by the ExacTrac X-ray 6D system. *Int J Radiat Oncol Biol Phys* 2007; 69(suppl):S684.
16. Macklis RM, Robinson C, Djemil T. Automated registration and correction of patient positioning for IGRT and body radiosurgery using the Novalis "ExacTrac" system. *Int J Radiat Oncol Biol Phys* 2006; 66(suppl):S644.
17. Li W, Bezjak A, Purdie TG, et al. Intrafractional target position accuracy for lung stereotactic body radiotherapy (SBRT) using cone-beam CT (CBCT) [abstract]. *Int J Radiat Oncol Biol Phys* 2009; 75(suppl):S160.

18. Gevaert T, Verellen D, Tournel K, et al. Setup accuracy of the Novalis ExacTrac 6DOF system for frameless radiosurgery. *Int J Radiat Oncol Biol Phys* 2012;82:1627-1635.
19. Ter Beek L, Wit F, Immink M, et al. Using ExacTrac for accurate positioning of breast cancer patients [abstract]. *Radiother Oncol* 2011; 99(suppl 1):S471.
20. Alonso-Arrizabalaga S, Gonzalez LB, Ferrando JVR, et al. Prostate planning treatment volume margin calculation based on the ExacTrac X-ray 6D image-guided system: margins for various clinical implementations. *Int J Radiat Oncol Biol Phys* 2007;69: 936-943.
21. Mornex F, Girard N, Beziat C, et al. Feasibility and efficacy of high-dose three-dimensional-conformal radiotherapy in cirrhotic patients with small-size hepatocellular carcinoma non-eligible for curative therapies-mature results of the French phase II RTF-1 trial. *Int J Radiat Oncol Biol Phys* 2006;66:1152-1158.

2.5.4. Conclusion

In our department, position corrections with the ExacTrac® X-ray6D system and target monitoring with the Snap Verification® tool allowed a reduction of the PTV margins for lung patients from 1.5 cm to 0.8 cm with target delineation using 4DCT or gated treatment. However, the prostate doesn't need any ITV delineation as confirmed in our 4D study. We can conclude that Snap Verification® combined with three gold markers may be an accurate method for the monitoring of target position and for the reduction of PTV margins up to 3 mm in prostate SBRT.

2.6. Discussion - section II

The planning target volume for the prostate irradiation includes the internal motion of the organ (intrafraction motion) and errors in target localization (interfraction motion).

We have shown above that respiratory-induced prostate motion is not significant (< 1 mm in LR and AP and < 2.5 mm in CC direction) and thus, should not be taken into consideration for margin calculation of stereotactic irradiation. Therefore, two aspects remain critical for SBRT and should be taken into account for the choice of the margins around the target volume: managing the random prostate motion and accurate localization of the organ.

Various studies have been carried out for the measurement of the prostate intrafraction motion [15, 22, 32, 34, 35, 58-61]. The localization and monitoring of the prostate [62-64] and the clinical consequences of daily variations [65] have been previously evaluated.
There are two ways to control the prostate movement:

1) with real-time target monitoring (that was described in section 2.5); and
2) by limiting the motion of the target: (e.g. immobilization and repositioning with endorectal balloons).

2.6.1. Limitation of prostate motion

Several aspects should be considered in order to considerably restrict the motion of the prostate for SBRT: patient position (prone *vs.* supine), the repletion of bladder and rectum and potential immobilization features (e.g. endorectal balloons, urinary catheter balloon).

2.6.1.1. Prone versus supine position

One recent publication determined the magnitude of the intrafraction motion of the prostate for IMRT. Mean ± standard deviation intrafraction prostate motion was 2.1±1.2 mm and 1.7 ± 1.4 mm for AP, 2.2 ± 2 mm and 1.6 ± 1.8 mm for SI, and 1±1.2 mm and 0.6 ± 0.9 mm for LR direction in the prone and supine positions, respectively [66]. The authors found a small difference in the magnitude of the intrafraction prostate motion when patients were treated prone *vs.* supine. Furthermore, treating in the prone position will accentuate internal organ motion related to free-breathing and should be avoided. Certainly, patients are more comfortable in the supine position and situations uncomfortable should be avoided so as to avoid uncontrolled motion during irradiation. In the majority of the SBRT trials the patients have been treated in supine position [39-44] but also in prone position [38].

2.6.1.2. Repletion of rectum and bladder

Variations in the bladder and rectum volume during the irradiation were reported for patients treated for prostate cancer [67-72]. These variations can be up to 80% relative to the average volumes.

Bladder movement was previously assessed with weekly CT scans [73, 74]. In order to reduce variations in bladder position, Miralbell *et al.* used a urinary catheter balloon. They observed an average motion of 5 mm [74].

Moreover, it was already demonstrated that prostate movement correlates well with rectal volume increases because of the gas in the rectum [16, 21, 75-77]. Rectal gas may have accounted for random errors in prostate motion of 1.3 – 2 mm [59, 78].

The role for an endorectal balloon (ERB) device during external beam radiation therapy was questioned in the last years [79-83]. The first application of an endorectal balloon is the rectum-wall sparing by pushing some parts of the rectum-wall away from the high dose gradients [84-93]. In order to reduce the PTV margins, the endorectal balloons are furthermore used for daily prostate immobilization [84-86, 94-97].

Though, the opinions regarding the utilization of an ERB for prostate immobilization are divided:

- D'Amico *et al.* reported their experience on prostate immobilization when using an EBR, in order to reduce inter- and intrafraction variations in prostate position [96]. They studied intrafraction motion with CT-images at 1 minute time interval with and without an air-filled (60cc) endorectal balloon and they concluded that prostate immobilization with ERB is possible. The ERB reduced the maximum prostate variation in any direction from 4 mm to ≤ 1 mm. Moreover, they didn't observe any prostate deviation during normal breathing [96]. In 2010, Wang *et al.* [80] studied the difference in the real-time prostate motion between patients undergoing radiotherapy with and without daily ERB. The prostate displacement for the non-ERB group is larger when compared to that of the balloon group. The differences found between the two groups are in the CC direction and mainly in the AP direction. The authors concluded that daily ERB had great impact on reducing large intrafraction prostate motion (>5 mm) [80]. The mean displacement of the prostate found by D'Amico *et al.* was 1.3 mm (range, 0–2.2 mm) with an ERB compared to 1.8 mm (range, 0–9.1 mm) ($p = 0.03$) without an ERB. They concluded that ERB reduced prostate motion variability. Maximum displacement was reduced from 4 mm to less than or equal to1 mm using a balloon [96].

- However, other reports didn't confirm these results and they didn't find any difference in systematic and random prostate motion with and without an ERB [81, 83]. The

main reason for large variations was the presence of gas between rectum-wall and ERB and therefore it was concluded that appropriate target positioning should be made especially for high-dose irradiations. The interfraction prostate motion variability and the on-line positioning accuracy were evaluated as well with an endorectal balloon device by El-Bassiouni *et al.* [81]. The patients were treated with conformal external-beam radiotherapy and weekly portal images. The mean displacements ± standard deviations of the ERB were 2 mm ± 1.4 mm, 4.1 mm ± 2 mm and 3.8 mm ± 3.3 mm in the LR, CC and AP directions, respectively. The authors concluded that internal motion and field setup variability in the presence of an ERB alone results in a suboptimal PTV margin in AP direction (> 1 cm) [81]. When Van Lin *et al.* investigated the systematic and random prostate errors they didn't find any difference between patients with and without an ERB [83]. Patients had implanted gold markers and daily off-line portal imaging correction. The maximum interfraction variation ± SD was 4.7 mm ± 1 mm in the AP direction. The gold markers reduced the systematic prostate displacements, while the ERB did not decrease the interfraction prostate motion. The AP prostate displacements may be explained by the presence of gas and stool near the ERB. It was concluded that ERB does not reduce the interfraction prostate motion and that the assumption that an ERB gives a constant rectal filling could not be confirmed [83].

Consequently, the utilization of an endorectal balloon seems to be appropriate for SBRT where reduction in PTV margins around the CTV are made up to 3-mm [98]. On the other hand, careful attention should be paid to systematic error of rectal balloon repositioning because of air leakage, suboptimal inflation or rectal cleaning [99] and patient discomfort. Despite the good ERB tolerability reported by several studies [86, 88, 100] patients may experience pain and discomfort when ERB is used [82]. Moreover, the use of an endorectal balloon might not be an ideal answer in prostate SBRT as the ERB approaches the rectal wall to prostate, which is contrary to the idea of a prostate-rectum separation.

The actual prostate SBRT trials have been treated the patients with empty rectum and full or intermediate bladder. However, Zellars *et al.* showed that large bladder volumes during radiotherapy are (1) difficult to achieve and (2) associated with posterior prostate displacement [101]. Their results suggest that an emptier bladder may be preferable to a full bladder late in therapy (to potentially decrease bladder and small bowel toxicity). In addition, the authors stated that an empty bladder and an empty rectum tend to maintain the prostate in similar positions early and late in therapy [101].

2.7. Conclusion – section II

In conclusion, a supine position seems more appropriate and will be used in the department's protocol for prostate SBRT. The patients will be treated supine in a fixed position that allows accurate daily reproducibility of the target.

While random prostate displacements may occur during the irradiation, because of the bladder or rectum filling, in our study we didn't observed any motion of the prostate linked to the normal breathing.

The interest of an endorectal balloon device remains unclear. The use of an ERB seems to be uncomfortable and painful for patients and not always an accurate method for prostate immobilization. Therefore, ERBs will not be used in our protocol for prostate SBRT. Patients will be treated with an empty rectum and intermediate bladder.

Cone-beam CT or kV repositioning combined with implanted gold markers are needed for the visualization of the interfraction variation. Moreover, real-time tracking and verification can be used for information on intrafraction prostate motion.

All these findings let us conclude that a reduction of the PTV margins up to 3 mm is possible, as also described by other SBRT experiences, given that appropriate techniques for delineation and monitoring of the target are available.

2.8. Bibliography – section II

[1] ICRU, "Prescribing, recording, and reporting photon beam therapy", ICRU Report No. 50, 1993.

[2] ICRU, "Prescribing, recording, and reporting photon beam therapy (supplement to ICRU Report No. 50)", ICRU Report No. 62, 1999.

[3] Benedict SH, Yenice KM, Followill D, *et al.* Stereotactic body radiation therapy: The report of AAPM Task Group 101. *Med Phys* 2010;37(8):4078-4101.

[4] Debois M, Oyen R, Maes F, *et al.* The contribution of magnetic resonance imaging to the three-dimensional treatment planning of localized prostate cancer. *Int J Radiat Oncol Biol Phys* 1999;45:857–865.

[5] Sannazzari GL, Ragona R, RuoRedda MG, Giglioli FR, Isolato G, Guarneri A. CT-MRI image fusion for delineation of volumes in three-dimensional conformal radiation therapy in the treatment of localized prostate cancer. *Br J Radiol* 2002;75:603-607.

[6] Gao Z, Wilkins D, Eapen L, *et al.* A study of prostate delineation referenced against a gold standard created from the visible human data. *Radiother Oncol* 2007;85:239–246.

[7] McLaughlin PW, Evans C, Feng M, Narayana V. Radiographic and anatomic basis for prostate contouring errors and methods to improve prostate contouring accuracy. *Int J Radiat Oncol Biol Phys* 2010;76:369-378.

[8] Villeirs GM, Verstraete KL, De Neve WJ, De Meerleer GO. Magnetic resonance imaging anatomy of the prostate and periprostatic area: a guide for radiotherapists. *Radiother Oncol* 2005;76:99-106.

[9] Khoo V, Dearnaley D, Finnigan D, *et al*. Magnetic resonance imaging (MRI): considerations and applications in radiotherapy treatment planning. *Radiother Oncol* 1997;42:1–15.

[10] Roach M, Faillace-Akazawa P, Malfatti C, *et al*. Prostate volumes defined by magnetic resonance imaging and computerized tomographic scans for three-dimensional conformal radiotherapy. *Int J Radiat Oncol Biol Phys* 1996;35(5):1011–1018.

[11] Rasch C, Barillot I, Remeijer P, *et al*. Definition of the prostate in CT and MRI: a multi-observer study. *Int J Radiat Oncol Biol Phys* 1999;43(1):57–66.

[12] Kagawa K, Lee WR, Schultheiss TE, Hunt MA, Shaer AH, Hanks GE. Initial clinical assessment of CT-MRI image fusion software in localization of the prostate for 3D conformal radiation therapy. *Int J Radiat Oncol Biol Phys* 1997;38:319-325.

[13] Chapet O, Udrescu C, De Bari B, *et al.* Do we really need a radiologist for the prostate delineation in radiotherapy? *Radiother Oncol* 2010;96 (Suppl. 1): S392-S419.

[14] Langen KM, Jones DTL. Organ motion and its management. *Int J Radiat Oncol Biol Phys* 2001;50:265-278.

[15] Huang E, Dong L, Chandra A, *et al.* Intrafraction prostate motion during IMRT for prostate cancer. *Int J Radiat Oncol Biol Phys* 2002;53:261–268.

[16] Ghilezan MJ, Jaffray DA, Siewerdsen JH, *et al.* Prostate gland motion assessed with cine-magnetic resonance imaging (cine-MRI). *Int J Radiat Oncol Biol Phys* 2005;62:406–417.

[17] Aubry JF, Beaulieu L, Girouard LM, *et al.* Measurements of intrafraction motion and interfraction and intrafraction rotation of prostate by three-dimensional analysis of daily portal imaging with radiopaque markers. *Int J Radiat Oncol Biol Phys* 2004;60:30–39.

[18] Beltran C, Herman MG, Davis BJ. Planning target margin calculations for prostate radiotherapy based on intrafraction and interfraction motion using four localization methods. *Int J Radiat Oncol Biol Phys* 2008;70:289–295.

[19] Pinkawa M, Pursch-Lee M, Asadpour B, *et al.* Image-guided radiotherapy for prostate cancer: Implementation of ultrasound-based prostate localization for the analysis of inter- and intrafraction organ motion. *Strahlenther Onkol* 2008;184:679–685.

[20] Rosewall T, Chung P, Bayley A, *et al.* A randomized comparison of interfraction and intrafraction prostate motion with and without abdominal compression. *Radiother Oncol* 2008;88:88–94.

[21] Mah D, Freedman G, Milestone B, *et al.* Measurement of intrafractional prostate motion using magnetic resonance imaging. *Int J Radiat Oncol Biol Phys* 2002;54:568–575.

[22] Britton KR, Takai Y, Mitsuya M, *et al.* Evaluation of inter- and intrafraction organ motion during intensity modulated radiation therapy (IMRT) for localized prostate cancer measured by a newly developed on-board image-guided system. *Radiat Med* 2005;23:14–24.

[23] Schaly B, Bauman GS, Song W, *et al.* Dosimetric impact of image-guided 3D conformal radiation therapy of prostate cancer. *Phys Med Biol* 2005;50:3083–3101.

[24] Vargas C, Martinez A, Kestin LL, *et al.* Dose–volume analysis of predictors for chronic rectal toxicity after treatment of prostate cancer with adaptive image-guided radiotherapy. *Int J Radiat Oncol Biol Phys* 2005;62:1297–1308.

[25] Worm ES, Hoyer M, Fledelius W, Poulsen PR. Three-dimensional, time-resolved, intrafraction motion monitoring throughout stereotactic liver radiation therapy on a conventional linear accelerator. *Int J Radiat Oncol Biol Phys* 2013;86(1):190-197.

[26] Beddar AS, Kainz K, Briere TM, *et al.* Correlation between internal fiducial tumor motion and external marker motion for liver tumors imaged with 4D-CT. *Int J Radiat Oncol Biol Phys* 2007;67:630-638.

[27] Hurkmans CW, van Lieshout M, Schuring D, *et al.* Quality assurance of 4D-CT scan techniques in multicenter phase III trial surgery versus stereotactic radiotherapy (radiosurgery or surgery for operable early stage (stage 1A) non-small-cell lung cancer [ROSEL] study). *Int J Radiat Oncol Biol Phys* 2011;80:918-927.

[28] Udrescu C, Jalade P, Michel-Amadry G, De Bari B, and Chapet O. Evaluation of the respiratory prostate motion with 4D CT scans acquisitions using three implanted markers. *Radiother Oncol* 2010;96 (Suppl. 1): S392-S419.

[29] Udrescu C, Jalade P, de Bari B, Michel-Amadry G, Chapet O. Evaluation of the respiratory prostate motion with four-dimensional computed tomography scan acquisitions using three implanted markers. *Radiother Oncol* 2012;103:266-269.

[30] Moseley DJ, White EA, Wiltshire KL, *et al.* Comparison of localization performance with implanted fiducial markers and cone-beam computed tomography for on-line image-guided radiotherapy of the prostate. *Int J Radiat Oncol Biol Phys* 2007;67:942–953.

[31] Nederveen AJ, Dehnad H, van der Heide UA, *et al.* Comparison of megavoltage position verification for prostate irradiation based on bony anatomy and implanted fiducials. *Radiother Oncol* 2003;68:81–88.

[32] Cheung P, Sixel K, Morton G, *et al.* Individualized planning target volumes for intrafraction motion during hypofractionated intensity-modulated radiotherapy boost for prostate cancer. *Int J Radiat Oncol Biol Phys* 2005;62:418–425.

[33] Vigneault E, Pouliot J, Laverdière J, *et al.* Electronic portal imaging device detection of radioopaque markers for the evaluation of prostate position during megavoltage irradiation: A clinical study. *Int J Radiat Oncol Biol Phys* 1997;37:205–212.

[34] Nederveen AJ, van der Heide UA, Dehnad H, *et al.* Measurements and clinical consequences of prostate motion during a radiotherapy fraction. *Int J Radiat Oncol Biol Phys* 2002;53:206–214.

[35] Litzenberg DW, Balter JM, Hadley SW, *et al.* Influence of intrafraction motion on margins for prostate radiotherapy. *Int J Radiat Oncol Biol Phys* 2006;65:548–553.

[36] Kupelian P, Willoughby T, Mahadevan A, *et al.* Multi-institutional clinical experience with the Calypso system in the localization and continuous, real-time monitoring of the prostate gland during external radiotherapy. *Int J Radiat Oncol Biol Phys* 2007;67:1088–1098.

[37] Alonso-Arrizabalaga S, Brualla Gonzalez L, Rosello Ferrando JV, *et al.* Prostate planning treatment volume margin calculation based on the ExacTrac X-Ray 6D image-guided system: Margins for various clinical implementations. *Int J Radiat Oncol Biol Phys* 2007;69:936–943.

[38] Madsen BL, Hsi RA, Pham HT, *et al.* Stereotactic hypofractionated accurate radiotherapy of the prostate (SHARP), 33.5 Gy in five fractions for localized prostate disease: First clinical trial results. *Int J Radiat Oncol Biol Phys* 2007;67:1099–1105.

[39] Tang CI, Loblaw DA, Cheung P, *et al.* Phase I/II study of a five-fraction hypofractionated accelerated radiotherapy treatment for low-risk localized prostate cancer: early results of pHART3. *Clinic Oncol* 2008;20:729-737.

[40] King CR, Brooks JD, Gill H, Presti JC. Long-term outcomes from a prospective trial of stereotactic body radiotherapy for low-risk prostate cancer. *Int J Radiat Oncol Biol Phys* 2012;82:877-882.

[41] Bolzicco G, Favretto MS, Scremin E, *et al.* Image-guided stereotactic body radiation therapy for clinically localized prostate cancer: preliminary clinical results. *Technol Cancer Res Treat* 2010;9:473-477.

[42] Friedland JL, Freeman DE, Masterson-McGary ME, Spellberg DM. Stereotactic body radiotherapy: An emerging treatment approach for localized prostate cancer. *Technol Cancer Res Treat* 2009;8:387-392.

[43] Boike TP, Lotan Y, Cho LC, *et al.* Phase I dose-escalation study of stereotactic radiation therapy for low- and intermediate-risk prostate cancer. *J Clin Oncol* 2011;29:2020-2026.

[44] Jabbari S, Weinberg VK, Kaprealian T, *et al.* Stereotactic body radiotherapy as monotherapy or post-external beam radiotherapy boost for prostate cancer: Technique, early toxicity, and PSA response. *Int J Radiat Oncol Biol Phys* 2012;82:228-234.

[45] Lee YH, Son SH, Yoon SC, et al. Stereotactic body radiotherapy for prostate cancer: A preliminary report. *Asia Pac J Clin Oncol* 2012 [Epub ahead of print].

[46] Delouya G, Carrier JF, Béliveau-Nadeau D, Donath D, Taussky D. Migration of intraprostatic fiducial markers and its influence on the matching quality in external beam radiation therapy for prostate cancer. *Radiother Oncol* 2010;96:43-47.

[47] Udrescu C, Jalade P, De Bari B, *et al.* Evaluation of implanted gold markers migration during irradiation of prostate cancer. *Int J Radiat Oncol Biol Phys* 2010;78(Supp): S674.

[48] Udrescu C, De Bari B, Rouvière O, *et al.* Does hormone therapy modify the position of the gold markers in the prostate during irradiation? A daily evaluation with kV-images. *Cancer Radiother* 2013;17:215-220.

[49] Voyant C, Biffi K, Leschi D, *et al.* Dosimetric uncertainties related to the elasticity of bladder and rectal walls: Adenocarcinoma of the prostate. *Cancer Radiother* 2011;15:270-8.

[50] Wang Z, Nelson JW, Yoo S, *et al.* Refinement of treatment setup and target localization accuracy using three-dimensional cone-beam computed tomography for stereotactic body radiotherapy. *Int J Radiat Oncol Biol Phys* 2009;73:571-577.

[51] Soete G, De Cock M, Verellen D, *et al.* X-ray-assisted positioning of patients treated by conformal arc radiotherapy for prostate cancer: comparison of setup accuracy using implanted markers versus bony structures. *Int J Radiat Oncol Biol Phys* 2007;67:823–827.

[52] Letourneau D, Martinez AA, Lockman D, *et al.* Assessment of residual error for online cone-beam CT-guided treatment of prostate cancer patients. *Int J Radiat Oncol Biol Phys* 2005;62:1239–1246.

[53] Willoughby TR, Kupelian PA, Pouliot J, *et al.* Target localization and real-time tracking using the Calypso 4D localization system in patients with localized prostate cancer. *Int J Radiat Oncol Biol Phys* 2006;65:528–534.

[54] Orton NP, Tome WA. The impact of daily shifts on prostate IMRT dose distributions. *Med Phys* 2004;31:2845–2848.

[55] Landoni V, Saracino B, Marzi S, *et al.* A study of the effect of setup errors and organ motion on prostate cancer treatment with IMRT. *Int J Radiat Oncol Biol Phys* 2006;65:587–594.

[56] Udrescu C, Chapet O, de Bari B, Michel-Amadry G, and Mornex F. The ExacTrac Snap Verification (SV), a new tool for ensuring the quality control for stereotactic body radiation therapy (SBRT). *Int J Radiat Oncol Biol Phys* 2009;75(Suppl.):S609.

[57] Udrescu C, Mornex F, Tanguy R, Chapet O. ExacTrac snap verification: a new tool for ensuring quality control for lung stereotactic body radiation therapy. *Int J Radiat Oncol Biol Phys* 2013;85:e89-e94.

[58] Shimizu S, Shirato H, Kitamura K, *et al.* Use of an implanted marker and real-time tracking of the marker for the positioning of prostate and bladder cancers. *Int J Radiat Oncol Biol Phys* 2000;48:1591–1597.

[59] Kotte AN, Hofman P, Lagendijk JJ, *et al.* Intrafraction motion of the prostate during external-beam radiation therapy: analysis of 427 patients with implanted fiducial markers. *Int J Radiat Oncol Biol Phys* 2007;69:419–425.

[60] Li HS, Chetty IJ, Enke CA, *et al.* Dosimetric consequences of intrafraction prostate motion. *Int J Radiat Oncol Biol Phys* 2008;71:801–812.

[61] Madsen BL, Hsi RA, Pham HT, *et al.* Intrafractional stability of the prostate using a stereotactic radiotherapy technique. *Int J Radiat Oncol Biol Phys* 2003;57:1285–1291.

[62] Kupelian PA, Willoughby TR, Meeks SL, *et al.* Intraprostatic fiducials for localization of the prostate gland: monitoring intermarker distances during radiation therapy to test for marker stability. *Int J Radiat Oncol Biol Phys* 2005;62:1291–1296.

[63] de Crevoisier R, Lagrange JL, Messai T, *et al.* Prostate localization systems for prostate radiotherapy. *Cancer Radiother* 2006;10:394–401.

[64] Smitsmans MHP, De Bois J, Sonke J-J, *et al.* Automatic prostate localization on cone-beam CT scans for high precision image-guided radiotherapy. *Int J Radiat Oncol Biol Phys* 2005;63:975–984.

[65] Kupelian PA, Langen KM, Zeidan OA, *et al.* Daily variations in delivered doses in patients treated with radiotherapy for localized prostate cancer. *Int J Radiat Oncol Biol Phys* 2006;66:876–882.

[66] Wilder RB, Chittenden L, Mesa AV, *et al.* A prospective study of intrafraction prostate motion in the prone vs. supine position. *Int J Radiat Oncol Biol Phys* 2010;77:165-170.

[67] Stroom JC, Koper PCM, Korevaar GA, *et al*. Internal organ motion in prostate cancer patients treated in prone and supine treatment position. *Radiother Oncol* 1999;51:237–248.

[68] Lebesque JV, Bruce AM, Kroes APG, *et al*. Variation in volumes, dose-volume histograms, and estimated normal tissue complication probabilities of rectum and bladder during conformal radiotherapy of T3 prostate cancer. *Int J Radiat Oncol Biol Phys* 1995;33:1109 –1119.

[69] Antolak JA, Rosen II, Childress CH, *et al*. Prostate target volume variations during a course of radiotherapy. *Int J Radiat Oncol Biol Phys* 1998;42:661– 672.

[70] Crook JM, Raymond Y, Salhani D, *et al*. Prostate motion during standard radiotherapy as assessed by fiducial markers. *Radiother Oncol* 1995;37:35– 42.

[71] Tinger A, Michalski JM, Cheng A, *et al*. A critical evaluation of the planning target volume for 3-D conformal radiotherapy of prostate cancer. *Int J Radiat Oncol Biol Phys* 1998;42:213–221.

[72] Roeske JC, Forman JD, Mesina CF, *et al*. Evaluation of changes in the size and location of the prostate, seminal vesicles, bladder, and rectum during a course of external beam radiation therapy. *Int J Radiat Oncol Biol Phys* 1995;33:1321–1329.

[73] Turner SL, Swindell R, Bowl N, *et al*. Bladder movement during radiation therapy for bladder cancer: Implications for treatment planning. *Int J Radiat Oncol Biol Phys* 1997;39:355–360.

[74] Miralbell R, Nouet P, Rouzaud M, *et al*. Radiotherapy of bladder cancer: Relevance of bladder volume changes in planning boost treatment. *Int J Radiat Oncol Biol Phys* 1998;41:741–746.

[75] Nichol AM, Brock KK, Lockwood GA, *et al.* A magnetic resonance imaging study of prostate deformation relative to implanted gold fiducial markers. *Int J Radiat Oncol Biol Phys* 2007;67:48–56.

[76] Beard CJ, Kijewski P, Bussiere M, *et al.* Analysis of prostate and seminal vesicle motion: Implications for treatment planning. *Int J Radiat Oncol Biol Phys* 1996;34:451–458.

[77] de Crevoisier R, Melancon AD, Kuban DA, *et al.* Changes in the pelvic anatomy after an IMRT treatment fraction of prostate cancer. *Int J Radiat Oncol Biol Phys* 2007;68:1529–1536.

[78] Boda-Heggemann J, Kohler FM, Wertz H, *et al.* Intrafraction motion of the prostate during an IMRT session: A fiducial based 3D measurement with Cone-beam CT. *Radiat Oncol* 2008;3:37.

[79] Smeenk RJ, Teh BS, Butler EB, van Lin ENJTh, Kaanders JHAM. Is there a role for endorectal balloons in prostate radiotherapy? A systematic review. *Radiother Oncol* 2010;95:277-282.

[80] Wang K, Vapiwala N, Scheuermann R, *et al.* Comprehensive study on real-time prostate gland motion between patient groups undergoing radiotherapy with and without daily endorectal balloon [Abstract]. *Int J Radiat Oncol Biol Phys* 2010;78:S683.

[81] El-Bassiouni M, Davis JB, El-Attar I, Studer GM, Lutolf UM, Ciernik IF. Traget motion variability and on-line positioning accuracy during external-beam radiation therapy of prostate cancer with an endorectal balloon device. *Strahlenther Onkol* 2006;182:531-536.

[82] Van Lin ENJTh, Hoffmann AL, van Kollenburg P, Leer JW, Visser AG. Rectal wall sparing effect of three different endorectal balloons in 3D conformal and IMRT prostate radiotherapy. *Int J Radiat Oncol Biol Phys* 2005;63:565-576.

[83] Van Lin ENJTh, van der Vight LP, Witjes JA, Huisman HJ, Leer JW, Visser AG. The effect of an endorectal balloon and off-line correction on the interfraction systematic and random prostate position variations: a comparative study. *Int J Radiat Oncol Biol Phys* 2005;61:278-288.

[84] Wachter S, Gerstner N, Dorner D, *et al.* The influence of a rectal balloon tube as internal immobilization device on variations of volumes and dose-volume histograms during treatment course of conformal radiotherapy for prostate cancer. *Int J Radiat Oncol Biol Phys* 2002;52:91–100.

[85] Teh BS, McGary JE, Dong L, *et al.* The use of rectal balloon during the delivery of intensity modulated radiotherapy (IMRT) for prostate cancer: more than just a prostate gland immobilization device? *Cancer J* 2002;8:476–83.

[86] Teh BS, Woo SY, Mai WY, *et al.* Clinical experience with intensity-modulated radiation therapy (IMRT) for prostate cancer with the use of rectal balloon for prostate immobilization. *Med Dosim* 2002;27:105–13.

[87] Ciernik IF, Baumert BG, Egli P, Glanzmann C, Lütolf UM. On-line correction of beam portals in the treatment of prostate cancer using an endorectal balloon device. *Radiother Oncol* 2002;65:39–45.

[88] Patel RR, Orton N, Tomé WA, Chappell R, Ritter MA. Rectal dose sparing with a balloon catheter and ultrasound localization in conformal radiation therapy for prostate cancer. *Radiother Oncol* 2003;67:285–94.

[89] Sanghani MV, Ching J, Schultz D, *et al.* Impact on rectal dose from the use of a prostate immobilization and rectal localization device for patients receiving dose escalated 3D conformal radiation therapy. *Urol Oncol* 2004;22:165–8.

[90] Hille A, Schmidberger H, Töws N, Weiss E, Vorwerk H, Hess CF. The impact of varying volumes in rectal balloons on rectal dose sparing in conformal radiation therapy of prostate cancer.A prospective three-dimensional analysis. *Strahlenther Onkol* 2005;181:709–16.

[91] Vlachaki MT, Teslow TN, Amosson C, Uy NW, Ahmad S. IMRT versus conventional 3DCRT on prostate and normal tissue dosimetry using an endorectal balloon for prostate immobilization. *Med Dosim* 2005;30:69–75.

[92] Elsayed H, Bölling T, Moustakis C, *et al.* Organ movements and dose exposures in teletherapy of prostate cancer using a rectal balloon. *Strahlenther Onkol* 2007;183:617–24.

[93] Van Lin EN, Kristinsson J, Philippens ME, *et al.* Reduced late rectal mucosal changes after prostate three-dimensional conformal radiotherapy with endorectal balloon as observed in repeated endoscopy. *Int J Radiat Oncol Biol Phys* 2007;67:799–811.

[94] McGary JE, Grant III W. A clinical evaluation of setup errors for a prostate immobilization system. *J Appl Clin Med Phys* 2000;1:138–47.

[95] Teh BS, Mai WY, Uhl BM, *et al.* Intensity-modulated radiation therapy (IMRT) for prostate cancer with the use of a rectal balloon for prostate immobilization: acute toxicity and dose-volume analysis. *Int J Radiat Oncol Biol Phys* 2001;49:705–12.

[96] D'Amico AV, Manola J, Loffredo M, *et al.* A practical method to achieve prostate gland immobilization and target verification for daily treatment. *Int J Radiat Oncol Biol Phys* 2001;51:1431–6.

[97] McGary JE, Teh BS, Butler EB, Grant III W. Prostate immobilization using a rectal balloon. *J Appl Clin Med Phys* 2002;3:6–11.

[98] Miralbell R, Molla M, Rouzaud M, *et al.* Hypofractionated boost to the dominant tumor region with intensity modulated stereotactic radiotherapy for prostate cancer: A sequential dose escalation pilot study. *Int J Radiat Oncol Biol Phys* 2010;78:50-57.

[99] Miralbell R, Molla M, Arnalte R, *et al.* Target repositioning optimization in prostate cancer: is intensity-modulated radiotherapy under stereotactic conditions feasible? *Int J Radiat Oncol Biol Phys* 2004;59:366-371.

[100] Woel R, Beard C, Chen MH, *et al.* Acute gastrointestinal, genitourinary, and dermatological toxicity during dose-escalated 3D-conformal radiation therapy (3DCRT) using an intrarectal balloon for prostate gland localization and immobilization. *Int J Radiat Oncol Biol Phys* 2005;62:392–6.

[101] Zellars RC, Roberson PL, Strawderman M, *et al.* Prostate position late in the course of external beam therapy: patterns and predictors. *Int J Radiat Oncol Biol Phys* 2000;47:655-660.

III. TREATMENT PLANNING FOR STEREOTACTIC IRRADIATION OF PROSTATE CANCER. TWO APPROACHES TO SPARE THE RECTUM AND THE BLADDER FROM HIGH DOSES OF IRRADIATION

3.1. Introduction

We have showed in section II that for prostate SBRT a well-defined planning target volume can be achieved with 3-mm margins around the CTV. The main purpose of this section was to evaluate the contribution of two original approaches in order to spare the rectum and the bladder from high doses:

1) a "lower" dose prescribed to the whole prostate with a higher dose delivered to the simultaneous integrated boost (SIB) into the macroscopic tumor.

2) with an injection of hyaluronic acid between the prostate and the rectum – with the intention to drastically restrict the dose to the rectum.

Several major aspects of the treatment planning will be described and evaluated for prostate SBRT, as recommended by the AAPM Task Group 101 [1]:

- The prescription of the dose and the number of treatment fractions;
- The PTV coverage;
- Hotspots within the target;
- The dose to the organs at risk (the bladder and the rectum);
- The beam energy and the number of beams;
- The evaluation of the plan with various and specific indices(e.g., the conformity index, homogeneity index);
- The evaluation of the gradient describing the dose fall-off outside the target (using the gradient index).

3.2. Prostate SBRT with simultaneous-integrated boost into the tumor

3.2.1. Rationale for a simultaneous-integrated boost irradiation

It appears that the local recurrence of the prostate cancer after radiotherapy occurs often at the same site as the primary tumor before irradiation [2-10].

There are two studies that initially demonstrated the recurrence of the tumor inside the prostate after radiotherapy with the use of imaging modalities [2, 3]. Cellini *et al.* used the

transrectal ultrasonography (TRUS) and MRI for the detection of the tumor sites and concluded on local recurrences at the site of primary disease in 12 out of 12 patients treated with radiotherapy [2]. The authors didn't give any information about the histopathology results before or at recurrence. Moreover, the sensitivity and specificity of the TRUS technique are very low and not accurate for the diagnosis of the tumor mass or in screening for prostate cancer [11-14]. Pucar *et al.* acquired only MRI exams for 9 patients before and after irradiation and the results established by pathology findings from salvage radical prostatectomy confirmed that 100% of patients had local recurrences of prostate cancer [3].

In 2012, three new studies on local recurrence of prostate cancer appear to encourage a focal boost irradiation:

- Groenendaal *et al.* published their results based on the development of a logistic regression model for the prediction of the presence of the tumor on a voxel level in the peripheral zone of the prostate. They found a high diagnostic performance and objective interpretation of the functional MR images for tumor delineations and encouraged the utility of this model for focal boost therapy of the prostate [15].
- Arrayeh *et al.* determined that dominant recurrent tumor was at the same location as dominant baseline tumor in 8 of 9 patients (89%) that were treated with radiotherapy with a mean dose of 75.9 Gy (range, 75-79 Gy) [4]. They used longitudinal MR imaging and MR spectroscopic imaging to evaluate the position of the tumor before and after the recurrence. Their results encourage a schema of integrated boost treatment into the dominant tumor at baseline (before irradiation), therefore improving the tumor control [4].
- Chopra *et al.* found that local recurrence after RT predominantly occurs in regions with higher histological tumor density but also in other locations, using TRUS at diagnosis and T2-MR image, apparent diffusion coefficient (ADC) map dynamic contrast enhanced (DCE) images at time of biochemical failure [7]. The authors encouraged the design of clinical trials that should prescribe doses to subregions of the prostate, but advise preventative measures against the start of focal-only irradiation to the visible tumors or to considerable increase the dose to the uninvolved prostate gland [7].

Consequently, the results of these studies suggest that an additional dose escalation might be required to improve the long term local control [16-21]. The purpose of this chapter is two-folded:

- To assess the number of fields and the beam energy for a stereotactic irradiation of the prostate cancer with a simultaneous integrated boost (SIB), using different quantitative indexes.
- To compare a prostate SBRT-SIB approach *versus* a SBRT irradiation of the whole prostate, in order to limit the dose to the rectum and to the bladder;

3.2.2. The effect of beam number and the choice of beam energy

For stereotactic body radiation therapy a large beam number is one of the key methods to obtain a higher conformity of the dose and to attain a rapid fall-off outside the target. There are several reasons to use an increased number of beams. One is the reduction of the entrance dose that is required especially for high doses per fraction. Though, the number of beams should be reasonable in the everyday practice. Another aspect that has an effect on the dose fall-off is the beam energy. High energies could affect the beam penumbra in a SBRT technique.

3.2.2.1. Evaluation of a SBRT plan with different indices

The evaluation of a SBRT plan or the comparison between different plans can be made using various indices: the conformity index (CI), the gradient index (GI) and the homogeneity index (HI). The level of conformity, the GI (the fall-off) and the HI are not always mentioned for the evaluation of a prostate SBRT plan. Hence, no specific values exist for the GI of prostate SBRT.

a) The conformity index (CI)

Shaw *et al.* first described the conformity index in 1993 in the RTOG guidelines for the radiosurgery quality assurance [22]. They initially defined it as the volume of the prescription isodose divided by the volume of the target:

$$Conformity\ Index_{RTOG} = \frac{Prescription\ Isodose\ Volume\ (PIV)}{Target\ Volume\ (TV)}$$

This conformity index formula was mainly reported in the literature for brain radiosurgery [23-27], but also for prostate and other localizations [28-32]. However, other studies have described additional methods for calculating the CI [33, 34]. These studies are well summarized in a critical review by Feuvret *et al.* [33, 34]:

Example 1:

$$Conformity\ Index_{SALT} = \frac{Target\ Volume\ covered\ by\ the\ Reference\ Isodose\ (TV_{RI})}{Target\ Volume\ (TV)}$$

Example 2 – Conformity index for healthy tissues:

$$Conformity\ Index_{Lomax} = \frac{Target\ Volume\ covered\ by\ the\ Reference\ Isodose\ (TV_{RI})}{Volume\ of\ the\ Reference\ Isodose\ (V_{RI})}$$

Example 3 – Global conformity index or conformation number (CN) (which gives information about both, target volume coverage and irradiation of organs at risk):

$$Conformation\ Number_{van't\ Riet} = \frac{TV_{RI}}{TV} \times \frac{TV_{RI}}{V_{RI}}$$

b) The homogeneity index (HI) or dose heterogeneity

The homogeneity index, also noted MDPD, is described by RTOG as the ratio of the maximum dose (MD) divided by the prescription dose (PD) [22, 35] and was used for plan evaluation for various localizations [24, 26, 36-38]:

$$Homogeneity\ Index_{RTOG} = \frac{Maximum\ Dose\ within\ the\ targe\ (MD)}{Prescription\ Dose\ (PD)}$$

The HI is also named "heterogeneity index" and is described by AAPM/TG101 as the ratio of the highest dose received by 5% of PTV to lowest dose received by 95% of PTV [1]. The homogeneity index (or dose inhomogeneity) was moreover calculated by other teams with the following formula:

$HI = (D_{5\%} - D_{95\%})/D_{mean}$ for prostate cancer [39] and ethmoid sinus [29], or

$HI = (D_{2\%} – D_{98\%})/D_P$ for intracranial radiosurgery,

where $D_{i\%}$ being the dose received by *i%* of the PTV.

c) The gradient index (GI)

It is known that high beam energies give large penumbra and therefore the dose gradient is expanded wide of the target. If the hot spots into the tumor are even required, then the wide gradients are undesirable. In 2006, Paddick and Lippitz proposed a dose gradient index (GI) for the evaluation of the radiosurgery plans for the treatment of vestibular schwannoma [40].

The gradient index is intended for the comparison of several treatment plans that have identical conformity index, but different dose gradients. The gradient dose can make the difference between equal plans and could verify which of the plans (or the prescription

isodoses) gives the sharpest dose fall-off gradient encompassing the target [40]. Paddick and Lippitz defined the GI as:

$$Gradient\ Index = \frac{The\ Volume\ of\ 50\%\ of\ Prescription\ Isodose}{The\ Volume\ of\ the\ Prescription\ Isodose}$$

They affirmed that this index "*can be used for any prescription isodose*". For example, if a plan is normalized to the 80% isodose, than the GI is the volume of the 40% isodose divided by the volume of the 80% isodose: GI = $V_{40\%}/V_{80\%}$. One of the advantages of the GI is that it can be used as an objective evaluation between different conformal plans, no matter the isodose used for normalization.

3.2.3. Publication

Herein, we describe our dosimetric experience with comparison studies that were performed with the purpose of assessing the number of beams and the beam energy for a stereotactic irradiation of prostate cancer with an integrated boost.

The comparison between plans was made using:

- Different parameters from the dose-volume histogram: mean dose (MD), maximum dose (MaxD), dose (D_i) received by a certain volume of an organ and the volume (V_i) of an organ that receives a certain dose or isodose (in percentage or in cubic centimeters);

- Different quantitative indices: the conformity index (CI), the homogeneity index (HI), the gradient index (GI).

The initial results were accepted for poster presentation at the SFPM meeting (5-7 June 2013) in Nice, France (Appendix 7). The related article is presented below.

The effect of the number of fields and beam energy on a stereotactic irradiation of prostate cancer with simultaneous integrated boost into the dominant intraprostatic lesion.
An evaluation with various indices

Corina UDRESCU, M.S.[1-2], Olivier CHAPET, M.D., PH.D.[1], Ronan TANGUY, M.D.[1], Marie-Pierre SOTTON, M.S.[2] and Patrice JALADE, PH.D.[2]

[1]Department of Radiation-Oncology, Centre Hospitalier Lyon Sud, Pierre-Bénite, France
[2]Department of Medical Physcis, Centre Hospitalier Lyon Sud, Pierre-Bénite, France

.

Département de Radiothérapie - Oncologie
Centre Hospitalier Lyon Sud
165, Chemin du Grand Révoyet
69495, PIERRE BENITE Cedex
FRANCE
Tel 00 33 4 78 86 42 51
Fax 00 33 4 78 86 42 65
E-mail: corina.udrescu@hotmail.com

Running title: Beam and energy for prostate SBRT-SIB

Conflict of interest: none.

Abstract

Purpose: The impact of the number of fields and beam energy was evaluated for prostate stereotactic body radiotherapy (SBRT) with a simultaneous-integrated boost (SIB) into the dominant-intraprostatic lesion (DIL).

Methods and Materials: Nine IMRT patients were used for prostate SBRT (5x6.5Gy) with a SIB (5x8Gy) into the DIL. The prostate and the tumor were delineated using an image registration between the computed tomography scan and the magnetic resonance acquisition. Three plans were created per patient with 7-, 9- and 11-fields and the beam energy of 16MV. A 7-field plan was first optimized and calculated. Subsequently, the 9- and 11-field arrangements were generated using identical optimization parameters. Moreover, a comparison between two energies (6MV vs. 16MV) was made for a 9-field technique. Whenever needed, the optimization parameters were modified to achieve the protocol's requirements. The plans were evaluated and compared using the conformity, the gradient and the homogeneity indices and the dose-volume histogram (DVH) parameters.

Results: The volume of the 5Gy isodose increased with the number of fields and the volume of the 10Gy isodose decreased with the number of fields. The volume of the 5Gy isodose didn't differ between energies ($p=0.06$), but the volume of the 10Gy isodose decreased significantly for 16MV ($p=0.002$). With comparable evaluation indices for both plans (6MV and 16MV), the 100% isodose coverage for the tumor decreased with an average of 5% for 16MV.

Conclusions: The fields' number and beam energy should be carefully selected for SBRT-SIB, as may result in a volume increase of low doses. However, clinical studies must validate the consequence of this issue. Additionally, the SBRT-IMRT combination results in a higher number of MUs and therefore the treatment duration could increase.

Keywords: Prostate cancer, Stereotactic body radiation therapy, Intensity-modulated radiation therapy, Simultaneous-integrated boost, dominant intraprostatic lesion, Beam and energy.

Introduction

Prostate cancer may have one or more dominant intraprostatic lesions, clinically visible on MRI, and secondary tumors that might not be detectable using the imaging methods. This made complex the safe development of a focal treatment irradiation and a whole prostate irradiation seemed more reasonable. Moreover, local recurrence after radiotherapy for localized prostate cancer often occurs at the site of primary dominant intraprostatic lesion (DIL) (1-4). This suggests that the control of microscopic cancer cells might require "reasonable" irradiation doses and the control of the macroscopic tumor might require higher doses (2).

Additional studies recommend that selective concomitant boost dose escalation should be delivered at the region of the visible tumor and could improve the tumor control probability (TCP) (5-7). Because of the rapid development of imaging for the detection of the intraprostatic lesions with magnetic resonance (MR) modalities (8-17) or 11C-Choline positron emission computed tomography scans (PET-CT) (18, 19), a focal irradiation is possible.

Several teams have reported results with a simultaneously integrated boost (SIB) into the DIL using intensity-modulated radiation therapy (IMRT) with conventional fractionation up to 90Gy (20-26). As it was suggested that this dose might not be high enough for long term prostate tumor control (27), SBRT-SIB delivery to the DIL has been recently reported (6, 28).

Stereotactic body radiation therapy (SBRT) in 5 fractions has been developed in the past years for the treatment of low- to intermediate-risk prostate cancer showing promising results in terms of local control (90% to 100% for doses between 6.7 Gy and 10 Gy per fraction) (29-36). SBRT doses for prostate cancer are usually delivered using a ring gantry helical accelerator (29), a robotic-arm system (30-34) and a standard accelerator with IMRT or custom blocking (29, 35, 36). Therefore, a combination of the two approaches (SBRT-SIB) could increase the tumor control while sparing the surrounding organs from higher doses (28).

On the other hand, the choice of a greater number of beams is recommended for SBRT (37) and should provide higher dose conformity and sharper dose fall-off outside the target. There are other reasons for using an increased number of beams for a stereotactic treatment. One reason is the reduction of the entrance dose, required especially for high doses per fraction. But the number of beams should be reasonable in the everyday practice. Another factor that has an effect on dose fall-off is the beam energy, because high energies for SBRT could affect the beam penumbra.

As part of a protocol in our department, the impact of the number of fields and of beam energy was evaluated for prostate SBRT with a simultaneous integrated boost into the dominant intraprostatic lesion, using different indices and dose-volume histogram (DVH) parameters.

Methods and Materials

Patients and technique

Nine IMRT plans were designed for a SBRT delivery (5 x 6.5 Gy) into the prostate with a SIB (5 x 8 Gy) to the dominant intraprostatic lesion. The prostate and the tumor were delineated using an image registration (Integrated Registration® software, GE Medical Systems) between the computed tomography scan and the magnetic resonance acquisition. The plans were created using Eclipse (Varian, Palo Alto) treatment planning system, version 10.0.28 and calculated with the Anisotropic Analytical Algorithm (AAA) for a 5-mm multileaf collimator.

Evaluation of fields' number

Three plans were created for each of the 9 prostate cases with different non-opposing field arrangements (7, 9 and 11) and beam energy of 16 MV. A 7-field plan (7F) was first optimized and calculated with specific criteria established for the protocol:

- The PTV1 was equal to 3-mm uniform margin around the prostate and the PTV2 was equal to 5-mm margin around the tumor and 3 mm posterior.
- The prescription was made on the 95% isodose line for PTV1 and 95% for PTV2 that had to cover at least 97% of the target volumes. Moreover, the 100% isodose lines for PTV1 and PTV2 had to cover at least 90% of the target volumes.
- The maximum dose didn't have to exceed 107% of the prescribed dose.
- The rectal- and bladder-wall were delineated with an internal expansion of 5 mm and 7 mm, respectively.
- The doses to the organs at risk (rectal- and bladder-wall) were optimized as low as possible while there are no guidelines for prostate SBRT.
- Sharp dose fall-off parameters were introduced in Eclipse TPS for the plan optimization and normal tissue objective (Table 1).

The first plan was always validated by a radiation oncologist ("the author"), specialist in prostate cancer. Subsequently, additional fields were inserted to the first plan in order to create the 9-field (9F) and 11-field (11F) arrangements. Identical optimization parameters were used for all three plans and were optimized with 300 iterations before plan calculation.

Small PTV margins (few millimeters) are recommended for a stereotactic irradiation (38) (which account for the inter- and intrafraction motion) and were selected for the present study as three intraprostatic gold markers are used for: a) a daily repositioning of the patient with image-guided systems (On Board Imager® from Varian or ExacTrac® from BrainLab) and b) the real-time monitoring of the target with the Snap Verification® tool (BrainLab).

Evaluation of beam energy

The protocol was subsequently used for 5 patients for plan comparison with two energies (6MV vs. 16MV) for a 9-field technique. Whenever needed, the optimization parameters were gradually modified to obtain the protocol's requirements as mentioned above (e.g., the coverage of the prescription dose). Both plans were optimized with 300 iterations before plan calculation.

Comparison method and statistics

A SBRT plan or the comparison between different plans can be evaluated using DVH parameters and/or various indices: the conformity index (CI), the gradient index (GI), the homogeneity index (HI). The level of conformity, the GI (fall-off) and the HI are rarely mentioned for the evaluation of a prostate SBRT plan (39).

However, in the current study, the comparison between plans was made with the evaluation of:

- Different conformity indices described by four groups and resumed by Feuvret et al. (40): CI_{RTOG} (prescription isodose volume/target volume) (41), CI_{SALT} (target volume covered by the reference isodose/target volume) (42), CI_{Lomax} (target volume covered by the reference isodose/volume of the reference isodose) (43) and $CI_{van'tRiet}$ (CI_{SALT} x CI_{Lomax}) (44);
- The gradient index (the volume of 50% of prescription isodose/volume of the prescription isodose) (45);
- The homogeneity index described by RTOG (MDPD = maximum dose /prescription dose) (41);

- The homogeneity index described by AAPM/TG101 as ($D_{5\%}$ - $D_{95\%}$)/D_{mean}, where $D_{i\%}$ is the dose received by i% of the target and D_{mean} is the average dose to the target (38).
- The entrance dose to the patient calculated using the treatment planning system for each field, at 5 mm from patient's skin, at the beam axis;
- The monitor units (MU) for each field;
- The maximum dose (Dmax) and the doses (in Gy) received by 2 cc (D2cc), 5 cc (D5cc), 10 cc (D10cc) and 25 cc (D25cc) of the volume of the organs at risk (rectal- and bladder-wall);
- The volumes (in percentage) of the rectal- and bladder-wall that receive the *i%* isodose ($V_{i\%}$).

The statistical analysis of the quantitative variables was performed using the student paired t-test. The analysis was made with a significance threshold set at $p<0.05$. The diagrams were created using the SPSS V19.0 software.

Results

The average (range) volumes delineated for all patients were of 82cc (range 54.5-145cc) for PTV1 and of 15cc (range 7.9-27.2cc) for PTV2. Because of the integrated boost into the prostate, the gradient index was calculated only for PTV1.

The number of fields

With similar PTV coverage all indices used for the evaluation were similar between the three plans (Table 2). The DVH comparison between the three plans is showed in Figure 1.

The average (±SD) values for the entrance dose received for every field and plan were of 7.8±1.7Gy, 6.3±1.2Gy and 5.8±1.2Gy for 7F, 9F and 11F, respectively. As expected, the mean (±SD) values per field for the monitor units decreased significantly as the number of fields increased and were of 480±89, 386±57 and 323±57 for 7F, 9F and 11F, respectively (7vs9, p=0.0001 and 9vs11, p<0.0001). However, the average (range) values for the total number of monitor units per plan didn't differ: 3357 (range 2741-4019), 3477 (range 3241-3873) and 3558 (range 3111-4323) for 7F, 9F and 11F, respectively (7vs9, p=0.17 and 9vs11, p=0.31).

The average (±SD) doses received by 2cc, 5cc, 10cc and 25cc of the rectal-wall were of 33.7±2.4Gy, 25.8±9.2Gy, 16.7±3.2Gy and 4.8±3.6Gy for 7F, of 33.2±2.6Gy, 24.7±3.7Gy,

15.8±3.3Gy and 4.7±3.4Gy for 9F, and of 33.1±2.8Gy, 24.5±3.8Gy, 15.1±3.2Gy and 4.3±3.1Gy for 11F, respectively. The average rectal-wall Dmax was 41Gy (range 39.9-41.9Gy), 41.1Gy (range 39.6-42.1Gy) and 41Gy (range 39.6-41.8Gy) for 7F, 9F and 11F, respectively.

The average doses received by 2cc, 5cc, 10cc and 25cc of the bladder-wall were of 28.9±3.9Gy, 21.5±6.3Gy, 13.9±7.3Gy and 4.9±4.7Gy for7F, of 28.8±3.9Gy, 21.3±6.4Gy, 13.6±7.1Gy and 5±4.9Gy for 9F and of 28.7±3.8Gy, 21.1±6.4Gy, 13.5±7.1Gy and 4.8±4.5Gy for11F, respectively. The average bladder-wall Dmax was 37.2Gy (range 33.8-41.1Gy), 37Gy (range 34-41Gy) and 36.9Gy (range 34-40.4Gy) for 7F, 9F and 11F, respectively.

Average and range values for $V_{100\%}$, $V_{90\%}$, $V_{80\%}$, $V_{70\%}$, $V_{50\%}$, $V_{47.5\%}$ and $V_{30\%}$ are presented in Table 3 for rectal- and bladder-wall and for the three plans (7F, 9F and 11F).

The volume of the 5Gy isodose increased with the number of fields by an average (range) of 9.1% (range 3.9-11.6%) for 7F vs 9F (p=0.0001) and by 5.8% (range 3.5-8.3%) for 9F vs 11F (p=0.0001) (Figure 2, left). On the contrary, the volume of the 10Gy isodose decreased with the number of fields by an average (range) of 18.4% (range 10.2-23.8%) for 7F vs 9F (p=0.0001) and by 7.5% (range 4.5-11.1%) for 9F vs 11F (p=0.0001) (Figure 2, right).

Evaluation of beam energy

With comparable evaluation indices for both plans (6MV and 16MV), the 100% isodose coverage for the tumor decreased with an average (range) of 5% (range 4-7%) for 16MV (Table 4). A typical DVH for an IMRT-SIB plan is illustrated in Figure 3.

The average (±SD) entrance doses received for every field and plan were of 9.1±2Gy and 6.2±1.3Gy for 6MV and 16MV, respectively. The mean (±SD) values per field for the monitor units were 476±75 and 392±55 for 6MV and 16MV, respectively. Moreover, the average (range) values for the total number of MU per plan were 4283 (range 4097-4516) and 3531 (range 3245-3735) for 6MV and 16MV, respectively and significantly differed between the two plans (p=0.002).

The average doses received by 2cc, 5cc, 10cc and 25cc of the rectal-wall were of 32.2±1.7Gy, 22.5±1.5Gy, 13.8±1.4Gy and 3.9±2.8Gy for 6MV and of 32.6±2.3Gy, 23.4±2.1Gy, 14.2±1.5Gy and 3.9±2.9Gy for 16MV, respectively. The average (range) rectal-wall Dmax was 41.4Gy (range 40.9-42.2Gy) and 40.7Gy (range 39.8-41.4Gy) for 6MV and 16MV, respectively.

The average doses received by 2cc, 5cc, 10cc and 25cc of the bladder-wall were of 29.3±2.5Gy, 19.4±2.9Gy, 11.4±3.7Gy and 2.2±0.4Gy for 6MV and of 29±2.8Gy, 19.4±3.6Gy, 11.5±3.6Gy and 2.2±0.7Gy for 16MV, respectively. The average (range) bladder-wall Dmax was 37.7Gy (range 34.7-40.8Gy) and 37.2Gy (range 34-40.4Gy) for 6MV and 16MV, respectively.

Average and range values for $V_{100\%}$, $V_{90\%}$, $V_{80\%}$, $V_{70\%}$, $V_{50\%}$, $V_{47.5\%}$ and $V_{30\%}$ are presented in Table 5 for rectal- and bladder-wall and for both plans (6MV and 16MV).

The volume of the 5Gy isodose didn't vary among plans (p=0.06) and the difference between 6MV and 16MV remained little with an average of 2.5% (range 0.6-4%) (Figure 4, left). On the other hand, the volume of the 10Gy isodose decreased significantly for 16MV (p=0.002) by an average value of 28.4% (range 23.9-34.5%) (Figure 4, right).

Discussion

Recently, Aluwini et al. reported biochemical control rates and results on toxicities for 50 patients treated with SBRT to a total dose of 38Gy in 4 fractions to the whole prostate and an integrated boost to 11Gy per fraction to the DIL (28). With a median follow-up of 23 months the 2-year actuarial biochemical control rate was 100%. The grade 2 and 3 gastrointestinal (GI) acute toxicities were seen in 12% and 2%, respectively. The late grade 2 GI toxicity was 3% during 2 years. Genitourinary (GU) grade 2, 3 toxicities were reported on 15%, 8% in the acute phase and 10%, 6% in the late phase, respectively (28). The authors suggested that a SBRT-SIB irradiation is feasible with low acute and late GU and GI toxicities (28). While the SBRT treatment was delivered using the Cyberknife® in the study of Aluwini et al., a standard accelerator can be used to deliver such treatment (29, 35, 36).

Number of fields and beam energy

The number of fields and the choice of beam energy in IMRT have been previously evaluated for a whole-irradiation of deep-seated targets (46) and for a SIB-DIL approach (24). To our knowledge, a comparison between different plans (high number of fields and energy) for a SBRT-SIB irradiation with a standard accelerator and using specific variables has never been performed.

In the study of Pirzkall et al., the authors concluded that for an IMRT homogeneous dose to the whole prostate the use of 6MV photons with at least 9 fields is comparable with the use of 18MV (46). In 2011, Ost et al. described a planning comparison study on 12 patients for a prostate irradiation with simultaneous integrated boost (24). They compared

results for 3, 5 and 7 IMRT fields with a volumetric irradiation and two different energies (6MV and 18MV). The authors didn't find any difference between energies, except for a decrease in the number of MUs for 18MV. However, they noted that increasing the number of fields allows a dose escalation to the DIL (24).

In the current study, no significant differences were found between plans in terms of DVH parameters or evaluation indices, except for the low doses (Figure 2). Furthermore, no major difference was observed between energies for PTV1 coverage, except for the volume of the SIB (PTV2) that had to be covered by the 100% isodose, which decreased by an average value of 5% and with a maximum difference up to 7% for one patient. Dose inhomogeneity within the PTV1 as a consequence of the penumbra of the PTV2-SIB volume was accepted and reported in Tables 2 and 4.

Careful attention should be considered for the choice of the number of fields and of the beam energy in terms of volume of low doses (Figures 2 and 4) which become important for a SBRT approach. Additionally, the SBRT-IMRT combination results in a higher number of MUs and therefore the treatment duration would increase.

We acknowledge that NTCP should be furthermore studied for healthy tissues although for a simultaneous integrated boost these values are patient dependent (based on each DIL location). For six prostate cancer patients, Nutting et al. compared a whole prostate irradiation (70Gy in 2Gy fractions) to a dose escalation to the dominant intraprostatic tumor nodule (DIPTN) of 90Gy and the remainder of the PTV treated with 70Gy (23). The authors reported a predicted TCP gain up to 27.5% (range 11.4-47.9%) for a α/β ratio of 1.49Gy when a DIPTN approach is used, for an increase in rectal NTCP with an average value of 1.8% (23). In addition, the authors stated that the NTCP values (or the doses to the organs at risk) depend also on the intraprostatic tumor(s) location compared to the one of the organs at risk.

Conclusion

There wasn't any dosimetric difference between 7, 9 or 11 fields, except for the volume of the 5Gy isodose which increases with the number of fields and for the volume of the 10Gy isodose which decreases with the number of fields. The volume of the 5Gy isodose didn't differ between 6MV and 16MV, but the volume of the 10Gy isodose decreased significantly for 16MV. With comparable evaluation indices for both plans (6MV and 16MV), the 100% isodose coverage for the tumor decreased by an average of 5% for 16MV. The choice of fields' number and beam energy should be selected carefully, as may result in

volume increase of low doses and which remain important for SBRT. However, clinical studies must validate the consequence of this statement.

Following this study, in our department we chose a 9-field conformation and 16MV beam energy as a good compromise for a stereotactic irradiation of prostate cancer with simultaneous integrated boost into the tumor.

Bibliography

1. Arrayeh E, Westphalen AC, Kurhanewicz J, et al. Does local recurrence of prostate cancer after radiation therapy occur at the site of primary tumor? Results of a longitudinal MRI and MRSI study. Int J Radiat Oncol Biol Phys 2012;82:e787-93.

2. Cellini N, Morganti AG, Mattiucci GC, et al. Analysis of intraprostatic failures in patients treated with hormonal therapy and radiotherapy: implications for conformal therapy planning. Int J Radiat Oncol Biol Phys 2002;53:595-9.

3. Chopra S, Toi A, Taback N, et al. Pathological predictors for site of local recurrence after radiotherapy for prostate cancer. Int J Radiat Oncol Biol Phys 2012;82:e441-8.

4. Westphalen AC, Coakley FV, Roach M 3rd, McCulloch CE, Kurhanewicz J. Locally recurrent prostate cancer after external beam radiation therapy: Diagnostic performance of 1.5-T endorectal MR imaging and MR spectroscopic imaging for detection. Radiology 2010;256:485-92.

5. Kim Y, Tome WA. Is it beneficial to selectively boost high-risk tumor subvolumes? A comparison of selectively boosting highrisk tumor subvolumes versus homogeneous dose escalation of the entire tumor based on equivalent EUD plans. Acta Oncol 2008;47:906–16.

6. Miralbell R, Mollà M, Rouzaud M, et al. Hypofractionated boost to the dominant tumor region with intensity modulated stereotactic radiotherapy for prostate cancer: A sequential dose escalation pilot study. Int J Radiat Oncol Biol Phys 2010;78(Issue 1):50-7.

7. van Lin EN, Futterer JJ, Heijmink SW, et al. IMRT boost dose planning on dominant intraprostatic lesions: Gold marker-based three-dimensional fusion of CT with dynamic contrast enhanced and 1H-spectroscopic MRI. Int J Radiat Oncol Biol Phys 2006;65:291–303.

8. Franiel T, Ludemann L, Taupitz M, Bohmer D, Beyersdorff D. MRI before and after external beam intensity-modulated radiotherapy of patients with prostate cancer: The feasibility of monitoring of radiation-induced tissue changes using a dynamic contrast-enhanced inversion-prepared dual-contrast gradient echo sequence. Radiother Oncol 2009;93:241-5.

9. Groenendaal G, Moman MR, Korporaal JG, et al. Validation of functional imaging with pathology for tumor delineation in the prostate. Radiother Oncol 2010;94:145-50.

10. Groenendaal G, van den Berg CAT, Korporaal JG, et al. Simultaneous MRI diffusion and perfusion imaging for tumor delineation in prostate cancer patients. Radiother Oncol 2010;95:185-90.

11. Kajihara H, Hayashida Y, Murakami R, et al. Usefulness of diffusion-weighted imaging in the localization of prostate cancer. Int J Radiat Oncol Biol Phys 2009;74:399-403.

12. Kim CK, Park BK, Han JJ, Kang TW, Lee HM. Diffusion-weighted imaging of the prostate at 3 T for differentiation of malignant and benign tissue in transition and peripheral zones: preliminary results. J Comput Assist Tomogr 2007;31:449-54.

13. Niaf E, Rouvière O, Mège-Lechevallier F, Bratan F, Lartizien C. Computer-aided diagnosis of prostate cancer in the peripheral zone using multiparametric MRI. Phys Med Biol 2012;57:3833-51.

14. Puech P, Potiron E, Lemaitre L, et al. Dynamic contrast enhanced-magnetic resonance imaging evaluation of intraprostatic prostate cancer: Correlation with radical prostatectomy specimens. Urology 2009;74:1094–9.

15. Villeirs GM, De Meerleer GO, De Visschere PJ, Fonteyne VH, Verbaeys AC, Oosterlinck W. Combined magnetic resonance imaging and spectroscopy in the assessment of high grade prostate carcinoma in patients with elevated PSA: A single-institution experience of 356 patients. Eur J Radiol 2011;77:340–5.

16. Westphalen AC, McKenna DA, Kurhanewicz J, Coakley FV. Role of magnetic resonance imaging and magnetic resonance spectroscopic imaging before and after radiotherapy for prostate cancer. J Endourol 2008;22:789-94.

17. Woodfield CA, Tung GA, Grand DJ, Pezzullo JA, Machan JT, Renzulli 2nd JF. Diffusion-weighted MRI of peripheral zone prostate cancer: comparison of tumor apparent diffusion coefficient with Gleason score and percentage of tumor on core biopsy. AJR Am J Roentgenol 2010;194:W316-22.

18. Chang JH, Lim Joon D, Lee ST, et al. Intensity modulated radiation therapy dose painting for localized prostate cancer using 11C-choline positron emission tomography scans. Int J Radiat Oncol Biol Phys 2012;83(5):e691-6.

19. Van den Bergh L, Koole M, Isebaert S, et al. Is there an additional value of 11C-Choline PET-CT to T2-weighted MRI images in the localization of intraprostatic tumor nodules? Int J Radiat Oncol Biol Phys 2012;83:1486-92.

20. Ares C, Popowski Y, Pampallona S, et al. Hypofractionated boost with high-dose-rate brachytherapy and open magnetic resonance imaging-guided implants for locally aggressive prostate cancer: a sequential dose-escalation pilot study. Int J Radiat Oncol Biol Phys 2009;75:656-63.

21. Fonteyne V, Villeirs G, Speleers B, et al. Intensity-modulated radiotherapy as primary therapy for prostate cancer: Report on acute toxicity after dose escalation with simultaneous integrated boost to intraprostatic lesion. Int J Radiat Oncol Biol Phys 2008;72:799–807.

22. Housri N, Ning H, Ondos J, et al. Parameters favorable to intraprostatic radiation dose escalation in men with localized prostate cancer. Int J Radiat Oncol Biol Phys 2011;80:614-20.

23. Nutting CM, Corbishley CM, Sanchez-Nieto B, Cosgrove VP, Webb S, Dearnaley DP. Potential improvements in the therapeutic ratio of prostate cancer irradiation: dose escalation of pathologically identified tumour nodules using intensity modulated radiotherapy. Br J Radiol 2002;75:151-61.

24. Ost P, Speleers B, De Meerleer G, et al. Volumetric arc therapy and intensity-modulated radiotherapy for primary prostate radiotherapy with simultaneous integrated boost to intraprostatic lesion with 6 and 18 MV: a planning comparison study. Int J Radiat Oncol Biol Phys 2011;79:920-6.

25. Pickett B, Vigneault E, Kurhanewicz J, Verhey L, Roach M. Static field intensity modulation to treat a dominant intra-prostatic lesion to 90 Gy compared to seven field 3-dimensional radiotherapy. Int J Radiat Oncol Biol Phys 1999;44:921–9.

26. Xia P, Pickett B, Vigneault E, Verhey LJ, Roach M 3rd. Forward or inversely planned segmental multileaf collimator IMRT and sequential tomotherapy to treat multiple dominant intraprostatic lesions of prostate cancer to 90 Gy. Int J Radiat Oncol Biol Phys 2001;51:244-54.

27. Eade TN, Hanlon AL, Horwitz EM, Buyyounouski MK, Hanks GE, Pollack A. What dose of external-beam radiation is high enough for prostate cancer? Int J Radiat Oncol Biol Phys 2007;68:682–9.

28. Aluwini S, van Rooij P, Hoogeman M, Kirkels W, Kolkman-Deurloo IK, Bangma C. Stereotactic body radiotherapy with a focal boost to the MRI-visible tumor as monotherapy for low- and intermediate-risk prostate cancer: early results. Radiat Oncol 2013;8:84.

29. Boike TP, Lotan Y, Cho LC, et al. Phase I dose-escalation study of stereotactic radiation therapy for low- and intermediate-risk prostate cancer. J Clin Oncol 2011;29:2020-6.

30. Bolzicco G, Favretto MS, Scremin E, Tambone C, Tasca A, Guglielmi R. Image-guided stereotactic body radiation therapy for clinically localized prostate cancer: preliminary clinical results. Technol Cancer Res Treat 2010;9:473-7.

31. Friedland JL, Freeman DE, Masterson-McGary ME, Spellberg DM. Stereotactic body radiotherapy: An emerging treatment approach for localized prostate cancer. Technol Cancer Res Treat 2009;8:387-92.

32. Jabbari S, Weinberg VK, Kaprealian T, et al. Stereotactic body radiotherapy as monotherapy or post-external beam radiotherapy boost for prostate cancer: Technique, early toxicity, and PSA response. Int J Radiat Oncol Biol Phys 2012;82:228-34.

33. King CR, Brooks JD, Gill H, Presti JC. Long-term outcomes from a prospective trial of stereotactic body radiotherapy for low-risk prostate cancer. Int J Radiat Oncol Biol Phys 2012;82:877-82.

34. Lee YH, Son SH, Yoon SC, et al. Stereotactic body radiotherapy for prostate cancer: A preliminary report. Asia Pac J Clin Oncol 2012 [Epub ahead of print]

35. Madsen BL, Hsi RA, Pham HT, Fowler JF, Esagui L, Corman J. Stereotactic hypofractionated accurate radiotherapy of the prostate (SHARP), 33.5 Gy in five fractions for localized prostate disease: First clinical trial results. Int J Radiat Oncol Biol Phys 2007;67:1099–105.

36. Tang CI, Loblaw DA, Cheung P, et al. Phase I/II study of a five-fraction hypofractionated accelerated radiotherapy treatment for low-risk localized prostate cancer: early results of pHART3. Clinic Oncol 2008;20:729-37.

37. Buyyounouski MK, Price RA, Harris EER, et al. Stereotactic body radiotherapy for primary management of early-stage, low- to intermediate-risk prostate cancer: report of the American Society for Therapeutic Radiology and Oncology emerging technology committee. Int J Radiat Oncol Biol Phys 2010;76:1297-304.

38. Benedict SH, Yenice KM, Followill D, et al. Stereotactic body radiation therapy: the report of AAPM Task Group 101. Med Phys 2010;37:4078-101.

39. Hossain S, Xia P, Huang K, et al. Dose gradient near target-normal structure interface for nonisocentric CyberKnife and isocentric intensity-modulated body radiotherapy for prostate cancer. Int J Radiat Oncol Biol Phys 2010;78:58-63.

40. Feuvret L, Noel G, Mazeron JJ, Bey P. Conformity index: A review. Int J Radiat Oncol Biol Phys 2006;64:333-42.

41. Shaw E, Kline R, Gillin M, et al. Radiation Therapy Oncology Group: radiosurgery quality assurance guidelines. Int J Radiat Oncol Biol Phys 1993;27:1231–9.

42. Lefkopoulos D, Dejean C, El-Balaa H, et al. Determination of dose-volumes parameters to characterise the conformity of stereotactic treatment plans. Proceedings of the 13th International Conference of the Use of Computers in Radiation Therapy. Heidelberg: Springer; 2000;p.356–8.

43. Lomax NJ, Scheib SG. Quantifying the degree of conformity in radiosurgery treatment planning. Int J Radiat Oncol Biol Phys 2003;55:1409-19.

44. van`t Riet A, Mak ACA, Moerland MA, Elders LH, van der Zee W. A conformation number to quantify the degree of conformality in brachytherapy and external beam irradiation: application to the prostate. Int J Radiat Oncol Biol Phys 1997;37:731-6.

45. Paddick I, Lippitz B. A simple dose gradient measurement tool to complement the conformity index. J Neurosurg 2006;105:194-201.

46. Pirzkall A, Carol MP, Pickett B, Xia P, Roach III M, Verhey LJ. The effect of beam energy and number of fields on photon-based IMRT for deep-seated targets. Int J Radiat Oncol Biol Phys 2002;53:434-42.

Table 1. Fall-off parameters used for IMRT optimization.

Parameter	Values for the study
Distance from target border [cm]	0.2
Start dose [%]	95
End dose [%]	47.5
Fall-off	5

Table 2. Average and range values for different variables used for the comparison of the three plans.

Variable	Dose associated to the isodose	Number of beams			t-test
		7F	9F	11F	
PTV coverage					
(P)V95% (%)	30.87 Gy	99.8 (99.5-100)	99.7 (99.3-100)	99.8 (99.3-100)	7vs9 (p=0.25) ; 9vs11 (p=0.58)
(T)V95% (%)	38 Gy	100 (99.9-100)	100 (99.7-100)	100 (99.7-100)	7vs9 (p=0.35) ; 9vs11 (p=0.27)
(P)V100% (%)	32.5 Gy	94.8 (91.8-96.5)	94.1 (91.4-97.1)	93.8 (88.4-97.8)	7vs9 (p=0.24) ; 9vs11 (p=0.6)
(T)V100% (%)	40 Gy	95.3 (92.6-98.7)	94.1 (87.2-99)	91.3 (84.1-97.1)	7vs9 (p=0.14) ; 9vs11 (p=0.09)
3D Dmax (Gy)		42 (41.2-42.8)	42 (41.1-43.3)	41.9 (41.1-43.6)	7vs9 (p=0.87) ; 9vs11 (p=0.42)
Evaluation indexes for the prostate					
(P)GI		3.8 (3.5-4.4)	3.7 (3.6-4)	3.8 (3.5-4.1)	7vs9 (p=0.48) ; 9vs11 (p=0.08)
(P)CI_{RTOG}		1.28 (1.17-1.4)	1.26 (1.17-1.38)	1.27 (1.16-1.39)	**7vs9 (p=0.02)** ; 9vs11 (p=0.49)
(P)CI_{SALT}		0.99 (0.98-1)	0.99 (0.98-1)	0.99 (0.98-1)	7vs9 (p=0.34) ; 9vs11 (p=0.34)
(P)CI_{Lomax}		0.78 (0.71-0.84)	0.79 (0.73-0.85)	0.78 (0.72-0.85)	**7vs9 (p=0.009)** ; 9vs11 (p=0.51)
(P)$CI_{van'tRiet}$		0.77 (0.71-0.84)	0.78 (0.72-0.83)	0.77 (0.72-0.84)	7vs9 (p=0.11) ; 9vs11 (p=1)
(P)HI		0.24 (0.23-0.25)	0.24 (0.23-0.25)	0.24 (0.23-0.25)	7vs9 (p=0.08) ; 9vs11 (p=0.08)
Evaluation indexes for the tumor					
(T)CI_{RTOG}		1.57 (1.33-1.81)	1.52 (1.33-1.7)	1.51 (1.28-1.7)	**7vs9 (p=0.01)** ; 9vs11 (p=0.51)
(T)CI_{SALT}		0.99 (0.99-1)	0.99 (0.99-1)	0.99 (0.98-1)	7vs9 (p=0.16) ; 9vs11 (p=0.16)
(T)CI_{Lomax}		0.64 (0.55-0.75)	0.66 (0.58-0.75)	0.66 (0.58-0.77)	**7vs9 (p=0.01)** ; 9vs11 (p=0.47)
(T)$CI_{van'tRiet}$		0.63 (0.54-0.74)	0.65 (0.58-0.74)	0.65 (0.57-0.76)	**7vs9 (p=0.02)** ; 9vs11 (p=0.67)
(T)MDPD		1.05 (1.03-1.07)	1.05 (1.03-1.08)	1.05 (1.03-1.09)	7vs9 (p=1) ; 9vs11 (p=0.55)
(T)HI		0.03 (0.03-0.04)	0.03 (0.03-0.04)	0.03 (0.03-0.04)	7vs9 (p=1) ; 9vs11 (p=0.59)

Table 3. Average and range values (in percentage) for the volume of organ (rectal- and bladder-wall) that receives a certain dose, for different number of fields.

Variable	Corresponded dose of the isodose (Gy)	Number of beams			t-test
		7F	9F	11F	
Rectal-wall values (%)					
$V_{100\%}$	32.5	7.9 (5.3-13)	7.3 (4.7-12.2)	7.1 (4.9-12)	**7vs9 (p=0.008)** ; 9vs11 (p=0.24)
$V_{90\%}$	29.25	11.9 (8.2-17)	11.3 (7.6-17.2)	11 (7.5-16.4)	7vs9 (p=0.06) ; 9vs11 (p=0.07)
$V_{80\%}$	26	15.2 (10.4-21.5)	14.6 (9.9-21.7)	14.1 (9.6-20.2)	7vs9 (p=0.13) ; 9vs11 (p=0.09)
$V_{70\%}$	22.75	19.4 (13.6-28.4)	18.3 (12.4-26.1)	17.6 (12.5-24.2)	**7vs9 (p=0.03)** ; 9vs11 (p=0.09)
$V_{50\%}$	16.25	32.1 (21.9-43.8)	29.8 (19.8-43.3)	28.7 (19.6-40.1)	**7vs9 (p=0.02)** ; 9vs11 (p=0.06)
$V_{47.5\%}$	15.44	34.6 (23.2-49.5)	31.9 (21-47.1)	30.7 (20.9-43.5)	**7vs9 (p=0.02)** ; 9vs11 (p=0.07)
$V_{30\%}$	9.75	56.3 (39-79.7)	53.8 (32.9-78)	49.8 (32.4-73.5)	7vs9 (p=0.07) ; **9vs11 (p=0.01)**
Bladder-wall values (%)					
$V_{100\%}$	32.5	3 (0.3-9.3)	2.9 (0.2-8.8)	2.6 (0.2-7.9)	**7vs9 (p=0.03)** ; 9vs11 (p=0.08)
$V_{90\%}$	29.25	5.9 (1.1-16.9)	5.8 (1-16.6)	5.7 (0.9-16.1)	**7vs9 (p=0.01)** ; 9vs11 (p=0.38)
$V_{80\%}$	26	8.1 (1.8-22.9)	7.9 (1.8-21.8)	8 (1.8-21.9)	7vs9 (p=0.16) ; 9vs11 (p=0.63)
$V_{70\%}$	22.75	10.6 (2.4-28.6)	10.6 (2.4-27.5)	10.5 (2.3-27.1)	7vs9 (p=0.8) ; 9vs11 (p=0.5)
$V_{50\%}$	16.25	19 (5.7-43.3)	18.7 (5.4-45.2)	18.2 (5.4-42.4)	7vs9 (p=0.38) ; 9vs11 (p=0.09)
$V_{47.5\%}$	15.44	20.4 (6.3-46.9)	20.2 (5.9-49.3)	19.6 (5.8-46.7)	7vs9 (p=0.65) ; 9vs11 (p=0.06)
$V_{30\%}$	9.75	31.5 (10.8-80.1)	31.8 (10.6-84.2)	30.7 (10.5-77.7)	7vs9 (p=0.61) ; 9vs11 (p=0.15)

Table 4. Average and range values for different variables used for the comparison of the two plans (6MV and 16MV).

Variable	Dose associated to the isodose	Beam Energy		t-test
		6 MV	16 MV	
PTV coverage				
(P)V95% (%)	30.87 Gy	99.9 (99.8-100)	99.8 (99.5-100)	p=0.1
(T)V95% (%)	38 Gy	100 (99.8-100)	100 (99.8-100)	p=0.37
(P)V100% (%)	32.5 Gy	95.4 (93.5-97.6)	94 (92.6-96.7)	p=0.06
(T)V100% (%)	**40 Gy**	**98.5 (98.2-98.8)**	**93.5 (91.9-94.7)**	**p=0.001**
3D Dmax (Gy)		42.1 (41.5-42.6)	41.6 (41.3-42.1)	**p=0.003**
Evaluation indexes for the prostate				
(P)GI		4 (3.8-4.3)	3.8 (3.6-4)	p=0.06
(P)CI_{RTOG}		1.31 (1.24-1.45)	1.27 (1.21-1.38)	p=0.058
(P)CI_{SALT}		0.99 (0.99-1)	0.99 (0.98-1)	p=0.07
(P)CI_{Lomax}		0.76 (0.69-0.8)	0.78 (0.73-0.81)	p=0.053
(P)$CI_{van'tRiet}$		0.75 (0.69-0.8)	0.77 (0.72-0.8)	p=0.1
(P)HI		0.24 (0.23-0.24)	0.24 (0.23-0.25)	p=0.17
Evaluation indexes for the tumor				
(T)CI_{RTOG}		1.52 (1.42-1.61)	1.46 (1.33-1.61)	p=0.053
(T)CI_{SALT}		0.99 (0.99-1)	0.99 (0.99-1)	p=0.17
(T)CI_{Lomax}		0.65 (0.62-0.7)	0.68 (0.62-0.74)	**p=0.042**
(T)$CI_{van'tRiet}$		0.65 (0.62-0.7)	0.67 (0.61-0.73)	p=0.09
(T)MDPD		1.05 (1.04-1.06)	1.04 (1.03-1.05)	p=0.06*
(T)HI		0.02 (0.02-0.03)	0.03 (0.03-0.04)	p=0.06*

Table 5. Average and range values (in percentage) for the volume of organ (rectal- and bladder-wall) that receives a certain dose, for 6MV and 16MV.

Variable	Corresponded dose of the isodose (Gy)	Beam Energy		t-test
		6 MV	16 MV	
Rectal-wall values (%)				
$V_{100\%}$	32.5	5.9 (4.5-7.6)	6.1 (4.6-7.7)	p=0.48
$V_{90\%}$	29.25	9.5 (7.2-11.9)	9.9 (7.6-12.2)	p=0.35
$V_{80\%}$	26	12.5 (9.2-16.3)	13 (9.9-15.9)	p=0.34
$V_{70\%}$	22.75	15.6 (12-20.4)	16.4 (12.4-20.2)	p=0.12
$V_{50\%}$	16.25	25.6 (19.4-33.9)	26.4 (19.6-33.7)	p=0.11
$V_{47.5\%}$	15.44	27.3 (20.5-35.9)	28.1 (20.8-35.9)	p=0.12
$V_{30\%}$	9.75	47.9 (32-63.9)	49.2 (32.8-64.2)	p=0.23
Bladder-wall values (%)				
$V_{100\%}$	32.5	2.1 (0.4-3)	1.7 (0.3-2.8)	p=0.09
$V_{90\%}$	29.25	3.9 (1.3-5.4)	3.8 (1-5.6)	p=0.49
$V_{80\%}$	26	5.4 (2.4-7.4)	5.5 (2.1-8)	p=0.69
$V_{70\%}$	22.75	7.2 (3.2-9.5)	7.4 (3.1-10.5)	p=0.38
$V_{50\%}$	16.25	12.8 (5.8-17.6)	13 (5.5-17.7)	p=0.66
$V_{47.5\%}$	15.44	13.8 (6.3-18.9)	13.9 (5.9-19)	p=0.64
$V_{30\%}$	9.75	21.5 (10.6-28.6)	21.8 (10.7-29.4)	p=0.24

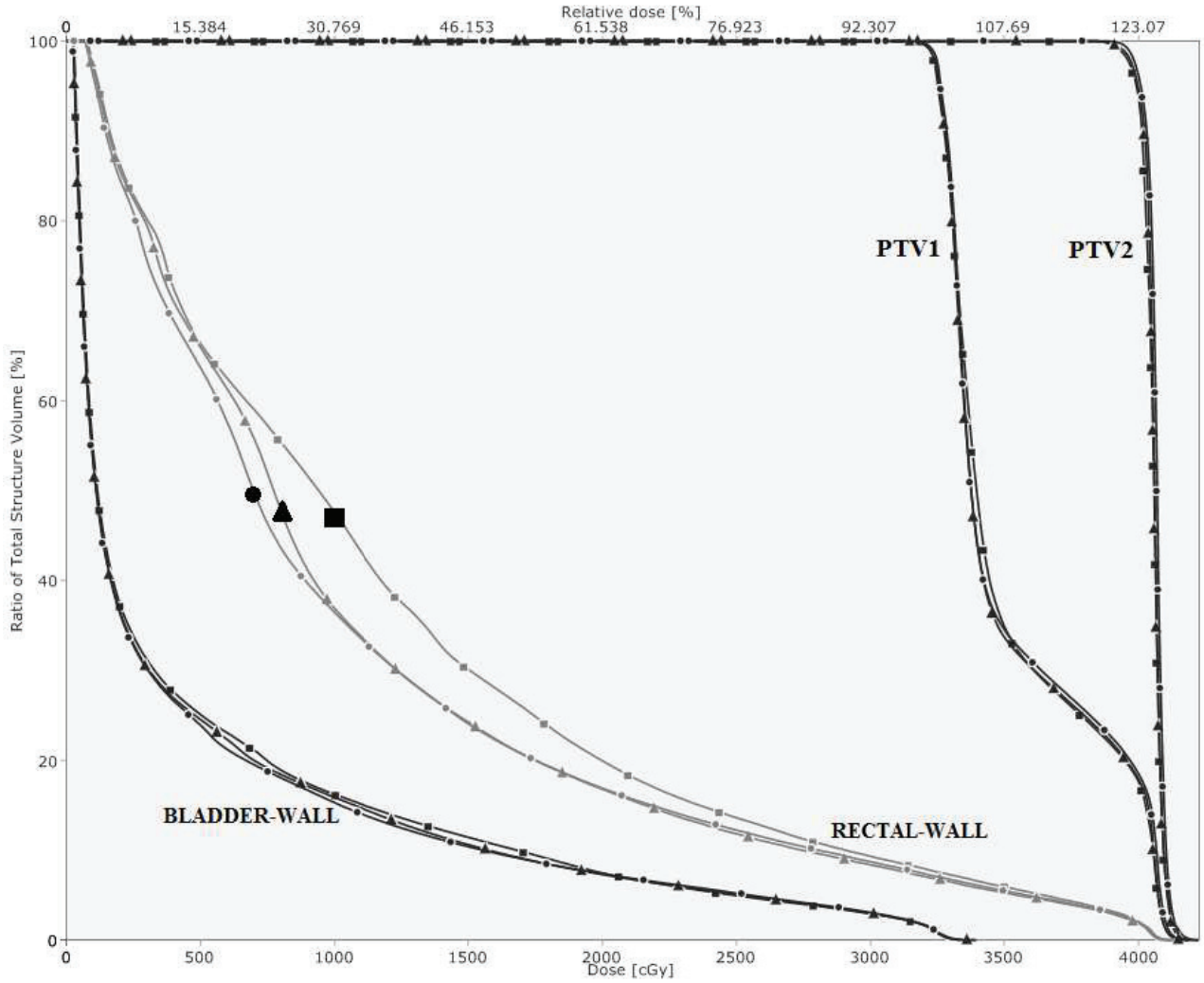

Figure 1. Dose-volume histograms of planning target volumes (PTV1-prostate and PTV2-tumor) and organs at risk (bladder- and rectal-wall) for 7-beam (*square*), 9-beam (*triangle*) and 11-beam (*circle*) conformations.

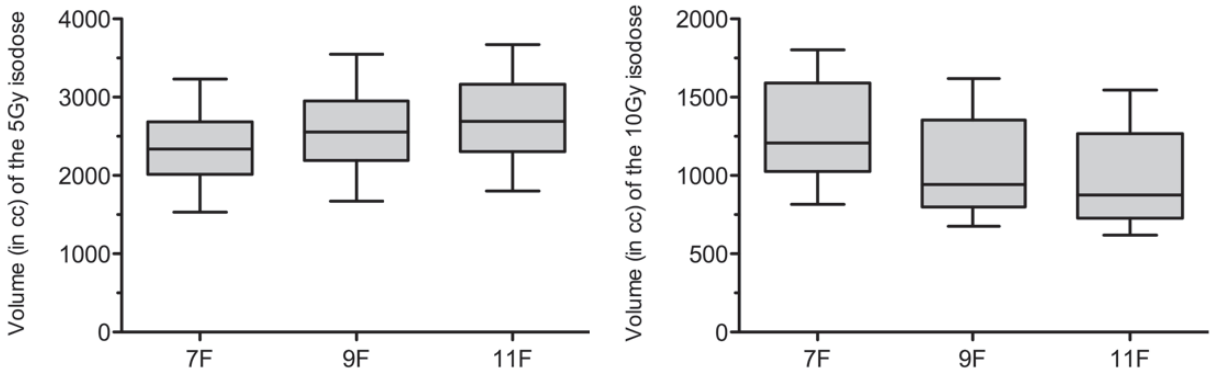

Figure 2. Volumes (in cubic centimeters) of the 5Gy (*left*) and 10Gy (*right*) isodoses for the 7-, 9- and 11-beam conformations.

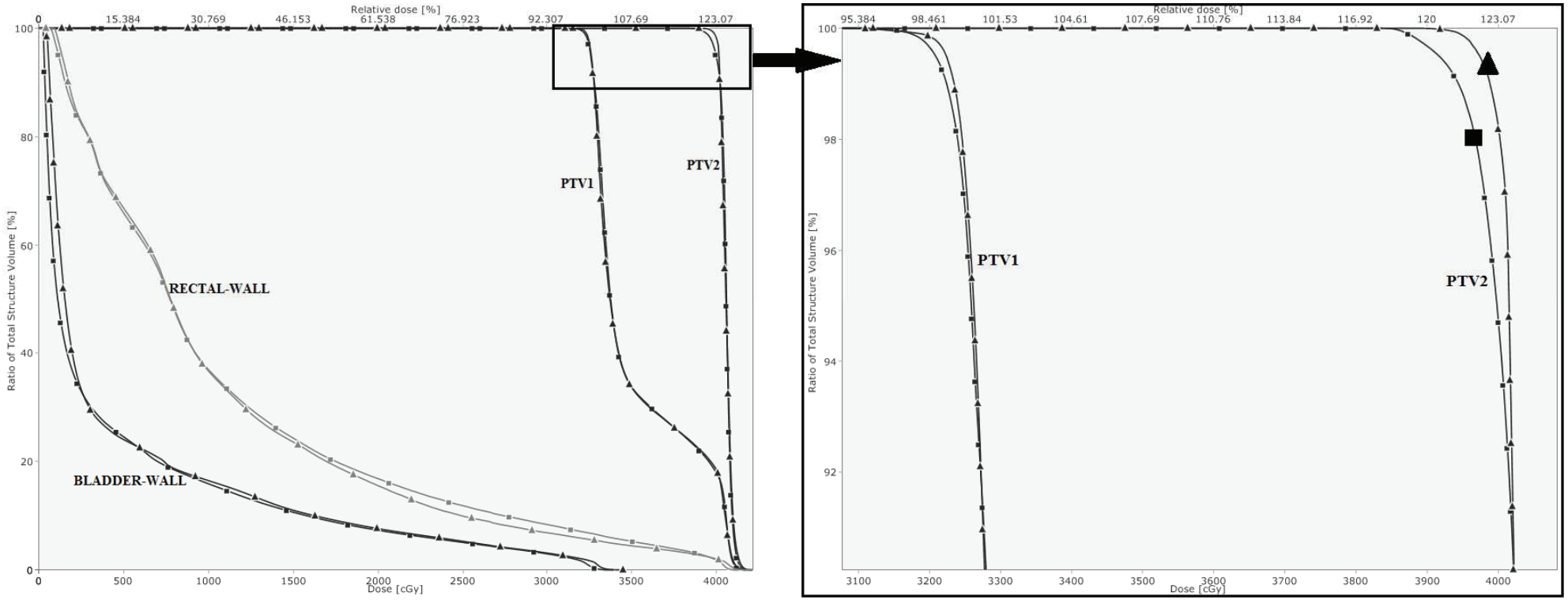

Figure 3. Dose-volume histograms of planning target volumes (PTV1-prostate and PTV2-tumor) and organs at risk (bladder- and rectal-wall) for 6MV (*triangle*) and 16MV (*square*) energies.

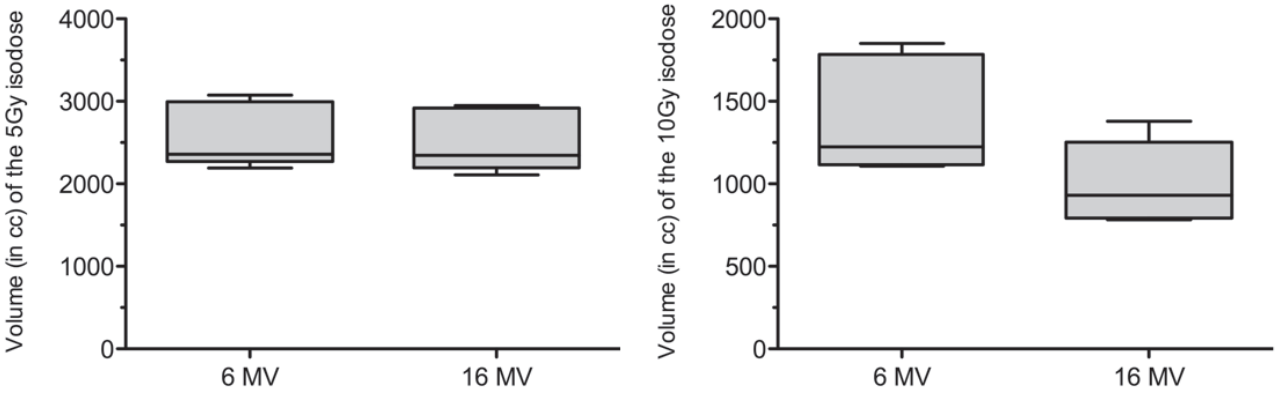

Figure 4. Volumes (in cubic centimeters) of the 5Gy (*left*) and 10Gy (*right*) isodoses for 6MV and 16MV beam energies.

3.2.4. Conclusion

The choice between different number of fields or different beam energies should be made carefully, as it could modify the low dose volume. However, clinical studies must validate the consequence of this statement for prostate SBRT.

Following this study we chose a 9-field conformation and 16MV beam energy in our department, as a good compromise for a stereotactic irradiation of prostate cancer with a SIB.

3.2.5. Prostate SBRT irradiation with a simultaneous-integrated boost versus a homogeneous SBRT irradiation

We have seen in the first part that doses between 6.5 Gy and 10 Gy per fraction are achievable for prostate SBRT and that the probability of a biochemical failure can be reduced. A recent retrospective study on 135 patients from 8 institutions reports the biochemical relapse-free survival (bRFS) rates for localized prostate cancer after stereotactic body radiotherapy [41]. For a median dose of 36.25 Gy (range 35 – 40 Gy) and a median follow-up of 60 months (range 60 - 72), the bRFS rate at 5 years was 97%. The authors observed that the bRFS rates for 35 Gy and for >36.25 Gy were 93% and 100%, respectively, which were not statistically significant on multivariate analysis (p=0.97) [41].

There are two relationships that should be taken into account for any SBRT approach: *the dose-response* (equal to tumor control) and *the dose-effect* (the consequence of this high dose on exposed healthy tissues).

Methodological improvement and technical innovation in stereotactic radiotherapy make possible the study of high dose escalations to the prostate. Consequently, the potential clinical interest of an integrated SBRT boost into the tumor is double:

- to avoid the local recurrence observed after standard RT;
- to spare the rectum and the bladder from higher doses of irradiation when a SBRT approach is planned.

3.2.6. Publication

In 2010, the team from the Radiotherapy-Oncology Department of Lyon Sud Hospital (HLS) initiated a study for the evaluation of a SBRT plan (32.5 Gy in 5 fractions) with a simultaneous integrated SBRT boost (40 Gy in 5 fractions) within the macroscopic tumor visible on MRI. This plan was compared with two homogeneous SBRT irradiations of the entire prostate (32.5 Gy and 40 Gy) in order to assess the potential dosimetric interest of an integrated SBRT boost approach. The imaging protocol was created in cooperation with the radiologists from the Department of Radiology (HLS) and from the Department of Urological Radiology (Edouard Herriot Hospital in Lyon), who have more than 15 years of experience in the interpretation of MR imaging for prostate cancer. The prostate and the tumor(s) were delineated for each patient on T2- and T1-MRI registrations and the radiologists were aware of the results of the biopsy-proven prostate cancer for all patients. Additional imaging modalities were available if necessary for the aid in tumor identification.

The initial results were presented at the 52nd Annual ASTRO Meeting (October 31 – November 4, 2010) in San Diego (Appendix 8, *abstract number 3288*) [42]. The study is presented below and was published in 2014 in *Physica Medica*.

Physica Medica 30 (2014) 320–325

Contents lists available at ScienceDirect

Physica Medica

journal homepage: http://www.physicamedica.com

Original paper

Potential interest of developing an integrated boost dose escalation for stereotactic irradiation of primary prostate cancer

C. Udrescu [a,b], O. Rouvière [c], C. Enachescu [a], M.-P. Sotton [b], J. Bouffard-Vercelli [d], P. Jalade [b], O. Chapet [a,*]

[a] Department of Radiation Oncology, Centre Hospitalier Lyon Sud, Lyon-Pierre Benite, France
[b] Department of Medical Physics, Centre Hospitalier Lyon Sud, Lyon-Pierre Benite, France
[c] Department of Urological Radiology, Hopital Edouard Herriot, Lyon, France
[d] Department of Radiology, Centre Hospitalier Lyon Sud, Lyon-Pierre Benite, France

ARTICLE INFO

Article history:
Received 24 May 2013
Received in revised form
19 September 2013
Accepted 23 September 2013
Available online 26 October 2013

Keywords:
Prostate cancer
Integrated boost
IMRT
Stereotactic body radiotherapy

ABSTRACT

Introduction: The stereotactic irradiation is a new approach for low-risk prostate cancer. The aim of the present study was to evaluate a schema of stereotactic irradiation of the prostate with an integrated-boost into the tumor.
Material and methods: The prostate and the tumor were delineated by a radiologist on CT/MRI fusion. A 9-coplanar fields IMRT plan was optimized with three different dose levels: 1) 5 × 6.5 Gy to the PTV1 (plan 1), 2) 5 × 8 Gy to the PTV1 (plan 2) and 3) 5 × 6.5 Gy on the PTV1 with 5 × 8 Gy on the PTV2 (plan 3). The maximum dose (MaxD), mean dose (MD) and doses received by 2% (D2), 5% (D5), 10% (D10) and 25% (D25) of the rectum and bladder walls were used to compare the 3 IMRT plans.
Results: A dose escalation to entire prostate from 6.5 Gy to 8 Gy increased the rectum MD, MaxD, D2, D5, D10 and D25 by 3.75 Gy, 8.42 Gy, 7.88 Gy, 7.36 Gy, 6.67 Gy and 5.54 Gy. Similar results were observed for the bladder with 1.72 Gy, 8.28 Gy, 7.01 Gy, 5.69 Gy, 4.36 Gy and 2.42 Gy for the same dosimetric parameters. An integrated SBRT boost only to PTV2 reduced by about 50% the dose difference for rectum and bladder compared to a homogenous prostate dose escalation. Thereby, the MD, D2, D5, D10 and D25 for rectum were increased by 1.51 Gy, 4.24 Gy, 3.08 Gy, 2.84 Gy and 2.37 Gy in plan 3 compared to plan 1.
Conclusions: The present planning study of an integrated SBRT boost limits the doses received by the rectum and bladder if compared to a whole prostate dose escalation for SBRT approach.

Introduction

Post-radiotherapy local recurrence occurs at the site of the primary tumor as first suggested by Cellini et al. [1] on 118 patients who underwent external beam radiotherapy at doses ≤70.2 Gy, with results from digital rectal examination, transrectal ultrasound and magnetic resonance imaging (but without reporting any pathological confirmation). In 2007, Pucar et al. presented the results of 9 patients with localized prostate cancer that were treated with IMRT with a median dose of 81 Gy (range 69–86.4 Gy) and supported the suggestion that post-RT local recurrence occurs at the site of the primary tumor [2]. The authors reported a direct visual comparison between pre-RT and post-RT imaging and pathological evaluation after salvage radical prostatectomy. They found that all 9 clinically significant tumor foci were visible and comparable between the three sets of tests. Their results may suggest that these irradiation doses might not be sufficient for the macroscopic disease and the authors suggested that their results support the practice of boosting the RT dose within the primary tumor, using imaging guidance.

Two recent teams studied the local recurrence of the prostate cancer after a radiation therapy and highlighted the major interest of the focal dose escalation. Chopra et al. demonstrated that a vast majority of low-intermediate prostate cancer patients (95%) recurred after radiotherapy (with doses between 60 and 79.2 Gy) at the original site of dominant tumor density at presentation [3]. The authors advised caution against the pursuit of focal-only radiotherapy to the radiologically visible dominant lesions or to substantial dose escalation to the uninvolved prostate gland; they also advised that careful design of clinical trials should be done for the higher radiation dose prescriptions to subregions of the prostate [3]. Arrayeh et al.

* Corresponding author. Département de Radiothérapie – Oncologie, Centre Hospitalier Lyon Sud, Chemin du Grand Révoyet, 69495 Pierre Benite Cedex, France. Tel.: +33 4 78 86 42 60; fax: +33 4 78 86 42 65.
E-mail address: olivier.chapet@chu-lyon.fr (O. Chapet).

1120-1797/$ – see front matter © 2013 Associazione Italiana di Fisica Medica. Published by Elsevier Ltd. All rights reserved.
http://dx.doi.org/10.1016/j.ejmp.2013.09.005

undertook a study to determine if local recurrence of prostate cancer after radiation therapy (75.9 Gy (range 74–79 Gy)) occurs at the same site as primary tumor before treatment, using longitudinal MR imaging and MR spectroscopic imaging to assess the dominant tumor locations at baseline and recurrence [4]. The prescribed doses seem to be insufficient and the authors determined that the dominant recurrent tumor was at the same location as dominant baseline tumor in 89% of patients and recommended that additional focal therapy using dose escalation could improve the local tumor control [4].

From all these studies it can be concluded that radiation doses between 60 and 90 Gy might not be sufficient for macroscopic disease control [1–4]. Hence, a concomitant focal therapy was subsequently developed.

The stereotactic irradiation is a recent concept of the radiotherapy (RT) for low-risk prostate cancers, resumed in 2010 in the stereotactic body radiotherapy (SBRT) reports of the American Society for Therapeutic Radiology and Oncology (ASTRO) [5] and of the American Association of Physicists in Medicine (AAPM) [6]. Several fractionations greater than 6.5 Gy per fraction were already evaluated and promising results were published in terms of biochemical control [7–15]. However, in all the related experiences, a homogenous irradiation of the whole prostate was performed.

The recent progress in dynamic MRI allows the visualization of the macroscopic prostatic lesions [16–22] and can open the way to a focal therapy [21–23]. Furthermore, the development of the image-guided radiotherapy (IGRT) techniques for the inter- and intrafraction prostate localization and its reposition (implanted markers with kV imaging or cone beam CT), offer a precise tracking of the prostate before and during the irradiation course [24–27]. The major interest of an integrated SBRT boost is to limit the dose to the organs at risk while increasing the dose to the macroscopic tumor. The aim of the present planning study was to evaluate a stereotactic prostate irradiation, with an integrated-boost dose escalation of 5 × 8 Gy to the macroscopic disease.

Material and methods

CT–MRI image registration

Nine patients with low- to intermediate-risk prostate cancer (according to D'Amico classification) followed the same procedure for the CT–MRI registration. Three porous gold markers (Eckert & Ziegler BEBIG) were first implanted into the prostate by an urologist or a radiologist. The markers are 3 mm long and 1.2 mm thick. After the implantation of those markers, each patient had two (T1-gadolinium dynamic contrast-enhanced (DCE) and T2-weighted) pelvic MRI acquisitions and one CT scan simulation (GE LightSpeed16®) with a slice thickness of 2.5 mm. MRI parameters were defined in order to optimize the clearness of both, markers and prostate. The T2-weighted images were acquired with a turbo spin echo sequence (TSE) (TR = 7449 ms, TE = 135 ms) with an axial slice thickness of 3 mm and no space between the slices (gap = 0 mm); the images were acquired using a Sense body coil 4 elements (a phased array coil for increased signal-to-noise ration and high-resolution body imaging), with a 332 × 243 matrix, a TSE factor of 19 and a field of view (FOV) of 200 × 200 mm.

The DCE-MRI protocol consisted of a three-dimensional spoiled gradient echo sequence (TR/TE = 7.2/4.2, slice thickness = 2 mm, 40 slices, flip angle = 20°). The FOV was 285 × 238 and the acquisition matrix 144 × 118. A dose of 0.2 ml/kg gadolinium (Multihance, Bracco Imaging France) was injected intravenously and the scans were repeated 19 times at 7 s.

Subsequently, registrations between these acquisitions were performed with Advantage Fusion® software (General Electric Medical Systems). All registrations were prepared by a radiation physician (OC) using the three markers.

Target and organs delineation

Three steps were needed for the delineation of structures:

1) Prostate delineation was performed by a radiation physician (OC) using the registration between the dosimetric CT scan and T2–MRI exam;
2) The delineation of the macroscopic tumor was performed by a radiologist using the registration between the CT scan and T1(gadolinium)–MRI exam;
3) The organs at risk were delineated by a radiation physician (OC) using the CT scan that was also used for planning purpose.

Irradiation technique

Two planning target volumes (PTV) were created for each patient: PTV1 was the prostate with a 3-mm uniform expansion and PTV2 was the tumor with a 5-mm volumetric expansion, reduced to 3 mm toward the rectum. Small margins (that account for inter- and intrafraction motion) were used as the daily repositioning and the target monitoring are made using the three gold markers and the OBI® system (Varian) and/or using the Snap Verification® tool of the ExacTrac® system (BrainLab). The PTV2 margins were voluntarily increased to 5 mm to cover potential uncertainty in image registration and tumor delineation. The reason for these small margins is to improve the dose fall-off outside of the target and help spare the nearby organs at risk, as recommended by AAPM Task Group for SBRT (TG101) [6].

Three plans were generated using Eclipse® TPS (Varian) with 16 MV linear accelerator and the pencil beam convolution (PBC) algorithm [28,29]. The technique consists of nine-coplanar fields with an IMRT optimization for three different dose levels:

a) 32.5 Gy in 5 fractions of 6.5 Gy to the PTV1 (Plan 1);
b) 40 Gy in 5 fractions of 8 Gy to the PTV1 (Plan 2); and
c) 32.5 Gy in 5 fractions of 6.5 Gy to the PTV1, combined with a simultaneous integrated boost (SIB) of 40 Gy in 5 fractions of 8 Gy to the PTV2 (Plan 3) (Fig. 1).

Biologically equivalent dose (BED) calculation

Assuming an α/β ratio of 1.5 Gy [30] and using the linear quadratic model, the equivalent doses delivered in 5 fractions for Plan 1 and Plan 2 are 76 Gy in 38 fractions of 2 Gy and 108 Gy in 54 fractions of 2 Gy, respectively. They were obtained from the equation of biologically equivalent dose (BED) previously applied by Madsen et al. for entire prostate SBRT irradiation [7]:

$$\mathrm{BED} = (nd) + \left(\frac{nd^2}{\frac{\alpha}{\beta}}\right)$$

For an equivalent irradiation delivered in 2 Gy per fraction the total doses for acute effects (for $\alpha/\beta = 10$ Gy) are 44.7 Gy and 60 Gy for Plan 1 and Plan 2, respectively. Assuming an α/β of 3 Gy for late effects, the equivalent doses in 2 Gy are 61.8 Gy and 88 Gy for plans 1 and 2, respectively.

PTV coverage and conformal index

At least 97% of the PTV1 and PTV2 had to be covered by the 95% isodoseline and the hot spot didn't exceed 107% of the prescribed dose.

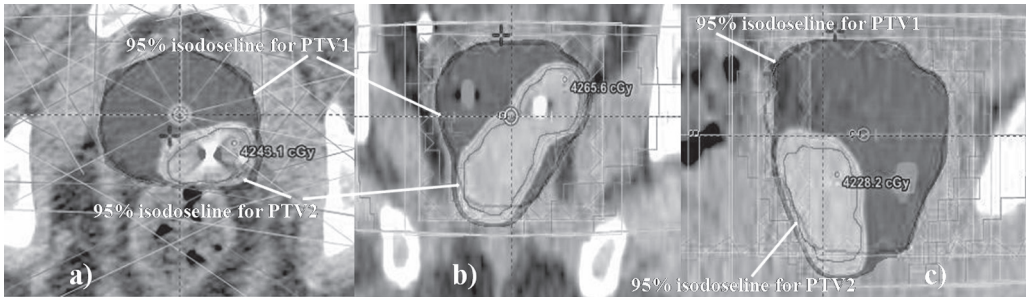

Figure 1. The dose distribution of a patient with an integrated-boost simulation in the axial plane (a), coronal plane (b) and sagittal plane (c).

The conformal index (CI) is a ratio-score that is used for stereotactic irradiation and that quantifies the correspondence between different volumes: the tumoral contour, the isodoses (prescribed, of reference, minimal and maximum) and/or the healthy tissues. The difference between conformal indexes described in the literature was already well resumed by Feuvret et al. [31]. In the present study the conformal index was noted for both PTV1 and PTV2, applying the formula:

$CI = V_{IR}/V_{PTV}$,
V_{IR} = 95% isodoseline volume, that covers the PTV
V_{PTV} = PTV volume,

whereas, the uniformity of the treatment plan was also verified by the visualization of the CT slices and of the dose-volume histograms, as suggested by Feuvret et al. A CI value between 1 and 2 proves a good dosimetric treatment plan [31]; however, for the SBRT irradiation, it is recommended to keep the CI around 1.2.

Organs at risk (OAR) dose evaluation

For all the three plans, the doses to the rectum, bladder and femoral heads were optimized to be as low as possible, without affecting the PTV coverage. The maximum dose (MaxD), mean dose (MD) and doses received by 2% (D2), 5% (D5), 10% (D10) and 25% (D25) of the rectal and bladder walls were used to compare the three SBRT-IMRT plans. The results below are expressed in average values.

The student paired *t*-test was used for the statistical analysis of the variables and was performed with the MedCalc® software (version 9.2.0.1). The analysis was made with a significance threshold set at $p < 0.05$.

Results

Prostate and tumor characteristics are described in Table 1.

PTV coverage and conformal index

The average PTV1 coverage by the 95% isodoseline was of 98.21% (range 97.8–98.96%), 98.39% (range 97.74–99.46%) and 98.85% (range 97.8–99.81%) for Plans 1, 2 and 3, respectively. For SIB irradiation, the average PTV2 coverage by the 95% isodoseline was of 99.36% (range 97.72–99.98%). Subsequently, the mean conformity index for PTV1 was of 1.13 (range 1.06–1.17), 1.06 (range 1.03–1.08) and 1.23 (range 1.14–1.29) for Plans 1, 2 and 3 respectively; the PTV2 in Plan 3 had a mean CI of 1.28 (range 1.15–1.55).

Doses to the rectal- and bladder-wall

Table 2 shows average (range) values for doses received by the rectal- and bladder-wall. A dose escalation to the entire prostate from 5 × 6.5 Gy (Plan 1) to 5 × 8 Gy (Plan 2) increased the MD, MaxD, D2, D5, D10 and D25 for rectum by 3.75 Gy, 8.42 Gy, 7.88 Gy, 7.36 Gy, 6.66 Gy and 5.54 Gy, respectively (Fig. 2). Similar results were observed for the bladder with respectively: 1.72 Gy, 8.28 Gy, 7.01 Gy, 5.69 Gy, 4.36 Gy and 2.42 Gy for the same dosimetric parameters (Fig. 3). A focal dose escalation only to the tumor (PTV2 in Plan 3) reduced the dose difference between Plan 1 and 2 by about 50% for the rectum and the bladder. This was not valid for the MaxD parameter. Thereby, the MD, D2, D5, D10 and D25 for rectum were increased only of 1.51 Gy, 4.24 Gy, 3.08 Gy, 2.84 Gy and 2.37 Gy in Plan 3 compared to Plan 1. The differences for bladder were respectively 0.43 Gy, 1.47 Gy, 1.30 Gy, 1.08 Gy and 0.76 Gy for the same parameters.

Discussion

Different experiences with a homogenous stereotactic irradiation for prostate cancer were reported [7–15]. Irradiation doses between 6.5 Gy and 10 Gy per fraction delivered in these studies provide important information:

1) SBRT for prostate cancer is technically feasible;
2) with a limited follow-up, the local control is excellent (between 80% and 100%);

Table 1
Prostate and tumor characteristics of the patients.

Patient	Clinical stage	PTV1-contour volume	Tumor localization and PTV2-contour volume
1	T2a N0M0	55.3 cc	Right-posterior, from base to apex 14.7 cc
2	T1c N0M0	79.5 cc	Right-posterior, at mid prostate 15.7 cc
3	T1c N0M0	89.6 cc	Right- and left-posterior 26.6 cc
4	T1c N0M0	111.5 cc	Antero-post, from base to apex 27.2 cc
5	T1c N0M0	145 cc	Left-posterior, from base to mid-prostate 8.9 cc
6	T1c N0M0	74.2 cc	Left-posterior, at apex 11.4 cc
7	T1c N0M0	69.3 cc	Right- and left-posterior 12.4 cc
8	T1c N0M0	54.5 cc	Left-posterior 7.9 cc
9	T1c N0M0	58.7 cc	Right-posterior, at mid-prostate 9.9 cc

Table 2
Average (range) values for rectal- and bladder-wall in the three plans.

Variable	6.5 Gy × 5 (Plan 1)	SBRT-SIB (Plan 3)	8 Gy × 5 (Plan 2)	*t*-Test	
				Plan 1 vs Plan 3	Plan 3 vs Plan 2
Rectal-wall					
D2cc (Gy)	31.3 (28.3–32.7)	35.6 (33.2–38.7)	39.2 (36.8–41.2)	$p = 0.002$	$p = 0.007$
D5cc (Gy)	28.8 (25.6–31.6)	31.9 (29.8–34.8)	36.2 (32.9–39.2)	$p = 0.005$	$p = 0.0009$
D10cc (Gy)	23.7 (17.8–29.2)	26.6 (23.3–30.7)	30.4 (24–35.8)	$p = 0.009$	$p = 0.002$
D25cc (Gy)	12.5 (9.1–18.1)	14.9 (11.9–16.8)	18.1 (13.7–24.1)	$p = 0.02$	$p = 0.005$
MD (Gy)	9.7 (7–14.3)	11.2 (9.2–13.4)	13.5 (10.2–18.8)	$p = 0.01$	$p = 0.004$
MaxD (Gy)	33.8 (32.8–34.5)	42 (40.3–43.2)	42.2 (41.5–42.9)	$p < 0.0001$	$\mathbf{p = 0.51}$
Bladder-wall					
D2cc (Gy)	30 (23.6–33.5)	31.5 (26–34)	37 (28.9–41.5)	$p = 0.01$	$p = 0.0001$
D5cc (Gy)	25.1 (15–32.2)	26.4 (17.5–32.4)	30.8 (19.1–39.8)	$p = 0.01$	$p = 0.0005$
D10cc (Gy)	19.5 (7.4–30.1)	20.6 (10.2–29.2)	23.8 (9.1–36.2)	$p = 0.03$	$p = 0.006$
D25cc (Gy)	10.2 (1.7–20.5)	10.9 (2.3–19.5)	12.6 (2–24.8)	$\mathbf{p = 0.08}$	$p = 0.03$
MD (Gy)	7.4 (2.6–16.6)	7.8 (3.2–16.1)	9.1 (3.2–20.4)	$\mathbf{p = 0.07}$	$p = 0.02$
MaxD (Gy)	33.7 (31.2–34.6)	37.3 (34.2–41.9)	42 (39.1–43.6)	$p = 0.01$	$p = 0.004$

3) a dose-effect could exist with rates of local control of 90% at 6.7 Gy per fraction and 100% at 9–10 Gy per fraction;
4) grade ≥ 3 rectal and urinary toxicities are low but GI and GU toxicities ≥ grade 2 are not negligible (18% and 31%, respectively) when higher doses are used [8];
5) three studies used a CyberKnife [9,12,13,15] and four studies demonstrated that the SBRT for prostate cancer can be completed with dedicated or conventional accelerators [7,8,10,11,14] as well.

In all these studies a homogenous irradiation of the whole prostate gland was performed. The significant rate of grade ≥2 rectal and urinary toxicities supports the interest of the integrated boost concept for the prostate SBRT. The results of the present planning study may suggest that a focal irradiation to the macroscopic tumor, visible on MRI, could preserve the rectum and bladder when the SBRT is delivered.

When Plan 2 is compared with Plan 3 no significant difference was found between the two plans in terms of maximum dose ($p = 0.51$). This may arise because the maximum dose evaluation is punctual, thus calculated on one voxel and occur especially for posterior tumors. However, the differences between Plans 2 and 3 for rectal-wall become significant ($p < 0.007$) from D2cc to D25cc and shows the importance of an SIB approach for dose escalation. Moreover, the differences between Plans 2 and 3 for bladder-wall are significant ($p < 0.03$) for all parameters (Table 2).

The intent of concomitant hypofractionated boost to the tumor region was previously described, using the *IMRT technique* [21,32,33]. In Miralbell et al. study, 50 patients were treated with a conventional external radiotherapy to the prostate (64–64.4 Gy), followed by an IMRT stereotactic boost to the dominant tumor (2 × 5 Gy, to 2 × 7 Gy) [32]. The approach showed excellent outcomes with an acceptable long-term toxicity. Only 2 patients presented Grade 3 acute urinary toxicity. The 5-year probabilities of ≥Grade 2 late urinary and low gastrointestinal toxicity-free survival were of 82.2% and 72.2%, respectively. The survival rates without biological recurrence are of 98%.

Willoughby et al. [33] reported the preliminary results on 31 patients with an advanced and localized prostate cancer, who were treated with 70 Gy in 28 fractions of 2.5 Gy to the entire prostate with concomitant irradiation (to an area corresponding to the peripheral zone) of 80 Gy in 28 fractions of 2.86 Gy. With a median follow-up of 70 months, the toxicity from the concomitant boost of 80 Gy has been limited. After 7 years, the overall survival, the biochemical relapse-free survival rate and the clinical progression disease-free survival rate were of 48%, 52% and 68%, respectively. The acute rectal toxicity scores were 0 and 1 in 68% and 32%, and the acute urinary toxicity scores were 0, 1 and 2 in respectively 35%, 52% and 13%. The Grade 2 late rectal toxicity was minimal (3% at 7 years) with no Grade 3 and the

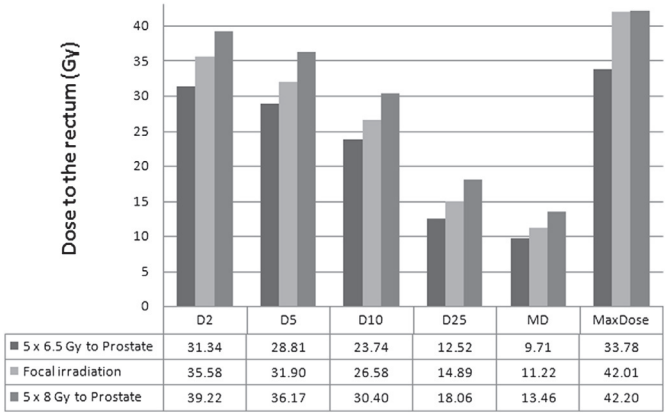

Figure 2. Average values (in Gy) of dosimetric parameters for the rectum-wall: mean dose, maximum dose and D_i (dose received by the "*i*" percentage of the rectum), for all the nine patients and for all three plans.

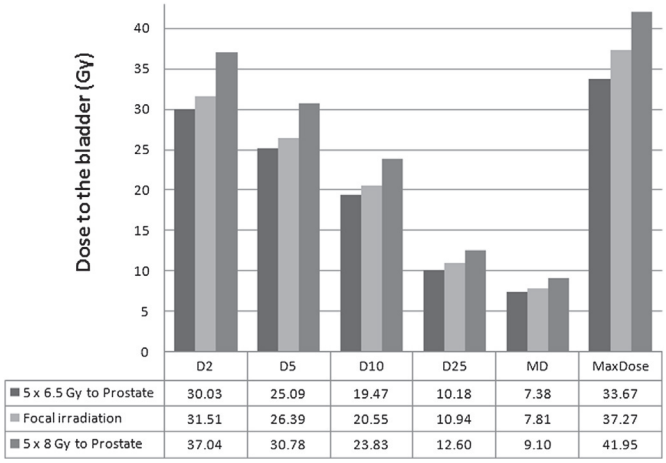

Figure 3. Average values (in Gy) of dosimetric parameters for the bladder: mean dose, maximum dose and D_i (dose received by the "*i*" percentage of the rectum), for all the nine patients and for all three plans.

Grade 2 late urinary toxicity was 11% with only 2 cases of Grade 3.

Delivering 74 Gy to the PTV and 80 Gy to the intraprostatic tumor (which was delineated by using the MRI), De Meerleer et al. did not observe any Grade 3 acute gastrointestinal (GI) toxicity. From the 15 patients treated in this study, only three presented Grade 2 GI toxicity. A Grade 2 genitourinary (GU) acute toxicity was seen for six patients, but no grade 2 or 3 toxicity was observed after 1 and 3 months after the treatment [21].

We acknowledge that the limitations of our study are the evaluation of the tumor control probability (TCP) and the normal tissue complication probability (NTCP). However, several studies assessed the TCP/NTCP for an irradiation of the entire prostate and for a selective concomitant boost on DIL, using doses of 2 Gy per fraction [34–36]. Nutting et al. estimated the TCP and NTCP for rectum using 6 IMRT plans with and without an SIB technique [35]. The authors compared a whole-prostate irradiation to a dose of 70 Gy (in 2 Gy per fraction) with an SIB boost to the dominant intraprostatic tumor nodule (DIPTN) to 90 Gy and the remainder of the PTV to 70 Gy. When the DIPTN was dose escalated, the TCP was increased by 27.5% (range 11.4–47.9%) ($p < 0.001$) for α/β ratio = 1.49. The average increase in rectal NTCP was 1.8% (range 0.7–2.6%). The authors also stated that the increase in rectal NTCP was low (0.9%) for patients having DIPTN in the lateral part of the peripheral zone of the prostate [35]. In 5 patients, Van Lin et al. evaluated the TCP and NTCP for two plans: 1) a $PTV_{prostate}$ irradiation of 70 Gy (2 Gy per fraction) with PTV_{DIL} of 90 Gy (2.57 Gy per fraction) and 2) a $PTV_{prostate}$ irradiation to 78 Gy (2 Gy per fraction) [36]. Overall, the TCP did not differ between plans with an average of 87.4% (range 85–89%) and 86% (range 83–88%) for $PTV_{prostate+DIL}$ and $PTV_{prostate}$, respectively. The average NTCP values for the rectal-wall were 3.8% (range 2–6%) and 5.6% (range 4–6%) for $PTV_{prostate+DIL}$ and $PTV_{prostate}$, respectively. Moreover, in 4 of 5 patients, the DIL-IMRT plan reduced the rectal-wall NTCP (range 1–3%) [36]. A recent paper of Chang et al. calculated the TCP and NTCP (α/β ratio = 3.1 Gy) for different plans (with and without DIL boost) [34]. The authors compared 1) a whole-prostate irradiation to 78 Gy ($Plan_{78}$), 2) a plan with 78 Gy to the prostate and 90 Gy to the DIL (defined on positron emission tomography scans) ($Plan_{78-90}$) and 3) a plan with 72 Gy to the prostate and 90 Gy to the DIL ($Plan_{72-90}$). The TCP values for $Plan_{78}$, $Plan_{78-90}$ and $Plan_{72-90}$ were 65%, 97% and 96%, respectively [34]. $Plan_{78-90}$ and $Plan_{72-90}$ had significantly higher TCP values than $Plan_{78}$ ($p = 0.002$ and $p = 0.001$). The average rectum NTCP values were 4.6%, 3.7% and 3.2% for $Plan_{78}$, $Plan_{78-90}$ and $Plan_{72-90}$, respectively, with no statistically significant differences between plans ($p = 0.082$) [34].

As described above, the concept of focal irradiation was already used for moderate hypofractionated IMRT and it was recently evaluated for stereotactic body radiotherapy of prostate cancer [23]. The first results of Aluwini et al. on 50 patients with low- to intermediate-risk prostate cancer are promising [23]. The patients were treated with SBRT to a total dose of 38 Gy in 4 daily fractions of 9.5 Gy with an integrated boost to 11 Gy per fraction to the dominant lesion visible on MRI. The 2-year biochemical control was 100%, while the EORTC/RTOG toxicity scales presented grades 2 and 3 GI acute toxicity in 12% and 2%, respectively, and grade 2 and grade 3 GU acute toxicities in 15% and 8%, respectively. The late grade 2 GI toxicity was seen in 3% of patients and the grade 2 and grade 3 GU late toxicities were seen in 10% and 6%, respectively.

The main benefit for the patients treated with such a technique would be high-dose escalation to the tumor (which translates into improved biochemical control), while irradiating the microscopic disease with a sufficient dose and limiting the augmentation of higher doses to the organs at risk. Moreover, the SBRT approach has a double advantage in terms of decrease number of fractions (and therefore the decrease of treatment costs) with an increase in patient's comfort.

Dosimetric parameters to apply for the organs at risk remain very difficult to define for an SBRT approach and therefore the purpose is to keep the doses as low as possible. In the present study the doses for rectum and bladder were optimized to be as low as possible. The dosimetric results of an IB-SBRT irradiation showed an increase of the doses to the rectum and bladder compared to homogenous SBRT irradiation of 32.5 Gy to the whole prostate. However, this increase in dose is limited to 50% when compared to homogenous SBRT dose escalation of 40 Gy to the whole prostate.

Conclusions

The present schema of integrated boost dose escalation was created to deliver a sufficient high-dose to the microscopic disease into the prostate while increasing the dose to the macroscopic tumor. This approach deeply limits the doses received by the rectum and the bladder compared to entire prostate dose escalation. Clinical studies need to validate this approach.

Conflicts of interest statement

None.

References

[1] Cellini N, Morganti AG, Mattiucci GC, Valentini V, Leone M, Luzi S, et al. Analysis of intraprostatic failures in patients treated with hormonal therapy and radiotherapy: implications for conformal therapy planning. Int J Radiat Oncol Biol Phys 2002;53:595–9.
[2] Pucar D, Hricak H, Shukla-Dave A, Kuroiwa K, Drobnjak M, Eastham J, et al. Clinically significant prostate cancer local recurrence after radiation therapy occurs at the site of primary tumor: magnetic resonance imaging and step-section pathology evidence. Int J Radiat Oncol Biol Phys 2007;69:62–9.
[3] Chopra S, Toi A, Taback N, Evans A, Haider MA, Milosevic M, et al. Pathological predictors for site of local recurrence after radiotherapy for prostate cancer. Int J Radiat Oncol Biol Phys 2012;82:e441–8.
[4] Arrayeh E, Westphalen AC, Kurhanewicz J, Roach III M, Jung AJ, Carroll PR, et al. Does local recurrence of prostate cancer after radiation therapy occur at the site of primary tumor? Results of a longitudinal MRI and MRSI study. Int J Radiat Oncol Biol Phys 2012;82:e787–93.
[5] Buyyounouski MK, Price RA, Harris EER, Miller R, Tomé W, Schefter T, et al. Stereotactic body radiotherapy for primary management of early-stage, low- to intermediate-risk prostate cancer: report of the American Society for Therapeutic Radiology and Oncology emerging technology committee. Int J Radiat Oncol Biol Phys 2010;76:1297–304.
[6] Benedict SH, Yenice KM, Followill D, Galvin JM, Hinson W, Kavanagh B, et al. Stereotactic body radiation therapy: the report of AAPM Task Group 101. Med Phys 2010;37:4078–101.
[7] Madsen BL, Hsi RA, Pham HT, Fowler JF, Esagui L, Corman J. Stereotactic hypofractionated accurate radiotherapy of the prostate (SHARP), 33.5 Gy in five fractions for localized prostate disease: first clinical trial results. Int J Radiat Oncol Biol Phys 2007;67:1099–105.
[8] Boike TP, Lotan Y, Cho LC, Brindle J, DeRose P, Xie XJ, et al. Phase I dose-escalation study of stereotactic radiation therapy for low- and intermediate-risk prostate cancer. J Clin Oncol 2011;29:2020–6.
[9] King CR, Brooks JD, Gill H, Pawlicki T, Cotrutz C, Presti Jr JC. Stereotactic body radiotherapy for localized prostate cancer: interim results of a prospective phase II clinical trial. Int J Radiat Oncol Biol Phys 2009;73:1043–8.
[10] Mantz C, Fernandez E, Zucker I, Harrison S. A phase II trial of Trilogy-based prostate SBRT: report of favorable toxicity and early biochemical outcomes [Abstract]. Int J Radiat Oncol Biol Phys 2008;72(Suppl. 1). S311.
[11] Tang CI, Loblaw DA, Cheung P, Holden L, Morton G, Basran PS, et al. Phase I/II study of a five-fraction hypofractionated accelerated radiotherapy treatment for low-risk localized prostate cancer: early results of pHART3. Clin Oncol 2008;20:729–37.
[12] Choi C, Cho C, Kim G, Park K, Jo M, Lee C, et al. Stereotactic radiation therapy of localized prostate cancer using CyberKnife [Abstract]. Int J Radiat Oncol Biol Phys 2007;69(Suppl. 3). S375.
[13] Fuller DB, Lee C, Hardy S, Jin H. Virtual HDR[sm] CyberKnife prostate treatment: toward the development of non-invasive HDR dosimetry delivery and early clinical observations [Abstract]. Int J Radiat Oncol Biol Phys 2007;69. S358.
[14] Loblaw A, Cheung P, D'Alimonte L, Deabreu A, Mamedov A, Zhang L, et al. Prostate stereotactic ablative body radiotherapy using a standard linear

accelerator: toxicity, biochemical, and pathological outcomes. Radiother Oncol 2013;107:153–8.
[15] Katz AJ, Santoro M, Diblasio F, Ashley R. Stereotactic body radiotherapy for localized prostate cancer: disease control and quality of life at 6 years. Radiat Oncol 2013;8:118.
[16] Morgan VA, Riches SF, Giles S, Dearnaley D, deSouza NM. Diffusion-weighted MRI for locally recurrent prostate cancer after external beam radiotherapy. AJR 2012;198:596–602.
[17] Groenendaal G, Moman MR, Korporaal JG, van Diest PJ, van Vulpen M, Philippens MEP, et al. Validation of functional imaging with pathology for tumor delineation in the prostate. Radiother Oncol 2010;94:145–50.
[18] Groenendaal G, van den Berg CAT, Korporaal JG, Philippens MEP, Luijten PR, van Vulpen M, et al. Simultaneous MRI diffusion and perfusion imaging for tumor delineation in prostate cancer patients. Radiother Oncol 2010;95:185–90.
[19] Franiel T, Ludemann L, Taupitz M, Bohmer D, Beyersdorff D. MRI before and after external beam intensity-modulated radiotherapy of patients with prostate cancer: The feasibility of monitoring of radiation-induced tissue changes using a dynamic contrast-enhanced inversion-prepared dual-contrast gradient echo sequence. Radiother Oncol 2009;93:241–5.
[20] Kajihara H, Hayashida Y, Murakami R, Katahira K, Nishimura R, Hamada Y, et al. Usefulness of diffusion-weighted imaging in the localization of prostate cancer. Int J Radiat Oncol Biol Phys 2009;74:399–403.
[21] De Meerleer G, Villeirs G, Bral S, Paelinck L, De Gersem W, Dekuyper P, et al. The magnetic resonance detected intraprostatic lesion in prostate cancer: planning and delivery of intensity-modulated radiotherapy. Radiother Oncol 2005;75:325–33.
[22] Azzeroni R, Maggio A, Fiorino C, Mangili P, Cozzarini C, De Cobelli F, et al. Biological oprimization of simultaneous boost on intra-prostatic lesions (DILs): sensitivity to TCP parameters. Phys Medica 2013;29(6):592–8.
[23] Aluwini S, van Rooij P, Hoogeman M, Kirkels W, Kolkman-Deurloo IK, Bangma C. Stereotactic body radiotherapy with a focal boost to the MRI-visible tumor as monotherapy for low- and intermediate-risk prostate cancer: early results. Radiat Oncol 2013;8:84.
[24] Kudchadker RJ, Lee AK, Yu ZH, Johnson JL, Zhang L, Zhang Y, et al. Effectiveness of using fewer implanted fiducial markers for prostate target alignment. Int J Radiat Oncol Biol Phys 2009;74:1283–9.
[25] Moman MR, van der Heide UA, Kotte ANTJ, van Moorselaar RJA, Bol GH, Franken SPG, et al. Long-term experience with transrectal and transperineal implantations of fiducial gold markers in the prostate for position verification in external beam radiotherapy; feasibility, toxicity and quality of life. Radiother Oncol 2010;96:38–42.
[26] van Haaren PMA, Bel A, Hofman P, van Vulpen M, Kotte ANTJ, van der Heide UA. Influence of daily setup measurements and corrections on the estimated delivered dose during IMRT treatment of prostate cancer patients. Radiother Oncol 2009;90:291–8.
[27] Vassiliev ON, Kudchadker RJ, Kuban DA, Frank SJ, Choi S, Nguyen Q, et al. Dosimetric impact of fiducial markers in patients undergoing photon beam radiation therapy. Phys Medica 2012;28:240–4.
[28] Zarza-Moreno M, Cardoso I, Teixeira N, Jesus AP, Mora G. The use of non-standard CT conversion ramps for Monte Carlo verification of 6 MV prostate IMRT plans. Phys Med Eur J Med Phys 2013;29(4):357–67.
[29] Siggel M, Ziegenhein P, Nill S, Oelfke U. Boosting runtime-performance of photon pencil beam algorithms for radiotherapy treatment planning. Phys Med Eur J Med Phys 2012;28(4):273–80.
[30] Brenner DJ, Martinez AA, Edmundson GK, Mitchell C, Thames HD, Armour EP. Direct evidence that prostate tumors show high sensitivity to fractionation (low alpha/beta ratio), similar to late-responding normal tissue. Int J Radiat Oncol Biol Phys 2002;52:6–13.
[31] Feuvret L, Noel G, Nauraye C, Garcia P, Mazeron J-J. Index de conformation et radiothérapie. Cancer/Radiothérapie 2004;8:108–19.
[32] Miralbell R, Mollà M, Rouzaud M, Hidalgo A, Toscan JI, Lozano J, et al. Hypofractionated boost to the dominant tumor region with intensity modulated stereotactic radiotherapy for prostate cancer: A sequential dose escalation pilot study. Int J Radiat Oncol Biol Phys 2010;78(1):50–7.
[33] Willoughby T, Reddy CA, Kupelian PA. Concomitant boost of the peripheral zone with hypofractionated radiotherapy in locally advanced prostate cancer patients: results of a Phase II protocol [Abstract]. Int J Radiat Oncol Biol Phys 2009;75(Suppl. 3). S82.
[34] Chang JH, Lim Joon D, Lee ST, Gong SJ, Anderson NJ, Scott AM, et al. Intensity modulated radiation therapy dose painting for localized prostate cancer using ^{11}C-choline positron emission tomography scans. Int J Radiat Oncol Biol Phys 2012;83:e691–6.
[35] Nutting CM, Corbishley CM, Sanchez-Nieto B, Cosgrove VP, Webb S, Dearnaley DP. Potential improvements in the therapeutic ratio of prostate cancer irradiation: dose escalation of pathologically identified tumour nodules using intensity modulated radiotherapy. Br J Radiol 2002;75:151–61.
[36] Van Lin EN, Fütterer JJ, Heijmink SW, van der Vight LP, Hoffmann AL, van Kollenburg P, et al. IMRT boost dose planning on dominant intraprostatic lesions: gold marker-based three-dimensional fusion of CT with dynamic contrast-enhanced and ^{1}H-spectroscopic MRI. Int J Radiat Oncol Biol Phys 2006;65:291–303.

3.3. The dosimetric contribution of an injection of hyaluronic acid between the prostate and the rectum

The hyaluronic acid (HA) is a polysaccharide that is found in an important quantity in human tissues, especially in the skin. When it exists in its natural form, it is "degrade" very fast by the enzymatic systems. The utility of the HA was already developed in medicine in urology, orthopedics or esthetics, so it was modified in order to be more stable in time (few months to few years).

A new and original approach for the rectum-wall sparing was first reported by Prada et al. using a hyaluronic acid injection for brachytherapy treatments or external beam radiation therapy in combination with brachytherapy for prostate cancer [43, 44]. The authors reported a very good tolerance of the spacer by the patients, with no side effects, no toxicity of rectal function and no pain. The stability of the HA was also reported by the authors 9 months after the injection. In consequence, the distance between the prostate and the rectum-wall is increased and probably the dose-effect to the rectum could be negligible. This implies that the rectal toxicity may be reduced, particularly for prostate SBRT.

In the last few years, the results of several clinical investigations were additionally reported with a different spacer, a polyethylene-glycol hydrogel [45-51].

3.3.1. Prostate hypofractionated radiotherapy with hyaluronic acid

Hence, based on the initial results of Prada *et al.*, a phase II study was started in 2010 in the Department of Radiotherapy-Oncology from HCL. The protocol evaluates the acute and late rectal toxicities of patients treated with a hypofractionated irradiation of 62 Gy in 20 fractions of 3.1 Gy. We have first started with a "moderate"-hypofractionated radiotherapy, as it was our first practice and because we wanted to acquire experience with hyaluronic acid injection. To our knowledge, it was the first study to use HA for exclusive external beam irradiation and an injection of HA under local anesthesia.

3.3.2. Publication

The first dosimetric results for 16 patients were presented as poster at the 54th Annual ASTRO Meeting (October 28 – 31, 2012) in Boston (Appendix 9, *abstract number 2499*) [52] and were furthermore accepted for publication in 2013 in the *International Journal of Radiation Oncology Biology Physics* [53]. The first clinical results for the 36 patients

included in the Phase II study RPAH1 were accepted for "*Digital Poster Discussion*" at ASTRO 2013 (Appendix 9, *abstract number 1065*) [54].

International Journal of
Radiation Oncology
biology • physics

www.redjournal.org

Clinical Investigation: Genitourinary Cancer

Prostate Hypofractionated Radiation Therapy: Injection of Hyaluronic Acid to Better Preserve The Rectal Wall

Olivier Chapet, MD, PhD,* Corina Udrescu, MS,*,† Marian Devonec, MD, PhD,‡ Ronan Tanguy, MD,* Marie-Pierre Sotton, MS,† Ciprian Enachescu, MD,* Marc Colombel, MD, PhD,§ David Azria, MD, PhD,|| Patrice Jalade, PhD,† and Alain Ruffion, MD, PhD‡

*Departments of *Radiation Oncology, †Medical Physics, and ‡Urology, Centre Hospitalier Lyon Sud, Pierre Benite, France; §Department of Urology, Hopital Edouard Herriot, Lyon, France; and ||Department of Radiation Oncology, Centre Val d'Aurelle, Montpellier, France*

Received Sep 20, 2012, and in revised form Nov 3, 2012. Accepted for publication Nov 13, 2012

Summary

The aim of this dosimetric study was to evaluate the contribution of a hyaluronic acid injection between the rectum and the prostate for reducing the risk of rectal toxicity in prostate hypofractionated irradiation. The hyaluronic acid injection significantly improved the dosimetric parameters of the rectal wall. A phase 2 study is underway to evaluate the rate of grade $\geq$2 late rectal toxicities when this injection is combined with a hypofractionated irradiation.

Purpose: The aim of this study was to evaluate the contribution of an injection of hyaluronic acid (HA) between the rectum and the prostate for reducing the dose to the rectal wall in a hypofractionated irradiation for prostate cancer.

Methods and Materials: In a phase 2 study, 10 cc of HA was injected between the rectum and prostate. For 16 patients, the same intensity modulated radiation therapy plan (62 Gy in 20 fractions) was optimized on 2 computed tomography scans: CT1 (before injection) and CT2 (after injection). Rectal parameters were compared: dose to 2.5 cc (D2.5), 5 cc (D5), 10 cc (D10), 15 cc (D15), and 20 cc (D20) of rectal wall and volume of rectum covered by the 90% isodose line (V90), 80% (V80), 70% (V70), 60% (V60), and 50% (V50).

Results: The mean V90, V80, V70, V60, and V50 values were reduced by 73.8% ($P<.0001$), 55.7% ($P=.0003$), 43.0% ($P=.007$), 34% ($P=.002$), and 25% ($P=.036$), respectively. The average values of D2.5, D5, D10, D15, and D20 were reduced by 8.5 Gy ($P<.0001$), 12.3 Gy ($P<.0001$), 8.4 Gy ($P=.005$), 3.7 Gy ($P=.026$), and 1.2 Gy ($P=.25$), respectively.

Conclusions: The injection of HA significantly limited radiation doses to the rectal wall.

Reprint requests to: Olivier Chapet, MD, PhD, Département de radiothérapie Oncologie, Centre Hospitalier Lyon Sud, Chemin du Grand Revoyet, 69495 Pierre Benite cedex, France. Tel: (33) 4-78-86-42-60; Fax: (33) 4-78-86-42-65; E-mail: olivier.chapet@chu-lyon.fr

Int J Radiation Oncol Biol Phys, Vol. 86, No. 1, pp. 72–76, 2013
0360-3016/$ - see front matter © 2013 Elsevier Inc. All rights reserved.
http://dx.doi.org/10.1016/j.ijrobp.2012.11.027

Conflict of interest: none.

Acknowledgments—This project was supported by the Department of Clinical Research, University Hospital, Lyon, France.

Introduction

The α/β ratio for prostate cancer, often estimated to be below 3 Gy (1-5), suggests that the dose per fraction could have a significant impact on local control in exclusive external beam irradiation of this cancer. Several phase 3 trials are comparing a hypofractionated irradiation (HF) with a dose per fraction between 2.4 Gy and 3 Gy with a normofractionated irradiation (NF) at 1.8-2 Gy. Recently, the first results of the Fox Chase Center phase 3 trial were presented (6). This superiority design study compared 76 Gy in 38 fractions of 2 Gy to 70.2 Gy in 26 fractions of 2.7 Gy. At 5 years, there was no difference between the 2 groups in terms of biochemical-free survival (BFS). This result suggests that a dose per fraction of 2.7 Gy might not be sufficient to induce a benefit and that a dose >3 Gy might be necessary. The results of the Arcangeli et al study (7) support this conclusion. Indeed, a dose of 62 Gy in 20 fractions of 3.1 Gy was compared with a dose of 80 Gy in 40 fractions of 2 Gy. At 3 years, the BFS was increased from 79% to 89% ($P = .035$) in the HF arm. The rate of grade $\geq$2 late rectal toxicities was 17% and 16% in the HF and NF arms, respectively. In several phase 2 trials, HF with doses per fraction of $\geq$3 Gy was associated with rates of grade $\geq$2 acute rectal toxicities of between 20% and 36% and a rate of late toxicities >15% (8-12). Rectal tolerance could therefore represent the main limitation to expanded use of HF in prostate cancer. An injection of hyaluronic acid (HA) in the space between the rectum and the prostate has been proposed as a method of improving rectal tolerance following brachytherapy and Prada et al (13, 14) highlighted the tolerability of this approach. In 2010, a phase 2 trial was initiated to evaluate the benefit of using HA as a spacer in a HF schema to better preserve the rectum. Dosimetric analyses of the first 16 patients included in the study are presented and discussed.

Methods and Materials

HA injection

All the patients included in the phase 2 study had a low- to intermediate-risk prostate cancer according to D'Amico classification (15). They received a transperineal injection of 10 cc of HA (NASHA Spacer gel, Q-Med AB, Uppsala, Sweden) between the rectum and the prostate under local anesthesia and ultrasound guidance. This injection was combined with an implantation of 3 gold markers used for a computed tomography/magnetic resonance imaging (CT/MRI) fusion and for treatment setup. The aim of the injection was to separate the prostate from the rectum and thereby reduce the dose received by the anterior rectum wall. An injection of this volume of HA was expected to separate the 2 organs by at least 1 cm (Fig. 1). No limitation of prostate volume was defined for the inclusion of patients in the study.

Dosimetric study

As part of the phase 2 trial, a dosimetric CT scan (GE LightSpeed16), with a slice thickness of 2.5 mm, was performed before (CT1) and after injection of HA (CT2). Patients were treated with a 7-field intensity modulated radiation therapy (IMRT) plan, optimized on the CT2. For the first 16 patients included in the present study, the same treatment plan was optimized on CT1 (without HA injection) for dosimetric comparison. All the patients were treated in the supine position. The rectum was empty on both CTs, and the bladder was in a state of intermediate repletion.

Definitions of volumes

Identical volumes were created on the 2 dosimetric CT scans. A clinical target volume 1 (CTV1) was defined by the delineation of the prostate and the first centimeter of the seminal vesicles. A CTV2 corresponded to the prostate alone. A planning target volume 1 (PTV1) was created by adding a volumetric expansion of 8 mm around the CTV1 (except in the posterior direction where the margin was reduced to 4 mm). A PTV2 was generated by adding the same margins around the CTV2. The rectum was delineated from 2 cm above to 2 cm below the CTV1. The rectal wall was defined by an internal expansion of 5 mm. The external contours of the bladder were totally delineated. An internal expansion of 7 mm was used to generate the bladder wall. The 2 femoral heads were identified up to the upper edge of the lesser trochanters.

Comparison of plans of treatment

The same 7-beam IMRT plan was optimized on the CT1 and CT2 with the photon energy of 16 MV. A dose of 3.1 Gy per fraction (total dose of 62 Gy) was prescribed. The dose to the PTV1 was 44 Gy in 20 fractions of 2.2 Gy (BED = 46 Gy with $\alpha/\beta = 1.5$ Gy) and 100% of the volume was covered by the isodose line of 42 Gy (95% of 44 Gy; 2.1 Gy per fraction). Whenever possible, 90% of the PTV1 had to receive 44 Gy. The PTV2 was covered by the 59 Gy isodose line (2.95 Gy per fraction: 95% of 3.1 Gy) and whenever possible, 90% of this volume received at least 3.1 Gy. The maximum dose point did not exceed 105% of the prescribed dose. The total number of fractions was 20 for a total dose of 62 Gy. The doses to the rectum and the bladder were optimized to be as low as possible. The maximum dose to the femoral heads did not exceed 46 Gy in 20 fractions.

Thickness of HA

Because the HA was better visualized on the MRI than on the CT, a fusion based on gold makers was used to improve the delineation of the spacer (Fig. 2). The thickness of HA between the prostate and the rectum was measured on the centerline of the prostate in 3 CT scan slices: (*1*) at the apex of the prostate, 5 mm above the most inferior portion of the prostate; (*2*) at the base of the prostate,

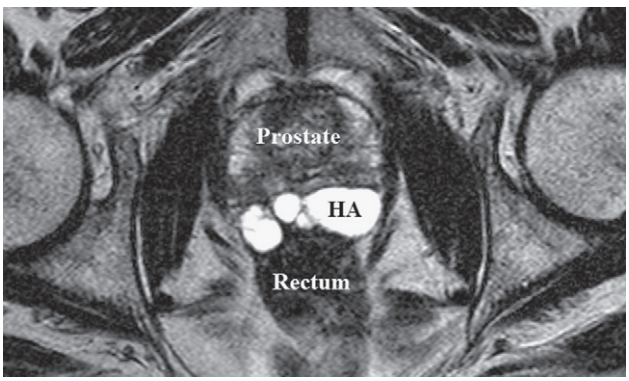

Fig. 1. Injection of hyaluronic acid (HA) between the rectum and the prostate.

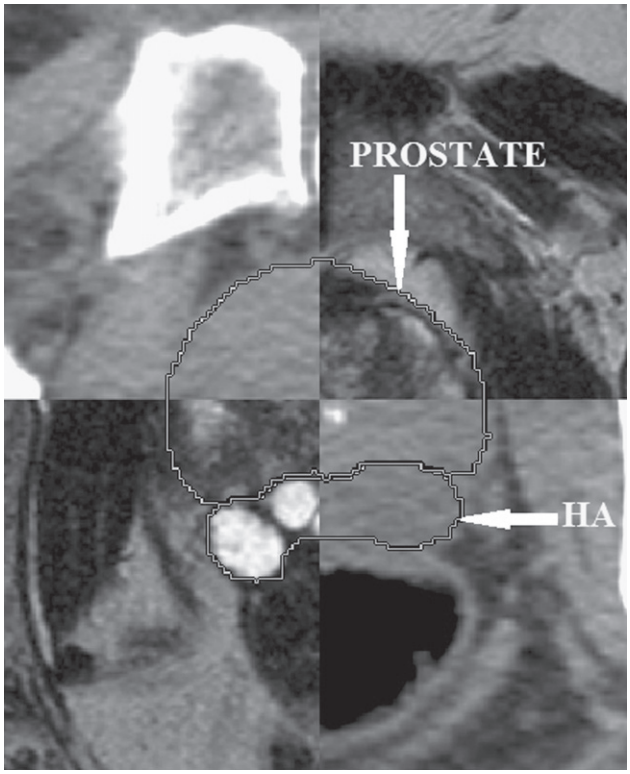

Fig. 2. Delineation of hyaluronic acid (HA) on computed tomography/magnetic resonance imaging fusion.

5 mm below the most superior portion of the prostate; and (*3*) on the median CT slice. For each patient, an average thickness value was calculated from the 3 measurements.

Analysis

The dosimetric comparison between CT1 and CT2 was performed on the first 16 patients included in the study. The volumes of rectum irradiated with and without HA were compared on the following dosimetric parameters: maximum dose (Dmax), minimum doses to 2.5 cc (D2.5), 5 cc (D5), 10 cc (D10), 15 cc (D15), and 20 cc (D20) of rectum and the volume of rectum receiving 90% (V90), 80% (V80), 70% (V70), 60% (V60), and 50% (V50) of the prescribed dose of 62 Gy. These quantitative dosimetric variables were performed using the Wilcoxon test for paired series (Wilcoxon matched-pairs test). The analysis was univariate, bilateral with a significance threshold set at $P<.05$. All tests were conducted using the SPSS V19.0 software.

To limit the potential impact of variation of rectal volume between the 2 CT scans, all results were calculated in cubic centimeters and not as percentage of volume. The same parameters were used for the bladder. For comparison, all the results were expressed as mean values for the 16 patients.

Results

Volume delineation

The mean prostate volume was 51.7 cc (range, 28.7-93.9 cc) on the CT1 and 52.7 cc (range, 31.4-92.7 cc) on the CT2. The PTV1 and PTV2 were 154.3 cc (range, 111.1-232.8 cc) and 129.1 cc (range, 88.7-204.4 cc), respectively, on CT1 and 161.1 cc (range, 117.8-240.0 cc) and 132.6 cc (range, 91.6-202.2 cc), respectively, on CT2.

The mean rectum-wall volume was 36.9 cc (range, 20-54 cc) on CT1 and 37.3 cc (range, 23.9-50 cc) on the CT2. For the bladder wall, the mean volume was 50.5 cc (range, 20-87 cc) on CT1 and 57.2 cc (range, 23.7-111.3 cc) on CT2.

PTV1 and PTV2 coverage

The 42 Gy isodose line (95% of the dose to the PTV1) covered 99.6% (range, 98.6%-100%) and 99.8% (range, 99.5%-100%) of the PTV1, on CT1 and CT2, respectively. The mean volume of PTV1 receiving 44 Gy (100% of dose) was 97.8% (range, 95.1%-100.0%) and 97.5% (range, 91%-99.9%) on CT1 and CT2, respectively. The mean volume of PTV2 covered by the 59 Gy isodose line (95% of 62 Gy) was 99.9% (range, 99.8%-100%) on CT1 and 99.6% (range, 95.3%-100%) on CT2. The isodose 62 Gy covered 91.1% (range, 90.0%-96.5%) of the PTV2 on the CT1 and 91.9% (range, 90%-99.4%) of the same PTV on CT2.

Rectal doses with and without HA

The average thickness of HA for the 16 patients was 11.5 mm (range, 8.3-16.4 mm). The average thickness of HA at the base, median, and apex of the prostate were 15.1 mm (range, 6.4-29 mm), 9.8 mm (range, 5-21.2 mm) and 9.9 mm (range, 3.2-21.5 mm). The detailed results of rectal doses with and without HA are summarized in Table 1. The mean values of V90, V80, V70, V60, and V50 were reduced by 73.8% ($P<.0001$), 55.7% ($P=.0003$), 43.0% ($P=.007$), 34% ($P=.002$), and 25% ($P=.036$), respectively. Similarly, the average values of D2.5, D5, D10, D15, and D20 were reduced by 8.5 Gy ($P<.0001$), 12.3 Gy ($P<.0001$), 8.4 Gy ($P=.005$), 3.7 Gy ($P=.026$), and 1.2 Gy ($P=.25$), respectively.

Discussion

HF is a promising approach to external beam irradiation in prostate cancer. It could potentially reduce the duration and cost of

Table 1 Variation of dosimetric rectal parameters (mean values and range) after injection of HA (hyaluronic acid)

	CT1 (without HA)	CT2 (with HA)
V100%	0.3 cc (0-2.63 cc)	0 cc
V90%	7.65 cc (4.4-18.9 cc)	2.1 cc (0.3-6.8 cc)
V80%	10.4 cc (5.8-25.2 cc)	4.6 cc (0.7-11.8 cc)
V70%	13.3 cc (7.2-36.6 cc)	7.6 cc (1.2-17.9 cc)
V60%	16.4 cc (8.9-48.9 cc)	10.9 cc (1.9-23.1 cc)
V50%	20.3 cc (10.8-62.8 cc)	15.1 cc (2.8-30.4 cc)
D2.5	60.9 Gy (59.7-62.1 Gy)	52.4 Gy (32.3-60.0 Gy)
D5	58.5 Gy (53.3-61.1 Gy)	46.2 Gy (24.6-57.6 Gy)
D10	45.7 Gy (33.9-57.4 Gy)	37.3 Gy (19.7-51.8 Gy)
D15	34.9 Gy (18.4-51.1 Gy)	31.2 Gy (16.5-45.7 Gy)
D20	27.0 Gy (19.7-42.4 Gy)	25.8 Gy (12.6-41.2 Gy)
Dmax	62.4 Gy (61.5-63.6 Gy)	61.2 Gy (59.7-62.7 Gy)

treatment per patient, improve the capacity of treatment in radiation oncology departments, and improve local control of the disease compared to a normal fractionation.

Some experiences have been reported with a dose per fraction of ≥3 Gy. When doses of 57 to 60 Gy (in 19-20 fractions of 3 Gy) were used, rates of late grade ≥2 rectal toxicity, <10%, were reported (16-19). Using the linear-quadratic (LQ) model and an α/β ratio of 4.8 Gy for grade ≥2 late rectal toxicity (20), the biochemical equivalent dose for 60 Gy in 20 fraction is 69 Gy in 2 Gy per fraction. In the Vesprini et al study (9), 121 patients were treated with 60 to 66 Gy in 20 to 22 fractions of 3 Gy with IMRT. There was a significant difference in the rate of late GI toxicity grade ≥2 when comparing the 66-Gy and 60-Gy cohorts (38% vs 8%, respectively, $P = .0003$), suggesting that increasing the number of fractions of 3 Gy from 20 to 22 may be sufficient to have a strong impact on rectal toxicity. Using the LQ model and the same α/β ratio of 4.8 Gy for grade ≥2 late rectal toxicity, the biochemical equivalent dose for 66 Gy in 22 fractions is 76 Gy in 2 Gy per fraction. Several studies seem to confirm the impact of a variation of dose per fraction or of fraction number on rectal toxicity. In a series of 52 patients treated at 69 Gy in 23 fractions of 3 Gy, Akimoto et al (11) reported a rate of 25% for grade ≥2 rectal bleeding. In the Rene et al study (10), 129 patients were treated at 66 Gy in 22 fractions of 3 Gy. With a median follow-up of 51 months, the worst crude rate of grade ≥2 GI toxicity seen at any time during follow-up was 25%. In the Lock et al study (8), 66 patients were treated at 63.2 Gy in 20 fractions of 3.16 Gy. Despite the use of arc-based IMRT and a daily repositioning of the prostate, 25% and 3% of patients experienced grade 2 and grade 3 rectal toxicities, respectively, with a median follow-up of 36 months.

On the basis of the experiences reported with doses >60 Gy in 20 fractions, a phase 2 study was initiated in 2010. Patients with low- to intermediate-risk prostate cancer according to the D'Amico classification (15) were treated at a dose of 62 Gy in 20 fractions of 3.1 Gy. An injection of HA between the rectum and the prostate was performed under local anesthesia. Experiences of injection of HA have already been published, and the authors demonstrated that this injection was well tolerated and offered superior preservation of the rectum wall in prostate HDR brachytherapy (13, 14) or external beam radiation therapy (21, 22).

Few other studies used different spacers between the prostate and the rectum with a prescribed standard doses of 78 Gy (39 fractions of 2 Gy) and IMRT planning (23-25). In the cadaveric study, Susil et al used 20 mL of hydrogel injection to create a mean separation of 12.5 mm (23). The average rectum volumes receiving 70 Gy with IMRT decreased from 19.9% before separation to 4.5% after separation. In their study, they concluded that 10 to 15 mm of separation is sufficient to achieve the rectal V70 reduction. For 8 prostate cancer patients, Weber et al injected approximately 10 mL of polyethylene glycol spacer to create 7 to 10 mm separation between the prostate and the rectum (24). Mean value for V70 with IMRT planning was 9.8% ± 5.4% before spacer insertion and decreased to 5.3% ± 3.3% after spacer injection. Following an injection of 10 mL of spacer gel in 18 patients with prostate cancer, Pinkawa et al observed distances of at least 6.6 mm in a medial plane in 89% of cases (25). They found that relative rectum volume within the 50, 60, 70, and 76 Gy isodose could be reduced by 22%, 35%, 56%, and 89% in IMRT treatment plans.

Although Prada et al (13, 14) needed only 3 to 7 mL of HA for a sufficient separation between the rectum and the prostate, in our experience this volume of HA was not sufficient and a full syringe of 10 mL was necessary to achieve at least 1 cm of HA thickness. Our study proposes an injection of HA for hypofractionated external beam irradiation. The results of the dosimetric comparison of treatment with and without HA confirm the potential benefit of the injection in preserving the rectal wall. A potential weakness of the study is that the 2 CT scans (with and without HA) were not performed in exactly the same conditions for the prostate and the rectum. However, the delineation of the prostates was similar on both CT scans, with mean volumes of 52.7 cc and 51.7 cc, respectively. All the rectal dosimetric parameters were expressed in cubic centimeters and not as percentage of volume to limit the impact of a variation of rectal dilatation between the 2 CT scans, as observed in other studies (24). Almost all rectal dosimetric parameters evaluated in this study were strongly improved by the injection of HA; only the punctual maximum dose does not seem to be reduced by the HA injection. This punctual Dmax remains equivalent to the treatment dose in the 2 plans (61.2 and 62.4 Gy). This result highlights that even with an injection of HA, a small volume of rectum may remain inside the PTV and receive a dose close to 62 Gy. Nevertheless, the large improvement of the D2.5 demonstrates that the volume of rectum exposed to high doses is greatly reduced by the injection of HA.

Conclusion

An injection of HA between the rectum and the prostate significantly improves the dosimetric parameters of the rectal wall. A phase 2 study is under way to evaluate the rate of grade ≥2 late rectal toxicities when this injection is combined with HF irradiation.

References

1. Carlson DJ, Stewart RD, Li XA, et al. Comparison of in vitro and in vivo α/β ratios for prostate cancer. *Phys Med Biol* 2004;49: 4477-4491.
2. Brenner DJ, Hall EJ. Fractionation and protraction for radiotherapy of prostate carcinoma. *Int J Radiat Oncol Biol Phys* 1999; 43:1095-1101.
3. Brenner DJ, Martinez AA, Edmundson GK. Direct evidence that prostate tumors show high sensitivity to fractionation (low alpha/beta ratio), similar to late-responding normal tissue. *Int J Radiat Oncol Biol Phys* 2002;52:6-13.
4. Wang JZ, Guerrero M, Li XA. How low is the α/β ratio for prostate cancer? *Int J Radiat Oncol Biol Phys* 2003;55:194-203.
5. Miralbell R, Roberts SA, Zubizarreta E, et al. Dose fractionation sensitivities of low/middle/high-risk prostate cancer deduced from seven international primary institutional datasets. *Int J Radiat Oncol Biol Phys* 2009;75(suppl 3):S81.
6. Pollack A, Walker G, Buyyounouski M, et al. Five year results of a randomized external beam radiotherapy hypofractionation trial for prostate cancer. *Int J Radiat Oncol Biol Phys* 2011;81:S1.
7. Arcangeli G, Saracino B, Gomellini S, et al. A prospective phase III randomized trial of hypofractionation versus conventional fractionation in patients with high-risk prostate cancer. *Int J Radiat Oncol Biol Phys* 2010;78:11-18.
8. Lock M, Best L, Wong E, et al. Phase II trial of arc-based hypofractionated intensity-modulated radiotherapy in localized prostate cancer. *Int J Radiat Oncol Biol Phys* 2011;80:1306-1315.
9. Vesprini D, Sia M, Lockwood G, et al. Role of principal component analysis in predicting toxicity in prostate cancer patients treated with hypofractionated intensity-modulated radiation therapy. *Int J Radiat Oncol Biol Phys* 2011;81:415-421.

10. Rene N, Faria S, Cury F, et al. Hypofractionated radiotherapy for favorable risk prostate cancer. *Int J Radiat Oncol Biol Phys* 2010;77: 805-810.
11. Akimoto T, Muramatsu H, Takahashi M, et al. Rectal bleeding after hypofractionated radiotherapy for prostate cancer: correlation between clinical and dosimetric parameters and the incidence of grade 2 or worse rectal bleeding. *Int J Radiat Oncol Biol Phys* 2004;60:1033-1039.
12. Faria SL, Souhami L, Joshua B, et al. Reporting late rectal toxicity in prostate cancer patients treated with curative radiation treatment. *Int J Radiat Oncol Biol Phys* 2008;72:777-781.
13. Prada PJ, Fernandez J, Martinez AA, et al. Transperineal injection of hyaluronic acid in anterior perirectal fat to decrease rectal toxicity from radiation delivered with intensity modulated brachytherapy or EBRT for prostate cancer patients. *Int J Radiat Oncol Biol Phys* 2007;69:95-102.
14. Prada PJ, Gonzalez H, Menéndez C, et al. Transperineal injection of hyaluronic acid in the anterior perirectal fat to decrease rectal toxicity from radiation delivered with low-dose-rate brachytherapy for prostate cancer patients. *Brachytherapy* 2009;8:210-217.
15. D'Amico AV, Whittington R, Malkowicz SB, et al. Biochemical outcome after radical prostatectomy, external beam radiation therapy, or interstitial radiation therapy for clinically localized prostate cancer. *JAMA* 1998;280:969-974.
16. Leborgne F, Fowler J. Late outcomes following hypofractionated conformal radiotherapy vs. standard fractionation for localized prostate cancer: A nonrandomized contemporary comparison. *Int J Radiat Oncol Biol Phys* 2009;74:1441-1446.
17. Coote JH, Wylie JP, Cowan RA, et al. Hypofractionated intensity-modulated radiotherapy for carcinoma of the prostate: Analysis of toxicity. *Int J Radiat Oncol Biol Phys* 2009;74:1121-1127.
18. Martin JM, Rosewall T, Bayley A, et al. Phase II trial of hypofractionated image-guided intensity-modulated radiotherapy for localized prostate adenocarcinoma. *Int J Radiat Oncol Biol Phys* 2007;69:1084-1089.
19. Dearnaley D, Syndikus I, Sumo G, et al. Conventional versus hypofractionated high-dose intensity-modulated radiotherapy for prostate cancer: Preliminary safety results from the CHHiP randomised controlled trial. *Lancet Oncol* 2012;13:43-54.
20. Tucker SL, Thames HD, Michalski JM, et al. Estimation of α/β for late rectal toxicity based on RTOG 94-06. *Int J Radiat Oncol Biol Phys* 2011;81:600-605.
21. Pinkawa M, Piroth MD, Holy R, et al. Quality of life after intensity-modulated radiotherapy for prostate cancer with a hydrogel spacer. *Strahlenther Onkol* 2012;188:917-925.
22. Hatiboglu G, Pinkawa, Vallee JP, et al. Application technique: Placement of a prostate-rectum spacer in men undergoing prostate radiation therapy. *BJU Int*, in press.
23. Susil RC, McNutt TR, DeWeese TL, et al. Effects of prostate-rectum separation on rectal dose from external beam radiotherapy. *Int J Radiat Oncol Biol Phys* 2010;76:1251-1258.
24. Weber DC, Zilli T, Vallee JP, et al. Intensity modulated proton and photon therapy for early prostate cancer with or without transperineal injection of a polyethylene glycol spacer: a treatment planning comparison study. *Int J Radiat Oncol Biol Phys* 2012;84: e311-e318.
25. Pinkawa M, Escobar Corral N, Caffaro M, et al. Application of a spacer gel to optimize three-dimensional conformal and intensity modulated radiotherapy for prostate cancer. *Radiother Oncol* 2011; 100:436-441.

3.3.3. Prostate SBRT with hyaluronic acid

The ultimate purpose of such approach of prostate-rectum separation is to be applied for stereotactic schemas used for the treatment of prostate cancer. Even with the expectation that small volumes of adjacent organs at risk will be irradiated with high doses during SBRT, it is estimated that the rectum would receive minor doses.

The "lowest" SBRT dose found in the literature for prostate cancer is 32.5 Gy (5 x 6.5 Gy). In our department, 42.5 Gy in 5 fractions seems a reasonable dose without a prostate-rectum separation. Therefore, an evaluation of a HA consequence with the latter dose was made in order to make this dose acceptable when a prostate-rectum separation exists.

To our knowledge, a PRS was never applied for a SBRT approach. In order to investigate the potential benefit of using PRS in SBRT, a dosimetric study was realized. An evaluation for prostate SBRT was made with two levels of dose: 32.5 Gy versus 42.5 Gy in 5 fractions, with or without a PRS.

3.3.4. Publication

The initial results were accepted for poster presentation at the ESTRO 31 conference (09-13 May, 2012) in Barcelona, Spain and the abstract has also been selected for "*Young scientists ESTRO Poster Session*" (Appendix 10, *abstract number PD-0278*) [55]. The related article is presented below and was published in 2014 in the *International Journal of Radiation Oncology Biology Physics*.

International Journal of Radiation Oncology biology • physics

www.redjournal.org

Physics Contribution

Dosimetric Implications of an Injection of Hyaluronic Acid for Preserving the Rectal Wall in Prostate Stereotactic Body Radiation Therapy

Olivier Chapet, MD, PhD,* Corina Udrescu, MS,*,† Ronan Tanguy, MD,* Alain Ruffion, MD, PhD,‡ Pascal Fenoglietto, MS,§ Marie-Pierre Sotton, MS,† Marian Devonec, MD, PhD,‡ Marc Colombel, MD, PhD,‖ Patrice Jalade, PhD,† and David Azria, MD, PhD§

**Department of Radiation Oncology, †Department of Medical Physics, and ‡Department of Urology, Centre Hospitalier Lyon Sud, Pierre Benite; §Department of Radiation Oncology, Centre Val d'Aurelle, Montpellier; and ‖Department of Urology, Hopital Edouard Herriot, Lyon, France*

Received Jul 6, 2013, and in revised form Oct 17, 2013. Accepted for publication Oct 28, 2013.

Summary

The benefit of a hyaluronic acid injection between the prostate and the rectal wall was evaluated for stereotactic irradiation. An important contribution of the hyaluronic acid was observed for rectal wall preservation (volume reduction of 90%). This effect, especially from the median plane to the apex of the prostate, could allow a dose escalation from 5 × 6.5 Gy to 5 × 8.5 Gy without significantly increasing the dose to the rectum.

Purpose: This study assessed the contribution of ahyaluronic acid (HA) injection between the rectum and the prostate to reducing the dose to the rectal wall in stereotactic body radiation therapy (SBRT).

Methods and Materials: As part of a phase 2 study of hypofractionated radiation therapy (62 Gy in 20 fractions), the patients received a transperineal injection of 10 cc HA between the rectum and the prostate. A dosimetric computed tomographic (CT) scan was systematically performed before (CT1) and after (CT2) the injection. Two 9-beam intensity modulated radiation therapy-SBRT plans were optimized for the first 10 patients on both CTs according to 2 dosage levels: 5 × 6.5 Gy (PlanA) and 5 × 8.5 Gy (PlanB). Rectal wall parameters were compared with a dose−volume histogram, and the prostate−rectum separation was measured at 7 levels of the prostate on the center line of the organ.

Results: For both plans, the average volume of the rectal wall receiving the 90% isodose line (V90%) was reduced up to 90% after injection. There was no significant difference ($P = .32$) between doses received by the rectal wall on CT1 and CT2 at the base of the prostate. This variation became significant from the median plane to the apex of the prostate ($P = .002$). No significant differences were found between PlanA without HA and PlanB with HA for each level of the prostate ($P = .77$, at the isocenter of the prostate).

Conclusions: HA injection significantly reduced the dose to the rectal wall and allowed a dose escalation from 6.5 Gy to 8.5 Gy without increasing the dose to the rectum. A phase 2 study is under way in our department to assess the rate of acute and late rectal toxicities when SBRT (5 × 8.5 Gy) is combined with an injection of HA. © 2014 Elsevier Inc.

Reprint requests to: Olivier Chapet, MD, PhD, Département de Radiothérapie Oncologie, Centre Hospitalier Lyon Sud, 165 Chemin du Grand Revoyet, 69495 Pierre Benite Cedex, France. Tel: (+33) 4-78-86-42-60; E-mail: olivier.chapet@chu-lyon.fr

Supported by Q-Med AB, Uppsala, Sweden, with grants and with hyaluronic acid injections provided to the University Hospital Lyon Sud.

Conflict of interest: none.

Int J Radiation Oncol Biol Phys, Vol. 88, No. 2, pp. 425−432, 2014
0360-3016/$ - see front matter
http://dx.doi.org/10.1016/j.ijrobp.2013.10.039

Introduction

Several studies have shown an α/β ratio for prostate cancer of less than 3 Gy, encouraging dose escalation (1-3). In previous years, a few trials have evaluated stereotactic body radiation therapy (SBRT) for low-risk to intermediate-risk prostate cancer (4-12). The treatment was delivered in 4 to 5 fractions of 6.5 Gy to 10 Gy using an image guided radiation therapy technique. Acute and late grade 1 to grade 3 urinary toxicities after SBRT are not negligible, and techniques for reducing the dose to the bladder must be studied. In addition, grade 1 to grade 2 acute and late rectal toxicities have been reported of 27% to 67% and 14% to 70%, respectively. To improve the patients' quality of life, a potential method of reducing the dose to the rectum may be a prostate-rectum separation (PRS). This approach has been described by Prada et al (13, 14) for brachytherapy treatments and by other teams during external beam radiation therapy (15-21). The main objective of the present study was to assess whether a hyaluronic acid (HA) injection between the rectum and the prostate could reduce the doses to the rectal wall in 2 SBRT approaches. The purpose of this work was 2-fold: (*1*) to evaluate the dose received by the rectum and to calculate the dose to the anterior rectal wall in a SBRT approach with HA and (*2*) to evaluate whether the rectal wall could be entirely preserved by an injection of HA when the dose to the prostate was increased from 6.5 Gy to 8.5 Gy per fraction.

Methods and Materials

Patients

As part of a phase 2 study for hypofractionated radiation therapy (62 Gy in 20 fractions of 3.1 Gy) (21), patients were treated for low-risk or intermediate-risk prostate cancer according to the D'Amico classification (22). Three gold markers were implanted into the prostate for image registration (Integrated Registration, GE Medical Systems) between the computed tomographic (CT) scan and T2 magnetic resonance imaging (T2-MRI) and for daily localization. A transperineal injection of 10 cc HA (NASHA Spacer gel, Q-Med AB, Uppsala, Sweden) was systematically performed between the rectum and the prostate, with the patient under local anesthesia, and under ultrasound guidance (Fig. 1). Inasmuch as the prostate and the HA were better visualized on T2-MRI than on the CT scan, the fusion was thereafter used for target and spacer contouring (Fig. 1a).

Treatment volume definition

For the first 10 patients included in the study, the following volumes were created on 2 CT scans, before (CT1) and after (CT2) the injection of HA:

1. A planning target volume (PTV) corresponding to a 3-mm uniform margin around the prostate (to account for interfraction and intrafraction motion); these small margins were feasible with the use of 3 gold markers for (a) daily kV repositioning and cone beam CT verification with the OBI system (Varian), (b) target monitoring with the Snap Verification tool of the ExacTrac system (BrainLab), or both.
2. The rectum was empty on both CTs and was delineated from 2 cm above to 2 cm below the prostate. The rectal wall was defined by an internal expansion of 5 mm.
3. The bladder was in intermediate repletion and was delineated on all CT slices. The bladder wall was defined using an internal expansion of 7 mm.

Comparison of the treatment plans

The SBRT plans were simulated using a 9-beam configuration with intensity modulated radiation therapy (IMRT). The plans were optimized on CT1 and CT2, according to 2 dosage levels: (*1*) 32.5 Gy in 5 fractions of 6.5 Gy (PlanA) (Biological Equivalent Dose $=$ 76 Gy in 38 fractions of 2 Gy with $\alpha/\beta = 1.5$ Gy) and (*2*) 42.5 Gy in 5 fractions of 8.5 Gy (PlanB) (Biological Equivalent Dose $\approx$ 110 Gy in 55 fractions of 2 Gy with $\alpha/\beta = 1.5$ Gy).

PlanA and PlanB were individually optimized and calculated for both CT1 and CT2.

In all plans, at least 97% of the PTV had to be covered by the 98% isodose line (Fig. 1b), and whenever possible, 90% of the PTV had to be covered by the 100% isodose line. The maximum dose point did not exceed 107% of the prescribed dose, and the doses to the rectal wall and the bladder wall were optimized to be as low as possible.

Statistical analysis

Initially, a general analysis was made for all patients. The volumes of the rectum and the bladder irradiated with and without HA were compared by the following dosimetric parameters: maximum dose (Dmax), dose to 2.5 cc (D2.5cc), 5 cc (D5cc), 10 cc (D10cc), and 15 cc (D15cc) of the organ, and the volumes of the organ receiving 90% (V90%), 80% (V80%), 70% (V70%), 60% (V60%), and 50% (V50%) of the prescribed doses. To limit a potential impact of variation in rectal and bladder volumes between the 2 CT scans, all results are given in cubic centimeters and not as percentage of volume. These quantitative dosimetric variables were analyzed by Wilcoxon test for paired series (Wilcoxon matched-pairs test). The analysis was univariate and bilateral, with a significant threshold set at $P<.05$. The tests were made with SPSS, version 19.0 software.

Then, for CT1 and CT2, the distances between the prostate and the rectum were measured at the center line of the prostate in 7 CT scan slices (Fig. 1d), following the representation of Kagawa et al (23): (*1*) at the base of the prostate and 5, 10, and 15 mm superior to the geometric isocenter of the prostate defined on the CT (noted as $+5$ mm, $+10$ mm, and $+15$ mm); (*2*) at the isocenter of the prostate (noted as 0 mm); and (*3*) at the apex of the prostate and 5, 10, and 15 mm inferior to the isocenter of the prostate (noted as -5 mm, -10 mm, and -15 mm).

Moreover, dose profiles were obtained in the 7 CT scan slices for the anterior rectal wall. They were measured at the center line of the prostate. The doses received by the rectal wall at 1 mm, 2 mm, 3 mm, 4 mm, and 5 mm of depth were noted for the 7 CT slices. The doses delivered to the anterior rectal wall were compared between CT1 and CT2 at different levels of the prostate by use of Wilcoxon test for matched series.

Additionally, a comparison was made between PlanA without HA and PlanB with HA for the doses received by the first

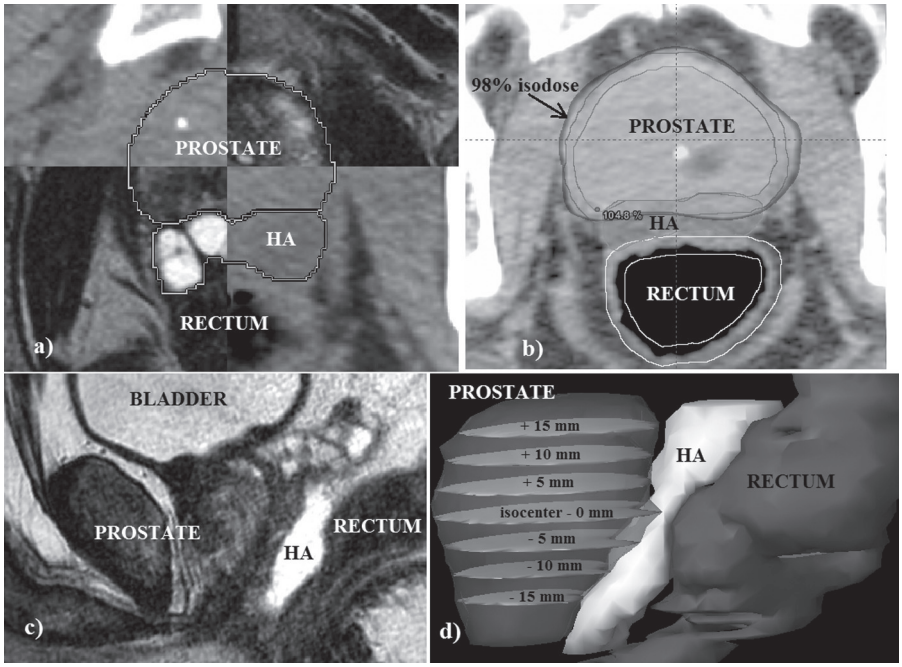

Fig. 1. (a) Axial view of image registration between the computed tomographic (CT) scan and the T2 magnetic resonance image (T2-MRI) with the delineation of the prostate and of the hyaluronic acid (HA). (b) Target covered by the 98% isodose and contour projections on the CT scan of the prostate, rectum, and HA. (c) Sagittal plane of the T2-MRI examination. (d) Illustration of different prostate levels, following the representation of Kagawa et al (22).

millimeter of the rectal wall at each level of the prostate. The test used for this comparison was Wilcoxon test for matched series.

Results

Volume delineation and PTV coverage

The mean prostate volumes were 52 cc (range, 30-93.9 cc) on CT1 and 52.4 cc (range, 32.5-92.7 cc) on CT2 ($P = .62$). The mean rectal wall volumes were 38.1 cc (range, 26-54 cc) on CT1 and 39.3 cc (range, 26.8-50.5cc) on CT2; there was no statistically significant difference between the 2 series ($P = .84$). For the bladder wall, the mean volumes were 51.4 cc (range, 17.8-87 cc) and 59 cc (range, 30.3-96.3 cc) on CT1 and CT2, respectively, with no statistically significant difference between the 2 series ($P = .1$).

For PlanA, the 98% isodose line covered 98.4% (range, 97.1%-100%) of the prostate on CT1 and 98.5% (range, 97.5%-100%) on CT2. The 100% isodose line covered 94.6% (range, 92.9%-98.9%) of the prostate on CT1 and 94.7% (range, 93.1%-96.8%) on CT2. For PlanB, the 98% isodose line covered 98.5% (range, 97.2%-100%) of the prostate on CT1 and 98.7% (range, 96.9%-99.9%) on CT2. The 100% isodose line covered 94.3% (range, 91.6%-98.7%) and 93.3% (range, 90.4%-98.4%) of the prostate on CT1 and CT2, respectively.

In PlanA for the bladder wall, the average values for Dmax were 33.8 Gy (range, 33.4-34.1 Gy) and 33.8 Gy (range, 33.4-34.3 Gy) for CT1 and CT2, respectively. The average values for the bladder wall in terms of V90%, V80%, V70%, V60%, and V50% were 2.2 cc, 3.4 cc, 4.7 cc, 6.3 cc, and 8.4 cc for CT1 and 3 cc, 4.3 cc, 5.7 cc, 7.4 cc, and 9.5 cc for CT2, respectively. Similar results were obtained for PlanB. The results for the rectal wall are presented below.

Prostate–rectum separation

The average PRS for the 10 patients is illustrated in Figure 2. On CT1, the average PRS was 1.67 cm (range, 0.66-3.34 cm), 0.74 cm (range, 0.1-2.17 cm), 0.29 cm (range, 0-1 cm), 0.07 cm (range, 0-0.2 cm), 0.15 cm (range, 0-0.48 cm), 0.16 cm (range, 0-0.32 cm), and 0.2 cm (range, 0-0.49 cm) for +5 mm, +10 mm, +15 mm, 0 mm, −5 mm, −10 mm, and −15 mm, respectively. On CT2, the average PRS was 1.73 cm (range, 0.7-4.27 cm), 1.2 cm (range, 0.23-2.05 cm), 1.13 cm (range, 0.64-2 cm), 1.01 cm (range, 0.54-1.56 cm), 1.02 cm (range, 0.54-1.52 cm), 1.14 cm (range, 0.6-1.53 cm), and 1.32 cm (range, 0.72-2.29 cm) for the same levels.

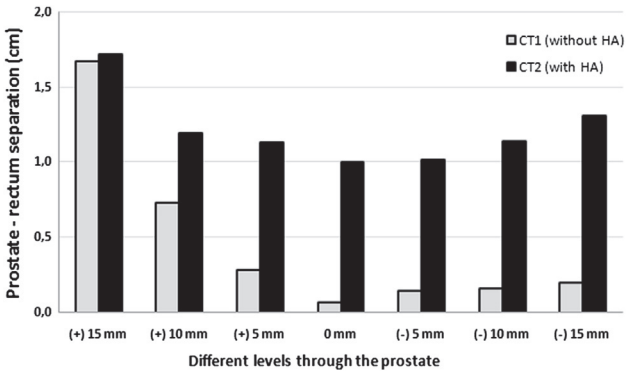

Fig. 2. Prostate–rectum separation before injection (CT1) of hyaluronic acid (HA) and after injection (CT2) at different levels of the prostate.

Rectal wall doses with and without HA

The spacer gel reduced the mean Dmax value to the rectal wall by 2.7 Gy for PlanA and by 2.5 Gy for PlanB. The mean values of V90%, V80%, V70%, V60%, and V50% were reduced by 90% ($P=.002$), 82% ($P=.002$), 70% ($P=.002$), 55% ($P=.002$), and 43% ($P=.002$) for PlanA and by 91% ($P=.002$), 77% ($P=.0059$), 62% ($P=.002$), 48% ($P=.004$), and 36% ($P=.0039$) for PlanB, respectively. In addition, the average values of D2.5cc, D5cc, D10cc, D15cc, and D20cc were reduced by 11 Gy ($P=.002$), 8 Gy ($P=.002$), 3 Gy ($P=.002$), 1.4 Gy ($P=.024$), and 1.2 Gy ($P=.014$) for PlanA and 12 Gy ($P=.002$), 10 Gy ($P=.001$), 4 Gy ($P=.013$), 2 Gy ($P=.04$), and 1.8 Gy ($P=.07$) for PlanB, respectively. The average, minimum, and maximum values for rectal wall doses on both plans and CT scans are shown in Table 1.

Impact of PRS on doses to the anterior rectal wall

CT1 before injection versus CT2 after injection

The average dose received by the rectal wall for all 10 patients is illustrated in Figure 3 for PlanA. The results are shown for each of the 7 CT slices. There was no significant difference ($P=.32$) between doses received by the rectal wall on CT1 and CT2 at the base of the prostate (+15 mm). However, this variation became significant especially from the median plane to the apex of the prostate (Fig. 3) on CT slice levels +10 mm ($P=.06$), +5 mm ($P=.002$), 0 mm ($P=.002$), −5 mm ($P=.002$), −10 mm ($P=.002$), and −15 mm ($P=.002$). Similar results were obtained for PlanB. The values of doses received by the first millimeter of the rectal wall are given in Table 2 for both plans and for both CT scans.

Rectal wall preservation with HA for dose escalation

No significant differences were found between PlanA (5 × 6.5 Gy) without spacer and PlanB (5 × 8.5 Gy) with spacer (Fig. 4) at each level of the prostate, regarding the doses received by the first millimeter of the rectal wall: +15 mm ($P=.27$), +10 mm ($P=.56$), +5 mm ($P=.9$), 0 mm ($P=.77$), −5 mm ($P=.19$), −10 mm ($P=.32$), and −15 mm ($P=.32$).

Discussion

SBRT dose escalation trials

A few experiences have been reported by different radiation therapy centers that developed the prostate SBRT in less than or equal to 5 fractions of 6.5 Gy to 10 Gy (5-12). The rate of local control was between 90% at 6.7 Gy per fraction and 100% at doses between 9 and 10 Gy per fraction. It appears that there may be a dose effect and that higher doses could give better local control. However, particular attention should be considered for genitourinary and gastrointestinal toxicities.

In a study by Madsen et al (5), 40 patients were included in a phase 1/2 trial and treated with a dose of 33.5 Gy in 5 fractions of 6.7 Gy. After a mean of 41 months of follow-up, grade 1-2 acute and late gastrointestinal toxicities were reported for 39% and 37.5% of the patients, respectively. Tang et al (8) treated 30 patients with doses of 35 Gy in 5 fractions of 7 Gy with an IMRT technique; with a median follow-up time of 12 months, acute and late grade 1-2 rectal toxicities were seen in 67% and 70% of patients, respectively. Friedland et al (10) presented the initial results for 112 patients with low-risk prostate cancer who were

Table 1 Average and range values for rectal wall doses on both plans and CT scans; average equivalent doses in 2 Gy/fraction (EQD2) are noted for normal tissue acute ($\alpha/\beta = 10$) and late ($\alpha/\beta = 3$ Gy) effects

	5 × 6.5 Gy (PlanA)				5 × 8.5 Gy (PlanB)			
	w/oHA		wHA		w/oHA		wHA	
Rectal wall variables	Average (range)	EQD2 (average) $\alpha/\beta = 3$ $\alpha/\beta = 10$	Average (range)	EQD2 (average) $\alpha/\beta = 3$ $\alpha/\beta = 10$	Average (range)	EQD2 (average) $\alpha/\beta = 3$ $\alpha/\beta = 10$	Average (range)	EQD2 (average) $\alpha/\beta = 3$ $\alpha/\beta = 10$
D2.5 (Gy)	30.3 (27.9-2.2)	54.9 40.6	19.4 (14.4-26.9)	26.7 22.4	40.3 (37.6-41.9)	89.1 60.7	27.9 (19.7-35.4)	47.9 36.2
D5 (Gy)	23.5 (18.5-8.9)	36.2 28.8	15.5 (10.7-20.8)	18.9 16.9	32.6 (26-37.3)	62.1 44.9	22.1 (15.2-30.7)	32.8 26.6
D10 (Gy)	13.2 (10.5-9.2)	14.9 13.9	10.2 (6.7-14.9)	10.3 10.2	19 (14.7-25.1)	25.8 21.9	14.9 (9.9-21.7)	17.8 16.1
D15 (Gy)	8.9 (6.5-13.4)	8.5 8.7	7.5 (4.1-11.4)	6.8 7.2	12.7 (9.2-18)	14.1 13.3	10.7 (6.1-16.4)	11.0 10.8
D20 (Gy)	6.5 (4.26-10.9)	5.6 6.1	5.3 (2.3-8.3)	4.3 4.9	9.2 (4.6-15)	8.9 9.1	7.4 (1.3-11.8)	6.6 7.1
V90% (cc)	3.2 (1.9-4.8)		0.3 (0-1.5)		3.5 (2.3-4.5)		0.3 (0-1.2)	
V80% (cc)	4.4 (3-6.7)		0.8 (0-2.8)		4.7 (3.2-6.5)		1.1 (0.1-3.2)	
V70% (cc)	5.4 (3.8-8.3)		1.6 (0-3.9)		5.8 (4.1-8.2)		2.2 (0.6-5.5)	
V60% (cc)	6.4 (4.7-9.9)		2.9 (0.4-5.7)		7.1 (5.1-9.9)		3.7 (1.1-7.6)	
V50% (cc)	7.9 (5.9-12)		4.5 (1.7-8.3)		8.9 (6.6-12)		5.7 (2-10.4)	

Abbreviations: CT = computed tomography; CT1 = CT before injection; CT2 = CT after injection; HA = hyaluronic acid; wHA = with HA; w/oHa = without HA.

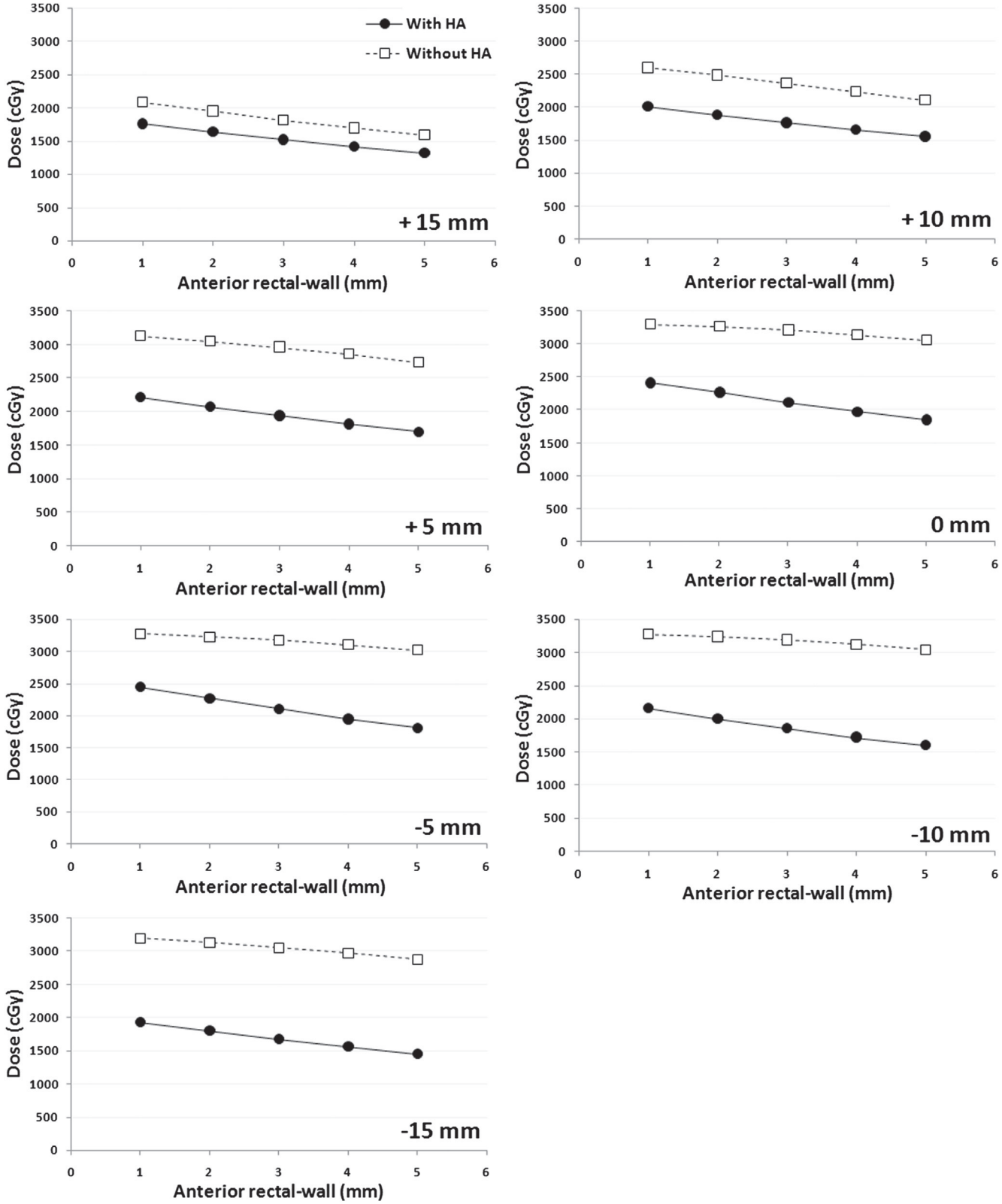

Fig. 3. Dose profile in the anterior rectal wall for PlanA, in CT1 (without hyaluronic acid [HA]) and in CT2 (with HA) at different levels through the prostate. 0 mm in x axis corresponds to the external surface of the anterior rectal wall.

treated with doses of 35 to 36 Gy in 5 consecutive fractions. With a median follow-up time of 24 months, only 1 patient experienced grade 3 rectal toxicity.

In 2012, King et al (7) published the long-term outcomes in 67 patients who received a dose of 36.25 Gy in 5 fractions of 7.25 Gy. With a median follow-up time of 2.7 years, late rectal grade 1-2

Table 2 Doses received by the first millimeter of the rectal wall at different levels of prostate: average and range values on both plans and CT scans

	5 × 6.5 Gy (PlanA)		5 × 8.5 Gy (PlanB)	
Level	w/oHA	wHA	w/oHA	wHA
+15 mm	20.8 Gy (10.1-29.1 Gy)	17.6 Gy (6.1-27.2 Gy)	29 Gy (12.8-39 Gy)	23.7 Gy (9.1-35.9 Gy)
+10 mm	26 Gy (11.8-32.8 Gy)	20.1 Gy (11.8-32.4 Gy)	35 Gy (15.6-43 Gy)	28 Gy (17.3-42 Gy)
+5 mm	31.3 Gy (20.8-33.7 Gy)	22.2 Gy (13.6-31.8 Gy)	41.5 Gy (32.7-43.7 Gy)	31.3 Gy (22.2-41.2 Gy)
0	33 Gy (32.5-33.5 Gy)	24.1 Gy (16-31.5 Gy)	43 Gy (42.4-43.6 Gy)	34.1 Gy (24.9-40.8 Gy)
−5 mm	32.7 Gy (31-33.8 Gy)	24.4 Gy (19-30.9 Gy)	42.9 Gy (41.8-43.9 Gy)	34.5 Gy (28.4-39.4 Gy)
−10 mm	32.8 Gy (31.5-33.7 Gy)	21.6 Gy (12.2-27.2 Gy)	42.8 Gy (41.4-43.8 Gy)	30 Gy (17.6-36.3 Gy)
−15 mm	32 Gy (26.4-33.2 Gy)	19.2 Gy (10.9-29.9 Gy)	42 Gy (35.6-43 Gy)	27 Gy (16-38.6 Gy)

Abbreviations: CT = computed tomography; CT1 = CT before injection; CT2 = CT after injection; HA = hyaluronic acid; wHA = with HA; w/oHa = without HA.

toxicities were seen in 16% of patients. Finally, Boike et al (6) presented the results of a phase 1 study with dose escalation for 3 arms: 45 Gy, 47.5 Gy, and 50 Gy in 5 fractions. Fifteen patients were included in each arm, with median follow-up times of 30, 18, and 12 months for the 3 groups, respectively. Acute grade 1-2 rectal toxicities were noted for each arm in 40%, 40%, and 54% of patients, respectively. Late grade 1-2 rectal toxicities were stated for each arm in 14%, 34%, and 33% of patients, respectively. For all patients, gastrointestinal grade $\geq$2 and grade $\geq$3 toxicities occurred in 18% and 2%, respectively.

In all those studies, SBRT seems to have been well tolerated, with no acute grade 3 and 4 rectal toxicities and few acute grade 1 and 2 toxicities. The late rectal toxicities appeared to be acceptable but the small number of patients and the median follow-up times, often below 2 to 3 years, were not sufficient to characterize late toxicities. All these results were published by expert centers in stereotactic radiation therapy, and the development of this irradiation technique in all departments of radiation oncology could lead to an increased risk of rectal toxicity. Therefore, to secure the development of SBRT, the use of a prostate—rectum spacer could be of interest.

Prostate—rectum separation

An original method has been described by Prada et al (13, 14) using an HA injection in the perirectal fat between the prostate and the anterior rectal wall. The authors reported that a 2-cm separation between the 2 organs significantly decreased the rectal dose from low-dose-rate (14) and high-dose-rate (13) brachytherapy. They confirmed that the spacer injection was very well tolerated by the patients and that the spacer remained stable for a minimum of 9 months and up to 1 year (13, 14).

To date, several studies have used different spacers between the prostate and the rectum (15-20). The authors prescribed a normal fractionation of 2 Gy for a total dose of 76 to 78 Gy in 38 to 39 fractions. The average value for the rectal volume that received 70 Gy (V70 Gy) with IMRT decreased from 10%-20% to 4.5%-7.5% after a PRS (16,18-20). The average spacer volume injection reported in these studies varied from 3 to 7 mL (13) to 10 to 30 mL (15-20) to obtain an average PRS between 7 mm and 20 mm. Although Prada et al (13) needed only 3 to 7 mL HA for a considerable PRS, in our practice a full syringe of 10 mL was necessary to obtain at least 1 cm of HA thickness (21). This volume of injection was used in the majority of studies (15-20).

In the present study, the rectal dosimetric parameters were expressed in cubic centimeters and not as percentage of volume to limit the impact of a variation of rectal dilatation between the 2 CT scans, as was observed in other studies (20). In the study by Madsen et al (5), the average V90% and V80% values were 3.66 cc and 5.20 cc, respectively. In 2007, the same authors observed 3 cases of grade 2 rectal bleeding that they associated with the volume of the rectum receiving 90% of the dose: 3.5 cc, 7.66 cc, and 3.47 cc. In the current report, when a spacer was used, the average results for V90% and V80% were considerably lower: 0.3 cc and 0.8 cc for PlanA and 0.3 cc and 1.1 cc for PlanB, respectively. As an example, it appears that 3.7 cc of the rectal wall received an average equivalent dose in 2 Gy per fraction of 54.5 Gy (α/β = 3 Gy) and 40.3 Gy (α/β = 10 Gy) in the study by Madsen et al (5) (33.5 Gy in 5 fractions) versus 41.3 Gy (α/β = 3 Gy) and 32.1 Gy (α/β = 10 Gy) in the current study using 42.5 Gy in 5 fractions with HA. This comparison allows us to assume that a PRS could decrease the risk of such toxicities, but clinical studies should confirm this hypothesis.

The patients included in the current work had a spacer injection from the base to the apex. However, this injection was not extended to the space between the rectum and the seminal vesicles. When an analysis is performed for the PRS at each segment of the prostate, the effect caused by the form of the prostate at the base and the distal shape of the rectum may possibly suggest that we could focus the spacer injection between the median and apex regions of the prostate. In addition, at the base of the prostate, the seminal vesicles may have a role to play because they are a "natural" spacer, and the impact of HA at the base is smallest compared with the other levels (Fig. 3).

Impact of HA spacer on SBRT dose escalation

An interesting observation can be made on the impact of the HA injection on SBRT dose escalation. We observed that a spacer allows irradiation dosage to be increased from 5 × 6.5 Gy (with no spacer) to 5 × 8.5 Gy without increasing the average D2.5 and D5 values. In Figure 4, the impact of a PRS can be observed for all levels of the prostate. The real dose-PRS benefit as a result of the spacer injection may be observed once more from the median to the apex regions of the prostate.

The results of this SBRT dosimetric comparison of treatment with and without a PRS confirm the potential benefit of a spacer in preserving the rectal wall from high doses.

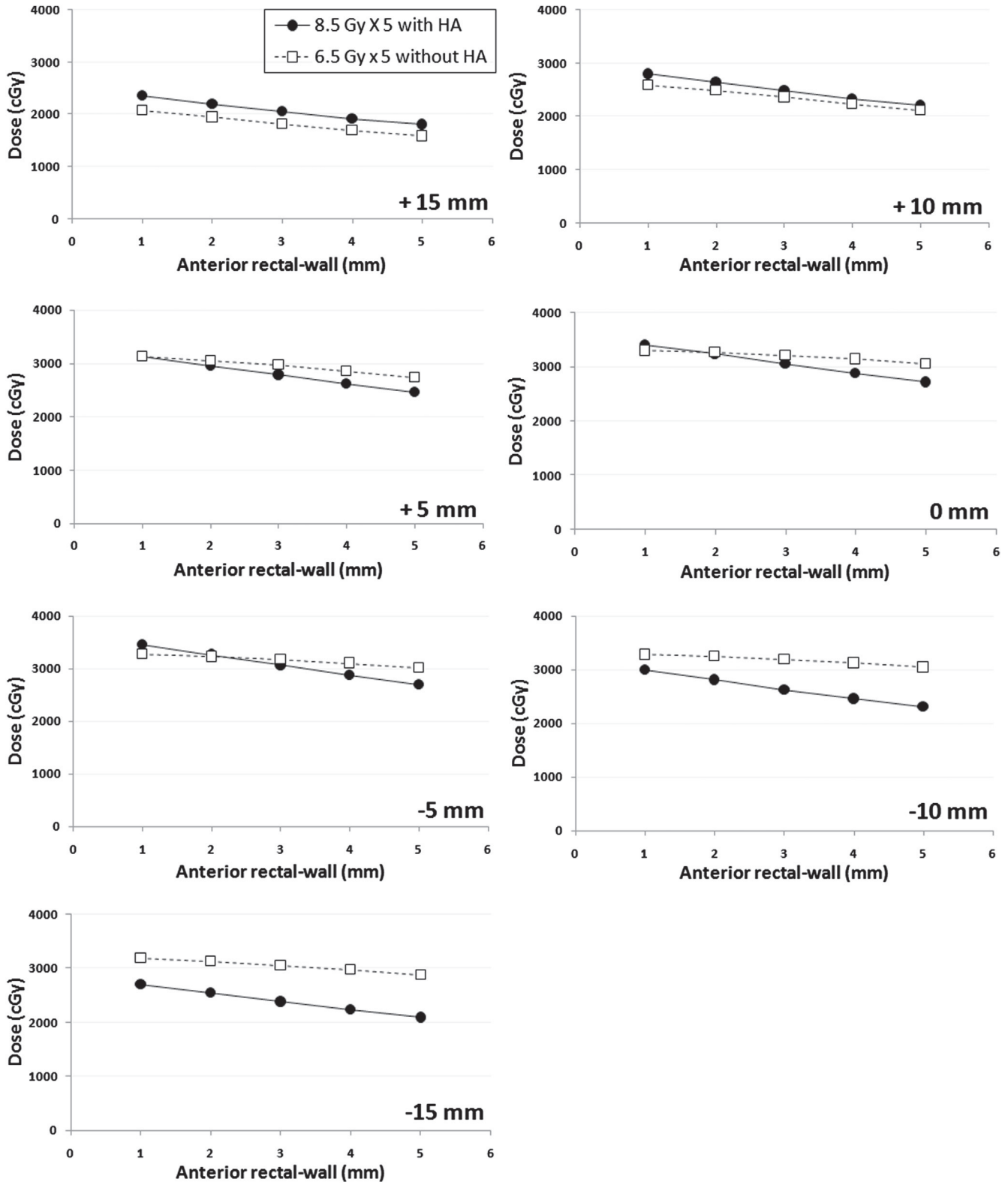

Fig. 4. Dose profile in the anterior rectal wall for PlanA without hyaluronic acid (HA) and for PlanB with HA at different levels through the prostate. 0 mm in x axis corresponds to the external surface of the anterior rectal wall.

Conclusions

In this study, the injection of a spacer limited the doses to the rectal wall. A spacer could secure the initiation and development of SBRT in many centers. A phase 2 study is under way in our department to assess the rates of late rectal toxicities when an IMRT-SBRT technique (5×8.5 Gy) is used with a spacer between the prostate and the rectal wall.

References

1. Yang J, Lamond J, Fowler J, et al. Effect of fractionation in stereotactic body radiation therapy using the linear quadratic model. *Int J Radiat Oncol Biol Phys* 2013;86:150-156.
2. Zaorsky NG, Studenski MT, Dicker AP, et al. Stereotactic body radiation therapy for prostate cancer: Is the technology ready to be the standard of care? *Cancer Treat Rev* 2013;39:212-218.
3. Brenner DJ, Martinez AA, Edmundson GK, et al. Direct evidence that prostate tumors show high sensitivity to fractionation (low alpha/beta ratio), similar to late-responding normal tissue. *Int J Radiat Oncol Biol Phys* 2002;52:6-13.
4. Buyyounouski MK, Price RA, Harris EER, et al. Stereotactic body radiotherapy for primary management of early-stage, low- to intermediate-risk prostate cancer: Report of the American Society for Therapeutic Radiology and Oncology emerging technology committee. *Int J Radiat Oncol Biol Phys* 2010;76:1297-1304.
5. Madsen BL, Hsi RA, Pham HT, et al. Stereotactic hypofractionated accurate radiotherapy of the prostate (SHARP), 33.5 Gy in five fractions for localized prostate disease: First clinical trial results. *Int J Radiat Oncol Biol Phys* 2007;67:1099-1105.
6. Boike TP, Lotan Y, Cho LC, et al. Phase I dose escalation study of stereotactic radiation therapy for low- and intermediate-risk prostate cancer. *J Clin Oncol* 2011;29:2020-2026.
7. King CR, Brooks JD, Gill H, et al. Long-term outcomes from a prospective trial of stereotactic body radiotherapy for low-risk prostate cancer. *Int J Radiat Oncol Biol Phys* 2012;82:877-882.
8. Tang CI, Loblaw DA, Cheung P, et al. Phase I/II study of a five-fraction hypofractionated accelerated radiotherapy treatment for low-risk localized prostate cancer: Early results of pHART3. *Clin Oncol* 2008;20:729-737.
9. Bolzicco G, Favretto MS, Scremin E, et al. Image-guided stereotactic body radiation therapy for clinically localized prostate cancer: Preliminary clinical results. *Technol Cancer Res Treat* 2010;9:473-477.
10. Friedland JL, Freeman DE, Masterson-McGary ME, et al. Stereotactic body radiotherapy: An emerging treatment approach for localized prostate cancer. *Technol Cancer Res Treat* 2009;8:387-392.
11. Jabbari S, Weinberg VK, Kaprealian T, et al. Stereotactic body radiotherapy as monotherapy or post-external beam radiotherapy boost for prostate cancer: Technique, early toxicity, and PSA response. *Int J Radiat Oncol Biol Phys* 2012;82:228-234.
12. Lee YH, Son SH, Yoon SC, et al. Stereotactic body radiotherapy for prostate cancer: A preliminary report. *Asia Pac J Clin Oncol* 2012 Sep 20 [Epub ahead of print]. http://dx.doi.org/10.1111/j.1743-7563.2012.01589.x.
13. Prada PJ, Fernandez J, Martinez AA, et al. Transperineal injection of hyaluronic acid in anterior perirectal fat to decrease rectal toxicity from radiation delivered with intensity modulated brachytherapy or EBRT for prostate cancer patients. *Int J Radiat Oncol Biol Phys* 2007;69:95-102.
14. Prada PJ, Gonzalez H, Menéndez C, et al. Transperineal injection of hyaluronic acid in the anterior perirectal fat to decrease rectal toxicity from radiation delivered with low-dose-rate brachytherapy for prostate cancer patients. *Brachytherapy* 2009;8:210-217.
15. Pinkawa M, Piroth MD, Holy R, et al. Quality of life after intensity-modulated radiotherapy for prostate cancer with a hydrogel spacer. *Strahlenther Onkol* 2012;188:917-925.
16. Pinkawa M, Escobar Corral N, Caffaro M, et al. Application of a spacer gel to optimize three-dimensional conformal and intensity modulated radiotherapy for prostate cancer. *Radiother Oncol* 2011;100:436-441.
17. Hatiboglu G, Pinkawa M, Vallée JP, et al. Application technique: Placement of a prostate-rectum spacer in men undergoing prostate radiation therapy. *BJU Int* 2012;110:e647-e652.
18. Song DY, Herfarth KK, Uhl M, et al. A multi-institutional clinical trial of rectal dose reduction via injected polyethylene-glycol hydrogel during intensity modulated radiation therapy for prostate cancer: Analysis of dosimetric outcomes. *Int J Radiat Oncol Biol Phys* 2013;87:81-87.
19. Susil RC, McNutt TR, DeWeese TL, et al. Effects of prostate-rectum separation on rectal dose from external beam radiotherapy. *Int J Radiat Oncol Biol Phys* 2010;76:1251-1258.
20. Weber DC, Zilli T, Vallee JP, et al. Intensity modulated proton and photon therapy for early prostate cancer with or without transperineal injection of a polyethylene glycol spacer: A treatment planning comparison study. *Int J Radiat Oncol Biol Phys* 2012;84:e311-e318.
21. Chapet O, Udrescu C, Devonec M, et al. Prostate hypofractionated radiation therapy: Injection of hyaluronic acid to better preserve the rectal wall. *Int J Radiat Oncol Biol Phys* 2013;86:72-76.
22. D'Amico AV, Whittington R, Malkowicz SB, et al. Biochemical outcome after radical prostatectomy, external beam radiation therapy, or interstitial radiation therapy for clinically localized prostate cancer. *JAMA* 1998;280:969-974.
23. Kagawa K, Lee WR, Schultheiss TE, et al. Initial clinical assessment of CT-MRI image fusion software in localization of the prostate for 3D conformal radiation therapy. *Int J Radiat Oncol Biol Phys* 1997;38:319-325.

3.4. Conclusion – section III

In conclusion, the actual results available in the literature for a prostate SBRT prove a good tumor local control with an acceptable tolerance.

Two SBRT approaches were described in this section for the localized prostate cancer: with an integrated boost into the tumor and with a prostate-rectum separation. Below are summarized the advantages and disadvantages of the two schema proposed for prostate cancer (Table 3.1).

A bifocal irradiation should be carefully initiated as the actual MR imaging is perhaps not sufficient for the precise detection of low-risk prostate cancer. This approach might prove its usefulness with the improvement of diagnostic imaging.

The HA injection is actually the safer technique for rectum protection during prostate SBRT. Afterward, the combination of these two approaches could result in an additional gain for bladder protection from higher doses.

Table 3.1. Summarized features of two approaches intended for prostate SBRT.

SBRT design	**Advantages**	**Disadvantages**
Bifocal	Rectum and bladder protection	With actual MRI acquisitions, tumors are not always detectable for low-risk prostate cancer
Hyaluronic Acid	Optimal protection of the rectum	No protection for the bladder Local or general anesthesia is needed

3.5. Bibliography – section III

[1] Benedict SH, Yenice KM, Followill D, *et al.* Stereotactic body radiation therapy: The report of AAPM Task Group 101. *Med Phys* 2010;37(8):4078-4101.

[2] Cellini N, Morganti AG, Mattiucci GC, *et al.* Analysis of intraprostatic failures in patients treated with hormonal therapy and radiotherapy: Implications for conformal therapy planning. *Int J Radiat Oncol Biol Phys* 2002;53:595-599.

[3] Pucar D, Hricak H, Shukla-Dave A, *et al.* Clinically significant prostate cancer local recurrence after radiation therapy occurs at the site of primary tumor: Magnetic resonance imaging and step-section pathology evidence. *Int J Radiat Oncol Biol Phys* 2007;69:62-69.

[4] Arrayeh E, Westphalen AC, Kurhanewicz J, *et al.* Does local recurrence of prostate cancer after radiation therapy occur at the site of primary tumor? Results of a longitudinal MRI and MRSI study. *Int J Radiat Oncol Biol Phys* 2012;82:e787-e793.

[5] Westphalen AC, Coakley FV, Roach M 3rd, McCulloch CE, Kurhanewicz J. Locally recurrent prostate cancer after external beam radiation therapy: Diagnostic performance of 1.5-T endorectal MR imaging and MR spectroscopic imaging for detection. *Radiology* 2010;256:485-492.

[6] Westphalen AC, McKenna DA, Kurhanewicz J, Coakley FV. Role of magnetic resonance imaging and magnetic resonance spectroscopic imaging before and after radiotherapy for prostate cancer. *J Endourol* 2008;22:789-794.

[7] Chopra S, Toi A, Taback N, *et al.* Pathological predictors for site of local recurrence after radiotherapy for prostate cancer. *Int J Radiat Oncol Biol Phys* 2012;82:e441-e448.

[8] Haider MA, Chung P, Sweet J, Toi A, Jhaveri K, Ménard C, *et al.* Dynamic contrast-enhanced magnetic resonance imaging for localization of recurrent prostate cancer after external beam radiotherapy. *Int J Radiat Oncol Biol Phys* 2008;70:425-430.

[9] Rouvière O, Valette O, Grivolat S, Colin-Pangaud C, Bouvier R, Chapelon JY, *et al.* Recurrent prostate cancer after external beam radiotherapy: value of contrast-enhanced dynamic MRI in localizing intraprostatic tumor - correlation with biopsy findings. *Urology* 2004;63:922-927.

[10] Kim CK, Park BK, Lee HM. Prediction of locally recurrent prostate cancer after radiation therapy: incremental value of 3T diffusion-weighted MRI. *J Magn Reson Imaging* 2009;29: 391-397.

[11] Kokeny GP, Cerri GG, de Oliveira Cerri LM, *et al.* Correlations among prostatic biopsy results, transrectal ultrasound findings and PSA levels in diagnosing prostate adenocarcinoma. *Eur J Ultrasound* 2000;12:103-113.

[12] Melchior SW, Brawer MK. Role of transrectal ultrasound and prostate biopsy. *J Clin Ultrasound* 1996;24:463-471.

[13] Pucar D, Sella T, Schoder H. The role of imaging in the detection of prostate cancer local recurrence after radiation therapy and surgery. *Curr Opin Urol* 2008;18:87-97.

[14] Kara T, Akata D, Akyol F, *et al.* The value of dynamic contrast-enhanced MRI in the detection of recurrent prostate cancer after external beam radiotherapy: Correlation with transrectal ultrasound and pathological findings. *Diagn Interv Radiol* 2011;17:38-43.

[15] Groenendaal G, Borren A, Moman MR, *et al.* Pathologic validation of a model based on diffusion-weighted imaging and dynamic contrast-enhanced magnetic resonance imaging for tumor delineation in the prostate peripheral zone. *Int J Radiat Oncol Biol. Phys* 2012;82:e537-e544.

[16] Pouliot J, Kim Y, Lessard E, *et al.* Inverse planning for HDR prostate brachytherapy used to boost dominant intraprostatic lesions defined by magnetic resonance spectroscopy imaging. *Int J Radiat Oncol Biol Phys* 2004;59:1196-1207.

[17] Van Lin ENJT, Futterer JJ, Heijmink SWTPJ, *et al.* IMRT boost dose planning on dominant intraprostatic lesions: Gold marker-based three-dimensional fusion of CT with dynamic contrast-enhanced and 1Hspectroscopic MRI. *Int J Radiat Oncol Biol Phys* 2006;65:291-303.

[18] Xia P, Pickett B, Vigneault E, Verhey LJ, Roach M 3rd. Forward or inversely planned segmental multileaf collimator IMRT and sequential tomotherapy to treat multiple dominant intraprostatic lesions of prostate cancer to 90 Gy. *Int J Radiat Oncol Biol Phys* 2001;51:244-254.

[19] Pickett B, Vigneault E, Kurhanewicz J, *et al.* Static field intensity modulation to treat a dominant intra-prostatic lesion to 90 Gy compared to seven field 3-dimensional radiotherapy. *Int J Radiat Oncol Biol Phys* 1999;43:921-929.

[20] Singh AK, Guion P, Sears-Crouse N, *et al.* Simultaneous integrated boost of biopsy proven, MRI defined dominant intra-prostatic lesions to 95 Gray with IMRT: Early results of a phase I NCI study. *Radiat Oncol* 2007;2:36.

[21] Miralbell R, Moll M, Rouzaud M, *et al.* Hypofractionated boost to the dominant tumor region with intensity modulated stereotactic radiotherapy for prostate cancer: A sequential dose escalation pilot study. *Int J Radiat Oncol Biol. Phys* 2010;78:50-57.

[22] Shaw E, Kline R, Gillin M, *et al*. Radiation Therapy Oncology Group: radiosurgery quality assurance guidelines. *Int J Radiat Oncol Biol Phys* 1993;27:1231–1239.

[23] Audet C, Poffenbarger BA, Chang P, *et al.* Evaluation of volumetric modulated arc therapy for cranial radiosurgery using multiple noncoplanar arcs. *Med Phys* 2011;38(11):5863-5872.

[24] Balagamwala EH, Suh JH, Barnett GH, *et al.* The importance of the conformality, heterogeneity, and gradient indices in evaluating Gamma Knife radiosurgery treatment plans for intracranial meningiomas. *Int J Radiat Oncol Biol Phys* 2012;83:1406-1413.

[25] Hazard LJ, Wang B, Skidmore TB, *et al.* Conformity of LINAC-based stereotactic radiosurgery using dynamic conformal arcs and micro-multileaf collimator. *Int J Radiat Oncol Biol Phys* 2009;73:562-570.

[26] Hong LX, Garg M, Lasala P, *et al.* Experience of micromultileaf collimator linear accelerator based single fraction stereotactic radiosurgery: Tumor dose inhomogeneity, conformity, and dose fall off. *Med Phys* 2011;38(3):1239-1247.

[27] Paddick I. A simple scoring ratio to index the conformity of radiosurgical treatment plans. *J Neurosurg* 2000;93:219-222.

[28] Baltas D, Kolotas C, Geramani K, *et al.* A conformal index (COIN) to evaluate implant quality and dose specification in brachytherapy. *Int J Radiat Oncol Biol Phys* 1998;40:515-524.

[29] Claus F, Mijnheer B, Rasch C, *et al.* Report of a study on IMRT planning strategies for ethmoid sinus cancer. *Strahlenther Onkol* 2002;178:572-576.

[30] Knoos T, Kristensen I, Nilsson P. Volumetric and dosimetric evaluation of radiation treatment plans: radiation conformity index. *Int J Radiat Oncol Biol Phys* 1998;42:1169-1176.

[31] Lomax NJ, Scheib SG. Quantifying the degree of conformity in radiosurgery treatment planning. *Int J Radiat Oncol Biol Phys* 2003;55:1409-1419.

[32] van`t Riet A, Mak ACA, Moerland MA, Elders LH, van der Zee W. A conformation number to quantify the degree of conformality in brachytherapy and external beam irradiation: application to the prostate. *Int J Radiat Oncol Biol Phys* 1997;37:731-736.

[33] Feuvret L, Noel G, Mazeron JJ, Bey P. Conformity index: A review. *Int J Radiat Oncol Biol Phys* 2006;64:333-342.

[34] Feuvret L, Noel G, Nauraye C, Garcia P, Mazeron JJ. Conformal index and radiotherapy. *Cancer Radiother* 2004;8:108-119.

[35] Shaw E, Scott C, Souhami L, *et al.* Single dose radiosurgical treatment of recurrent previously irradiated primary brain tumors and brain metastases: final report of RTOG protocol 90-05. *Int J Radiat Oncol Biol Phys* 2000;47:291-298.

[36] Wolff D, Stieler F, Welzel G, *et al.* Volumetric modulated arc therapy (VMAT) vs. serial tomotherapy, step-and-shoot IMRT and 3C-conformal RT for treatment of prostate cancer. *Radiother Oncol* 2009;93:226-233.

[37] Ohtakara K, Hayashi S, Hoshi H. Dose gradient analyses in Linac-based intracranial stereotactic radiosurgery using Paddick's gradient index: Consideration of the optimal method for plan evaluation. *J Radiat Res* 2011;52:592-599.

[38] Hossain S, Xia P, Huang K, *et al.* Dose gradient near target-normal structure interface for nonisocentric CyberKnife and isocentric intensity-modulated body radiotherapy for prostate cancer. *Int J Radiat Oncol Biol Phys* 2010;78:58-63.

[39] Lafond C, Gassa F, Odin C, *et al.* Comparison between two treatment planning systems for volumetric modulated arc therapy optimization for prostate cancer. *Physica Medica* 2012;*in press*.

[40] Paddick I, Lippitz B. A simple dose gradient measurement tool to complement the conformity index. *J Neurosurg* 2006;105:194-201.

[41] Kupelian P, Katz AJ, Freeman D, *et al.* Long-term efficacy of stereotactic body radiotherapy for localized prostate cancer: A multi-institutional pooled analysis. *J Clin Oncol* 2013;Suppl 6, abstract 9.

[42] Chapet O, Udrescu C, Sotton MP, *et al.* Potential interest of developing a focal dose escalation in stereotactic irradiation of prostate cancer. *Int J Radiat Oncol Biol Phys* 2010;78(Suppl.):S780-S781.

[43] Prada PJ, Fernandez J, Martinez AA, *et al.* Transperineal injection of hyaluronic acid in anterior perirectal fat to decrease rectal toxicity from radiation delivered with intensity modulated brachytherapy or EBRT for prostate cancer patients. *Int J Radiat Oncol Biol Phys* 2007;69:95-102.

[44] Prada PJ, Gonzalez H, Menéndez C, *et al.* Transperineal injection of hyaluronic acid in the anterior perirectal fat to decrease rectal toxicity from radiation delivered with low-dose-rate brachytherapy for prostate cancer patients. *Brachytherapy* 2009;8(2):210-7.

[45] Christodouleas JP, Susil RC, McNutt TR, *et al.* The impact of a rectal-prostate spacer on proton radiation of the prostate: A planning study [Abstract]. *Int J Radiat Oncol Biol Phys* 2010;78:S134.

[46] Hatiboglu G, Pinkawa, Vallée JP, *et al.* Application technique: placement of a prostate-rectum spacer in men undergoing prostate radiation therapy. *BJU Int* 2012;110:E647-E652.

[47] Pinkawa M, Escobar Corral N, Caffaro M, *et al.* Application of a spacer gel to optimize three-dimensional conformal and intensity modulated radiotherapy for prostate cancer. *Radiother Oncol* 2011;100:436-441.

[48] Pinkawa M, Piroth MD, Holy R, *et al.* Quality of life after intensity-modulated radiotherapy for prostate cancer with a hydrogel spacer. *Strahlenther Onkol* 2012;188:917-925.

[49] Song DY, Herfarth KK, Uhl M, *et al.* A multi-institutional clinical trial of rectal dose reduction via injected polyethylene-glycol hydrogel during intensity modulated radiation therapy for prostate cancer: Analysis of dosimetric outcomes. *Int J Radiat Oncol Biol Phys* 2013 *Article in press*.

[50] Susil RC, McNutt TR, DeWeese TL, *et al.* Effects of prostate-rectum separation on rectal dose from external beam radiotherapy. *Int J Radiat Oncol Biol Phys* 2010;76:1251-1258.

[51] Weber DC, Zilli T, Vallee JP, *et al.* Intensity modulated proton and photon therapy for early prostate cancer with or without transperineal injection of a polyethylene glycol spacer: a treatment planning comparison study. *Int J Radiat Oncol Biol Phys* 2012; 84:e311-e318.

[52] Chapet O, Udrescu C, Ruffion A, *et al.* Injection of hyaluronic acid (HA) to better preserve the rectal wall in prostate hypofractionated radiation therapy (HFR). *Int J Radiat Oncol Biol Phys* 2012 ;84(Suppl.):S406.

[53] Chapet O, Udrescu C, Devonec M, *et al.* Prostate hypofractionated radiation therapy: injection of hyaluronic acid to better preserve the rectal wall. *Int J Radiat Oncol Biol Phys* 2013;86:72-76.

[54] Chapet O, Decullier E, Faix A, *et al.* Hypofractionated intensity modulated radiation therapy with injection of hyaluronic acid for localized prostate cancer: results of a phase 2 study (RPAH1). *Int J Radiat Oncol Biol Phys* 2013;87(Suppl.):S173.

[55] Udrescu C, Ruffion A, Sotton MP, *et al.* Injection of hyaluronic acid (HA) preserves the rectal wall in prostate stereotactic body radiation therapy (SBRT). *Radiother Oncol* 2012;103(Suppl.): S109-S110.

IV. QUALITY ASSURANCE OF A SBRT-IMRT PLAN

4.1. Introduction

One of the principles of the stereotactic body radiation therapy (SBRT) is that the delivered dose at the time of treatment must perfectly match with the planned dose. This feature is difficult to be attained, even if it is mandatory for the SBRT approach. This can be translated into:

a) accurate general performance of the accelerator, and
b) precise verification of the plan before the patient's treatment (quality assurance on the patient-specific level).

The issue of the quality assurance (QA) of the medical accelerators is more complex for SBRT-IMRT and therefore will not be discussed in this section. It requires precise recommendations in terms of: treatment planning commissioning (TPS), calculation algorithms, multileaf collimator verification, utilization of diode phantoms or evaluation methods for the QA of delivery process [1-4]. However, the QA of a SBRT-dedicated accelerator is mandatory in every department and has been previously developed [5, 6]. Moreover, the QA should meet the criteria described in the AAPM TG142 for machines that are used for SBRT treatments (e.g., precision < 1 mm/0.5 deg. for position indicators) [6]. An overview of the technical considerations of the QA for SBRT is moreover described in several reports for medical physicists of AAPM Task Group 101, Task Group 142 and IAEA Technical Report No. 430 [5-7].

In the IAEA report, it is recommended to perform the QA before each irradiation of the patient with an IMRT technique [5]. In this section we present several issues of SBRT-IMRT QA for prostate cancer in pre-treatment patient-specific quality controls.

4.2. Detectors for IMRT QA

Many and different systems have previously been described and validated for the QA comparison between calculated and measured doses of an IMRT treatment plan delivery. Ionization chamber (for absolute dose measurements in a few points) and films (radiographic or radiochromic - for relative dose in a plane and dose distribution verification) in combination with

water-equivalent phantoms have been the reference for IMRT and/or VMAT QA [8-13]. However, the evaluation method is very long, thus time-consuming.

Two-dimensional (2D) detector arrays, such as electronic portal imaging device (EPID® from Varian) [14-24], MapCHECK array (Sun Nuclear, Melbourne, FL) and MatriXX ion chamber array (IBA Dosimetry, GmbH, Schwarzenbrook, Germany) [25-33], are often used to validate planar dose distributions.

In the past years, three-dimensional (3D) detector arrays (specifically designed for rotational irradiation), such as Delta$^{4®}$ system (ScandiDos AB, Uppsala, Sweden) [34-42] and ArcCHECK® device (Sun Nuclear, Melbourne, FL) [39, 43-50], or Octavius® phantom [34, 51] and 3D dosimeters (gel dosimetry) [52-56], have been developed and evaluated for IMRT and volumetric modulated arc therapy (VMAT) QA.

It is essential to understand the characteristics and the limitations of each new detector and therefore a thorough evaluation is needed. It is difficult to compare the results with criteria used for film, ionization chamber, 2D and 3D detector arrays. For example, the 3D gamma evaluation is more complex than the 2D evaluation. On the other hand, relative results (e.g. films) are less complete and different than absolute measurements (e.g. Delta$^{4®}$).

4.2.1. Electronic portal imaging device, Varian

The EPID® from Varian is a flat-panel 2D detector attached to the gantry and always opposite to the head of the accelerator (Figure 4.1). The EPID is an amorphous silicon detector with the resolution 1024 x 768 and pixel size 0.39 mm. In our department, the portal imager is calibrated before each set of measurements.

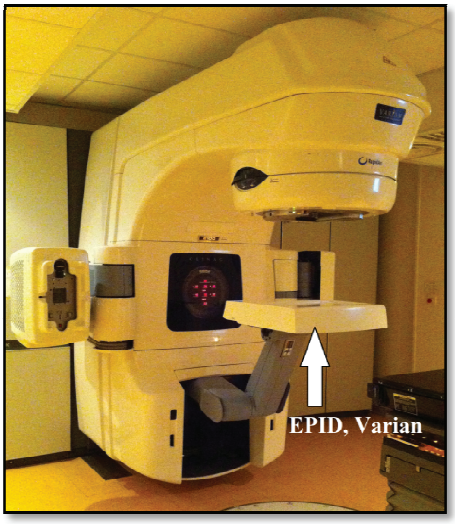

Figure 4.1. The electronic portal imaging device (EPID®), Varian

The EPID measures the fluence of each beam and the measurements are evaluated with the Portal Dosimetry® software, included in Eclipse®TPS (Varian Medical Systems, Palo Alto, CA). The dose profiles are aligned for each beam according to the clinical procedure at Lyon Sud Hospital. However, several issues remain:

- the measurement of the fluence can't be compared with profile depth measurement in water (which is the gold standard in radiotherapy);
- this fluence measurement is compared to a predictive response of the portal which is strongly linked to the TPS modelisation.
- it's an accelerator-dependent detector (always attached to the gantry)

If the EPID is a practical device in the QA procedure with very good tools for the analysis, it cannot provide an analysis of the 3D dose distribution.

4.2.2. Three-dimensional diode arrays for pre-treatment verification of IMRT

Delta$^{4®}$ and ArcCheck® are three-dimensional diode arrays dedicated for beam dosimetry QA. The systems are intended for the measurement of radiotherapy dose distributions that are measured and compared to the dose distribution, as calculated by the treatment planning system. They can be used for measurements from stationary beams (modulated or un-modulated) and measurements from dynamic beams. The QA analysis can be made on combination of dose maps from total delivery, dose maps from a field or dose maps from one segment. The high sensitivity of diodes compared to that of an ion chamber (more than 15 000 times) and the small sensitive

volume of the diodes allow measurements of high accuracy. There are several advantages of the 3D diode arrays:

- they are independent of the TPS and of the accelerator;
- provide 3D absolute measurements;
- allow measurements in the real geometry and condition as at the time of the treatment (gantry, collimator, table).

The two systems are furthermore described below.

4.2.2.1. The Delta$^{4®}$ system, ScandiDos

The Delta^4 system (Figure 4.2) consists of two orthogonal arrays within a cylindrical polymethylmethacrylate (PMMA) phantom (density of 1.19 g cm-3) that are synchronized with the accelerator. The two crossed arrays consist of three removable electrometers/detector-array units: 1 main unit and 2 wing units, though composing four quarters [57]. The four quarters have 5 degrees difference from the diagonals, which allow the user to change from standard orientation to reversed orientation (the orthogonal planes are at 40° and 130° from the horizontal midline of the phantom). Thus, the angle difference between the arrays and the radiation beam changes by 10 degrees and permit to avoid the beam incidence along one of the detectors [57]. The phantom is 40 cm in length, 22 cm in diameter and it weighs 27 Kg (but a transfer support that holds the phantom is provided). The detector boards include a total number of 1069 p-type silicon diodes with a cylindrical shape. The size of one diode is 0.78 mm^2 and has an active volume of 0.04 mm^3. The distance between diodes is 5 mm in the central area (6x6 cm) and 10 mm in the outer area (20x20 cm). A daily output correction can be applied and measures the overall response of the Delta^4 with respect to a treatment plan. The daily correction factor can be adjusted by measuring a 10x10 cm opened-field. A trigger signal from the accelerator is used to measure the dose for each pulse of accelerator, thus improving the signal-to-noise ratio.

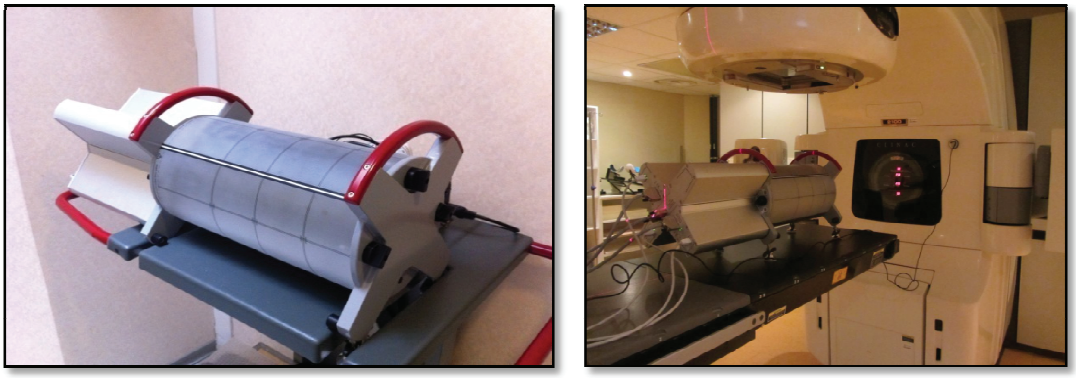

Figure 4.2. The Delta$^{4®}$ system, ScandiDos.

a) Delta$^{4®}$ Detectors Calibration

The calibration of the Delta$^{4®}$ is a cross-calibration, as described by the constructor [57]. The reference dose was first established with a ionization chamber in the calibration phantom (PMMA, Plexiglas material with a density of 1.19 g/cm^3). Then, the diode boards were removed from the Delta$^{4®}$ phantom and were placed perpendicular to the beam axis in the calibration phantom (acrylic). At Lyon Sud Hospital, both, relative (for one photon energy) and absolute (for available energies), calibrations were performed for main detector board and the two wing boards, at 5 cm water equivalent depth (for buildup) and 95 cm SSD. For the *relative calibration*, an individual relative sensitivity factor was determined for every detector, which compensate for detector-to-detector differences. This calibration was done by irradiating the detector board in different positions inside a large field with a constant number of monitor units. The *absolute calibration* factor was determined per detector board. The detector was put into the same position as the chamber and irradiated with 100 monitor units [57].

As recommended by ScandiDos, the original plans were recalculated on a virtually computed tomography scan provided by the company. The detectors from the two planes can measure the composite dose distribution of the entire plan and of each beam or sub-beam in only one measurement allowing thus a 4D treatment QA. The interpolation algorithm, provided with the software and that calculates doses at points where no detectors are present, was previously described [38]. In addition, dose profiles can be obtained to compare the planned dose against the detector measurement and measured dose distributions can be superimposed on the patient's anatomy (Delta^{4DVH} Anatomy$^{®}$). Furthermore, the local and global comparisons between the calculated and the measured dose distributions can be made using the three methods available in

the Delta^4 software: the dose deviation (%), the distance to agreement (mm) and the gamma index evaluation.

b) Evaluation studies for Delta$^{4®}$

Many authors have already described validation studies with the Delta^4 phantom [36-38, 41, 42] and reported good angular response, reproducibility and uniformity of the diodes.

In 2009, Feygelman *et al.* provided a complete description and characterization of the Delta^4 and demonstrated its applicability for IMRT QA [36].

Bedford *et al.* performed test with Delta^4 for angular response, linearity of segment dose and dose rate dependence [37]. The variation in response was found to be less than 0.5%, the linearity of segment dose was within 0.5% and the Delta^4 responded to all dose rates within 0.5% of the ionization chamber [37]. Additionally the authors compared Delta^4 results with those obtained with ionization chamber (0.6 cm^3 Farmer chamber) and film (EDR2 and Gafchromic EBT) in a water-equivalent phantom for IMRT and VMAT. They found a maximum difference of 2.5% when Delta^4 was compared with the ionization chamber and about -2% to +7% when compared to film (measured compared to planned dose with 3%/3mm criteria) [37].

The results of 264 clinical cases using Delta^4 for helical tomotherapy IMRT QA were presented by Geurts *et al.* [42]. The authors compared existing IMRT QA results with ionization chamber and Gafchromic® EBT films (International Specialty Products) to diode phantom results. The maximum observed difference (in low dose-gradient regions) was of 0.7% with a mean difference of 0.1% between the diode phantom and ionization chamber measurements and the authors concluded that phantom measurements closely match the planned dose distributions in high and low dose-gradient regions [42]. All 264 plans (head and neck, lung, partial breast, pelvic nodes, prostate, rectum, whole brain, whole breast and other) resulted in at least 90% of the diodes passing the established criteria (3%/3mm) when compared to the calculated dose, with a mean value of 97.5%. An interesting analysis was made by the investigators in terms of average time required to complete the total IMRT QA per patient (from creation of the QA plans to data analysis). The average time required in completing film and ionization chamber IMRT QA was 1.5 hours per patient and with the Delta^4 was 0.5 hours [42].

Korreman *et al.* reported the dosimetric verification measurements of RapidArc treatment delivery performed with the Delta^4 phantom [41]. The delivery of treatment plans were consistent

with the dose calculated in the Eclipse 8.5. TPS as verified with the Delta$^{4®}$ phantom. Moreover, the phantom results showed high reproducibility of consecutive delivery within the same day and from day to day (gamma values above 1 in none of the measured points and dose deviation less than 1%) [41].

Sadagopan *et al.* characterized, commissioned and evaluated the QA capabilities of the Delta$^{4®}$ for IMRT delivery [38]. They evaluated the system's reproducibility, stability, pulse-rate dependence, dose-rate dependence, angular dependence, linearity of dose response, energy response and also the interpolation algorithm. The short-term reproducibility was evaluated for 904 diodes over 10 irradiations and was found to be 0.1% (range 0-1%). The long-term reproducibility was measured 5 times over a period of 3 months and was found to be 0.5%. Moreover, the decrease in sensitivity was 0.9%/kGy for a 6 MV beam. The dose response was found to be linear within 0.25%, no dose rate dependence was observed and the diode dose-per-pulse response was less than 0.25%. The uncorrected angular dependence varied by ±2.5%. Additionally, Sadagopan *et al.* suggested that from their experience it's essential to renormalize the dose distribution in the high dose region and to exclude detectors that receive less than a certain minimum dose for the IMRT QA analysis [38]. The authors concluded that the Delta$^{4®}$ device is accurate and reproducible and that its interpolation algorithm is valid [38].

4.2.2.2. The ArcCheck® system, SunNuclear

The ArcCheck is a cylindrical water-equivalent (PMMA) phantom with a 3D array of 1386 diode detectors (size 0.8 x 0.8 mm) with 10 mm detector spacing (Figure 4.3). The size of one diode is 0.64 mm^2 has an active volume of 0.019 mm^3. The detectors are arranged in a spiral model, thus a helical geometry (HeliGrid^{TM}), with 21 cm array diameter and length. The purpose of the helical geometry is to increase the spatial sampling rate and reduce detector overlap from the beam's eye view. A ring encircles the inner cavity that can be left empty or filled with a homogeneous insert. "*The center of the phantom (15 cm diameter) is designed to accommodate different inserts such as a solid homogeneous core, a dosimetric core with ion chamber(s) or diode arrays, an imaging QA core, a core with heterogeneous materials for dose studies, etc"* [49, 58]. The ArcCheck measures the entrance and exit doses and the software displays QA dose maps that are a recalculation of the dose resulting from the beam fluence. The filter that is available in the software extracts a cylindrical dose plane from the imported 3D volume for direct

dose comparison with the measured values [58]. The device measures both relative and absolute dose measurements and in the 15 cm diameter cavity insert with an ionization chamber can be added for absolute dose measurement.

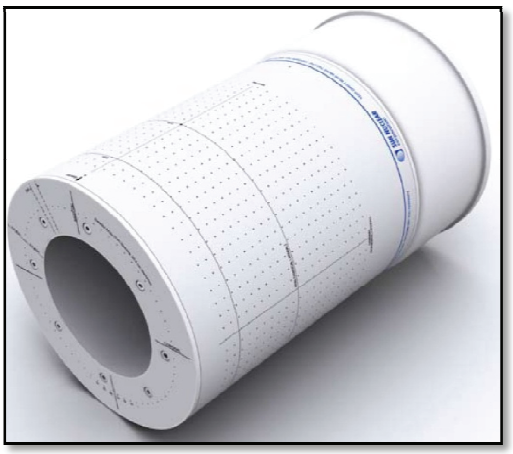

Figure 4.3. The ArcCheck® system, SunNuclear.

a) Correction factors and ArcCheck Calibration

There are four correction factors that are applicable for the ArcCheck measurement: background correction, diode sensitivity correction (array calibration), angular correction and absolute correction (dose calibration), as described by the constructor [58].

- The *background correction* creates a background correction factor for each detector [58];
- The *array calibration* measures and normalizes the relative sensitivity differences between the detectors (and it's performed at Sun Nuclear and the factors are stored in the array calibration file); the correction factors were applied to the raw measurements from each detector, ensuring that all detectors will have the same sensitivity and will eliminate the response differences between individual detectors [58];
- The *angular correction* corrects for the diodes angular dependence (is measured at Sun Nuclear and stored in the array calibration file) [58];
- The *dose calibration* that creates a dose calibration factor for converting the ArcCheck relative dose values to absolute dose values (was performed in the HCL department before starting the measurements). The absolute dose was performed in a 10 x 10 cm2

open field with the array at a depth where the dose was known from a measurement with a ionization chamber whose calibration was referenced. A flat-water phantom was used in the treatment planning system such that the chamber position was the same as the detector position in ArcCheck and has the same amount of buildup.

Three controls are available to set up the pass/fail criteria for the measurement points.

b) Percent difference (%Diff)

Van Dyk % Difference is the percent difference between any measured point and the corresponding plan point normalized to a common point (typically maximum dose point). For the ArcCheck, the percent difference is the tolerable difference between the measurement and calculated points. If the difference exceeds the allowed percent difference, the distance to agreement test is invoked [58].

c) DTA (mm)

The DTA is a radius in millimeters around the measured point. This test refers to points where the difference between measured and planned values of the points exceeds the selected percent difference (described above). Using the distance to agreement criteria, a measured point passes if, within a circle of DTA mm, there exists at least one calculated point that is greater than or equal to and at least one calculated point that is less than or equal to the value of the measured point. In the ArcCheck software, the plot shows all the measurement points that are not in agreement (the points that record a higher value are shown in red (hot), while those that record a lower value are shown in blue (cold)) [58].

d) Threshold (TH)

In the ArcCheck software, the threshold is the percent contour above which all plan points are included in the DTA analysis. By selecting a threshold value, the detectors that are outside of the area of interest can be excluded. The default value is 10, which means that detectors whose values fall within the 0 to 10 % range will be excluded from the statistical values to the right of the TH box. The lower the TH is, the more detectors will be included. The optimum TH value is between 5 and 10 because this will include the detectors that are in the penumbra region but exclude detectors that are in the scattered radiation regions [58].

e) Evaluation studies for ArcCheck®

Kozelka *et al.* reported the repetition rate, field size dependence and angular position dependence of ArcCheck [45]. They noted differences < 0.3% at lower repetition rates (40 MU/min) with the plug in place and field size dependence and angular position dependence were obvious.

Feygelman *et al.* reported response equalization of the individual detectors, minor field size dependence and angular response dependence for ArcCheck [39]. The percentage measured dose difference (ArcCheck-ion chamber) changed from -0.7% to 1.7% for the hollow phantom, and from -1.1% to 1.3% for the PMMA plug insert [39]. The authors reported that the largest difference between the calculated and the measured dose was observed up to 7% for angular dependence in the axial plane.

Recently, Li *et al.* performed test for the ArcCheck QA system and evaluated the suitability of the system for IMRT and VMAT verification [47]. Additionally, the investigators tested the device for short term reproducibility, dose linearity, dose rate dependence, dose per pulse dependence, field size dependence, out of field dependence and directional dependence [47]. They showed that the system performed well for all tests except for directional dependence, which varied from a minimum of -4.9% to a maximum of 9.1%. Li *et al.* suggested that the good field size dependence and out of field dependence implies that the ArcCheck diodes are less sensitive to low energy scattered photons, which is an important aspect of IMRT and VMAT QA because of the complexity of the plans and the magnitude of segment numbers [47]. For the patient IMRT and VMAT QA, the pass rates exceeded 95% and 93%, respectively. The authors stated that the ArcCheck QA system is completely suitable for clinical IMRT and VMAT verification [47].

In 2012, Kafir *et al.* designed a nonhomogeneous insert for the ArcCheck and demonstrated the possibility to verify the dose distribution with inhomogeneities and that it can be used clinically for routine QA of volumetric modulated arc therapy (VMAT) for lung SBRT [49]. Their result with the ArcCheck showed the uncertainties of dose calculations with inhomogeneities, with decrease in passing rates up to 3.6%.

Petoukhova *et al.* evaluated the dosimetric accuracy of HybridArc (BrainLAB, Feldkirchen, Germany) plans, using ArcCheck diode array (without and with an insert containing

a ionization chamber), calculated with Monte Carlo and Pencil Beam dose algorithms [46]. The absolute dose distributions measured and calculated with the Monte Carlo algorithm at the cylinder of the phantom gave good agreement (for 2%/2mm criteria). The difference between calculated and measured distributions significantly differed for ArcCheck, and the Monte Carlo algorithm was found to be superior [46].

4.3. Evaluation of IMRT QA

In order to validate an IMRT plan, the comparison between the calculated dose distribution and the measured dose distribution is performed by means of dose profile and gamma index evaluation. Low *et al.* developed a technique for the quantitative evaluation of two related dose distributions (the comparison method between calculated and measured dose distributions) that is referred to as gamma evaluation (or gamma index) [59-61]. The principle is that the gamma evaluation compares the measured dose distribution (of each beam or of the entire plan) by a detector with the planned dose distribution calculated by the treatment planning system. The *dose deviation* method provides the difference between the measured dose and the planned dose in one point and is recommended for use in regions with low dose gradients. *The distance-to-agreement (DTA)* method gives the shortest distance from the measured to the calculated point and is recommended for use in regions with high dose gradients. Thus, *the gamma index* combines both, the dose deviation and the DTA [38, 59]. Consequently, pass/fail criteria for dose deviation DTA and gamma index have to be adapted for each QA device that is used, as methods of IMRT QA evaluation vary from institution to institution.

Nelms and Simon conducted in 2007 an IMRT QA survey to users of an electronic 2D diode array [62]. The authors reported that most of the institutions perform absolute dose comparisons rather than relative dose comparisons and that the most used criteria are 3% and 3 mm for percentage difference analysis and for distance-to-agreement analysis, respectively [62]. Moreover, the most common criterion used for the analysis of an IMRT plan is the combination of 3% and 3 mm criteria.

The evaluation parameters used at Lyon Sud Hospital are: the average value of the gamma index (Gmean) has to be inferior to 0.5, the maximum value of the gamma index (Gmax) has to be inferior to 3 and the percentage of points in a definite evaluation area (region of interest) with a gamma index <1 (%G<1) needs to be greater or equal to 97%. The region of

interest for EPID evaluation that is used at Lyon Sud Hospital is "MLC+1cm". The pass/fail criteria are set at 4% and 3mm for percentage difference and distance-to-agreement, respectively.

At Lyon Sud Hospital, for the IMRT QA, films and the EPID have been used for more than 10 years, as well as the gamma evaluation [2]. Recently, RapidArc from Varian has been implemented in the Department or Radiation-Oncology. In 2010, two 3D diode arrays (Delta^4 and ArcCheck) were considered in order to improve the QA for IMRT and rotational treatments and were evaluated for conventional irradiations as well as for SBRT. Feygelman *et al.* compared and evaluated the two 3D arrays [39]. The authors found vast differences between the two devices, mainly due to low passing rates for the peripheral detectors of the ArcCheck and high passing rates for the Delta^4. They stated that both detectors measure two different things because of the completely different geometries [39].

The purpose of the current section is two-folded:

1. To assess the sensitivity of the Delta^4 three-dimensional diode array;
2. To evaluate the SBRT-IMRT plans of 5 prostate cases with a simultaneous integrated boost into the tumor and to assess if pre-treatment IMRT QA assure correct validation if the measurements are acquired at gantry angle of 0° or if the QA should be done with the gantry at treatment angles. Three independent measurement systems were used for this study.

4.4. Publication

The first study was intended to evaluate the degree of sensitivity of the Delta$^{4®}$ system with submillimetric MLC offsets and subdegree gantry errors. The initial results were presented as poster at the SFPM meeting in 2013 (5-7 June) in Nice, France (Appendix 11). The related article is presented below.

Sensitivity test of a 3D diode array system for small MLC and gantry errors in IMRT delivery

Corina Udrescu[1-2], Benjamin Pignata[2], Ronan Tanguy[1], Olivier Chapet[1], Julien Ribouton[2], Gaelle Kerneur[2], and Patrice Jalade[2]

[1]Department of Radiation Oncology, Centre Hospitalier Lyon Sud, Pierre-Benite, France
[2]Department of Medical Physics, Centre Hospitalier Lyon Sud, Pierre Benite, France

Corresponding author:
Corina Udrescu, M.S.
Département de Radiothérapie-Oncologie
Centre Hospitalier Lyon Sud
165 Chemin du Grand Revoyet
69495 PIERRE BENITE cedex
FRANCE
Tel : + 33 4 78 86 42 60
Fax : + 33 4 78 86 42 65
corina.udrescu@hotmail.com

Abstract

Purpose

The diode arrays are used for dose detection and are designed for three-dimensional (3D) dose verification before intensity-modulated radiotherapy (IMRT). They were characterized in the past and showed excellent reproducibility, linearity and dose-rate independence. The purpose of this work was to verify the sensitivity of a 3D diode array for small MLC and gantry offsets in IMRT.

Methods

Ten IMRT plans (5 prostate and 5 head and neck) were used. Systematic MLC errors were introduced for one leaf (errors of -0.2 mm, -0.5 mm, -0.7 mm, -1 mm, -2 mm, -3 mm, -5 mm and -10 mm) for each control point. Subsequently, gantry errors were made for the same plans (errors of 0.2°, 0.5°, 0.7°, 1°, 2°, 2.5°, 3°, 4° and 5°). The modified files were then imported for irradiation under the accelerator. The 3D diode array was used to acquire and analyze the data. All the measurements were acquired consequently for each patient. In order to estimate the repeatability errors, standard deviations (SD) of the maximum gamma (Gmax) and the percentage of points with area gamma < 1 (%G<1) were calculated for 20 consecutively beams with no offsets.

Gmax and %G<1 values were noted for both global gamma evaluation (GGE) (normalization dose) and for local gamma evaluation (LGE) (local detector dose) with pass/fail criteria of 2% and 2mm. Gmax and %G<1 were evaluated for each modified field when compared with the measured field with no introduced error (0 mm or 0°). Because we had one leaf with a small offset we evaluated only the Gmax and the %G<1 and not the mean gamma.

Results

The repeatability results for Gmax and %G<1 were of 3.5% and 0.51%, respectively, for local gamma evaluation and of 0.7% and 0.21%, respectively, for global gamma evaluation.

The MLC and gantry offsets had a noticeable impact on the plan evaluation when the measured dose distributions with offsets were compared with the measured dose distributions without offsets (0mm and 0°). For all the ten plans we observed modifications in Gmax starting with 0.2 mm for MLC plans ($p<0.0001$, for LGE and GGE) and with 0.2° for the gantry errors ($p=0.001$ for LGE and $p=0.0007$ for GGE). On the other hand, the submillimetric and subdegree offsets didn't affect the clinical evaluation of the plan when the measured dose with offsets was compared with the planned dose without offsets.

Conclusions

The present 3D diode array system seems to be a very sensitive instrument for the quality assurance of the IMRT plans. In our study it detected submilimetric and subdegree errors for MLC and gantry, respectively. In clinical use these small errors may not be detected and could be hidden by the residual error between planned and delivered dose.

Keywords: Three-dimensional array, sensitivity, intensity-modulated radiotherapy, MLC and gantry errors

1. INTRODUCTION

Delta$^{4®}$ system is a device for dose detection and it's designed for three-dimensional (3D) dose verification (between the measured and planned dose distributions) for intensity modulated radiotherapy (IMRT) and volumetric modulated arc therapy (VMAT). In 2009, Feygelman *et al.* provided a complete description and characterization of the Delta^4 3D array and demonstrated its applicability for IMRT QA.[1] It was already evaluated in the past and showed excellent reproducibility, linearity, uniformity of the diodes, good angular response and dose-rate independence.[1-9] Moreover, the sensitivity of Delta^4 was recently assessed for intentional errors with increasing the number of monitor units (MU) by 3%, widening of the MLC banks (≥2mm) and collimator rotation error (≥2°).[2]

The purpose of this work was to evaluate the sensitivity of the Delta^4 device for very small (submilimetric and subdegree) multileaf collimator (MLC) and gantry errors in intensity modulated radiotherapy delivery.

2. MATERIALS AND METHODS

2.A. Treatment planning and errors

Ten patients were treated with IMRT on a Clinac 2100CD from Varian (5 prostate and 5 head and neck cases) with doses that varied from 28 to 76 Gy in 2 Gy per fraction. The treatment plans were calculated in the Eclipse® treatment planning system (TPS) version 10.0.28 (Varian Medical Systems, Palo Alto, CA) using the Analytical Anisotropic Algorithm (AAA) and the 120 Millennium MLC (Varian) and thus, they were used for the present study.

In Table I are noted the number and position of the leaves and the gantry angles that were used for the current paper. The isocenter of the field is situated between the 30th leaf and the 31st leaf. Systematic MLC errors were intentionally introduced in the TPS for one leaf (errors of -0.2

mm, -0.5 mm, -0.7 mm, -1 mm, -2 mm, -3 mm, -5 mm and -10 mm) and for each control point. Subsequently, gantry errors were introduced for a certain angle (errors of 0.2°, 0.5°, 0.7°, 1°, 2°, 2.5°, 3°, 4° and 5°) (Table I).

TABLE I. Gantry angle and leaf positions that were used for the present study are presented for each patient. The isocenter is situated between the 30th leaf and the 31st leaf.

		Gantry errors	**MLC errors**	
Localization	**Patient**	**Gantry angle**	**Leaf position**	**Gantry angle**
Prostate	1	315°	30B	255°
	2	45°	35B	255°
	3	255°	34B	255°
	4	105°	26B	255°
	5	180°	30B	255°
Head and	6	255°	26B	255°
head and neck	7	45°	32B	255°
	8	90°	32B	255°
	9	0°	30B	255°
	10	10°	37B	255°

2.B. Delta$^{4®}$ system and measurements

The modified files were then exported for irradiation under the accelerator. The Delta^4 system (ScandiDos, Uppsala, Sweden) was used to acquire and analyze the data (Figure 1). All the measurements were acquired consequently for each patient. In order to estimate the repeatability

errors, standard deviations of: the percentage of points having a gamma<1 (%G<1), the maximum gamma (Gmax) and the mean gamma (Gmean) were calculated for 20 consecutively beams with no offsets.

The Delta^4 is a 3D diode array that consists of two crossed and perpendicular planes within a cylindrical polymethylmethacrylate (PMMA) phantom (density of 1.19 g/cm^3, relative electron density of 1.147 g/cm^3 and 217 HU). The 2 orthogonal diode arrays (called units) are synchronized with the accelerator (to measure the dose for each pulse of accelerator) and consist of three removable electrometers/detector-array units: 1 main unit and 2 wing units. The phantom has a total length of 72 cm (40 cm in length and 22 cm in diameter) and it weighs 27 Kg (but a transfer support that holds the phantom is provided). The detector boards include a total number of 1069 p-type silicon diodes with a cylindrical shape. The size of one diode is 0.78 mm^2 and has an active volume of 0.04 mm^3. The distance between diodes is 5 mm in the central area (6x6 cm^2) and 10 mm in the outer area (20x20 cm^2). A daily output correction can be applied and measures the overall response of the Delta^4 with respect to a treatment plan. Herein, the output correction factor was not applied as it was not essential for the purpose of this study.

FIG. 1. The Delta$^{4®}$ system.

2.C. Analysis and statistics

The percentage of points having a gamma<1 (%G<1) and the Gmax variables were noted for both global gamma evaluation (GGE) (normalization dose) and local gamma evaluation (LGE) (local detector dose). The pass/fail criteria were of 2% and 2mm for dose deviation and distance-to-agreement, respectively. For GGE and LGE, each variable was evaluated 2 times with:

a) *a "clinical evaluation"* of the field – where for each beam (with or without offsets) the measured dose was compared with the planned dose from the TPS;

b) *a "reference evaluation*" – where for each modified field, the measured dose with offset was compared to the measured dose with no offset (0 mm or 0°, that was considered "the reference").

Because we had a single leaf with a small offset we evaluated only the Gmax and the %G<1 and not the mean gamma.

The statistical analysis of the quantitative variables was performed using the student paired t-test and the analysis was made with a significance threshold set at $p<0.05$. The diagrams were made using the SPSS V20.0 software.

3. RESULTS

3.A. Repeatability results

For the "clinical evaluation" of the fields and the GGE, the repeatability results were of 0.21%, 0.7% and 1.7% for %G<1, Gmax and Gmean, respectively. The LGE evaluation shows similar results: 0.51%, 3.54% and 1.8% for %G<1, Gmax and Gmean, respectively.

3.B. Clinical evaluation

As it can be observed in Figure 2(a) (for MLC offsets) and Figure 4(a) (for gantry offsets), when the measured dose distributions with errors were compared to the planned dose

distributions without errors, the Gmax variable increased starting with 2mm and 2°, but with no significant differences ($p>0.05$) for MLC and gantry errors (Table II). Moreover, the submillimetric and subdegree offsets didn't affect the plan evaluation.

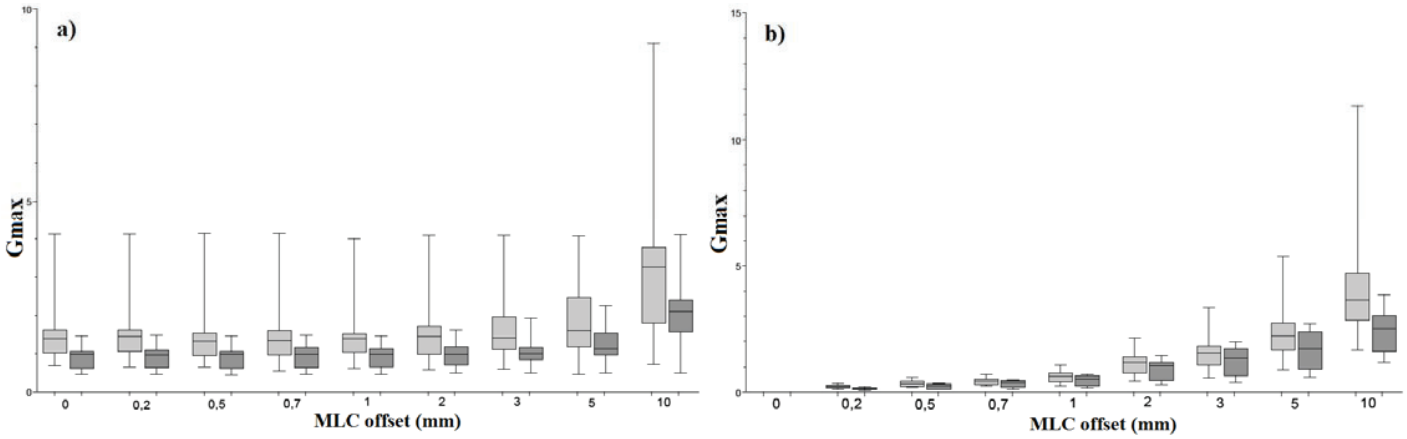

FIG. 2. Maximum gamma (Gmax) values plotted against MLC offsets (in millimeters) for local gamma evaluation (light grey) and for global gamma evaluation (dark grey). The results are presented for both, "clinical evaluation" (left) and "reference evaluation" (right).

TABLE II. Average, minimum and maximum values for maximum gamma (Gmax) for MLC and gantry offsets in terms of local and global gamma evaluations. The results represent the *"clinical evaluation"* where the measured doses with offsets were compared to the planned doses without offsets (0mm and 0°) and the *p*-value gives the significance.

	Gmax for MLC offsets					**Gmax for Gantry offsets**			
	Local gamma	***p***	**Global gamma**	***p***		**Local gamma**	***p***	**Global gamma**	***p***
0 mm	1.58 [0.69–4.13]	*n.a.*	0.91 [0.46–1.47]	*n.a.*	**0°**	1.52 [1.01–2.78]	*n.a.*	1.19 [0.79–2.59]	*n.a.*
0.2 mm	1.58 [0.66–4.13]	*=0.91*	0.91 [0.46–1.48]	*=0.52*	**0.2°**	1.51 [0.95–2.71]	*=0.75*	1.18 [0.70–2.5]	*=0.58*
0.5 mm	1.57 [0.66–4.14]	*=0.6*	0.91 [0.44–1.46]	*=0.82*	**0.5°**	1.51 [0.96–2.68]	*=0.83*	1.16 [0.70–2.48]	*=0.45*
0.7 mm	1.59 [0.54–4.15]	*=0.82*	0.93 [0.45–1.48]	*=0.32*	**0.7°**	1.52 [0.96–2.64]	*=0.91*	1.16 [0.71–2.38]	*=0.41*
1 mm	1.57 [0.62–4.01]	*=0.85*	0.92 [0.45–1.46]	*=0.3*	**1°**	1.57 [0.93–2.65]	*=0.4*	1.2 [0.72–2.41]	*=0.68*
2 mm	1.63 [0.59–4.09]	*=0.5*	0.97 [0.49–1.62]	*=0.2*	**2°**	1.73 [0.99–2.75]	*=0.12*	1.41 [0.73–2.47]	*=0.05*
3 mm	1.68 [0.6–4.09]	*=0.39*	1.05 [0.49–1.92]	*=0.1*	**2.5°**	1.87 [0.93–2.84]	*=0.05*	1.59 [0.76–2.56]	*=0.01*
5 mm	1.93 [0.69–4.07]	*=0.04*	1.27 [0.49–2.26]	*=0.01*	**3°**	2.06 [0.97–3.02]	*=0.01*	1.76 [0.77–2.72]	*=0.006*
10 mm	3.55 [0.72–9.1]	*=0.001*	2.09 [0.49–4.11]	*=0.0006*	**4°**	2.91 [1–4.54]	*=0.007*	2.32 [0.77–3.67]	*=0.001*
					5°	6.91 [1.02–29.21]	*=0.07*	2.99 [0.79–5.98]	*=0.003*

Similar results can be observed in Figure 3(a) and Figure 5(a) in terms of %G<1 for MLC and gantry offsets, respectively. The %G<1 didn't affect the plan evaluation for both global and local evaluations when the measurements with offsets were compared to the planned dose distributions (Table III).

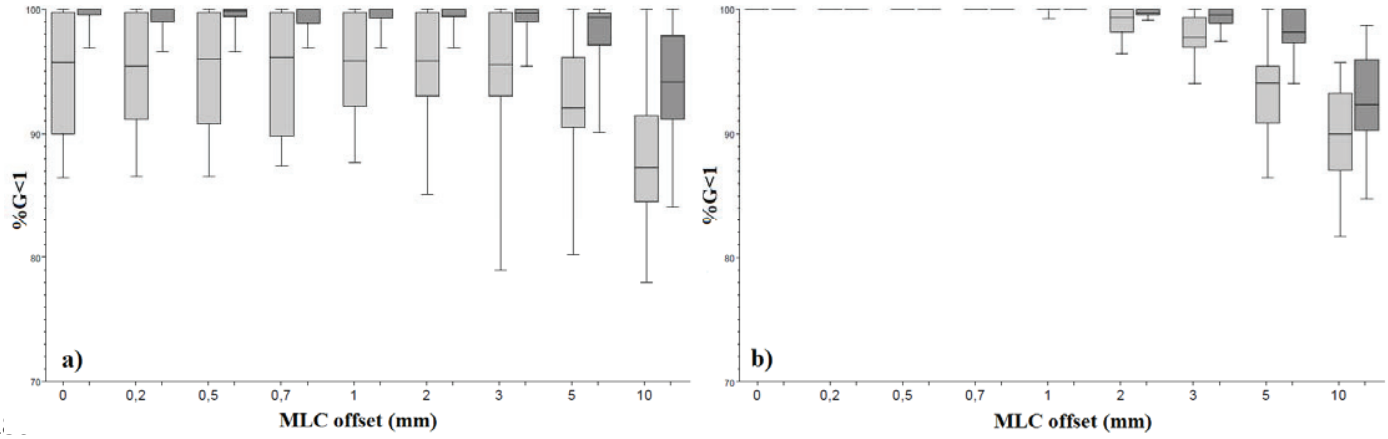

FIG. 3. Percentage of points that have a gamma index <1 (%G<1) plotted against MLC offsets (in millimeters) for local gamma evaluation (light grey) and for global gamma evaluation (dark grey). The results are presented for both, “clinical evaluation” (left) and “reference evaluation” (right).

TABLE III. Average, minimum and maximum values for the percentage of points having a gamma<1 (%G<1) for MLC and gantry offsets in terms of local and global gamma evaluations. These results represent the *"clinical evaluation"* where the measured doses with offsets were compared to the planned doses without offsets (0 mm and 0°).

	%G<1 for MLC offsets					**%G<1 for Gantry offsets**			
	Local gamma	***p***	**Global gamma**	***p***		**Local gamma**	***p***	**Global gamma**	***p***
0 mm	95.2 [86.5 - 100]	*n.a.*	99.6 [96.9 - 100]	*n.a.*	**0°**	93.7 [83.6 – 99.7]	*n.a.*	98.7 [91.4 - 100]	*n.a.*
0.2 mm	95.3 [86.6 - 100]	*=0.4*	99.5 [96.6 – 100]	*=0.34*	**0.2°**	94.3 [86 – 100]	*=0.05*	98.7 [92.5 – 100]	*=0.9*
0.5 mm	95.4 [86.6 - 100]	*=0.21*	99.4 [96.6 – 100]	*=0.1*	**0.5°**	94.3 [85.9 – 100]	*=0.13*	98.5 [91.7 – 100]	*=0.44*
0.7 mm	95.3 [87.4 – 100]	*=0.58*	99.4 [96.9 – 100]	*=0.09*	**0.7°**	94.5 [86.2 – 100]	*=0.03*	98.5 [93 – 100]	*=0.66*
1 mm	95.6 [87.7 – 100]	*=0.25*	99.5 [96.9 – 100]	*=0.47*	**1°**	94.3 [85.5 – 100]	*=0.16*	98.6 [93 – 100]	*=0.84*
2 mm	95.4 [85.1 – 100]	*=0.7*	99.5 [96.9 – 100]	*=0.63*	**2°**	93 [82.7 – 100]	*=0.2*	97.4 [89.9 – 100]	*=0.01*
3 mm	94.5 [79 – 100]	*=0.53*	99.2 [95.4 - 100]	*=0.07*	**2.5°**	91.4 [80.1 – 100]	*=0.01*	96.6 [89.6 – 100]	*=0.009*
5 mm	92.6 [80.2 – 100]	*=0.03*	98 [90.1 – 100]	*=0.05*	**3°**	89.6 [78.2 – 100]	*=0.005*	95.7 [88.3 – 100]	*=0.005*
10 mm	87.8 [78 – 100]	*=0.002*	93.6 [84.1 – 100]	*=0.002*	**4°**	84.6 [70.9 – 98.7]	*=0.003*	92.4 [83.8 – 100]	*=0.0005*
					5°	79.8 [60.8 – 98.7]	*=0.001*	87.5 [69.9 – 100]	*=0.0003*

3.C. Reference evaluation

However, the MLC offsets (Figure 2, b) and gantry offsets (Figure 4, b) had a noticeable impact on the plan evaluation in terms of maximum gamma when the measured dose distribution with offsets is compared with the measured dose distribution with no offset (0 mm and 0°). For all the ten plans significant modifications were noted for Gmax, starting with 0.2 mm for MLC

offset (p<0.0001 for LGE and GGE) and with 0.2° for gantry offset (p=0.001 and p=0.0007, for LGE and GGE, respectively) (Table IV).

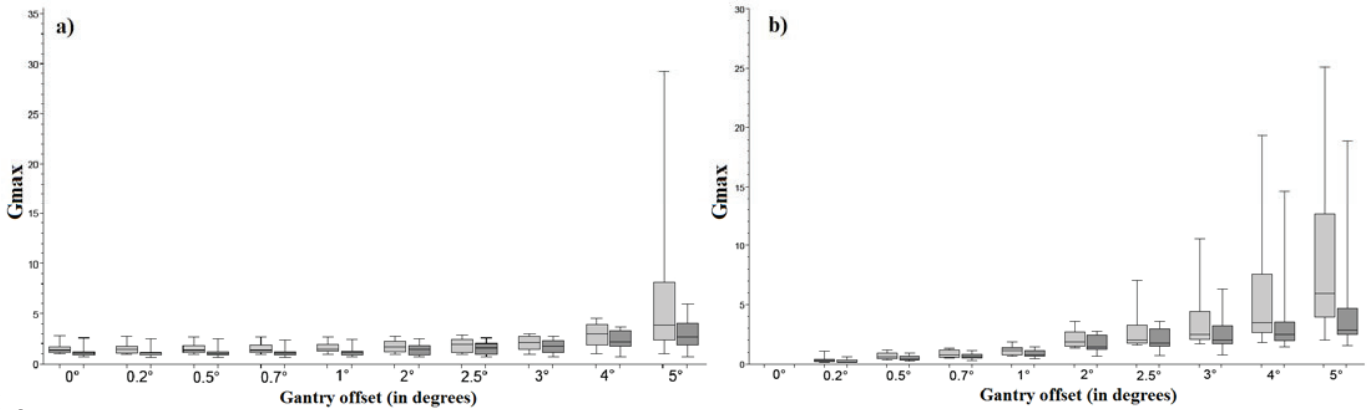

FIG. 4. Maximum gamma (Gmax) values plotted against gantry offsets (in degrees) for local gamma evaluation (light grey) and for global gamma evaluation (dark grey). The results are presented for both, "clinical evaluation" (left) and "reference evaluation" (right).

TABLE IV. Average, minimum and maximum values for maximum gamma (Gmax) for MLC and gantry offsets in terms of local and global gamma evaluations. These results represent the *"reference evaluation"* where the measured doses with offsets were compared to the measured doses without offsets (0 mm and 0°).

	Gmax for MLC offsets					**Gmax for Gantry offsets**			
	Local gamma	***p***	**Global gamma**	***p***		**Local gamma**	***p***	**Global gamma**	***p***
0.2 mm	0.23 [0.13 - 0.36]	*<0.0001*	0.14 [0.07 – 0.23]	*<0.0001*	**0.2°**	0.38 [0.18 – 1.12]	*=0.001*	0.26 [0.14 – 0.63]	*=0.0007*
0.5 mm	0.36 [0.21 - 0.59]	*<0.0001*	0.24 [0.12 – 0.36]	*<0.0001*	**0.5°**	0.70 [0.38 – 1.24]	*<0.0001*	0.5 [0.25 – 0.97]	*=0.0001*
0.7 mm	0.44 [0.25 – 0.7]	*<0.0001*	0.35 [0.11 – 0.5]	*<0.0001*	**0.7°**	0.87 [0.54 – 1.3]	*<0.0001*	0.67 [0.31 – 1.18]	*<0.0001*
1 mm	0.61 [0.25 – 1.07]	*<0.0001*	0.48 [0.17 – 0.71]	*<0.0001*	**1°**	1.17 [0.69 – 1.84]	*<0.0001*	0.89 [0.45 – 1.45]	*<0.0001*
2 mm	1.16 [0.45 – 2.16]	*<0.0001*	0.91 [0.31 – 1.45]	*=0.0001*	**2°**	2.05 [1.36 – 3.61]	*<0.0001*	1.66 [0.71 – 2.75]	*<0.0001*
3 mm	1.63 [0.58 – 3.36]	*=0.0001*	1.25 [0.39 - 2]	*=0.0001*	**2.5°**	2.74 [1.59 – 7.06]	*=0.0006*	2.04 [0.73 – 3.6]	*=0.0001*
5 mm	2.37 [0.9 – 5.37]	*=0.0002*	1.68 [0.61 – 2.70]	*=0.0001*	**3°**	3.76 [1.67 – 10.54]	*=0.003*	2.55 [0.81 – 6.33]	*=0.0006*
10 mm	4.31 [1.68 – 11.33]	*=0.0007*	2.41 [1.2 – 3.87]	*<0.0001*	**4°**	6.23 [1.8 – 19.36]	*=0.014*	3.82 [1.44 – 14.62]	*=0.01*
					5°	9.04 [1.99 – 25.08]	*=0.006*	4.79 [1.54 – 18.86]	*=0.01*

A less important difference was observed concerning the %G<1 (when the measured dose with offset was compared with the measured dose without offset) for MLC (Figure 3, b) and gantry (Figure 5, b) errors. The differences were significant starting with 2 mm (p=0.03) and 1° (p=0.02) (for LGE) and 2mm (p=0.01) and 2° (p=0.005) (for GGE) for MLC and gantry offsets, respectively (Table V).

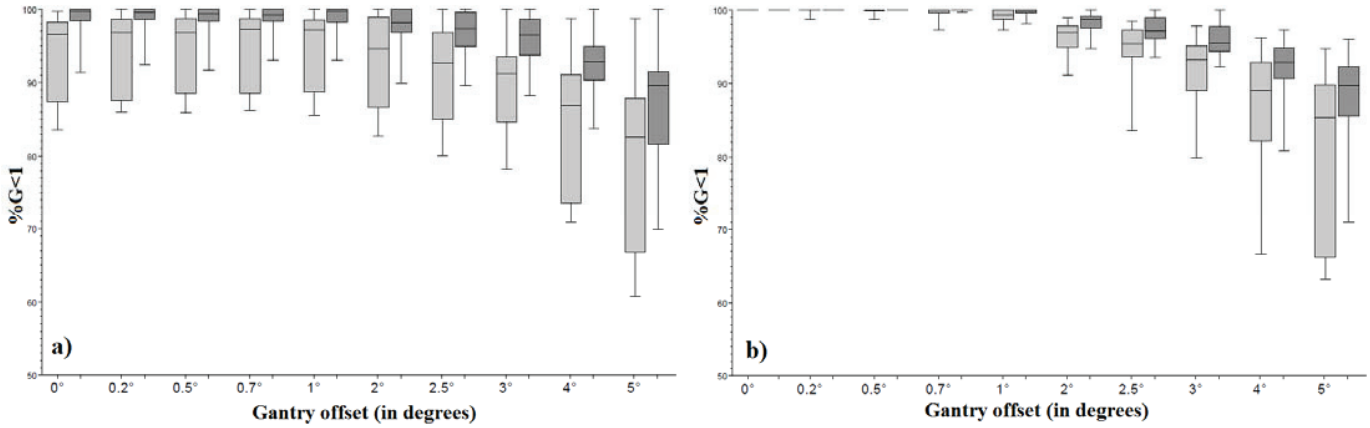

FIG. 5. Percentage of points that have a gamma index <1 (%G<1) plotted against gantry offsets (in degrees) for local gamma evaluation (light grey) and for global gamma evaluation (dark grey). The results are presented for both, "clinical evaluation" (left) and "reference evaluation" (right).

TABLE V. Average, minimum and maximum values for the percentage of points having a gamma<1 (%G<1) for MLC and gantry offsets in terms of local and global gamma evaluations. These results represent the *"reference evaluation"* where the measured doses with offsets were compared to the measured doses without offsets (0mm and 0°).

	%G<1 for MLC offsets					**%G<1 for Gantry offsets**			
	Local gamma	***p***	**Global gamma**	***p***		**Local gamma**	***p***	**Global gamma**	***p***
0.2 mm	100 [100 - 100]	*=1*	100 [100 – 100]	*=1*	**0.2°**	99.9 [98.7 – 100]	*=0.34*	100 [100 – 100]	*=1*
0.5 mm	100 [100 - 100]	*=1*	100 [100 – 100]	*=1*	**0.5°**	99.8 [98.7 – 100]	*=0.25*	100 [100 – 100]	*=1*
0.7 mm	100 [100 – 100]	*=1*	100 [100 – 100]	*=1*	**0.7°**	99.6 [97.3 – 100]	*=0.18*	100 [99.7 – 100]	*=0.34*
1 mm	99.9 [99.2 – 100]	*=0.34*	100 [100 – 100]	*=1*	**1°**	99.2 [97.3 – 100]	*=0.02*	99.7 [98.1 – 100]	*=0.17*
2 mm	98.9 [96.4 – 100]	*=0.03*	99.7 [99.1 – 100]	*=0.01*	**2°**	96.2 [91.1 – 98.9]	*=0.0009*	98.2 [94.7 – 100]	*=0.005*
3 mm	97.7 [94 – 100]	*=0.002*	99.3 [97.4 - 100]	*=0.02*	**2.5°**	94.4 [83.6 – 98.4]	*=0.002*	97.2 [93.5 – 100]	*=0.001*
5 mm	93.7 [86.5 – 100]	*=0.0005*	98.2 [94 – 100]	*=0.01*	**3°**	92 [79.9 – 97.8]	*=0.001*	95.9 [92.3 – 100]	*=0.0003*
10 mm	89.7 [81.7 – 95.7]	*<0.0001*	92.7 [84.8 – 98.7]	*=0.0003*	**4°**	86.3 [67 – 96.2]	*=0.002*	92 [80.9 – 97.3]	*=0.0003*
					5°	81.2 [63.2 – 94.7]	*=0.0007*	87.9 [71 – 96]	*=0.0007*

4. DISCUSSION

4.A. Delta$^{4®}$ system evaluation

Bedford *et al.* performed test with Delta^4 for angular response, linearity of segment dose and dose rate dependence.[4] The variation in response was found to be less than 0.5%, the linearity of segment dose was within 0.5% and the Delta^4 responded to all dose rates within 0.5% of the ionization chamber.[4] Additionally the authors compared Delta^4 results with those obtained with ionization chamber (0.6 cm^3 Farmer chamber) and film (EDR2 and Gafchromic EBT) in a water-

equivalent phantom for IMRT and VMAT. They found a maximum difference of 2.5% when Delta^4 was compared with the ionization chamber and about -2% to +7% when compared to film (measured compared to planned dose with 3%/3mm criteria).[4]

The results of 264 clinical cases were presented by Geurts *et al.* using Delta^4 for helical tomotherapy IMRT QA.[9] The authors compared existing IMRT QA results with ionization chamber and Gafchromic® EBT films (International Specialty Products) to diode phantom results. The maximum observed difference (in low dose-gradient regions) was of 0.7% with a mean difference of 0.1% between the diode phantom and ionization chamber measurements and the authors concluded that phantom measurements closely match the planned dose distributions in high and low dose-gradient regions.[9] All 264 plans (head and neck, lung, partial breast, pelvic nodes, prostate, rectum, whole brain, whole breast and other) resulted in at least 90% of the diodes passing the established criteria (3%/3mm) when compared to the calculated dose, with a mean value of 97.5%. An interesting analysis was made by the investigators in terms of average time required to complete the total IMRT QA per patient (from creation of the QA plans to data analysis). The average time required in completing film and ionization chamber IMRT QA was 1.5 hours per patient and with the Delta^4 was 0.5 hours.[9]

Korreman *et al.* reported the dosimetric verification measurements of RapidArc treatment delivery performed with the Delta^4 phantom.[8] The delivery of treatment plans were consistent with the dose calculated in the Eclipse 8.5. TPS as verified with the Delta$^{4®}$ phantom. Moreover, the phantom results showed high reproducibility of consecutive delivery within the same day and from day to day (gamma values above 1 in none of the measured points and dose deviation less than 1%).[8]

Sadagopan *et al.* characterized, commissioned and evaluated the QA capabilities of the Delta$^{4®}$ for IMRT delivery.[5] They evaluated the system's reproducibility, stability, pulse-rate

dependence, dose-rate dependence, angular dependence, linearity of dose response, energy response and also the interpolation algorithm. The short-term reproducibility was evaluated for 904 diodes over 10 irradiations and was found to be 0.1% (range 0-1%). The long-term reproducibility was measured 5 times over a period of 3 months and was found to be 0.5%. Moreover, the decrease in sensitivity was 0.9%/kGy for a 6 MV beam. The dose response was found to be linear within 0.25%, no dose rate dependence was observed and the diode dose-per-pulse response was less than 0.25%. The uncorrected angular dependence varied by ±2.5%. Additionally, Sadagopan *et al.* suggested that from their experience it's essential to renormalize the dose distribution in the high dose region and to exclude detectors that receive less than a certain minimum dose for the IMRT QA analysis.[5] The authors concluded that the Delta$^{4®}$ device is accurate and reproducible and that its interpolation algorithm is valid.[5]

4.B. Delta$^{4®}$ sensitivity

Recently, Fredh *et al.* investigated the ability of three QA systems to detect linear accelerator-related errors for rotational IMRT.[2] They introduced intentional errors that included 3% increased number of monitor units, a widening of the MLC bank with 2 mm and 4 mm, and rotation error of the collimator by 2° and 5°. When they used 2%/2mm criteria and 95% as a pass rate the Delta^4 detected 15 out of 20 errors. The authors stated that the impact of the errors in the prostate plans appear to be more important when looking at the DVH than for the gamma evaluation (when the planned dose without errors was compared to the one with errors).[2] We acknowledge that one limitation of our study is that we didn't evaluate the impact of these submillimetric and subdegree errors on dose-volume histogram,[2, 10, 11] but this wasn't the purpose of our study. Moreover, the results from the current study cannot be compared to those of Fredh *et al.* (2 mm and 4 mm offsets for the MLC bank) because herein submillimetric errors were introduced only for one leaf.

To our knowledge, Delta^4 sensitivity tests were not performed so far for submillimetric MLC errors and gantry offsets. In the present work, the Delta^4 system detected these submillimetric and subdegree introduced errors when a "reference evaluation" was performed. However, in "clinical evaluation" these errors cannot be seen in terms of %G<1 and Gmax. On the other hand, in "clinical evaluation", the Delta^4 software was able to identify the leaf and the control points that were modified, starting with a 2 mm offset (Figure 6).

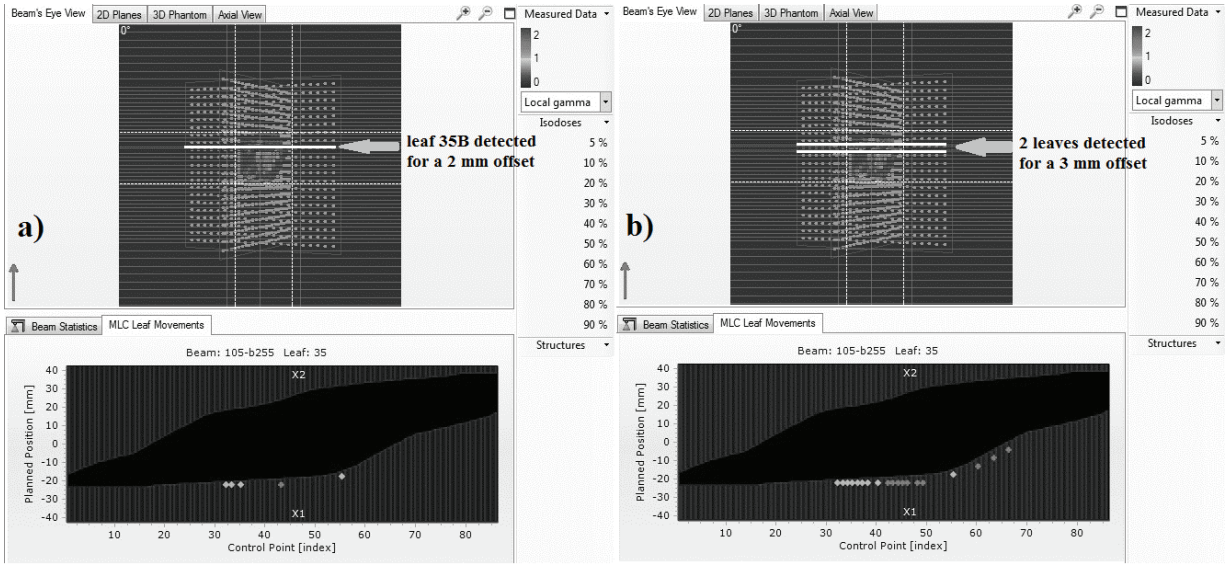

Figure 6. Illustration of the Delta$^{4®}$ software with an example of a case (patient 2) where: a) the leaf and the control points that were modified are detected by the system, starting with a 2 mm offset. b) two leaves are detected when 3 mm MLC offsets are introduced.

5. CONCLUSION

The Delta^4 system seems to be a very sensitive instrument for the quality assurance of the IMRT plans. In our study it detected submilimetric and subdegree errors for MLC and gantry, respectively. In clinical use (comparison between the measured dose and planned dose) these small errors may not be detected and could be hidden by the residual error between planned and delivered dose.

Bibliography

[1]V. Feygelman, K. Forster, D. Opp, and G. Nilsson, "Evaluation of a biplanar diode array dosimeter for quality assurance of step-and-shoot IMRT," *J. Appl. Clin. Med. Phys*. **10**, 64-78 (2009).

[2]A. Fredh, J. B. Scherman, L. S. Fog, *et al., "*Patient QA systems for rotational radiation therapy: A comparative experimental study with intentional errors," *Med. Phys.* **40**, 031716-1-9 (2013).

[3]G. Nilsson, "Delta4 – a new IMRT QA device," *Med. Phys.* **34**, 2432 (2007).

[4]J. L. Bedford, Y. K. Lee, P. Wai, C. P. South, and A. P. Warrington, "Evaluation of the Delta[4] phantom for IMRT and VMAT verification," *Phys. Med. Biol.* **54**(9), N167-N176 (2009).

[5]R. Sadagopan, J. A. Bencomo, R. L. Martin, *et al.,* "Characterization and clinical evaluation of a novel IMRT quality assurance system," *J. Appl. Clin. Med. Phys*. **10**, 104-119 (2009).

[6]V. Feygelman, G. Zhang, C. Stevens, B. E. Nelms, "Evaluation of a new VMAT QA device, or the "X" and "O" array geometries," *J. Appl. Clin. Med. Phys.* **12**(2), 146-168 (2011).

[7]S. Korreman, *et al.,* "RapidArc verification measurements using three different dosimetric systems," *Int. J. Radiat. Oncol. Biol. Phys.* **72**(1), S645-S646 (2008).

[8]S. Korreman, J. Medin, and F. Kjaer-Kristoffersen, "Dosimetric verification of RapidArc treatment delivery," *Acta. Oncol.* **48**, 185-191 (2009).

[9]M. Geurts, J. Gonzalez, and P. Serrano-Ojeda, "Longitudinal study using a diode phantom for helical tomotherapy IMRT QA," *Med. Phys.* **36**(11), 4977-83 (2009).

[10]H. Zhen, B. E. Nelms, and W. A. Tomé, "Moving from gamma passing rates to patient DVH-based QA metrics in pretreatment dose QA," *Med. Phys.* **38**, 5477–5489 (2011).

[11]B. E. Nelms, H. Zhen, and W. A. Tomé, "Per-Beam, planar IMRT QA passing rates do not predict clinically relevant patient dose errors," *Med. Phys.* **38**, 1037–1044 (2011).

4.5. Publication

The purpose of the second study was to assess the impact of irradiation geometry on pre-treatment evaluation of prostate SBRT-IMRT plans with an integrated boost. The early results were presented as poster presentation at the SFPM meeting in 2013 (5-7 June) in Nice, France (Appendix 11). The results are presented below as an article.

The Impact of Gantry Angle on Pre-treatment Verification. Quality Assurance of IMRT-SBRT for Prostate Cancer Using Three Different Detectors

Corina UDRESCU, M.S.[1-2], Ronan TANGUY, M.D.[1], Olivier CHAPET, M.D., PH.D.[1], Marie-Pierre SOTTON, M.S.[2], Patrice JALADE, PH.D.[2]

[1]Department of Radiation Oncology, Centre Hospitalier Lyon Sud, Pierre-Benite, France

[2]Department of Medical Physics, Centre Hospitalier Lyon Sud, Pierre Benite, France

Corresponding author:

Corina Udrescu, M.S.

Département de Radiothérapie-Oncologie

Centre Hospitalier Lyon Sud

165 Chemin du Grand Revoyet

69495 PIERRE BENITE cedex

FRANCE

Tel : + 33 4 78 86 42 60

Fax : + 33 4 78 86 42 65

corina.udrescu@hotmail.com

Running title: Quality assurance for prostate IMRT-SBRT

Conflict of interest: none.

Abstract

Introduction

The purpose of this work was to evaluate the impact of the irradiation geometry on the QA for prostate IMRT-SBRT using one dependent-device from the accelerator and two independent-units from the accelerator.

Materials and Methods

The prostate and the tumor were delineated by a radiologist on CT/MRI registrations of 5 patients. As part of a protocol, a 9-coplanar fields IMRT plan was optimized following a schema of prostate SBRT (5x6.5Gy) with a simultaneous integrated boost into the tumor (5x8Gy). All the beams were consecutively verified 3 times for each patient and each phantom (EPID, Delta^4 and ArcCheck) with the gantry at: a) 0° (Plan G0), b) 90° (G90) and c) at their original angulations (242°,270°,297°,328°,0°,38°,76°,101°,127°), named GFbyF (field-by-field). The plans G90 and GFbyF were compared with G0 using two evaluation indexes (global gamma evaluation (GGE) and local gamma evaluation (LGE)) as differences of: percentage of detectors with gamma<1 (%G<1), maximum gamma (Gmax) and mean gamma (Gmean) (pass/fail criteria of 4%/3mm).

Results

An average difference (in absolute value) of 0.2% (range 0-0.9%) was found between G0 and GFbyF for EPID. For the independent-units from the accelerator higher values were observed for GGE with a maximum difference between G0 and GFbyF plans in terms of %G<1 up to 2.7% and 8.3% for Delta^4 and ArcCheck, respectively. Per-field differences between G0 and GFbyF were seen as well for Gmax with maximum differences up to 1.5 and 1.7 for Delta^4 and ArcCheck, respectively.

Conclusion

Usually the IMRT plan verification is made using all beams with gantry at 0°. However, it is important to verify the irradiation plans in the exact situation as at the time of treatment. We have showed here that there is an important difference in the evaluation of a stereotactic IMRT plan as it depends of the irradiation condition. These differences could be explained by the impact of the MLC weight and the couch attenuation. Therefore, it can be recommended that the IMRT verification is made with a detector independent from the

accelerator and in the exact configuration of the irradiation as at the time of the treatment (gantry angle and couch position).

Keywords: 3D diode array phantom, EPID, quality assurance, IMRT, prostate SBRT

Introduction

The intensity-modulated radiotherapy (IMRT) is a complex treatment technique, because of complicate fluence maps, many segments, and high constraints (used for beam optimization and dose calculation) along with mechanical and physical limitations of the accelerator. Therefore, the quality assurance (QA) for an IMRT plan requires a particular attention [1-3]. Additionally, the dosimetry verification and the QA of a stereotactic irradiation have a particular place in the patient treatment procedures [4, 5]. This is due to the high gradient doses that are delivered per fraction. The QA of an IMRT plan can be made using an accelerator-dependent and/or -independent detector. Usually, all the beams are verified at the gantry, collimator or table angles set at zero degrees (0°). However, it was already demonstrated that gravity may have an impact on the dynamic multileaf collimator (MLC) contained by the treatment head of the accelerator [6, 7]. The gantry angle dependence in IMRT pre-treatment patient-specific quality controls was recently presented with measurements of a dependent-device from the accelerator, the EPID [8].

The electronic portal imaging device (EPID®) (Varian Medical Systems, Palo Alto, CA) - a flat-panel 2D detector placed opposite and attached to the gantry of the accelerator – is dedicated to IMRT QA and has been already evaluated [9-12].

Three-dimensional (3D) diode arrays are independent-units from the accelerator and were described and evaluated, in the recent years, for stability and dosimetric verification measurements of IMRT and volumetric modulated arc therapy (VMAT) treatment delivery. The Delta^4 (Scandidos, Uppsala, Sweden) is a 3D diode array with two orthogonal planes inserted in a cylindrical PMMA or Plastic Water® phantom that is well suited for routine machine QA and pre-treatment verification for IMRT or VMAT plans [13-21]. The ArcCheck® 3D diode array (Sun Nuclear, Melbourne, USA) was first evaluated as a prototype [22, 23] and subsequently the commercial version was studied for IMRT, VMAT and HybridArc QA [18, 24-28].

In 2010, a protocol was created in our department for prostate stereotactic body radiation therapy (SBRT) with a simultaneous integrated boost (SIB) into the dominant intraprostatic lesion (DIL), as recently described by other teams [29].

The purpose of this work was to evaluate how the irradiation geometry could affect the IMRT QA for prostate SBRT-SIB plans, using a 2D detector (EPID®) and two 3D independent-units from the accelerator (Delta$^{4®}$ and ArcCheck®).

Materials and Methods

Treatment planning and verification plans

Treatment plans for 5 patients were created using a protocol for prostate SBRT with a simultaneously integrated boost into the macroscopic tumor. The prostate and the tumor were delineated by a radiologist on an image registration (Integrated Registration®, General Electric Medical Systems) between the computed tomography (CT) and the magnetic resonance imaging (MRI). The SBRT-IMRT plans were calculated in Eclipse® treatment planning system (TPS) using the Pencil Beam Convolution (PBC) algorithm, 9 non-opposing 16MV beams and a Clinac 2100CD from Varian. The prescribed doses were 32.5 Gy in 5 fractions of 6.5 Gy to the prostate and 40 Gy in 5 fractions of 8 Gy to the tumor. Three verification plans were subsequently created in the TPS for each phantom by recalculating each patients plan onto the three phantoms. In our previous version of Eclipse (version 8.6) the table (carbon-fibre type) wasn't included for the PBC recalculation of the verification plan. Therefore, in order not to bias the gamma analysis, the posterior fields passing through the table (2 fields for each patient) were not included in this study.

Measurements

All the beams were consecutively verified 3 times for each phantom (as illustrated in Figure 1 for the Delta^4 system) with the gantry at:

a) 0° (Plan G0) (Figure 1,a);
b) 90° (Plan G90) (Figure 1,b);
c) and in the treatment configuration (242°, 270°, 297°, 328°, 0°, 38°, 76°, 101°, 127°), named Plan GFbyF (field-by-field) (Figure 1, c).

The three different systems that were used to verify each plan (G0, G90 and GFbyF) are briefly described below:

a) EPID®, Varian

The EPID® (aS1000, IAS 3) is a flat-panel 2D amorphous silicon detector placed opposite and attached to the gantry of the accelerator, with a resolution of 1024 x 768 and a pixel size of 0.39 mm. In our department, the portal imager is calibrated before each measurement. After the measurements are acquired they are then evaluated with the Portal Dosimetry® software, included in Eclipse®TPS (Varian Medical Systems, Palo Alto, CA). The dose profiles are aligned for each beam according to the clinical procedure at the Lyon

Sud Hospital. However, even if the EPID is a practical device in the QA procedure with very good tools for the analysis, it is a dependent-detector from the accelerator and moreover it cannot provide an analysis of the 3D dose distribution.

b) Delta$^{4®}$, ScandiDos

The Delta$^{4®}$ system is a 3D array that includes 1069 p-type silicon diodes in a cylindrical polymethylmethacrylate (PMMA) phantom and is dedicated for the QA of IMRT, rotational irradiation and machine QA. The device is an independent-unit from the accelerator, but synchronized to the machine. The stability of the Delta$^{4®}$ in terms of linearity of dose, reproducibility, repeatability, angular dependence, dose rate dependence, pulse-rate dependence was already demonstrated [13-21]. Each detector board was initially calibrated in our department for relative and absolute dose, as previously described. Delta$^{4®}$ detectors measure the dose distributions of the plans and an interpolation algorithm calculates the doses at points where detectors are missing, thus allowing a 3D dose comparison.

c) ArcCheck®, Sun Nuclear

The ArcCheck® is a cylindrical water-equivalent (PMMA) phantom with a 3D array of 1386 diodes, arranged in a helical geometry. Repetition rate, field size dependence, angular position dependence, short term reproducibility, dose linearity, dose rate dependence, dose per pulse dependence, and out of field dependence were previously reported [18, 24-28]. The ArcCheck® software displays 3D dose maps that are a recalculation of the dose measured at the entrance and exit of the beam.

The characteristics of the three devices are summarized in Table 1.

Plan evaluation and statistics

For the three devices, the evaluation of dose distributions (measured doses compared with the planned doses) was based on gamma analysis (or gamma index) [30] performed with our clinical criteria: 4% dose difference and 3 mm distance-to-agreement. In our department, the acceptability criteria for gamma evaluation is a combination of three parameters [31] and involve that more than 97% of the points (or diodes) should have a gamma value less than one, maximum gamma must be < 3 and average gamma should be < 0.5. The measurements were not corrected for daily output variation in order to consider the real treatment delivery.

The plans G90 and GFbyF were compared with the plan G0 using the global gamma evaluation for EPID. For Delta$^{4®}$ and ArcCheck®, two gamma comparisons were made: the global gamma evaluation (GGE) and the local gamma evaluation (LGE). For each gamma evaluation, the comparison between two plans was made using three variables: the percentage

of points (diodes) having a gamma<1 (%G<1), the maximum gamma (Gmax) and the mean gamma (Gmean).

The Wilcoxon matched-pairs test was used to analyze the difference between two plans. All tests were bilateral with a significant threshold set at $p<0.05$ and were made using the SPSS V19.0 software.

Results

The gamma passing rates (%G<1) and the values for the maximum gamma (Gmax) and for the average gamma (Gmean) are presented in Table 2 for all three detectors.

EPID®

A total of 45 beams were verified for each plan. Ten of these beams were excluded from analysis, as they were posterior oblique and passed through the couch. In Table 2 are presented the EPID results for the three plans. For %G<1, average differences (absolute values) of 0.1% (range 0-1.1%) and 0.2% (range 0-0.9%) were noted for the 35 beams when G0 is compare with G90 ($p=0.13$) and with GFbyF ($p=0.0002$), respectively (Figure 2). For Gmax, average differences (absolute values) of 0.1 (range 0-0.4) and 0.1 (range 0-0.6) were noted for the 35 beams when G0 is compare with G90 ($p=0.13$) and with GFbyF ($p=0.0002$), respectively. For Gmean, no differences were found between the three plans.

Delta^{4}®

A total of 35 beams were evaluated for each plan (as the posterior oblique fields were excluded) (Table2). The Delta^4 results for the three plans are illustrated in Figure 3 for the global gamma evaluation (Figure 3,a) and for the local gamma evaluation (Figure 3,b).

GGE

For %G<1, average differences (absolute values) of 0.7% (range 0-4.3%) and 0.8% (range 0-2.7%) were noted for the 35 beams when G0 is compare with G90 ($p=0.0007$) and with GFbyF ($p<0.0001$), respectively. For Gmax, average differences (absolute values) of 0.2 (range 0-0.9) and 0.4 (range 0-1.5) were noted for the 35 beams when G0 is compare with G90 ($p<0.0001$) and with GFbyF ($p<0.0001$), respectively. For Gmean, the average differences were 0.1 (range 0-0.2) for G0 vs G90 ($p<0.0001$) and 0.1 (range 0-0.1) for G0 vs GFbyF ($p<0.0001$).

LGE

For %G<1, average differences (absolute values) of 3.1% (range 0.8-9%) and 2.2% (range 0-6.2%) were noted for the 35 beams when G0 is compare with G90 ($p<0.0001$) and with GFbyF ($p=0.0001$), respectively. For Gmax, average differences (absolute values) of 0.3 (range 0-1) and 0.5 (range 0-1.4) were noted for the 35 beams when G0 is compare with G90 ($p=0.0003$) and with GFbyF ($p=0.0007$), respectively. For Gmean, the average differences were 0.1 (range 0-0.2) for G0 vs G90 ($p<0.0001$) and 0.1 (range 0-0.2) for G0 vs GFbyF ($p<0.0001$).

ArcCheck®

A total of 20 beams were evaluated for each plan (several files were lost and the posterior oblique fields were not comprise) (Table2). The ArcCheck results for the three plans are illustrated in Figure 4 for the global gamma evaluation (Figure 4,a) and for the local gamma evaluation (Figure 4,b).

GGE

For %G<1, average differences (absolute values) of 4.4% (range 0.2-15.5%) and 3.4% (range 0-8.3%) were noted for the 20 beams when G0 is compare with G90 ($p=0.23$) and with GFbyF ($p=0.12$), respectively. For Gmax, average differences (absolute values) of 0.9 (range 0.1-3.3) and 0.5 (range 0.1-1.7) were noted for the 20 beams when G0 is compare with G90 ($p=0.4$) and with GFbyF ($p=0.11$), respectively. For Gmean, the average differences were 0.1 (range 0-0.3) for G0 vs G90 ($p=0.13$) and 0.05 (range 0-0.2) for G0 vs GFbyF ($p=0.81$).

LGE

For %G<1, average differences (absolute values) of 4.7% (range 0.6-9.6%) and 5% (range 0-13%) were noted for the 20 beams when G0 is compare with G90 ($p=0.54$) and with GFbyF ($p=0.005$), respectively. For Gmax, average differences (absolute values) of 1.1 (range 0.1-3.6) and 1.1 (range 0.1-3.7) were noted for the 20 beams when G0 is compare with G90 ($p=0.33$) and with GFbyF ($p=0.02$), respectively. For Gmean, the average differences were 0.1 (range 0-0.2) for G0 vs G90 ($p=0.49$) and 0.1 (range 0-0.3) for G0 vs GFbyF ($p=0.03$).

For ArcCheck, the observed differences (per field) between 2 plans seemed higher than for the other detector, but didn't reach the significant threshold, probably because of the smaller number of data available.

Discussion

In 2007, Nelms and Simon conducted a survey on planar IMRT QA analysis using an electronic 2D diode array device [32]. Survey results showed that a significant percentage of institutions (32.8%) used the single-gantry method for IMRT QA instead of field-by-field analysis [32].

Bedford *et al.* performed several tests for Delta^4 performance and the authors reported the accurate behavior of the system. They showed that the angular response was uniform over the complete range of gantry angles, but the couch attenuation was found to be an issue for IMRT and VMAT plans [16].

The intent of the present study was not to compare three QA devices, but to assess the importance of verifying an IMRT plan with an independent-unit from the accelerator and especially in the treatment configuration.

Recently, Monti *et al.* investigated the pre-treatment patient-specific per-field QA performed with the EPID at the gantry angle of 0° and at the treatment angles [8]. They found that the gamma index was dependent on gantry angles but the difference between fields measured at 0° and no-0° was small, with a mean value of -0.3%. In the present study, we found a similar result for %G<1 of EPID with a small average difference (in absolute value) of 0.2% (range 0-0.9%) (Figure 2). To our knowledge, this issue wasn't evaluated and quantified so far with cylindrical diode arrays, independent-units from the accelerator. In the current work, higher values were observed for GGE with a maximum difference between G0 and GFbyF plans in terms of %G<1 up to 2.7% and 8.3% for Delta^4 and ArcCheck, respectively. Per-field differences between G0 and GFbyF were seen as well for Gmax with maximum differences up to 1.5 and 1.7 for Delta^4 and ArcCheck, respectively.

These prostate IMRT-SIB plans might be considered of high difficulty with complex dose distributions because of the simultaneous integrated boost into the tumor (relatively small size). This could explain the low gamma evaluation values. Moreover, an IMRT plan does not involve IMRT QA to pass a particular acceptance test, but to be evaluated in the real treatment condition as the patient would be treated in (collimator, gantry and table angles, as well as couch attenuation).

In our department, we recently acquired the Delta^4 system for machine QA and treatment verification for IMRT and RapidArc plans. Furthermore, we continue to evaluate the optimal utilization of the pass/fail criteria for the new 3D diode array.

Conclusion

Usually the IMRT plan verification is made using all beams with gantry at 0°. However, it is important to verify the irradiation plans in the exact situation as at the time of treatment. We have showed here that there are important differences in the evaluation of a stereotactic IMRT plan as it depends of the irradiation geometry. These differences could be explained by the impact of the MLC weight and the couch attenuation. Therefore, it can be recommended that the IMRT verification is made with a detector independent from the accelerator and in the exact configuration of the irradiation as at the time of the treatment.

Bibliography:

[1] Ezzell GA, Galvin JM, Low D, *et al.* Guidance document on delivery, treatment planning, and clinical implementation of IMRT: report of the IMRT subcommittee of the AAPM radiation therapy committee. *Med Phys* 2003;30(8):2089-2115.

[2] Alber M, Broggi S, De Wagter C, *et al.* ESTRO Booklet No. 9 Guidelines for the verification of IMRT. Edited by G. Mijnheer, 2008, ESTRO, Brussel.

[3] Intensity Modulated Radiation Therapy Collaborative Working Group, "Intensity-modulated radiotherapy: current status and issues of interest". *Int J Radiat Oncol Biol Phys* 2001;51(4):880-914.

[4] Benedict SH, Yenice KM, Followill D, *et al.* Stereotactic body radiation therapy: the report of AAPM Task Group 101. *Med Phys* 2010; 37: 4078-4101.

[5] Klein EE, Hanley J, Bayouth J, *et al.* AAPM Task Group 142 report: Quality assurance of medical accelerators. *Med Phys* 2009;36:4197–4212.

[6] LoSasso T. IMRT delivery performance with Varian multileaf collimator. *Int J Radiat Oncol Biol Phys* 2008;71:S85-S88.

[7] Sastre-Padro M, Welleweerd J, Malinen E, Eilertsen K, Olsen DR, Ven der Heide UA. Consequences of leaf calibration errors on IMRT delivery. Phys Med Biol 2007;52:1147-1156.

[8] Monti AF, Berlusconi Chiara, Gelosa S. Gantry angle dependence in IMRT pre-treatment patient-specific quality controls. *Phys Medica* 2013;29:204-207.

[9] Van Elmpt W, McDermott L, Nijsten S, Wendling M, Lambin P, Mijnheer B. A literature review of electronic portal imaging for radiotherapy dosimetry. *Radiother Oncol* 2008;88:289-309.

[10] Roxby K, Crosbie J. Pre-treatment verification of intensity modulated radiation therapy plans using a commercial electronic portal dosimetry system. *Australasian Phys Eng Sci Med* 2010;33:51-57.

[11] Van Zijtveld M, Dirkx MLP, de Boer HCJ, Heijmen BJM. Dosimetric pre-treatment verification of IMRT using an EPID; clinical experience. *Radiother Oncol* 2006;81(2):168-175.

[12] Van Esch A, Depuydt T, Huyskens DP. The use of an aSi-based EPID for routine absolute dosimetric pre-treatment verification of dynamic IMRT fields. *Radiother Oncol* 2004;71(2):223-234.

[13] Fredh A, Bengtsson Scherman J, Fog LS, *et al.* Patient QA systems for rotational radiation therapy: A comparative experimental study with intentional errors. *Med Phys* 2013;40:031716-1 – 031716-9.

[14] Nilsson G. Delta4 – a new IMRT QA device. *Med Phys* 2007;34:2432.

[15] Feygelman V, Forster K, Opp D, Nilsson G. Evaluation of a biplanar diode array dosimeter for quality assurance of step-and-shoot IMRT. *J Appl Clin Med Phys* 2009;10:64-78.

[16] Bedford JL, Lee YK, Wai P, South CP, Warrington AP. Evaluation of the Delta^4 phantom for IMRT and VMAT verification. *Phys Med Biol* 2009;54(9):N167-N176.

[17] Sadagopan R, Bencomo JA, Martin RL, *et al.* Characterization and clinical evaluation of a novel IMRT quality assurance system. *J Appl Clin Med Phys* 2009;10:104-119.

[18] Feygelman V, Zhang G, Stevens C, Nelms BE. Evaluation of a new VMAT QA device, or the "X" and "O" array geometries. *J Appl Clin Med Phys* 2011;12(2):146-168.

[19] Korreman S, *et al.* RapidArc verification measurements using three different dosimetric systems. *Int J Radiat Oncol Biol Phys* 2008;72(1):S645-S646.

[20] Korreman S, Medin J and Kjaer-Kristoffersen F. Dosimetric verification of RapidArc treatment delivery. *Acta Oncol* 2009;48:185-191.

[21] Geurts M, Gonzalez J, Serrano-Ojeda P. Longitudinal study using a diode phantom for helical tomotherapy IMRT QA. *Med Phys* 2009;36(11):4977-83.

[22] Létourneau D, Publicover J, Kozelka J, Moseley DJ, Jaffray DA. Novel dosimetric phantom for quality assurance of volumetric modulated arc therapy. *Med Phys* 2009;36:1813–1821.

[23] Yan G, Lu B, Kozelka J, Liu C and Li JG. Calibration of a novel four-dimensional diode array. *Med Phys* 2010;37:108-115.

[24] Kozelka J, Robinson J, Nelms B, *et al.* Optimizing the accuracy of a helical diode array dosimeter: a comprehensive calibration methodology coupled with a novel virtual inclinometer. *Med Phys* 2011;38(9):5021-5032.

[25] Petoukhova AL, van Egmond J, Eenink MGC, *et al.* The ArcCheck diode array for dosimetric verification of HybridArc. *Phys Med Biol* 2011;56:5411-5428.

[26] Li G, Zhang Y, Jiang X, *et al.* Evaluation of the ArcCHECK QA system for IMRT and VMAT verification. *Phys Medica* 2013;29(3):295-303.

[27] Fakir H, Gaede S, Mulligan M, Chen JZ. Development of a novel ArcCheck^{TM} insert for routine quality assurance of VMAT delivery including dose calculation with inhomogeneities. *Med Phys* 2012;39(7):4203-4208.

[28] Eenink MGC, van Egmond, Roijen EJA, de Goede A, Petoukhova AL and Rietveld P. Evaluation of a helical diode array detector for IMRT quality assurance. *Radiother Oncol* 2010;95(1):S456.

[29] Aluwini S, van Rooij P, Hoogeman M, *et al.* Stereotactic body radiotherapy with a focal boost to the MRI-visible tumor as monotherapy for low- and intermediate-risk prostate cancer: early results. *Radiat Oncol* 2013; 8:84.

[30] Low DA, Harms WB, Mutic S, Purdy JA. A technique for the quantitative evaluation of dose distributions. *Med Phys* 1998;25:656-661.

[31] Stock M, Kroupa B and Georg D. Interpretation and evaluation of the gamma index and the gamma index angle for the verification of IMRT hybrid plans. *Phys Med Biol* 2005;50:399-411.

[32] Nelms BE, Simon JA. A survey on planar IMRT QA analysis. *J Appl Clin Med Phys* 2007;8(3):2448.

Table 1. Characteristics of the three IMRT QA devices used in the present study.

	EPID	Delta4	ArcCheck
Phantom			
Material	Exterior plastic housing	PMMA (density of 1.19g/cm^3;relative electron density of 1.147g/cm^3, 217HU)	PMMA
Shape	Plane	Cylindrical	Cylindrical
Dose distribution	2D	3D	3D
Array geometry	Flat-panel	2 perpendicular planes (crossed-planes)	Helical geometry (HeliGrid®) with 1 cm offset
Dimensions		The cylinder: 22 cm (diameter) x 40 cm (length) Total length: 72 cm	27 cm x 43 cm
Detection area per plane	40 x 30 cm^2 (1024x768 pixels)	20 x 20 cm^2	21 cm (array diameter and length)
Diodes			
Total number		1069	1386
Type	Amorphous-silicon	p-type silicon (p-Si)	n-type (SunPoint®) (silicon-based pn junction diode)
Active detector volume	For aS1000 IAS 3	0.04 mm^3	0.019 mm^3
Active detector area	Pixel size: 0.39 mm	0.78 mm^2	0.64 mm^2 (0.8mm x 0.8mm)
Active thickness		1 mm (in diameter) and 0.05 mm (thick)	0.03 mm^2
Distance between diodes		Central area (6x6cm): 5 mm Outer area (20x20cm): 10 mm	10 mm (1 cm pitch)
Sensitivity (nC/Gy)		5	32
Sensitivity decrease		0.8% per kGy (6MV beam)	0.5% per kGy (6MV beam) 1.5% per kGy (10MeV beam)
Measurement	At the detection plane	Measurement in the target	Measures the entrance and exit dose
Build up (water equivalent)	Copper build-up plate of 1 mm thickness	1.2 cm to 13.2 cm for nearest detector board	2.9 cm physical detector depth
Weight		27 Kg	16 Kg
Other	Mounted on a robotic-arm	Transfer support that holds the phantom Available 6D HexaMotion®; DVH Anatomy	Retractable homogeneous acrylic insert ; DVH

PMMA=polymethylmethacrylate (Acrylic); DVH = dose-volume histogram; 3D=three-dimensional

Table 2. Global and local evaluations for three devices and all plans, in terms of percentage of points having a gamma <1 (%G<1), maximum gamma (Gmax) and average gamma (Gmean). Results for the posterior-oblique fields were not included.

	Global Gamma Evaluation			Local Gamma Evaluation		
	%G<1	**Gmax**	**Gmean**	**%G<1**	**Gmax**	**Gmean**
EPID®						
G0						
Average±SD	99.4±0.3	2.2±0.6	0.3±0.04			
Median (range)	99.3 (98.6-99.9)	2.2 (1.2-3.5)	0.3 (0.2-0.3)			
G90						
Average±SD	99.3±0.3	2.3±0.7	0.3±0.04			
Median (range)	99.3 (98.4-99.9)	2.2 (1.3-3.7)	0.3 (0.2-0.3)			
GFbyF						
Average±SD	99.2±0.4	2.4±0.6	0.3±0.04			
Median (range)	99.2 (98.2-99.9)	2.3 (1.3-4.1)	0.3 (0.2-0.3)			
Delta$^{4®}$						
G0						
Average±SD	99.8±0.4	1±0.2	0.2±0.03	96.2±1.7	1.7±0.3	0.3±0.04
Median (range)	100 (98.5-100)	0.9 (0.6-1.6)	0.2 (0.2-0.3)	96.3 (92.5-98.7)	1.7 (1-2.3)	0.3 (0.2-0.4)
G90						
Average±SD	99.1±1.1	1.2±0.3	0.3±0.04	93.1±2.5	2±0.4	0.4±0.05
Median (range)	99.6 (95.3-100)	1.1 (0.8-1.9)	0.3 (0.2-0.4)	93.2 (85.8-97)	1.9 (1.3-3)	0.4 (0.3-0.5)
GFbyF						
Average±SD	98.9±1	1.3±0.4	0.3±0.05	94.7±2.5	2.1±0.5	0.4±0.06
Median (range)	98.9 (96.9-100)	1.3 (0.7-2.3)	0.3 (0.2-0.4)	94.8 (89.8-99.6)	1.9 (1-3.2)	0.4 (0.2-0.5)
ArcCheck®						
G0						
Average±SD	93.6±2.9	2.2±0.8	0.6±0.1	86.6±4.5	2.8±0.8	0.7±0.1
Median (range)	94.1 (87.3-98.3)	2 (1.2-3.9)	0.6 (0.5-0.8)	87.5 (78.1-93.2)	2.9 (1.5-5)	0.7 (0.5-0.8)
G90						
Average±SD	94.4±4.7	1.9±0.8	0.6±0.1	85.9±3.6	3.3±1.4	0.7±0.1
Median (range)	95.9 (80.3-100)	1.7 (1-4.6)	0.6 (0.5-0.8)	87.4 (80.3-90.7)	3 (1.7-5.9)	0.7 (0.6-0.8)
GFbyF						
Average±SD	92.1±3.5	1.9±0.5	0.6±0.1	83±5.2	3.7±1.2	0.7±0.1
Median (range)	92.6 (85.7-98.3)	1.8 (1.3-3.2)	0.6 (0.5-0.7)	83.8 (73.7-98.3)	3.5 (1.8-5.9)	0.7 (0.5-0.9)

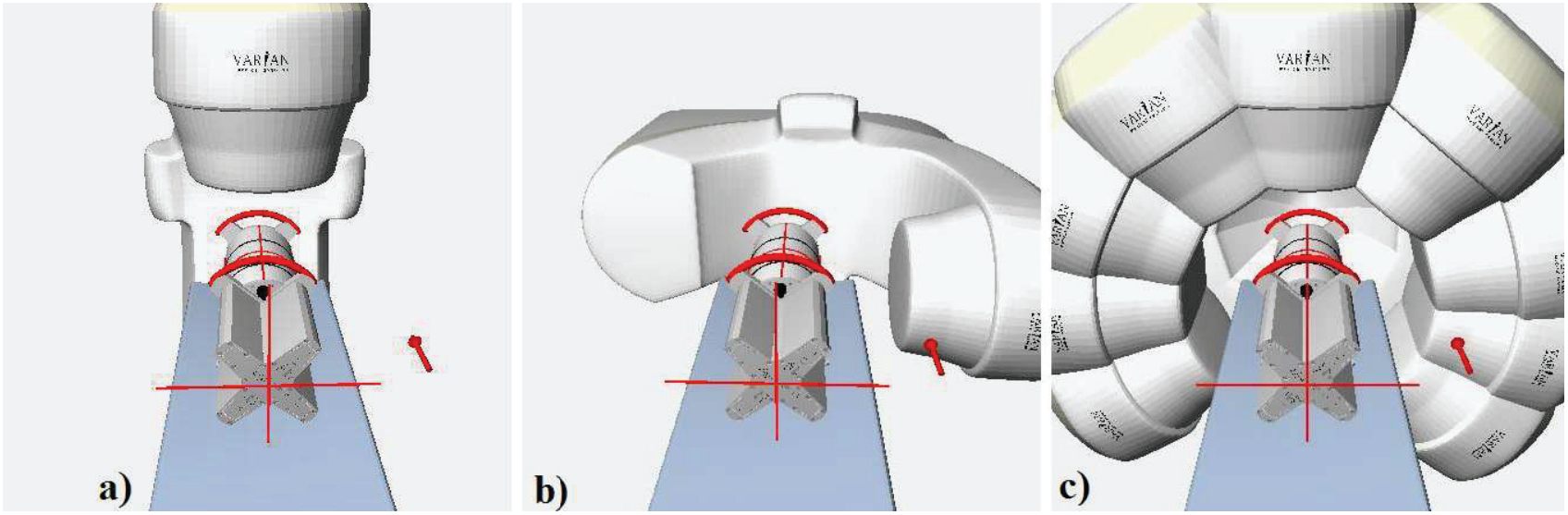

Figure 1. Three angle configurations for IMRT QA.

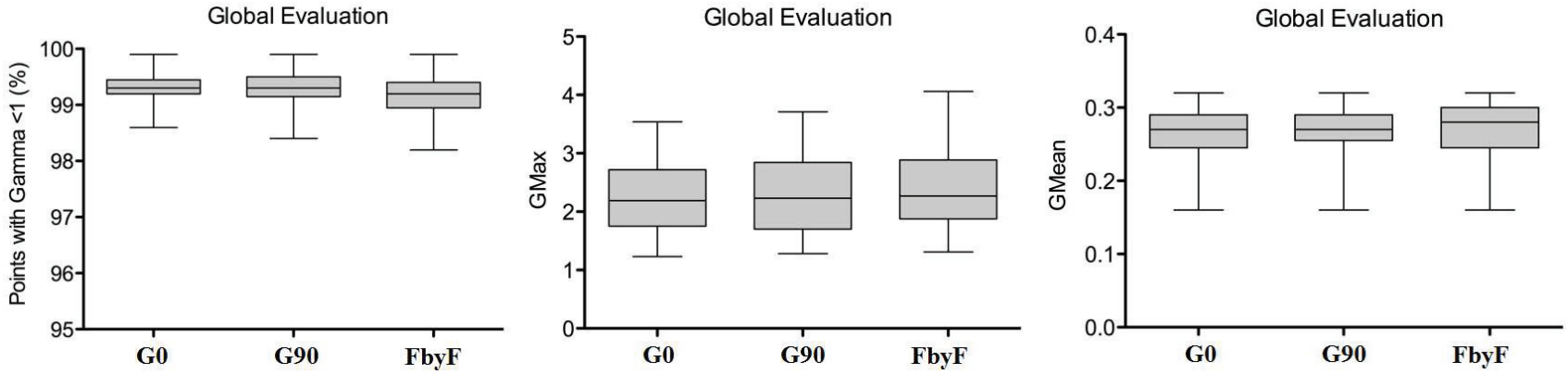

Figure 2. Results for the EPID.

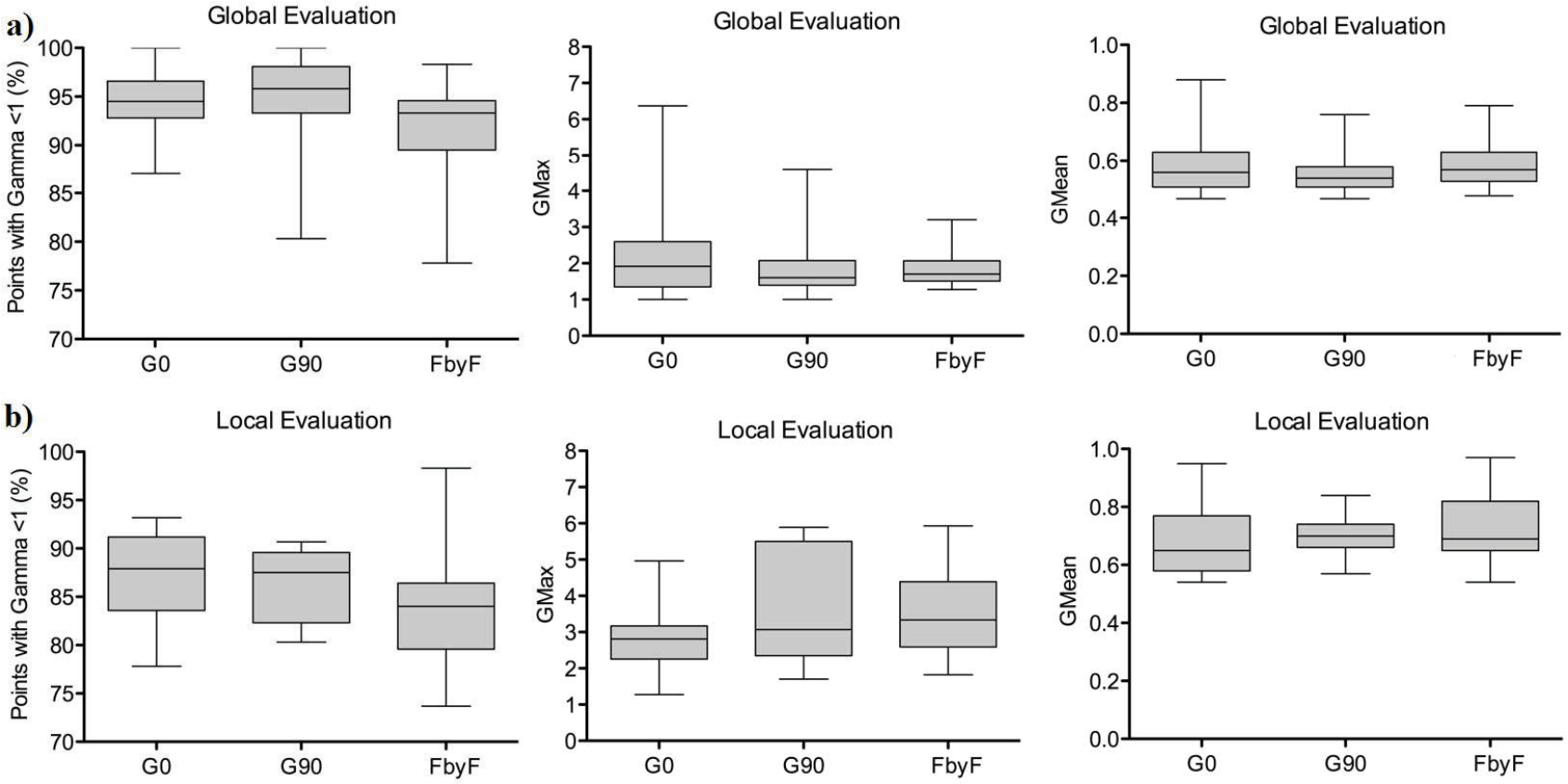

Figure 3. Results for the Delta^4 system.

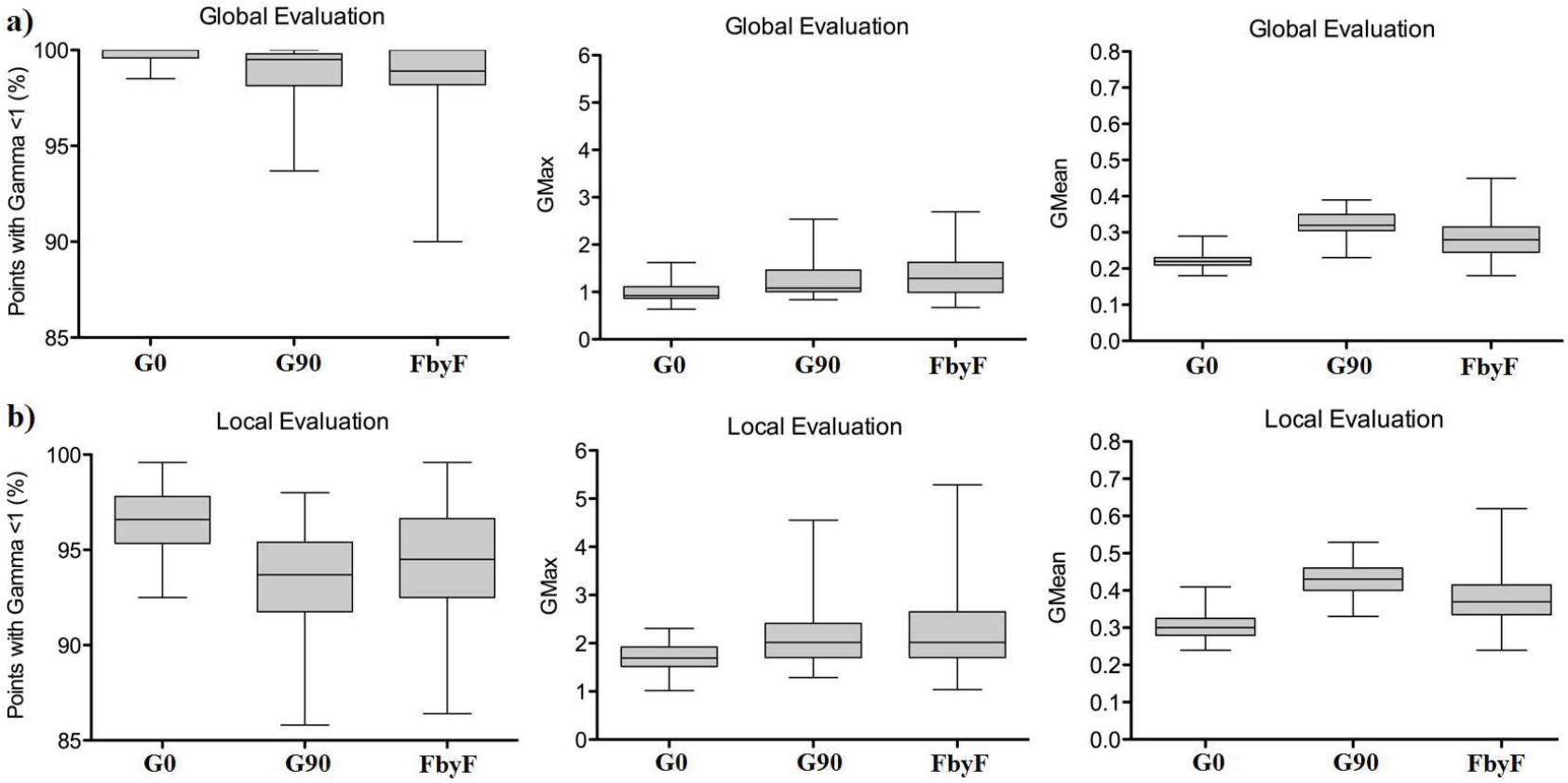

Figure 4. Results for the ArcCheck system.

4.6. Conclusion – section IV

The Delta$^{4®}$ system was found to be a sensitive 3D diode array and suitable for the IMRT QA.

An IMRT plan, with or without SBRT, should be verified using the geometry of the irradiation, including the beams that pass throughout the couch.

4.7. Bibliography – section IV

[1] Ezzell GA, Galvin JM, Low D, *et al.* Guidance document on delivery, treatment planning, and clinical implementation of IMRT: report of the IMRT subcommittee of the AAPM radiation therapy committee. *Med Phys* 2003;30(8):2089-2115.

[2] Alber M, Broggi S, De Wagter C, *et al.* ESTRO Booklet No. 9 Guidelines for the verification of IMRT. Edited by G. Mijnheer, 2008, ESTRO, Brussel.

[3] Intensity Modulated Radiation Therapy Collaborative Working Group, "Intensity-modulated radiotherapy: current status and issues of interest". *Int J Radiat Oncol Biol Phys* 2001;51(4):880-914.

[4] Essers M, de Langen M, Dirkx ML, Heijmen BJ. Commissioning of a commercially available system for intensity-modulated radiotherapy dose delivery with dynamic multileaf collimation. *Radiother Oncol* 2001;60:215-224.

[5] IAEA TRS 430. Commissioning and quality assurance of computerized planning systems for radiation treatment of cancer. Technical Reports Series (TRS) No. 430. Vienna, Austria: International Atomic Energy Agency; 2004.

[6] Klein EE, Hanley J, Bayouth J, *et al.* AAPM Task Group 142 report: Quality assurance of medical accelerators. *Med Phys* 2009;36:4197–4212.

[7] Benedict SH, Yenice KM, Followill D, *et al.* Stereotactic body radiation therapy: the report of AAPM Task Group 101. *Med Phys* 2010; 37: 4078-4101.

[8] Ranade MK, Li JG, Dubose RS, Kozelka J, Simon WE, Dempsey JF. A prototype quantitative film scanner for radiochromic film dosimetry. *Med Phys* 2008;35(2):473-479.

[9] Pallotta S, Marrazzo L and Bucciolini M. Design and implementation of a water phantom for IMRT, arc therapy, and tomotherapy dose distribution measurements. *Med Phys* 2007;34:3724-3731.

[10] Zeidan OA, Stephenson SAL, Meeks SL, *et al.* Characterization and use of EBT radiochromic film for IMRT dose verification. *Med Phys* 2006;33(11):4064-4072.

[11] Ling CC, Zhang P, Archambault Y, *et al.* Commissioning and quality assurance of RapidArc radiotherapy delivery system. *Int J Radiat Oncol Biol Phys* 2008;72:575-581.

[12] Pai S, Das IJ, Dempsey JF, *et al.* TG-69: radiographic film for megavoltage beam dosimetry. *Med Phys* 2007;34(6):2228-2258.

[13] Wilcox E, Daskalov G, Nedialkova L. Comparison of the epson expression 1680 flatbed and the vidar VXR-16 dosimetry PRO film scanners for use in IMRT dosimetry using gafchromic and radiographic film. *Med Phys* 2007;34(1):41-48.

[14] Van Elmpt W, McDermott L, Nijsten S, Wendling M, Lambin P, Mijnheer B. A literature review of electronic portal imaging for radiotherapy dosimetry. *Radiother Oncol* 2008;88:289-309.

[15] Roxby K, Crosbie J. Pre-treatment verification of intensity modulated radiation therapy plans using a commercial electronic portal dosimetry system. *Australasian Phys Eng Sci Med* 2010;33:51-57.

[16] Van Zijtveld M, Dirkx MLP, de Boer HCJ, Heijmen BJM. Dosimetric pre-treatment verification of IMRT using an EPID; clinical experience. *Radiother Oncol* 2006;81(2):168-175.

[17] Van Esch A, Depuydt T, Huyskens DP. The use of an aSi-based EPID for routine absolute dosimetric pre-treatment verification of dynamic IMRT fields. *Radiother Oncol* 2004;71(2):223-234.

[18] Vial P, Greer PB, Hunt P, Oliver L, Baldock C. The impact of MLC transmitted radiation on EPID dosimetry for dynamic MLC beams. *Med Phys* 2008;35(4):1267-1277.

[19] Basran PS, Woo MK. An analysis of tolerance levels in IMRT quality assurance procedures. *Med Phys* 2008;35(6):2300-2307.

[20] Essers M, Hoogervorst BR, van Herk M, Lanson H, Mijnheer BJ. Dosimetric Characteristics of a Liquid-Filled Electronic Portal Imaging Device. *Int J Radiat Oncol Biol Phys* 1995;33(5):1265 – 1272.

[21] Iori M, Cagni E, Paiusco M, Munro P and Nahum AE. Dosimetric verification of IMAT delivery with a conventional EPID system and a commercial portal dose image prediction tool. *Med Phys* 2010;37:377-390.

[22] Van Esch A, Bohsung J, Sorvari P, *et al.* Acceptance tests and quality control (QC) procedures for the clinical implementation of intensity modulated radiotherapy (IMRT) using inverse planning and the sliding window technique: experience from five radiotherapy departments. *Radiother Oncol* 2002;65:53-70.

[23] McDermott LN, Wendling M, van Asselen B, *et al.* Clinical experience with EPID dosimetry for prostate IMRT pre-treatment dose verification. *Med Phys* 2006;33(10):3921—3930.

[24] Chen J, Chuang CF, Morin O, Aubin M, Buliot J. Calibration of an amorphous-silicon flat panel portal imager for exit-beam dosimetry. *Med Phys* 2006;33(3):584-594.

[25] Han Z, Ng SK, Bhagwat MS, Lyatskaya Y and Zygmanski P. Evaluation of MatriXX for IMRT and VMAT dose verifications in peripheral dose regions. *Med Phys* 2010;37:3704-3714.

[26] Jursinic PA, Sharma R, Reuter J. MapCHECK used for rotational IMRT measurements: step-and-shoot, tomotherapy, RapidArc. *Med Phys* 2010;37(6):2837-2846.

[27] Jursinic PA, NelmsBE. A 2-D diode array and analysis software for verification of intensity modulated radiation therapy delivery. *Med Phys* 2003;30(5):870-879.

[28] Letourneau D, Gulam M, Yan D, Oldham M, Wong JW. Evaluation of a 2D diode array for IMRT quality assurance. *Radiother Oncol* 2004;70(2):199-206.

[29] Li JG, Yan G, Liu C. Comparison of two commercial detector arrays for IMRT quality assurance. *J Appl Clin Med Phys* 2009;10(2):62-74.

[30] Amerio S, Boriano A, Bourhaleb F, *et al.* Dosimetric characterization of a large area pixel-segmented ionization chamber. *Med Phys* 2004;31(2):414-420.

[31] Stasi M, Giordanengo S, Cirio R, *et al.* D-IMRT verification with a 2D pixel ionization chamber: dosimetric and clinical results in head and neck cancer. *Phys Med Biol* 2005;50(19):4681-4694.

[32] Poppe B, Blechschmidt A, Djouguela A, *et al.* Two-dimensional ionization chamber arrays for IMRT plan verification. *Med Phys* 2006;33(4):1005-1015.

[33] Spezi E, Angelini AL, Romani F, Ferri A. Characterization of a 2D ion chamber array for the verification of radiotherapy treatments. *Phys Med Biol* 2005;50(14):3361-3373.

[34] Fredh A, BengtssonScherman J, Fog LS, *et al.* Patient QA systems for rotational radiation therapy: A comparative experimental study with intentional errors. *Med Phys* 2013;40:031716-1 – 031716-9.

[35] Nilsson G. Delta4 – a new IMRT QA device. *Med Phys* 2007;34:2432.

[36] Feygelman V, Forster K, Opp D, Nilsson G. Evaluation of a biplanar diode array dosimeter for quality assurance of step-and-shoot IMRT. *J Appl Clin Med Phys* 2009;10:64-78.

[37] Bedford JL, Lee YK, Wai P, South CP, Warrington AP. Evaluation of the Delta^4 phantom for IMRT and VMAT verification. *Phys Med Biol* 2009;54(9):N167-N176.

[38] Sadagopan R, Bencomo JA, Martin RL, *et al.* Characterization and clinical evaluation of a novel IMRT quality assurance system. *J Appl Clin Med Phys* 2009;10:104-119.

[39] Feygelman V, Zhang G, Stevens C, Nelms BE. Evaluation of a new VMAT QA device, or the "X" and "O" array geometries. *J Appl Clin Med Phys* 2011;12(2):146-168.

[40] Korreman S, *et al.* RapidArc verification measurements using three different dosimetric systems. *Int J Radiat Oncol Biol Phys* 2008;72(1):S645-S646.

[41] Korreman S, Medin J and Kjaer-Kristoffersen F. Dosimetric verification of RapidArc treatment delivery. *Acta Oncol* 2009;48:185-191.

[42] Geurts M, Gonzalez J, Serrano-Ojeda P. Longitudinal study using a diode phantom for helical tomotherapy IMRT QA. *Med Phys* 2009;36(11):4977-83.

[43] Létourneau D, Publicover J, Kozelka J, Moseley DJ, Jaffray DA. Novel dosimetric phantom for quality assurance of volumetric modulated arc therapy. *Med Phys* 2009;36:1813–1821.

[44] Yan G, Lu B, Kozelka J, Liu C, Li JG. Calibration of a novel four-dimensional diode array. *Med Phys* 2010;37(1):108-115.

[45] Kozelka J, Robinson J, Nelms B, *et al.* Optimizing the accuracy of a helical diode array dosimeter: a comprehensive calibration methodology coupled with a novel virtual inclinometer. *Med Phys* 2011;38(9):5021-5032.

[46] Petoukhova AL, van Egmond J, Eenink MGC, *et al.* The ArcCheck diode array for dosimetric verification of HybridArc. *Phys Med Biol* 2011;56:5411-5428.

[47] Li G, Zhang Y, Jiang X, *et al.* Evaluation of the ArcCheck QA system for IMRT and VMAT verification. *Phys Medica* 2013;29(3):295-303.

[48] Olofsson N, *et al.* Evaluation of IMRT beam complexity metrics to be used in the IMRT QA process. 2012 Master of science thesis. http://www.gu.se/digitalAssets/1360/1360092_niklas-olofsson-rapport.pdf

[49] Fakir H, Gaede S, Mulligan M, Chen JZ. Development of a novel ArcCheck^{TM} insert for routine quality assurance of VMAT delivery including dose calculation with inhomogeneities. *Med Phys* 2012;39(7):4203-4208.

[50] Eenink MGC, van Egmond, Roijen EJA, de Goede A, Petoukhova AL and Rietveld P. Evaluation of a helical diode array detector for IMRT quality assurance. *Radiother Oncol* 2010;95(1):S456.

[51] Van Esch A, Clermont C, Devillers M and Iori M. On-line quality assurance of rotational radiotherapy treatment delivery by means of a 2D ion chamber array and the Octavius phantom. *Med Phys* 2007;34(10):3825-3837.

[52] Crescenti RA, Scheib SG, Schneider U, Gianolini S. Introducing gel dosimetry in a clinical environment: customization of polymer gel composition and magnetic resonance imaging parameters used for 3D dose verifications in radiosurgery and intensity modulated radiotherapy. *Med Phys* 2007;34(4):1286-1297.

[53] Gustavsson H, Karlsson A, Back SA. MAGIC-type polymer gel for three-dimensional dosimetry: intensity-modulated radiation therapy verification. *Med Phys* 2003;30(6):1264-1271.

[54] Low DA, Dempsey JF, Venkatesan R, *et al.* Evaluation of polymer gels and MRI as a 3-D dosimeter for intensity-modulated radiation therapy. *Med Phys* 1999;26(8):1542-1551.

[55] Islam KT, Dempsey JF, Ranade MK, Maryanski ML and Low DA. Initial evaluation of commercial optical CT-based 3D gel dosimeter. *Med Phys* 2003;30(8):2159-2168.

[56] Babic S, Battista J, Jordan K. Three-Dimensional dose verification for intensity-modulated radiation therapy in the radiological physics centre head-and-neck phantom using optical computed tomography scans of ferrous xylenol-orange gel dosimeters. *Int J Radiat Oncol Biol Phys* 2008;70(4):1281-1291.

[57] www.scandidos.com

[58] www.sunnuclear.com

[59] Low DA, Harms WB, Mutic S, Purdy JA. A technique for the quantitative evaluation of dose distributions. *Med Phys* 1998;25:656-661.

[60] Low DA, Dempsey JF. Evaluation of the gamma dose distribution comparison method. *Med Phys* 2003;30:2455-2464.

[61] Van Dyk J, Barnett RB, Cygler JE, Shragge PC. Commissioning and quality assurance of treatment planning computers. *Int J Radiat Oncol Biol Phys* 1993;26:261-273.

[62] Nelms BE, Simon JA. A survey on planar IMRT QA analysis. *J Appl Clin Med Phys* 2007;8(3):2448.

V. GENERAL CONCLUSION

The present work evaluated a stereotactic body radiation therapy approach for the prostate cancer. The results obtained in this study allow to conclude the following:

- a prostate SBRT is technically feasible using a standard accelerator and an intensity-modulated radiation therapy;
- careful attention should be paid for the implementation of the SBRT starting with the target's delineation; If the radiation physician is not an expert in prostate cancer, a radiologist contour is required to improve the delineation of the target;
- respiratory-induced prostate motion shouldn't be a concern, but rectal and bladder filling or patient's position during treatment (prone versus supine) may have an impact on prostate random motion;
- intraprostatic fiducials are the gold standard for prostate repositioning and are mandatory for target repositioning during SBRT. Herein, the stability of these markers was demonstrated, but an insignificant shrinkage of the prostate may arise if hormone-therapy is administrated before or during radiotherapy. This shrinkage shouldn't affect the accuracy of target repositioning.
- Small margins for planning target volume definition are possible up to 3 mm if the patient and the target are localized and monitored with real-time tracking.
- The combination of a 9-beam conformation with 16 MV beam energy showed an excellent PTV coverage without increasing the low- and high-dose gradients to the organs at risk.
- Two approaches for sparing the rectal-wall from high doses have been evaluated. The first approach is a simultaneous-integrated boost into the dominant intraprostatic lesion. The results showed a decrease of the dose to both, rectal- and bladder-wall, when compared to a homogeneous higher dose. The second approach was an injection of a spacer gel between the rectum and the prostate. The high doses to the anterior rectal-wall were significantly reduced and allowed an increase of the prescription dose from 32.5 Gy to 42.5 Gy without increasing the dose to the rectum.
- A stereotactic irradiation with intensity-modulated radiotherapy requires accurate quality assurance before starting patient's treatment. The novel three-dimensional diode arrays

seem additionally to be suitable for the evaluation of the treatment plan. However, pre-treatment patient-specific quality controls should be done at treatments angles and using the real irradiation geometry of the plan, as at the time of the treatment (including gantry, collimator and table rotations).

Appendix 1

Hypofractionated Radiotherapy for Prostate Cancer – Review of clinical trials

Lukka et al., 2005 - Canada

Patients: Men with early-stage T1-T2 adenocarcinoma of the prostate were randomly assigned to receive prostate irradiation in two arms: 66 Gy in 33 fractions over 45 days (long arm- 470 patients) or 52.5 Gy in 20 fractions over 28 days (short arm- 466 patients), with daily fractions. The patients were treated in supine position with a full-bladder before each treatment.

Dosimetric parameters: The irradiation was done with a ≥ 10 MV linear accelerator, using a four-field technique or using three fields for patients with prosthetic hip. The PTV was the prostate alone with a 1.5 cm margin on all sited, and sometimes reduced to 1 cm posteriorly. The dose was prescribed at the isocenter and the dose within the target volume was maximum 5% from the isocenter dose.

Repositioning: Patient position verification was done with port films of the anterior and lateral pelvic views on the first day of treatment. Furthermore, the first 30 patients from each center underwent real-time review.

Results: The median follow-up time for all patients was 5.7 years [4.5 – 8.3 years]. 236 patients in the long arm and 263 patients in the short arm experienced biochemical or clinical failure (BCF). At 5-years, the Kaplan-Meier rates of BCF in the long and short arms were 52.95% and 59.95%, respectively, with a difference of – 7 % (90% CI, -12.58% to -1.42%). PSA failure was experienced for long and short arms by respectively 50 % and 55.8 % of patients (using Vancouver criteria) and respectively 37.7 % and 42.3 % of patients (using Houston criteria). Overall survival at 5-years was 85.2 % in the long arm and 87.6 % in the short arm.

Acute Toxicity: Grade 3 or 4 GI or GU were experienced by 7 % and 11.4 % in the long and short arm, respectively (risk difference = - 4.4 %, 95% CI).

Late toxicity: 3.2 % of patients experienced severe toxicities in both arms, where GU represented two thirds of these events.

Yeoh et al., 2003 – Australia

Patients: 120 patients with localized early-stage prostate cancer (T1-T2N0M0) were randomly assigned to one of the two dose regimens: 64 Gy in 32 fractions within 6.5 weeks (61 patients) or 55 Gy in 20 fractions within 4 weeks (59 patients). Based on a $\alpha/\beta = 3$ Gy for late radiation effects, the study suggested that the two regimens are equitoxic.

Dosimetric parameters: The irradiation technique used four-field (AP and laterals) or three-field (anterior and two posterior oblique/lateral) with the dose prescribed to the isocenter and delivered using external beam 6 – 23 MV photons. The PTV was the prostate only (and maximum the base of the seminal vesicles, if necessary), with a 1.5 cm 95% isodose margin.

Repositioning: not described; the localization of the prostate was based on two-dimensional CT data, without rectal shielding.

Results: The median duration for the nadir PSA was 16.8 months [0.8 – 28.3], after the end of the treatment. The actuarial 4-year biochemical relapse-free survival rate was 85.8% for all patients and 86.2% and 85.5% in the hypofractionated and conventional arms, respectively. No difference in clinically toxicity or treatment efficacy between the two arms.

Toxicity: The median duration of follow-up was 43.5 months [23 - 62] and no difference in clinically significant toxicity was noticed. For the analysis of the GI toxicity, no differences were present between the two regimens, other than a mild rectal bleeding, which occurred more frequently at 2 years (42% vs 27%) in patients who received hypofractionated RT. No differences were found between two arms in any of the urinary symptoms that increased in 1 month after treatment.

Pollack et al., 2006 – Philadelphia

Patients: Randomized patients with intermediate- (IR) to high-risk (HR) prostate cancer (T1-T3 adenocarcinoma) were treated with doses of 76 Gy in 38 fractions at 2 Gy per fraction (Arm I) or 70.2 Gy in 26 fractions at 2.7 Gy per fraction (Arm II). Assuming and $\alpha/\beta = 1.5$ Gy, Arm II was considered to be equivalent to 84.4 Gy in 2 Gy per fraction. Patients were simulated in the supine position in an α-cradle with a Plexiglas holder to immobilize the feet. Before simulation, the patients were asked to empty the rectum and to have a moderately full bladder.

Dosimetric parameters: For the Arm I and Arm II the prescribed dose was delivered with respectively step-and-shoot conventional fractionation intensity-modulated radiation

therapy (CIMRT) and hypofractionation intensity-modulated radiation therapy (HIMRT). Fused images between the CT scan and MRI exam were used to contour the prostate, seminal vesicles, rectum, bladder, etc. PTV was chosen function of the patients' stage, but for the CIMRT it was 8 mm in all dimensions except posteriorly (the prostate-rectal interface), in which the margin was 5 mm. For HIMRT the margins were smaller, the desired PTV was 7 mm in all dimensions, except posteriorly, in which the margin was 3 mm.

Repositioning: Daily B-mode acquisition and targeting ultrasound alignment

Results: Up to 4 months of androgen deprivation was permitted, and long-term androgen deprivation was used for high-risk patients. There were no significant differences in the makeup of the patients in the two treatment arms. There were statistically higher volume percentages of the rectum treated to more than both the high (V50 Gy) and low (V31 Gy) dose cutpoints in Arm II, as compared with Arm I (V65 Gy and V40 Gy). A similar pattern was observed for the bladder. The only covariate shown to be related to increased acute rectal reactions was the composite DVH V65 Gy/V50 Gy parameter. With a median follow-up of 39 months, 5-year BF (nadir + 2) was 21% (95% CI, 12-37%) for the standard arm and 17% (95% CI, 10-28%) for the hypofractionated arm.

GI Toxicity: There were no statistically significant differences in acute GI toxicity during treatment. However, there were slightly more men with Grade 2 reactions in Arm II (9 vs. 4 in Arm I). At 3-months follow-up visit, about 85% experienced no GI side effects with < 5% experiencing Grade 2. Changes in GI morbidity demonstrate that at Weeks 2, 3 and 4 of treatment, there was a slight, but significant increase in mean maximum toxicity seen in the HIMRT arm.

GU Toxicity: The majority of patients in both Arms experienced Grade 1-2 GU side effects during treatment. At the first 3-months follow-up visit, the majority experienced no GU side effects with < 10% experiencing Grade 2 toxicity. There was no statistical difference in acute toxicity at the 3-months follow-up visit. A smaller bladder volume at planning was independently associated with an increase in acute effects.

Coote et al., 2009 – Manchester

Patients: This Phase I/II study included 60 patients that all received neoadjuvant hormone therapy. The first 30 patients received 57 Gy in 19 fractions (equivalent to 73 Gy in 2 Gy per fraction assuming an $\alpha/\beta=1.5$) and the second group of 30 patients received 60 Gy in 20 fractions (equivalent to 77 Gy). The patients were simulated supine with CT slices of 5-mm increments, with an empty bladder and without formal immobilization.

Dosimetric parameters: The PTV1 were the prostate and the seminal vesicles, with a margin of 1 cm except the prostate-rectal interface where the margin was 0.7 cm. The PTV2 was the prostate alone with no margin. The treatment planning was made using IMRT technique, using 5 isocentric fields (posterior, right- and left-lateral oblique fields and right- and left-anterior oblique fields – 180°, 255°, 325°, 35° and 105°). IMRT was delivered using an 8-MV step-and-shoot multileaf collimator once daily, 5 times per week. The plans provided excellent PTV coverage with on average 98.4% (SD=0.7) of the volume receiving 95% of the prescribed dose.

Repositioning: Portal images were taken of the setup fields daily during Week 1 and weekly after. A shrinking action level protocol was used to ensure a treatment accuracy of 3 mm.

Results: At 24-month follow-up, 44/60 patients were alive and well with no biochemical evidence of disease recurrence. 12 patients had developed disease recurrence by the Phoenix criteria.

Acute Toxicity: No patient experienced any RTOG Grade 3 or 4 urinary or bowel toxicity and only 10% and 15% respectively, reported Grade 2 GU and GI toxicity.

Late Toxicity: At 2-years, GU late effects (RTOG criteria) were only 4.25% of patients experiencing Grade 2 bladder toxicity. There was one case of Grade 3 urinary toxicity. At 2-years, there was 4% Grade 2 bowel toxicity. There was no Grade 3 or 4 bowel toxicity.

Kupelian et al., 2007 – Cleveland

Patients: 770 patients were included in the study, with 34% considered to be low risk, 28% intermediate risk and 38% high risk. 459 patients received neoadjuvant or adjuvant androgen deprivation. Patients were set-up with minimal immobilization in the supine position.

Dosimetric parameters: IMRT was used to deliver a nominal dose of 70 Gy in 28 fractions of 2.5 Gy, within 5.5 weeks. The treatment was delivered with a 10-MV photon beam using dynamic multileaf collimators and five-field beam arrangement (2 lateral beams, 2 anterior oblique and one anterior beam).

Repositioning: Daily localization for treatment was performed using the BAT transabdominal ultrasound system.

Results: The 5-year biochemical relapse-free survival (bRFS) was adequate for all patients with no significant difference between the ASTRO (A-bRFS) and nadir+2 (N-bRFS) definitions. The overall 5-year A-bRFS and N-bRFS rates were 82% and 83%. For patients

with low-, intermediate- and high-risk disease, the 5-year rates were respectively 95%, 85% and 68% (for A-bRFS) and respectively 94%, 83% and 72% (for N-bRFS).

Acute GI and GU Toxicity: The RTOG acute rectal toxicity scores were 0 in 51%, 1 in 40% and 2 in 9%. The RTOG acute urinary toxicity scores were 0 in 33%, 1 in 48%, 2 in 18% and 3 in 1% of patients.

Late rectal toxicity: The RTOG late rectal toxicity scores were 0 in 89.6%, 1 in 5.9%, 2 in 3.1%, 3 in 1.3% and 4 in 0.1%. The actuarial late RTOG Grade 2 or worse rectal toxicity rate at 5-years was 6%.

Late urinary toxicity: The RTOG late urinary toxicity scores were 0 in 90.5%, 1 in 4.3%, 2 in 5.1% and 3 in 0.1%. The actuarial late Grade 2 or worse RTOG urinary toxicity rate at 5-years was 7%.

Livsey et al., 2003 – Manchester

Patients: Outcomes of 705 men who had biopsy proven, clinically localized prostate cancer (T1-T4 N0M0) and a pretreatment PSA value were analyzed. Patients were CT simulated supine, without formal immobilization and were asked to empty their bladder and bowel immediately before CT simulation and treatment.

Dosimetric parameters: All patients received conformal radiotherapy to the prostate with a standard 4-field conformal technique (opposed anterior and posterior and opposed lateral portals) using 8-20 MV photons. The PTV was the CTV (prostate plus all/base of the seminal vesicles dependent on risk criteria) with 1-cm margin and received the prescribed dose of 50 Gy in 16 fractions, during 22 days. The multileaf collimator leaves were fitted to the PTV with a penumbra margin of 0.7 cm to ensure the coverage of the PTV by the 95% isodose line.

Repositioning: no specification;

Results: Overall survival at 5-years was 83.1%, with a disease-specific survival of 91%. The biochemical-free survival (bNED) was significantly associated with treatment PSA, stage and Gleason score. For patients grouped into good, intermediate and poor groups, their disease-specific survival at 5-years was, respectively, 96%, 91% and 86%. The actuarial bNED rates for these groups with 5-year bNED were of, respectively, 82%, 56% and 39%.

Toxicity: Using the RTOG scoring system for late toxicity for a subgroup of 101 patients, the late bladder morbidity was Grade 0/1, 90%; Grade 2, 9%; and Grade 3, 1%; Bowel toxicity was recorded as Grade 0, 65%; Grade 1, 30%; and Grade 2, 5%. There was no ≥ Grade 3 toxicity.

Appendix 2

Stereotactic Body Radiation Therapy for Prostate Cancer - Review of Clinical Trials

Madsen et al., 2007 – Seattle

Patients: The Phase I/II trial included 40 patients treated with stereotactic hypofractionated accurate radiotherapy of the prostate (SHARP), with 33.5 Gy in 5 fractions of 6.7 Gy daily (equivalent to 78 Gy for an $\alpha/\beta=1.5$, with acute effects equivalent of 46.6 Gy for an $\alpha/\beta=10$; for late rectal effects $\alpha/\beta=3$ was taken into consideration). The patients were in a flex-prone position on a specially designed cushion and were placed on a diet to minimize gas and took daily simethicone to reduce rectal dilatation and movement during treatment. CT scan and MRI image fusion was done for treatment planning purpose.

Dosimetric parameters: Six stationary noncoplanar fields were designed with custom blocking including a 4-5 mm margin from the prostate to the block edge. The dose was prescribed to the isocenter with 100% of the prostate GTV to be covered by the 90% isodose line. No DVH constraints were placed on the rectum, as they didn't know what to expect with regard to toxicity. The dose was kept as low as feasible.

Repositioning: Daily repositioning was made using orthogonal images based on three fiducial markers implanted in the apex, base and mid-gland of the prostate.

Results: Using the ASTRO definition, the 48-month freedom from relapse rate was 70% and with nadir + 2 ng/mL definition it was 90%.

Acute Toxicity: Grade 1 or 2 acute RTOG toxicity at 1 month for GU and GI was 49% and 39%, respectively. Only one Grade 3 acute GU toxicity was reported.

Late Toxicity: Late Grade 1 or 2 toxicity reported at any time after 30 days follow-up for GU and GI was, respectively 45% and 37.5%. No late Grade 3 or higher toxicity was reported. The 48-month actuarial rate of GU Grade 1 toxicity was 25.8% and Grade 2 toxicity was 16.1%. For late Grade 1 and 2 GI toxicities, the 48-month actuarial rates are 34.4% and 9.4%, respectively.

King et al., 2009 – Stanford

Patients: A total of 41 patients with low-risk prostate cancer were treated with a total dose of 36.25 Gy in 5 fractions of 7.25 Gy (assuming an $\alpha/\beta=1.5$, the equivalent biological dose is 90.6 Gy at 2 Gy per fraction). The patients were simulated with a CT scan at 1.25 mm slice thickness and treated supine, in an alpha cradle.

Dosimetric parameters: Cyberknife was used to deliver the SBRT with the dose prescribed to the PTV that consisted of an expansion of the prostate by 5 mm, reduced to 3 mm in the posterior direction. The prescription dose had to cover 95% of the planning target volume and the normalization was required to the 89-90% isodose line. The rectal DVH goals were <50% rectal volume receiving 50% of the prescribed dose, <20% receiving 80% of the dose, <10% receiving 90% of the dose and <5% receiving 100%.

Repositioning: Image-guided SBRT was used daily, based on three gold fiducials.

Results: With a median follow-up of 33 months, no patient has experienced PSA failure regardless of the biochemical failure definitions used (ASTRO or nadir+2).

Toxicity: Only 2 patients (5%) experienced RTOG Grade 3 late urinary toxicity and none with Grade 3 rectal toxicity. There was no Grade 4 toxicity. The first 21 patients received daily treatment (QD) and the remaining 20 patients were treated every other day (QOD). No patient in the QOD group reported a quality of life (QOL) score 4-5 for any of the symptoms, whereas in the QD group 8 patients (38%) reported a score of 4-5 for any individual symptoms and 5 patients (24%) reported a score of 4-5 for the overall quality of life. They were all statistically significant. For the urinary QOL there was no significant difference between the QD and QOD groups.

Choi et al., 2007 – Korea

Patients: Results of a clinical experience has been reported on 44 patients treated for low to high risk prostate cancer with CyberKnife® SBRT. This report, available in abstract form only, details the results at 13 months of follow-up of the treatment of 10 patients with low-risk prostate cancer (PSA less than 10, Gleason less than 6, stage T1b-T2a), 9 intermediate-risk prostate cancers (PSA 10-20, Gleason 7), and 25 high-risk patients (PSA $\geq$ 20, or Gleason $\geq$ 8).

Dosimetric parameters: The patients received stereotactic treatment with a CybeKnife® unit to a total dose of 32-36 Gy in 4 fractions of 8-9 Gy per fraction, with the exception of one patient who received 24 Gy in 3 fractions of 8 Gy.

Repositioning: Real-time tracking of implanted markers with CyberKnife.

Results: 3-year overall survival rate was 100%, with a 3-year biochemical failure-free rate of 78.3%. There were only 4 patients with biochemical failure.

Toxicity: Grade 1 or 2 acute rectum toxicity was experienced by 14 patients and Grade 1 or 2 acute urinary bladder toxicity was experienced by 17 patients. There were no Grade 3 or greater acute toxicities.

Mantz et al., 2008 – Florida

Patients: In this abstract, 58 patients were treated with a total dose of 36.25 Gy prescribed to the prostate in 5 fractions of 7.25 Gy, delivered on an every-other-day schedule. Protocol inclusion criteria required T1c to T2a stage, PSA ≤10ng/mL, Gleason score 6 or less, prostate volume less than 60 cc, and an IPSS voiding score of less than 18.

Dosimetric parameters: The SBRT PTV was created by 3-mm uniform expansion of the prostate volume. SBRT was delivered with a Linear accelerator-based using the Trilogy® system. Point dose maxima of 50%, 85%, 105% and 125% were assigned as treatment planning constraints to the femoral heads, rectum, bladder and urethra, respectively.

Repositioning: Cone Beam CT image guidance was used prior to each fraction for correction of target setup error, and the Calypso 4D Localization System was used during treatment for target tracking.

Results: Mean PSA for all patients demonstrated a rapid decline over the first 6 months of follow-up, from a pretreatment value of 7.6 ng/mL, to a 6-month post-treatment value of 1.0 ng/mL. No biochemical failures have been noted to date.

Urinary Toxicity: At 1-month, Grades 1-2 urinary frequency, dysuria and retention were reported by respectively 43.1%, 15.5% and 18.9% of patients. At 6-months, Grade 1 urinary frequency, dysuria and retention were reported by respectively 16.7%, 0% and 6.7% of patients. No patient reported Grade 3 or greater urinary toxicity at any time.

Rectal Toxicity: At 6-months, 3 patients reported Grade 1 proctitis and 1 patient reported Grade 1 rectal bleeding.

Appendix 3

- Abstracts and posters at the ESTRO 29 meeting (September 12-16, 2010) in Barcelona;

Abstract Nb.

1177 CLINICAL RESULTS OF IMAT IN ADENOCARCINOMA PROSTATE CANCER
E. Madon (Italy), V. Richetto, S. Gribaudo, S. La Sala, S. Di Gregorio, U. Monetti, A. Mussano, E. Roberto, A. Urgesi

1178 CO-MORBID CONDITIONS AND LATE RECTAL TOXICITY ON PROSTATE CANCER PATIENTS TREATED BY 3DCRT.
R. Fuentes-Raspall (Spain), G. Oliu-Isern, A. Roselló, J. M. Inoriza-Belzunce

1179 COMBRETASTATIN-A4-PHOSPHATE DURING PROSTATE RADIOTHERAPY, A RESPONSE ASSESSMENT USING MULTI-FUNCTIONAL MRI
R. Alonzi (United Kingdom), A. Padhani, N. J. Taylor, Q. Ng, H. Mandeville, U. Patel, J. J. Stirling, P. Hoskin

1180 COMPARISION OF PRONE AND SUPINE TREATMENT POSITION FOR PATIENTS WITH PROSTATE CANCER – AN ANALYSIS OF DOSE VOLUME HISTOGRAMS FOR TOMOTHERAPY.
T. Bajon (Poland), T. Piotrowski, B. Bak, J. Kazmierska, B. Blasiak

1181 COMPARISON OF HIGH-DOSE EBRT AND EBRT WITH BRACHYTHERAPY BOOST IN TREATMENT OF PROSTATE CANCER PATIENTS.
B. Smolska-Ciszewska (Poland), L. Miszczyk, B. Bialas, M. Gawkowska-Suwinska, G. Plewicki, M. Fijalkowski, M. Giglok, K. Behrendt, E. Nowicka, A. Zajusz

1182 CONE-BEAM CT VERIFICATION FOR PROSTATE RADIOTHERAPY: MANUAL VERSUS AUTOMATIC REGISTRATION
N. Rosenfelder (United Kingdom), A. Aitken, N. van As, V. Khoo

1183 CONTOURING VARIABILITY OF THE PENILE BULB ON CT IMAGES: IMPACT ON A MULTI-INSTITUTIONAL COMPARISON
L. Perna (Italy), C. Fiorino, E. Maggiulli, G. Fellin, T. Rancati, S. VIlla, V. Vavassori, R. Valdagni, C. Cozzarini

1184 CYBERKNIFE ROBOTIC IMAGE-GUIDED STEREOTACTIC RADIOTHERAPY FOR ISOLATED RECURRENT PRIMARY, LYMPH NODE OR METASTATIC PROSTATE CANCER
B. A. Jereczek-Fossa (Italy), D. Zerini, L. Fariselli, G. Beltramo, C. Fodor, L. Santoro, F. Gherardi, C. Ascione, I. Bossi-Zanetti, R. Mauro, L. C. Bianchi, A. Bergantin, A. Vavassori, G. B. Ivaldi, O. De Cobelli, B. Rocco, E. Scardino, G. Musi, F. Verweij, V. Matei, R. Orecchia

Abstract Nb.

1185 DETAILED HISTOLOGICAL VALIDATION OF DYNAMIC CONTRAST ENHANCED (DCE) MRI IN THE PROSTATE: WHAT DOES KTRANS TELL US?
M. Moman (Netherlands), G. Groenendaal, M. Philippens, A. Borren, A. Boeken Kruger, P. J. van Diest, P. van der Groep, U. van der Heide, M. van Vulpen

1186 DO WE REALLY NEED A RADIOLOGIST FOR THE PROSTATE DELINEATION IN RADIOTHERAPY?
O. Chapet (France), C. Udrescu, B. De Bari, O. Rouviere, F. Lorchel, S. Mengue, T. Chekrine, A. D'Hombres, N. Girouin, J. Bouffard- Vercelli

1187 EARLY REPORT ON ACUTE TOXICITY AFTER IMRT/IGRT WITH TOMOTHERAPY IN LOCALIZED PROSTATE CANCER
R. Cendales (Spain), F. Schnitman, L. Schiappacasse, R. Matute, C. Minguez, D. Sevillano

1188 EFFECTIVENESS OF PERMANENT PROSTATE BRACHYTHERAPY IN YOUNG MEN WITH LONG-TERM FOLLOW-UP
N. Salem (France), F. Bladou, J. M. Boher, G. Gravis, J. Walz, M. Resbeut

1189 EVALUATION OF DOSE DISTRIBUTION WITH AND WITHOUT SIMULTANEOUS INTEGRATED BOOST FOR HIGH RISK PROSTATE CANCER
A. Vicedo-Gonzalez (Spain), M. Garcia, J. Pastor, L. Brualla, G. Domingo, J. V. Roselló, J. Lopez Torrecilla

1190 EVALUATION OF FE SIMULATION FOR PELVIC ORGANS MOTION MODELING IN PROSTATE CANCER 3DCRT USING CBCT SCANS
A. Mohammad (France), M. B. BOUBAKER, A. Noel, P. Aletti

1191 EVALUATION OF THE RESPIRATORY PROSTATE MOTION WITH 4D CT SCANS ACQUISITION USING THREE IMPLANTED MARKERS
C. Udrescu (France), P. Jalade, G. Michel-Amadry, B. De Bari, O. Chapet

1192 EXCELLENT ACUTE TOXICITY OF SALVAGE TOMOTHERAPY TO PROSTATIC BED AND PELVIS IN 55 PATIENTS
F. Alongi (Italy), C. Cozzarini, C. Fiorino, A. Fodor, S. Broggi, G. M. Cattaneo, R. Calandrino, N. Di Muzio

DO WE REALLY NEED A RADIOLOGIST FOR THE PROSTATE DELINEATION IN RADIOTHERAPY?

Olivier CHAPET [1], Corina UDRESCU [1-2], Berardino DE BARI [1], Olivier ROUVIERE [4], Fabrice LORCHEL [1], Sylvie MENGUE [1], Tarik CHEKRINE [1], Anne d'HOMBRES [1], Nicolas GIROUIN [4], Juliette BOUFFARD-VERCELLI [3]

[1] - Department of Radiation Oncology, [2] – Department of Medical Physics, [3] – Department of Radiology, Centre Hospitalier Lyon Sud, PIERRE BENITE, FRANCE
[4] – Department of Urologic Radiology, Hopital Edouard Herriot, Lyon, FRANCE

Purpose:

Prostate delineation on the CT scan is associated with high inter-observer variations. The aim of this study was to evaluate if a fusion of the dosimetric CT scan with a MRI (integrating a radiologist prostate delineation) could reduce the inter-observer variations and improve the radiation oncologist contouring.

Materials/ Methods:

Five patients (pts) with a prostate cancer underwent a 3 gold markers implantation by an urologist surgeon or radiologist. → Each patient had a CT scan simulation (GE LightSpeed16®), a T2-MRI and a fusion on the markers was made using the Advantage GE Fusion software.

The prostate was delineated on the T2-MRI by 3 radiologists (**Group R**) experts in prostate cancer

Six physicians, 3 experts (Group E) and 3 non-experts (Group NE) in prostate cancer, delineated 3 contours on each patients' CT scan

Using only the CT scan
(CT)

Having the CT/T2-MRI fusion available
(CT/T2)

Having the CT/T2-MRI fusion available with radiologists' prostate delineation made on the MRI only
(CT+CR)

A percentage of common contoured volume (CCV) was calculated for the group R on T2-MRI and for the groups E and NE on CT, CT/MRI and CT+CR, using the following formula:

$$CCV = \frac{\text{common volume of all the physicians of the group}}{\text{delineated volume of the physician}} \times 100$$

Results:

Table: Mean percentages of common contoured volumes in the two groups for all the patients.

	Patient 1	Patient 2	Patient 3	Patient 4	Patient 5	All Patients
CT E	73	59	76	76	71	71 ± 13
CT/T2 E	70	60	75	77	68	70 ± 15
CT+ CR E	74	82	82	80	78	79 ± 10
CT NE	68	59	68	66	72	67 ± 9
CT/T2 NE	51	50	73	67	66	62 ± 12
CT+ CR NE	78	79	82	80	76	79 ± 7
Radiologists on T2- MRI	84	85	90	86	85	86 ± 5

•Experts and non-experts contour evaluations:

The percentage of common volume delineated on CT scan only is poor in the two, E and NE, groups (cf Table).
A fusion CT/MRI-T2 did not improve the percentage of common volume obtained with CT in the group E and even altered it in the group NE.

•The impact of the radiologist prostate delineation on the radiation physicians contours:

Compared to CT and CT/T2, having the radiologists' delineation available on the MRI (CT-CR) improved the percentage of common volume to the same value of 79% in groups E and NE.

•Radiologists contours on T2-MRI:

Regarding the prostate delineations of all the patients on the T2-MRI, there was a mean percentage of common volumes of 86 ± 5%, between the radiologists contours.

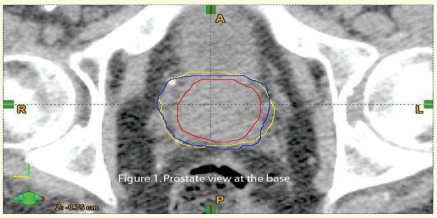

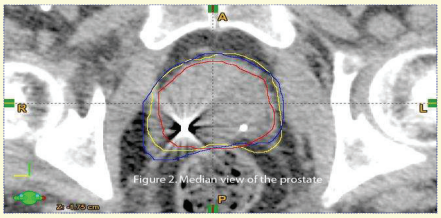

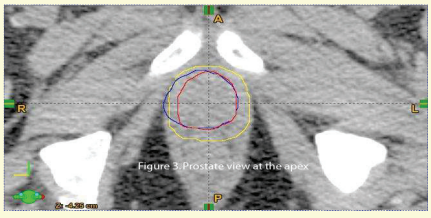

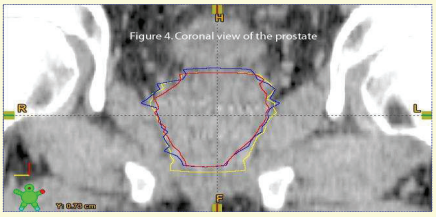

Figures: Example for one patient of the prostate views at the base (fig. 1), middle (fig. 2), at the apex (fig. 3) and coronal view. The union functions for the 3 non-experts contours were created for each case apart:

- for the dosimetric CT scan only (yellow);
- for the CT/T2-MRI fusion, without the radiologists contour (blue);
- for the CT/T2-MRI fusion, with the radiologists contour on the T2-MRI (red).

Conclusions:

The inter-radiologists reproducibility is high in the delineation of the prostate on T2-MRI.

A CT/MRI fusion with a radiologist contour improves the delineation of any physician and the differences between E and NE disappeared.

A fusion without the radiologist contours decreases the quality of the delineation in NE and should not be used.

EVALUATION OF THE RESPIRATORY PROSTATE MOTION WITH 4D CT SCANS ACQUISITIONS USING THREE IMPLANTED MARKERS

Corina UDRESCU [1-2], Patrice JALADE [2], Géraldine MICHEL-AMADRY [2], Berardino DE BARI [1], Olivier CHAPET [1]
1 - Department of Radiation Oncology,
2 – Department of Medical Physics,
Centre Hospitalier Lyon Sud, PIERRE BENITE, FRANCE

Background:

An important consideration for the development of stereotactic irradiation in prostate cancer is to take into account the potential intra-fraction respiratory motion in order to design the planning target volume (PTV) and the daily repositioning accuracy.

Purpose:

The objective of this study was to analyze and measure the respiratory prostate motion on the 10 phases of a 4D CT scan.

Materials and Methods:

➢ ***Patients:*** Ten patients, with a low to intermediate risk cancer, had 3 gold markers (3mm x 1.2mm) implanted in the prostate. All the patients were treated supine using specific immobilization.

➢ ***4D Acquisitions:*** - A 4D scan was acquired for each patient using a General Electric LightSpeed16® CT scan, with slice thicknesses of 2.5 mm;

- Ten CT scan phases of the respiratory cycle were created using 4D Advantage®GE software.

➢ ***The prostate motion was measured on :***

1°) a simple visual analysis of the dynamic 4D CT s can sequences.

2°) each phase of the respiratory cycle according th e following procedure :

➢ For each CT scan phase, 2 digitally reconstructed radiographs (DRRs) were created at 0° and 90° (image p ixel size = 0.02 cm).

➢ On the two DRRs, the coordinates (x, y, z) of each marker's center were defined from the isocenter of the CT scans.

➢ The amplitude of the motion was calculated by comparing the markers' coordinates on the 10 scans.

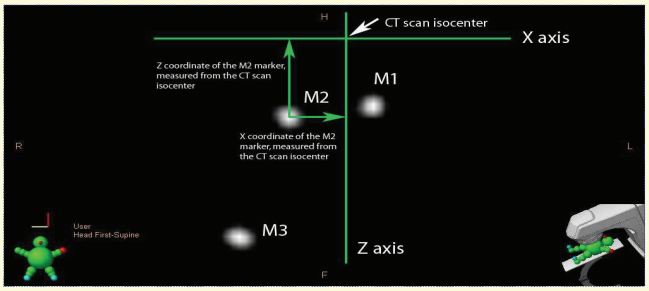

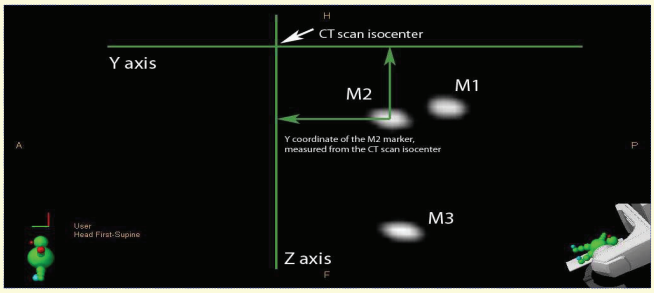

Figures 1 and 2. Anterior and left lateral digitally recontructed radiographs (DRRs), of one phase of a 4D CT scan

Results:

- No difficulty was faced in defining the coordinates of the markers on each CT scan series;
- The mean values of the markers coordinates in x, y and z were respectively 1.15 (ranged from 0.4 to 2.5 cm), 1.48 (0 to 3.6 cm) and 2.26 cm (0.4 to 5.6 cm) from the CT scan isocenter;
- No prostate motion was observed on a simple visual analysis of the dynamic 4D CT scan sequences;
- With a more specific analysis on the DRR, using the fiducials' coordinates on each of the ten respiratory phases, the prostate motion remained below 1 mm in left-right and anterior-posterior directions, for all the patients;
- In the cranio-caudal direction the prostate motion remained undetectable, thereby below the slice thickness of 2.5 mm.

Conclusions:

Even if important prostate displacement can occur during the prostate treatment due to the bladder or rectum filling, in our study we didn't observe any motion of the prostate, linked to the respiration.

Taking into consideration the slice thickness of the CT scan (2.5 mm), our study shows that the prostate motion with the respiration, if present, remains always below 2.5 mm.

Appendix 4

- Abstract and poster at the 52nd Annual ASTRO Meeting (October 31 – November 4, 2010) in San Diego;

3051 Conceptual Design of PET-linac System for Molecular-guided Radiotherapy

M. Ishikawa[1], S. Yamaguchi[1], S. Tanabe[1], G. Bengua[2], K. Sutherland[1], R. Suzuki[2], N. Miyamoto[1], K. Nishijima[1], N. Katoh[1], H. Shirato[1]

[1]*Graduate School of Medicine, Sapporo 060-8638, Japan,* [2]*Department of Medical Physics, Hokkaido University Hospital, Sapporo 060-8648, Japan*

Purpose/Objective(s): Molecular imaging is an important modality for recognizing tumor location. If a planar molecular-image of the tumor can be taken during patient setup verification in radiotherapy, it may be possible to accurately confirm that the irradiation field adequately covers the tumor. We will report the results of our feasibility study on a PET-Linac system for patient setup verification using a parallel-plane PET configuration.

Materials/Methods: We assumed that the parallel-plane PET system consisted of a pair of position sensitive scintillation detector array placed 60 cm away from each other. Each detector array is equipped with 11,664 GSO scintillator crystals (2.5 x 2.5 x 25 mm^3). Monte Carlo simulations using Geant4 were performed on a simple geometry for patient setup verification. A 24 cm x 24 cm cylindrical water phantom embedded with four spherical ^{18}F gamma-ray sources (25 kBq/cc) having diameters of 8, 16, 24, 32 mm was placed in between the plane detector arrays. The background gamma rays in the water phantom were varied by assuming contrast ratios relative to the tumor of 1:50, 1:20, 1:10, and 1:5. Acquisition time was assumed to be 60 seconds, and the planar image was reconstructed using an ML-EM algorithm. To evaluate the feasibility of molecular-imaging based setup verification, 3 observers were asked to determine the setup displacements using in-house software which allowed the co-registration of the original image and reconstructed image.

Results: The average discrepancies at higher contrast (e.g., 1:50) were less than 1.46 mm for all spherical-source diameters. Even at low contrast (e.g., 1:5), average discrepancies were less than 1.20 mm for the spherical sources with diameters larger than 16 mm. It means that accurate patient setup can be done independent of the contrast. Recognition of the 8 mm spherical source was difficult at lower contrast, however, setting the contrast higher than 1:20 resulted a discrepancy of less than 1.15 mm.

Conclusions: Conceptual design of parallel-plane PET system was considered for the initial patient setup verification in radiation therapy. From the Monte Carlo simulations performed for a simple geometry, molecular-imaging based patient setup verification was found to be feasible up to an accuracy of about 1.5 mm. Moreover, spatial resolution was judged as sufficient for verifying that the irradiation field adequately covers the tumor.

Author Disclosure: M. Ishikawa, None; S. Yamaguchi, None; S. Tanabe, None; G. Bengua, None; K. Sutherland, None; R. Suzuki, None; N. Miyamoto, None; K. Nishijima, None; N. Katoh, None; H. Shirato, None.

3052 Evaluation of Implanted Gold Markers Migration during Irradiation of Prostate Cancer

C. M. Udrescu[1,2], P. Jalade[2], B. De Bari[1], O. Rouviere[3], A. Ruffion[4], G. Michel-Amadry[2], O. Chapet[1]

[1]*Department of Radiation Oncology, Centre Hospitalier Lyon Sud, Lyon, France,* [2]*Department of Medical Physics, Centre Hospitalier Lyon Sud, Lyon, France,* [3]*Department of Urological Radiology, Hopital Edouard Herriot, Lyon, France,* [4]*Department of Urology, Centre Hospitalier Lyon Sud, Lyon, France*

Purpose/Objective(s): In order to improve the prostate localization, gold markers are frequently implanted into the organ before the beginning of an external beam irradiation treatment. However, the accuracy of the prostate repositioning may depend on the potential migration of the markers during the course of irradiation. The purpose of this work was to analyze if the gold markers could migrate between the first and last session of irradiation.

Materials/Methods: Ten patients were treated for a low or intermediate risk prostate cancer at the dose of 74 Gy to 76 Gy in 37 to 38 fractions, 3 of them receiving 6 months of androgen deprivation. Three gold markers were implanted in the prostate by an urologist surgeon or a radiologist: at the base (M1), laterally (M2) and apex (M3). The markers were 3 mm long and 1.2 mm thickness. Two kV images (pixel size of the image = 0.02 cm) were acquired every day at 0° and 90° for the prostate repositioning. The coordinates of the middles of the markers M1 and M2 were daily measured on the two kV images on x, y and z axes, from the center of the third marker (M3) taken as reference for all the fractions and patients (coordinates: 0, 0, 0). The distances between the markers were extrapolated from the coordinates by the formula: D_{ij} = square root of $[(x_j-x_i)^2+(y_j-y_i)^2+(z_j-z_i)^2]$. The initial mean distance value between two markers was calculated from the distances measured on the first five kV pairs. The final mean distance value was calculated from the last five kV pairs. For each patient apart, a mean variation of distance between two markers, during the course of irradiation, was thereby obtained by subtraction of the final mean value from the initial one.

Results: A total number of 1062 distances were calculated for all the patients and all the marker pairs. A small reduction of the distances between the three markers were noted for all the patients with a mean SD of 0.65 mm (0.23-1.25). No increased distances were seen. Between the first five and the last five measurements, the mean variation of distance between 2 seeds was 1.1 mm, with a minimum of 0 mm and a maximum value of 3.3 mm. This distance variations between 2 seeds was <1 mm, 1 to 2 mm, 2 to 3 mm and >3 mm respectively in 50%, 33.3%, 10%, and 6% of all the measurements (10 pts x 3 distances). The average reductions of distance between the two markers M1M2, M2M3, and M1M3 were 1.26 mm (0.2- 3.3 mm), 1.26 mm (0-3.1 mm) and 1.25 mm (0.4- 3 mm), respectively.

Conclusions: The constant reduction of the distances between the 3 markers is more likely in favor of a reduction of the prostate volume during irradiation than a migration of the makers. This reduction of distances remained very low and should not affect the accuracy of the prostate repositioning.

Author Disclosure: C.M. Udrescu, None; P. Jalade, None; B. De Bari, None; O. Rouviere, None; A. Ruffion, None; G. Michel-Amadry, None; O. Chapet, None.

3053 The Influence of an Endorectal Balloon on Intrafraction Prostate Motion

R. Smeenk[1], R. J. W. Louwe[1], K. M. Langen[2], A. P. Shah[2], P. A. Kupelian[2], E. N. J. T. van Lin[1], J. H. A. M. Kaanders[1]

[1]*Radboud University Nijmegen Medical Centre, Nijmegen, Netherlands,* [2]*M.D. Anderson Cancer Center Orlando, Orlando, FL*

Purpose/Objective(s): To investigate the prostate immobilizing properties of an endorectal balloon (ERB) during prostate IMRT.

EVALUATION OF IMPLANTED GOLD MARKERS MIGRATION DURING IRRADIATION OF PROSTATE CANCER

Corina UDRESCU [1-2], Patrice JALADE [2], Berardino DE BARI [1], Olivier ROUVIERE [3], Alain RUFFION [4], Géraldine MICHEL-AMADRY [2], Olivier CHAPET [1]

[1] -Department of Radiation Oncology, [2] –Department of Medical Physics, EA3738, Centre Hospitalier Lyon Sud, PIERRE BENITE, FRANCE

[3] – Department of Urologic Radiology, Hôpital Edouard Herriot, LYON, FRANCE

[4] – Department of Urology, Centre Hospitalier Lyon Sud, PIERRE BENITE, FRANCE

Background:

The development of new techniques for prostate irradiation such as intensity modulation, hypo-fractionation or stereotactic schema demands a high level of accuracy in prostate localization. Intra-prostatic gold markers are recommended to be implanted into the prostate for a better daily repositioning before and also during the irradiation:

- Improving the prostate localization
- Allowing a reduction of the Planning Target Volume (PTV)

The accuracy of the prostate repositioning might be affected by a potential migration of the markers during the course of irradiation.

Purpose:

The purpose of this study was to evaluate if the intra-prostatic gold fiducials could migrate during the radiotherapy course, using daily OBI- kV control images. This method will estimate also if this migration will affect the prostate repositioning accuracy.

Materials and Methods:

Patients:

- Ten patients were treated for a low or intermediate risk prostate cancer at the dose of 74Gy to 76Gy in 37 to 38 fractions, 5 of them receiving 6 months of androgen deprivation.
- Three gold markers were implanted in the prostate by an urologist surgeon or a radiologist: at the base (M1), laterally (M2) and apex (M3). The markers were 3 mm long and 1.2 mm thickness.
- All the patients were treated supine using specific immobilization.

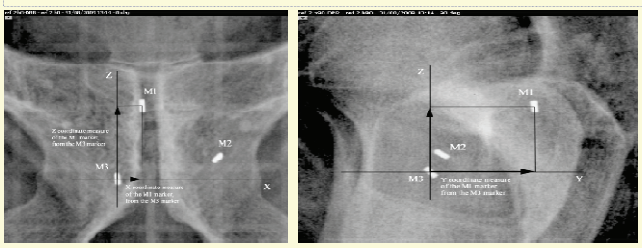

Figure 1 and 2. Example of an anterior and left lateral OBI kV images. The M3 marker was chosen as reference (x, y, z) = (0, 0, 0) for all the images. The x and z coordinates of the other two markers were measured on the anterior acquisition and the y coordinates on the left lateral acquisition.

kV- Acquisitions:

- Two kV images (pixel size of the image = 0.02 cm) were acquired every day at 0° and 90° for the prostate repositioning.
- The coordinates of the middles of the markers M1 and M2 were daily measured on the two kV images on x, y and z axes, from the center of the third marker (M3) taken as reference for all the fractions and patients (coordinates: 0,0,0).
- The distances between the markers were extrapolated from the coordinates by the formula:

$$D_{ij} = \text{square root of } [(x_j-x_i)^2+(y_j-y_i)^2+(z_j-z_i)^2$$

Analysis:

- A mean variation of the distance between the markers (from the first to the last fraction) was calculated for all the measurements.
- For each patient apart, a general variation of the distance between two markers, during the course of irradiation, was thereby obtained by subtraction of the final distance value (at the end of the treatment) from the initial one (at the beginning of the treatment).
- The initial value (at the beginning of the treatment) of the distance between two markers was obtained by calculating the mean of the distances measured on the first 5 kV pairs.
- The final value (at the end of the treatment) of the distances between two markers was obtained by calculating the mean of the distances measured on the last 5 kV pairs.

Results:

- 758 images were acquired for this study and 708/758 images were available for analysis, corresponding to 354 pairs of kV images (50 images couldn't be evaluated due to technical problems);
- Only reductions of distances between two markers were observed and no increased distances were measured.

General analysis of distance variations (dvar) between markers on all kV images:

- 676 dvar remained below 1 mm;
- an increase of distance equal or above 1 mm was observed on 102 dvar, but did not exceed 2,7 mm;
- a decrease of distance equal or superior to 1 mm was noted on 254 dvar, where the maximum value was of 3.7 mm.

Table 1. Dvar values (first 5 vs last 5 kV images) between two markers. All values are in mm.

Patient	M1M2	M2M3	M3M1
1	- 3.3	- 1.9	- 0.7
2	- 0.4	0.03	- 0.4
3	- 1.3	- 1.6	- 1.3
4	- 1.5	- 3.1	- 2.9
5	- 1.6	- 0.2	- 1.1
6	0.9	- 0.3	0.5
7	- 1.5	- 2.9	- 3.0
8	- 1.0	- 1.0	- 0.8
9	0.2	- 1.2	- 0.7
10	- 0.9	- 0.4	- 1.1
Average variation	- 1.26	- 1.26	- 1.25
Minimum values	- 0.2	- 0.03	- 0.4
Maximum values	- 3.3	- 3.1	- 3.0

Analysis of the Dvar (from the first 5 to the 5 last measurements):

- For all the patients, the Dvar values between two seeds are presented in the Table 1.
- The mean variation of all the distances between two seeds was 1.26 mm, with a minimum of 0.03 mm and a maximum value of 3.3 mm.
- The average reductions of distances between two markers apart, M1M2, M2M3 and M1M3 were 1.26 mm [0.2– 3.3 mm], 1.26 mm [0.03- 3.1 mm] and respectively 1.25 mm [0.4- 3 mm].
- The distance variations were < 1 mm, 1 to 2 mm, 2 to 3 mm and > 3 mm in 50%, 33.3%, 10% and 6% of cases, respectively. It means that no variation greater than 4 mm was present in any direction (antero-posterior, superior-inferior or left-right).

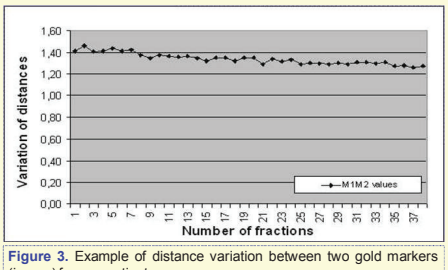

Figure 3. Example of distance variation between two gold markers (in mm) for one patient.

Impact of Hormonotherapy:

- In this study, five patients received a neo- adjuvant hormone-therapy during 6 months.
- These patients had a total number of 15 Dvar values, where only four were greater than 2.5 mm and did not exceed 3.1 mm.
- A plot for one patient M1M2 distance values is presented in Figure 3.
- The reduction of the distance between two markers was observed even in the absence of the hormone-therapy.

Conclusions:

The constant reduction of the distances between the 3 markers is more likely in favour of a reduction of the prostate volume during irradiation than a migration of the makers.

This reduction of distances remained very low and did not affect the accuracy of the prostate repositioning, a very important aspect especially for the hypo-fractionation, IMRT and/or stereotactic body radiation therapy (SBRT).

In our department we will continue to use this repositioning method, reducing the PTV margins around the prostate for the standard IMRT treatments, hypo-fractionated radiotherapy and SBRT.

Appendix 5

- A protocol for the quality control of the On Board Imager (OBI®, Varian Medical Systems) initiated at Lyon Sud Hospital, France.

Fantômes nécessaires pour le contrôle de qualité de l'OBI

ID	Nom du fantome	Description	Photos
123546	**Catphan 504**	Contrôle de Qualité des images CBCT	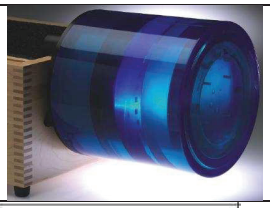
123546	Phantom 2 – **Las Vegas**	Test pour la qualité de l'image PV	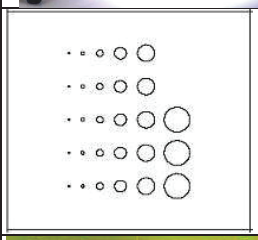
123546	**PCB Blade Calibration (La Plaque Vert)**	Détermination du Pixel Central du kVD a l'OBI et contrôle des mâchoires du kVS	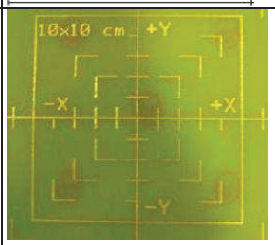
123546	Isocentre **Cube** Assy **5 cm** (**2 mm ball**)	Précision du positionnement de l'isocentre de l'OBI et de l'isocentre MV lors de la rotation du Bras	
123546	18FG **Leeds** Test Objects (CQ XRay)	Contrôle de Qualité des images kV de l'OBI	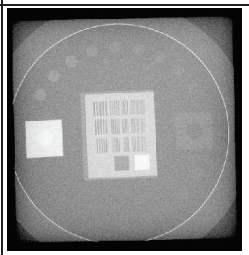
123546	**Marquer – Block**		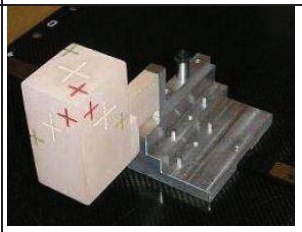

I. Protocole pour une acquisition CBCT (Cone Beam CT)

Fantôme utilise : Catphan 504

Paramètres de positionnement:

- positionnement par les lasers
- Table : Lat = ; Lng = cm ; Vert = cm
- Epaisseur de coupe : 2.5 mm
- Field of View: 25 cm
- Mode: High Quality Head
- Filtre : Full Fan

Centrage du fantôme Catphan 504 :

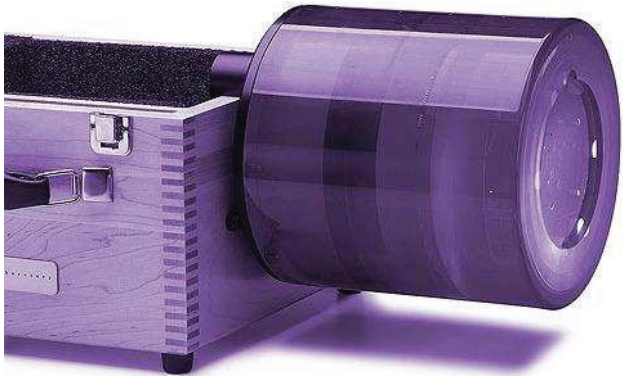

1. Positionnez la boite en bois du fantôme Catphan sur la table de traitement. Celle-ci doit être ouverte de façon à ce qu'elle ne bascule pas lors que on accroche le fantôme comme le montre la figure 1 (le couvercle ouvert agit comme un contrepoids).
2. Assurez-vous de placer le fantôme en débord de la table (la table ne doit pas interférée dans l'image.
3. Utiliser un niveau à Bulle, sur la longueur du fantôme, pour aligner celui-ci horizontalement.
4. Centrer le Catphan en utilisant les lasers et les marques d'alignement qui se trouve sur le fantôme (point blanc que l'on voit sur la Figure 1).
5. Acquérir une acquisition CBCT et effectuer les contrôles suivants:

a. Reproductibilité HU (CTP404) : *Résolution en densité pour des tensions de 80kV, 100kV et 120 kV:*

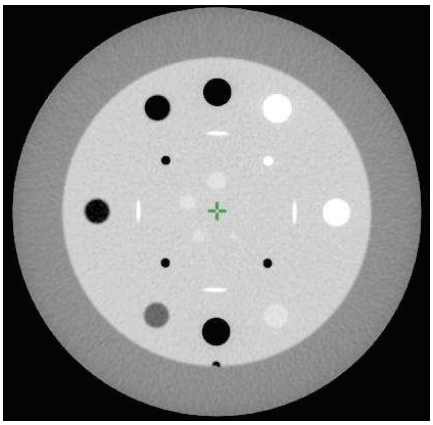

1. Sélectionnez l'image d'une coupe (figure 2) qui permet le contrôle de la résolution en densité, à l'aide du Page Up / Down.
2. Utilisez la fonction Tools-Measure-Histogram pour faire un carrée dans chaque substance homogène. Assurez-vous que le carrée ne dépasse pas le bord de la substance à mesurer.
3. Relever les mesures en unité Hounsfield (HU) dans le tableau 1 de la feuille de résultats. On contrôlera notamment qu'aucune dérive significative n'est notée par rapport à la valeur de référence relevée à l'acceptance de l'OBI.
   Par exemple, un Scanner en mode « Head » avec le filtre « Bow Tie », doit donner pour une région remplie d'air une valeur HU de -1000 ± 40.
4. Répétez les étapes ci-dessus pour les 3 tensions du tube.

Tableau 1 : Résolution en densité.

Matériel	HU Moyenne attendue	Localisation	HU Mesure			Tolérance	Résultats
			80 kV	100 kV	120 kV		
Air	-1000	12 heures				< | 40 HU |	P / F
PMP	-200	11 heures				< | 40 HU |	P / F
LDPE	-100	9 heures				< | 40 HU |	P / F
Polystyrène	-35	7 heures				< | 40 HU |	P / F
Acrylique	120	5 heures				< | 40 HU |	P / F
Delrin	340	3 heures				< | 40 HU |	P / F
Téflon	990	1 heure				< | 40 HU |	P / F

b. *Test pour la Résolution à Bas Contraste (CTP515) :*

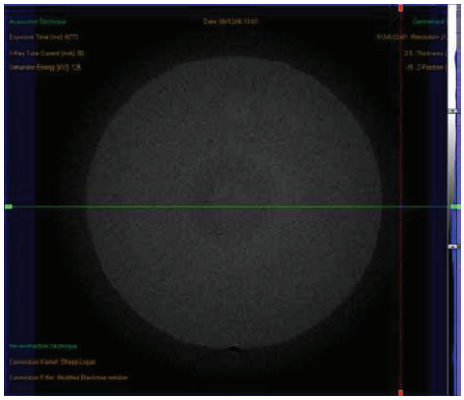

Le test pour la résolution à bas contraste sera effectué pour vérifier la capacité de visualiser des objets à bas contraste. Vous devriez voir au moins l'un des objets de contraste 1%.

c. Test pour la Résolution à Haut Contraste (CTP528) :

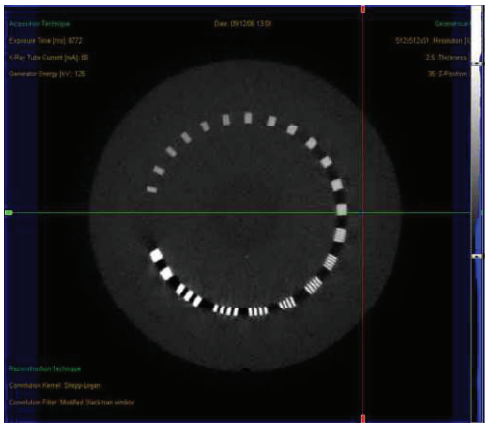

1. Le test pour la résolution à haut contraste sera effectué pour vérifier la résolution spatiale. Il mesure le nombre de paires de lignes (line pairs) par mm.
2. Avec le Full Fan, nous devrions pouvoir compter 7 paires de lignes par mm.
3. Avec le Half Fan, nous devrions pouvoir compter 6 paires de lignes par mm.
4. Si les paires de lignes sont floues, il faut refaire la calibration géométrique.
5. Notez les repères discernables dans la feuille de résultats.

Rm : Si la résolution à haut contraste n'est pas bonne (paires de lignes floues), une calibration géométrique et / ou une calibration du bras doivent être effectuées.
Si le problème n'est pas résolu par une nouvelle calibration, informer le SAV Varian.

d. Uniformité HU (CTP486) :

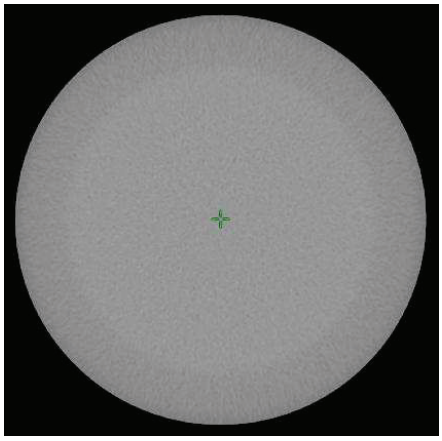

1. Sélectionnez la coupe du Catphan 486 qui affiche le module Uniformité HU ;
2. Utilisez la fonction Tools-Measure-Histogram pour faire un carrée dans la substance homogène, pour chaque position : centre, haut, droit, gauche et en bas.
3. Relever les mesures en unité Hounsfield (HU) dans le tableau 2 de la feuille de résultats. On contrôlera notamment qu'aucune dérive significative n'est notée par rapport à la valeur de référence relevée à l'acceptance de l'OBI.
4. Par exemple, un Scanner en mode « Head » avec le filtre « Bow Tie », doit donner pour une région remplie d'air une valeur HU de -1000 ± 40.
5. Répétez les étapes ci-dessus pour les 3 tensions du tube.

Tableau 2. Uniformité HU :

Position du ROI		Centre	Haut	Droit	Gauche	Bas
Mesure HU (pour chaque tension du tube)	80 kV					
	100 kV					
	120 kV					
Tolérance		<| 40 HU |	< | 40 HU |	< | 40 HU |	< | 40 HU |	< | 40 HU |
Résultats		P / F	P / F	P / F	P / F	P / F

e. Contrôle de la linéarité :

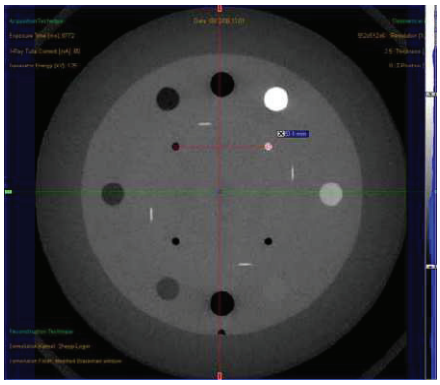

1. Sélectionnez la coupe qui affiche le module Linéarité spatiale, à l'aide du Page Up / Down.
2. Vérifiez la distance, en mesurant les distances entre les trous de vérification, situés dans le fantôme Catphan, en utilisant la fonction pour la mesure de distance (Measure-Distance). Les mesures doivent s'inscrire dans une précision de 1% de la distance réelle.
3. Notez les valeurs dans le tableau 3 de la feuille de résultats.

Tableau 3: Linéarité spatiale.

Dimensions du carré formé par les cylindres	Haut	Droit	Gauche	Bas
Longueur Mesure				
Longueur attendue	5.0 cm	5.0 cm	5.0 cm	5.0 cm
Tolérance	≤ 0.2 cm	≤ 0.2 cm	≤ 0.2 cm	≤ 0.2 cm
Résultats	P / F	P / F	P / F	P / F

f. Epaisseur de Coupe (CTP404).

1. On mesure l'image d'une rampe qui fait un angle de 23° par rapport à l'axe z. (épaisseur de coupe). L'image obtenue est la projection suivant x (barre horizontale) ou suivant y (barre verticale) de la rampe. Cette image projetée correspond au cosinus de l'angle de la rampe avec x ou y.
2. L'épaisseur de coupe correspond à la projection de la rampe suivant l'axe z, ce qui représente le sinus de l'angle de la rampe avec l'axe z.
3. Au final la relation entre l'épaisseur de coupe et l'image observée est donc tg 23° =0.42.
4. Soit épaisseur de coupe= mesure x 0.42.

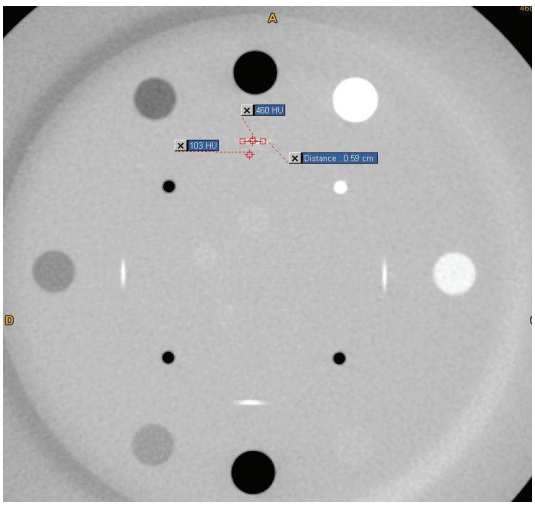

Tableau 4. Epaisseur de Coupe.

Position du fil	Haut	Droit	Gauche	Bas
Epaisseur de coupe (mm)	2.5	2.5	2.5	2.5
Mesure attendue (=épaisseur / 0.42)	5.95 mm	5.95 mm	5.95 mm	5.95 mm
Mesure (mm)				
Tolérance de la Mesure	5.65 – 6.25 mm	5.65 – 6.25 mm	5.65 – 6.25 mm	5.65 – 6.25 mm
Résultats	P / F	P / F	P / F	P / F

II. Tests du déplacement du Bras de Détecteur pendant le mouvement Vertical

	Position Verticale départ/ final	Position Verticale	Déplacement Long	Déplacement Lat.
Valeur Mesure	KVD à (-50, 0, 0)			
Valeur Attendu		48.2 +/- 0.2 cm	≤ 0.2 cm	≤ 0.2 cm
Résultats		P / F	P / F	P / F
Valeur Mesure	KVD à (-30, 0, 0)			
Valeur Attendu		28.2 +/- 0.2 cm	≤ 0.2 cm	≤ 0.2 cm
Résultats		P / F	P / F	P / F

Test Mécanique	Valeur Attendu (cm)	Valeur Mesure (cm)	Différence (cm)	Spécification	P / F
Distance KVS avec le Bras à 270 et KVS à (100, 0,0)	85.2			≤ 0.2 cm	
Distance KVD avec le Bras à 90 et KVD et (50, 0,0)	48.2			≤ 0.2 cm	

III. Protocole contrôle qualité pour la précision du positionnement de l'isocentre de l'OBI et de l'isocentre MV lors de la rotation du bras

Fantôme utilise : Cube 5cm

Paramètres de positionnement:

- Placer le mylar en T afin que « la barre du T » soit coté pied
- Ecarter les rails de la table afin qu'il ne soient pas dans l'image.
- Utiliser la barre de contention en F_2H_2
- Centrage du cube par les lasers
- DSP : 97.5 cm sur la croix noire au centre du cube
- Champ : 7 x 7 cm
- Table : Lat = 0 ; Lng = 116.7 cm ; Vrt = 2.5 cm ;
- Pour MV : Valeur Bras = Bras ;
- Pour KV : Valeur Bras = Valeur KVS (kV Source) ;
- For kV images : KVD = 40 cm ;
- KVS : kV = 40 ; mA = 25 ; mS = 4 ;

Contrôles:

a.) Pour la détermination de la précision du positionnement de l'isocentre de l'OBI et de l'isocentre MV, on va acquérir des images MV et KV pour les positions suivantes du Bras et du KVS :

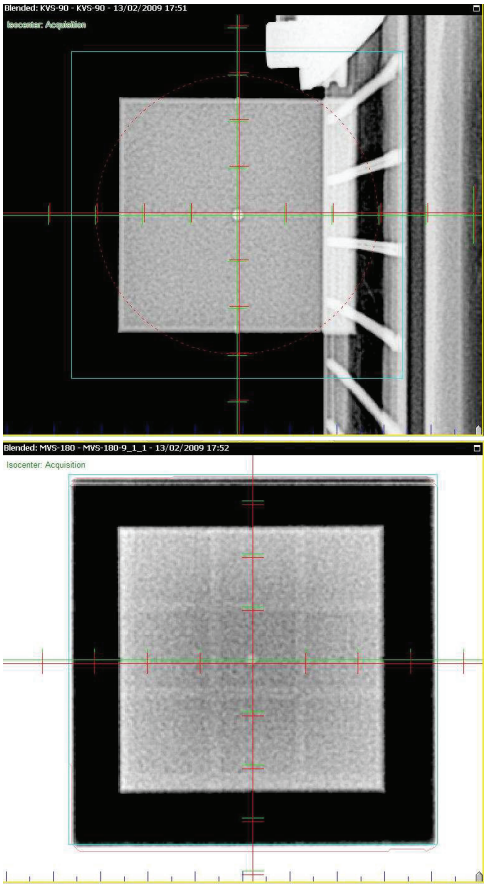

1.) Acquisition MV180: MVS = 180
2.) Acquisition kV90: B = 180 ; kVS = 90
3.) Acquisition kV0: B = 90 ; kVS = 0
4.) Acquisition MV90: MVS=90
5.) Acquisition kV270: B = 0 ; kVS = 270
6.) Acquisition MV0: MVS = 0
7.) Acquisition kV180: B = 270 ; kVS = 180
8.) Acquisition MV270: MVS = 270

b.) Centrer la croix verte dans le centre de la bille et regardez en bas les décalages, entre la croix rouge qui représente le centre de l'image et la croix verte que l'on place au centre de la bille.

c.) Les valeurs en bas de l'écran représente le décalage entre l'axe de l'image kV ou MV et l'isocentre de l'accélérateur matérialisé par les lasers. Il est donc important de s'assurer auparavant par un contrôle mécanique que les lasers qui ont servis au centrage du cube soient correctement positionnés à l'isocentre de l'accélérateur.
On notera les valeurs dans le tableau 5, de la feuille de résultats.

d.) La tolérance est de +/- 2 mm.

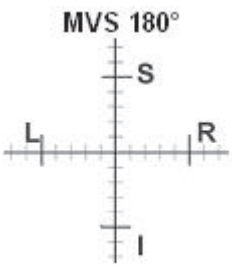

S/I =_____
G/D=_____

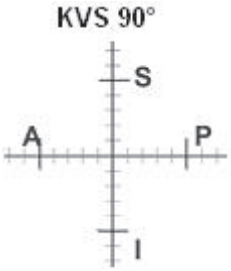

S/I=_____
A/P=_____

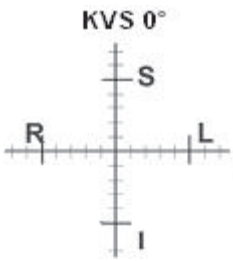

S/I=_____
D/G=_____

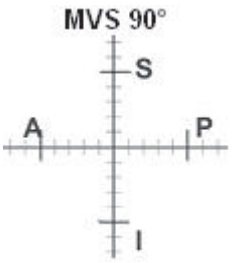

S/I=_____
A/P=_____

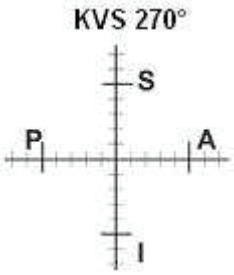

S/I=_____
P/A=_____

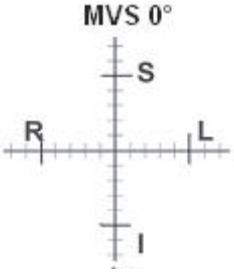

S/I=_____
D/G=_____

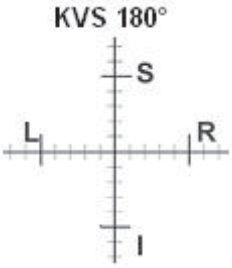

S/I=_____
G/D=_____

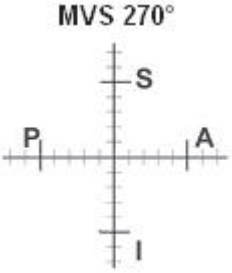

S/I=_____
P/A=_____

Tolérance: +/- 2 mm Résultats: P / F

Tableau 5. Décalage

Acquisition	Décalage (mm)			Tolérance
	D-G (x)	A-P (y)	S-I (z)	
MVS = 180				± 2 mm
kVS = 90				± 2 mm
kVS = 0				± 2 mm
MVS = 90				± 2 mm
kVS = 270				± 2 mm
MVS = 0				± 2 mm
kVS = 180				± 2 mm
MVS = 270				± 2 mm

IV. Protocole – test pour le contrôle de positionnement du kVD

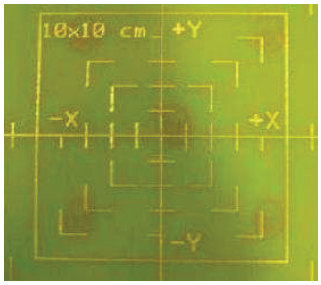

Fantôme utilise: **La Plaque Vert**
Protocole Eclipse :
Plan :
Paramètres de positionnement:

- Contention : F_3H_3
- DSP : 100 cm sur la plaque
- Set Up par les lasers
- kVS : kV= 40, mA= 25, mS= 4
- Table : Lat = 0 ; Lng = 125,3 cm ; Vrt = 0.1 cm
- B = kVS = 0°
- Position des mâchoires : 10 cm pour chaque mâchoire
- kVD = 40 cm, kVD = 50 cm, kVD = 60 cm, kVD = 80 cm

Contrôles:

1. Placez la plaque verte sur la table en respectant tout les paramètres de positionnement.
2. Acquérir l'image kV pour les différentes positions du kVD (40, 50, 60 et 80 cm)
3. Notez les décalages affichée en bas d'écran en déplacent la croix vert dans le centre de la plaque.
4. Mesurez à l'aide des repères de la plaque les dimensions du carré de 10 cm de coté.

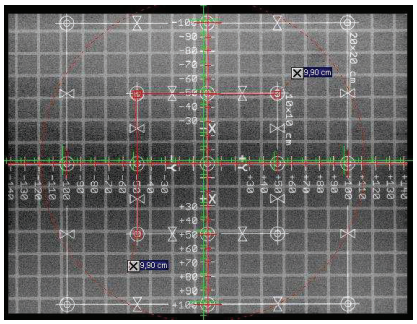

Résultats (P / F)	Pixel Central	Mâchoire Y1	Mâchoire Y2	Mâchoire X1	Mâchoire X2
KVD = 40 cm					
KVD = 50 cm					
KVD = 60 cm					
KVD = 80 cm					
Spécification	+ / - 1 mm	+ / - 2.5 mm	+ / - 2.5 mm	+ / - 2.5 mm	+ / - 2.5 mm

V. Protocole – test pour le contrôle des mâchoires

Fantôme utilise: **La Plaque Vert**
Plan :
Paramètres de positionnement:

- Contention : F_3H_3
- DSP : 100 cm sur la plaque
- Set Up par les lasers
- kVD = 40 cm ; kVS : kV= 40, mA= 25, mS= 4
- Table : Lat = 0 ; Lng = 125,3 cm ; Vrt = 0.1 cm
- B = kVS = 0°
- Position des mâchoires :
  - P1 = 10 cm pour chaque mâchoire
  - P2 = 20 cm pour chaque mâchoire

Contrôles:

1. Placez la plaque verte sur la table en respectant tout les paramètres de positionnement.
2. Acquérir l'image kV pour une position de kVD = 40 cm et pour chaque position de mâchoire (10 cm et 20 cm).
3. Mesurez chaque mâchoire avec une tolérance de +/- 2.5 mm.

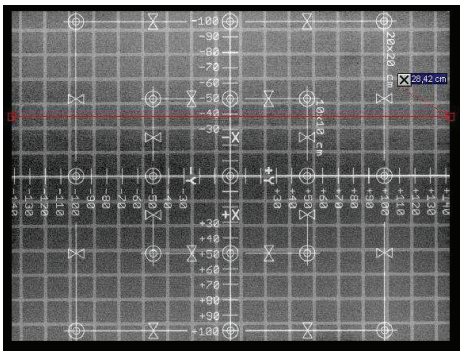

Résultats (P / F)	Pixel Central	Mâchoire Y1	Mâchoire Y2	Mâchoire X1	Mâchoire X2
P1 = 10 cm					
P2 = 20 cm					
Spécification	+ / - 1 mm	+ / - 2.5 mm	+ / - 2.5 mm	+ / - 2.5 mm	+ / - 2.5 mm

VI. Test pour l'agrandissement

Fantôme utilise: **La Plaque Vert**

Plan :

Paramètres de positionnement:

- Contention : F_3H_3
- DSP : 100 cm sur la plaque
- Set Up par les lasers
- kVD = 40 cm ; kVS : kV= 40, mA= 25, mS= 4
- Table : Lat = 0 ; Lng = 125,3 cm ; Vrt = 0.1 cm
- B = kVS = 0°

Contrôles:

1. Placez la plaque verte sur la table en respectant tout les paramètres de positionnement.
2. Placez le conne d'électron sur la première plaque et puis la deuxième plaque alignée aussi par les lasers.
3. Acquérir l'image kV pour une position de kVD = 40 cm.
4. Vérifiez que les deux centres des plaques se superposent.

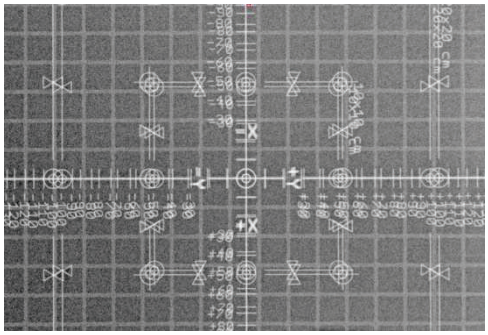

VII. Protocole – Test de Leeds (pour la qualité de l'image KV)

Fantôme utilise: Leeds Test
Plan :
Paramètres de positionnement:

- Le fantôme est placé sur le kVD.
- Le filtre Cooper est positionne sur le fantôme
- kVD = 40 cm ; kVS : kV= 40, mA= 25, mS= 4
- « ABC » activé pour le mode Flouro
- B = kVS = 0°

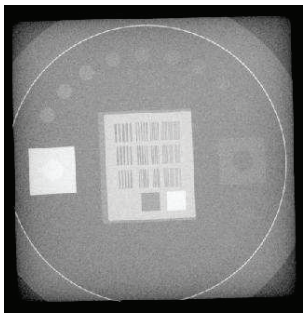

Contrôles:

1. Acquérir des images kV pour différentes positions du kVD (40, 50, 60, 80) et pour chaque mode (radiographique ou flouro).
2. Le mode radiographique : pour la résolution spatiale on doit voir en moins 10 repères et pour le contraste résolution 12 disques.
3. Le mode flouro : pour la résolution spatiale on doit voir en moins 8 repère et pour le contraste résolution 11 disques.

	Mode Radiographique				Mode Flouro			
kVD cm	40	50	60	80	40	50	60	80
Résultats résolution Spatiale								
Spécification	> 10eme repère				> 8eme repère			
Test Contraste Résolution								
Spécification	> 12 disque				> 11 disque			
Résultats	P / F				P / F			

VIII. Protocole – test pour la qualité de l'image MV

Fantôme utilise: Las Vegas (Phantom 2)
Protocole Eclipse :
Plan :

Paramètres de positionnement:

- Contention : F_2H_2
- DSP = 100 cm sur la croix du fantôme
- Set Up par les lasers
- Champ : 20 x 20 cm
- Table : Lat = 0 ; Lng = 120,3 cm ; Rot = 0 ; Vert = 1,9 cm
- Tourner la table et vérifier les
- B = 0 ; MV [50, 0, 0]
- Débit de dose = 100 UM/min ; X6
- Double exposition avant sauvegarde

Contrôles:

1. Placez le fantôme sur la table en respectant tous les paramètres pour le set up.
2. Acquérir une image portale du fantôme et effectuer les contrôles suivants :
   a.) Indique avec une croix sur le formulaire, le numéro des repères circulaires visibles sur l'image, pour chaque ligne.
   b.) Pour chaque énergie, respectez les spécifications dans la figure en bas.

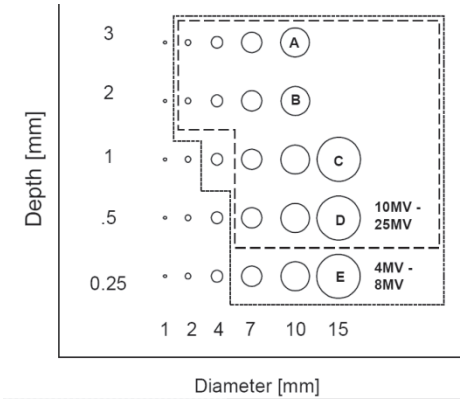

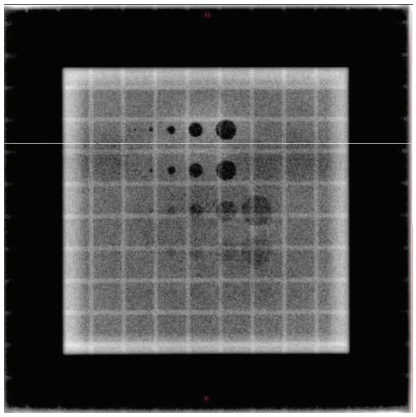

IX. Contrôle qualité de l'imageur portale (Bruit et homogénéité)

1. Acquisition d'images portales

- Avant l'irradiation cliquer sur *Maintenance* puis *Acquire Image*

Conditions d'irradiation :

Distance source- détecteur : 140 cm
Champ 27 x 20 cm2 cassette entière
Nombre d'UM délivrés : 1
Energie 6 MV et débit de dose 100 UM/ min

- Pour ce contrôle, la table ne doit pas être interposée entre la source et le détecteur ;
- Procéder à l'irradiation de la cassette entière 27x20 cm2 ; l'image apparaît (Remarque : on peut régler le contraste de l'image avec l'icône)
- Pour analyser les images aller dans : C:Programs/Files/Varian/Oncology/Treatment/AM/Images
- Pour évaluer le bruit et l'homogénéité, on délimite des zones d'intérêt ou ROI (1 centrale, 4 périphériques et 2 comprenant la quasi-totalité de la matrice)
- Remplir le tableau n°1.

Tolérance pour l'homogénéité : ± 5%
Bruit : ne doit pas dépasser la tolérance fixée par le fabricant par rapport au contrôle initial.

ROI	X	Y	DX	DY	Min	Max	Moy	DS	Homogénéité	Bruit
Haut gauche	800	100	100	100						
Bas gauche	800	550	100	100						
Centre	460	330	100	100						
Haut droite	120	100	100	100						
Bas droite	100	550	100	100						
Vertical	250	200	1	300						
Horizontal	250	200	450	1						

Appendix 6

- Abstract and poster at the 51st Annual ASTRO Meeting (November 1-5, 2009) in Chicago;

for radiotherapy have received the marker implant in different body regions (lung, liver, breast, cervix, prostate, pancreas and other sites in abdomen) using ultrasound or CT-guidance without need for anesthetics. The shape of the marker can be adjusted into a single clump, a clump with a string, a clump-string-clump form, or a string alone. Once implanted, the marker is visible with kilo voltage imaging.

Results: An evaluation of the marker implantation procedure, safety, x-ray visualization, and positioning movements during the therapy period will be presented.

Conclusions: Increasingly, we must be certain of exact localization of tumor targets by using markers in IGRT. The fine-needle marker presented here allows implantation into almost any tumor with minimal risks of internal bleeding or infection and can be implanted safely and precisely using guidance with ultrasound or CT. The Gold Anchor™ is developed for visualization with kilo voltage equipment during radiotherapy.

Author Disclosure: I. Naslund, Owner of Naslund Medical, E. Ownership Interest; P. Wersall, None; E. Castellanos, None; C. Beskow, None; S. Nyrén, None.

2954 The Exactrac Snap Verification (SV), a New Tool for Ensuring the Quality Control for Stereotactic Body Radiation Therapy (SBRT)

C. M. Udrescu[1], O. Chapet[1], B. de Bari[1], G. Michel-Amadry[2], F. Mornex[1]

[1]*Department of Radiation Oncology, Centre Hospitalier Lyon Sud, Pierre Benite, France,* [2]*Department of Medical Physics, Centre Hospitalier Lyon Sud, Pierre Benite, France*

Purpose/Objective(s): The intra-fraction patient (pt) imaging and verification provided by ExacTrac SV allows tracking possible isocenter displacement within the pt throughout treatment by SBRT and realignment during the treatment. The purpose of this study was (1) to measure the intra-fraction variations of isocenter position, (2) to study the amplitude of variation function of the fraction duration and (3) to evaluate the impact of the table movement on pt positioning, using SV.

Materials/Methods: ExacTrac SV uses X-ray real-time images acquired at any moment during treatment delivery or between fields to instantly detect and visualize isocenter displacement (beam on or off). The displacement can be measured using the fusion of the bony structures or the implanted markers with the DRRs. A tolerance margin indicates if a patient setup correction is needed or not. We already evaluated 5 pts who were treated with the ExacTrac X-ray 6D, for T1-T2 lung (4 pts) or liver (1 pt) tumors, using SBRT (mean treatment fields number = 9). The pts had a SV at each fraction, before each treatment beam. Finally, 477 beams were verified with a measure of the isocenter displacement. The time from the pt installation on the table to each SV was systematically noted. Three ''SV time'' groups were identified: SV performed at less than 10 minutes (group 1 = 36 beams), between 11 and 20 minutes (group 2 = 255 beams) and more than 21 minutes (group 3 =186 beams), after patient setup.

Results: The mean isocenter deviation for all the beams and all the fractions was 2.37 mm. The total mean time of one fraction was 22 minutes [9- 36 minutes]. The mean deviations were 1.8mm [1 - 8], 2.12mm [0 - 8] and 2.7mm [0 - 8] for group 1, 2 and 3, respectively. For the same groups, the percentages of deviation $\geq$ 3 mm were 2.6% (1/36), 20% (51/255) and 25% (46/186) and the percentage of deviation $\geq$ 5 mm were 5.2% (2/36), 4% (10/255) and 14% (26/186) respectively. In 3 pts, a table rotation was necessary. The mean isocenter deviations increased from 1.92mm before table rotation (178 beams) to 2.88mm for the first beam treated after rotation (35 beams). Pain, cough, or talk may explain the observed deviations in a few situations.

Conclusions: SV allows detecting isocenter deviations, which increase in amplitude and frequency with the fraction duration. It makes possible and highly suitable the intra-fraction verification for the SBRT, taking in account clinical condition and technical issues. With high-quality images at low X-ray doses, SV gives an accurate targeting from the beginning to the end of each fraction, inducing confidence to escalate the dose. SV appears to be an important tool for ensuring the quality control for SBRT. At the time of the meeting, results for more patients treated for lung, liver and prostate cancers will be available.

Author Disclosure: C.M. Udrescu, None; O. Chapet, None; B. de Bari, None; G. Michel-Amadry, None; F. Mornex, None.

2955 Favorable IMRT Experience Treating Obese Prostate Cancer Patients in the Prone Position using Electromagnetic Tracking and a "Belly Board"

M. D. Logsdon, J. K. Bareng, L. Olson, A. Ryan, S. W. Lee

Radiological Associates of Sacramento, Sacramento, CA

Purpose/Objective(s): We sought to extend the use of electromagnetic localization and tracking technology (Calypso Medical Technologies, Seattle, WA) to obese men with large anterior-posterior (AP) separations who would otherwise not be eligible to have their prostate localized and/or tracked if they were treated in a supine position.

Materials/Methods: Four patients of large girth (weights 189-326 lbs) were treated. The A-P dimensions of these patients precluded electromagnetic localization and tracking when they were in a supine position. This is due to the specifications of the tracking system, which limits the maximum distance from the array to the transponders to prevent gantry collision. These patients were placed in the prone position for both the treatment planning CT as well as daily radiation treatments. The first patient was treated on a solid slab of Styrofoam. In an attempt to minimize prostate motion caused by respiration, the remaining three patients were treated on a conventional ''belly board.'' PTV prescription doses ranged from 77.4-79.2 Gy. Tracking limits were set to 5 mm for all dimensions except for 4 mm posterior.

Results: Localization and tracking were accomplished successfully for all 173 fractions. The tracking logs for all patients demonstrated patterns of prostate motion attributable to breathing, predominantly in the AP axis with lesser effect along the superior-inferior (SI) axis and no effect on the lateral axis. For the first patient, the excursions due to respiratory motion were typically ± 1 mm in the SI axis and ± 2 mm in the AP axis. When a ''belly board'' was used for the subsequent 3 patients, the excursions were decreased and were typically ± 0.5 mm in the SI axis and ± 1 mm in the AP axis. Beam pauses and/or interruptions for patient repositioning were no more frequent than for more slender patients treated in the supine position.

The ExacTrac Snap Verification (SV), a New Tool for Ensuring the Quality Control for Stereotactic Body Radiation Therapy (SBRT)

Corina Udrescu (1), Olivier Chapet (1), Berardino de Bari (1), Géraldine Michel-Amadry (2), Françoise Mornex (1),

(1) Department of Radiation Oncology, UA 37-38, Centre Hospitalier Lyon Sud, Pierre Benite, France;

(2) Department of Medical Physics, Centre Hospitalier Lyon Sud, Pierre Benite, France

Abstract:

Purpose/Objective(s): The intra-fraction patient (pt) imaging and verification provided by ExacTrac® SV allows tracking possible isocenter displacement within the pt throughout treatment by SBRT and realignement during the treatment. The purpose of this study was (1) to measure the intra-fraction variations of isocenter position, (2) to study the amplitude of variation function of the fraction duration and (3) to evaluate the impact of the table movement on pt positioning, using SV.

Materials/Methods: ExacTrac® SV uses X-ray real-time images acquired at any moment during treatment delivery or between fields to instantly detect and visualize isocenter displacement (beam on or off). The displacement can be measured using the fusion of the bony structures or the implanted markers with the DRRs. A tolerance margin indicates if a patient setup correction is needed or not. We already evaluated 5 pts who were treated with the ExacTrac® X-ray 6D, for T1-T2 lung (4 pts) or liver (1 pt) tumors, using SBRT (mean treatment fields number = 9). The pts had a SV at each fraction, before each treatment beam. Finally, 477 beams were verified with a measure of the isocenter displacement. The time from the pt installation on the table to each SV was systematically noted. Three "SV time" groups were identified: SV performed at less than 10 minutes (group 1 = 36 beams), between 11 and 20 minutes (group 2 = 255 beams) and more than 21 minutes (group 3 =186 beams), after patient setup.

Results: The mean isocenter deviation for all the beams and all the fractions was 2.37 mm. The total mean time of one fraction was 22 minutes [9- 36 minutes]. The mean deviations were 1.8mm [1 - 8], 2.12mm [0 - 8] and 2.7mm [0 - 8] for group 1, 2 and 3, respectively. For the same groups, the percentages of deviation ≥ 3 mm were 2.6% (1/36), 20% (51/255) and 25% (46/186) and the percentage of deviation ≥ 5 mm were 5.2% (2/36), 4% (10/255) and 14% (26/186) respectively. In 3 pts, a table rotation was necessary. The mean isocenter deviations increased from 1.92mm before table rotation (178 beams) to 2.88mm for the first beam treated after rotation (35 beams). Pain, caugh or talk may explain the observed deviations in a few situations.

Conclusions: SV allows detecting isocenter deviations, which increase in amplitude and frequency with the fraction duration. It makes possible and highly suitable the intra-fraction verification for the SBRT, taking in account clinical condition and technical issues. With high-quality images at low X-ray doses, SV gives an accurate targeting from the beginning to the end of each fraction, inducing confidence to escalate the dose. SV appears to be an important tool for ensuring the quality control for SBRT. At the time of the meeting, results for more patients treated for lung, liver and prostate cancers will be available.

The ExacTrac® system

- Uses low energy X-rays;
- Snap Verification acquires images at any moment during the treatment, or between two beams;
- Instantly detects and visualizes the isocenter displacements even if the beam is on or off;
- Makes possible displacement measurements using fusions between the DRRs and the bony structures or implanted markers.
- A tolerance margin established by our department indicates if a patient setup correction is needed or not.

ExacTrac® X-Ray 6D

Introduction

The ExacTrac® imaging system offers an important precision for the real time positioning of the patient for every fraction and also for an easy set-up of the patient at all times during the SBRT treatment.

The Snap Verification allows:

- an accurate verification of the patient position;
- a monitoring of the isocenter displacements during the beam on or off;
- and, if it's necessary, a target realignment during the SBRT treatment.

Objectives:

1.) To measure the intra-fraction variations of the isocenter position,

2.) To study the amplitude of the variation function of the fraction duration,

3.) To evaluate the impact of the table movement on the patient positioning, using Snap Verification.

Patients and Methods:

- Seventeen (17) patients treated for T1-T2 lung (16 patients) or liver (1 patient) tumors had a Snap Verification before each treatment beam.
- 1651 beams were verified with a measure of the isocenter displacement;
- The mean treatment fields number was 8 [3 – 14 beams];

The « SV- time » groups:

The time from the patients set-up on the treatment table to each Snap Verification was systematically noted:

Group 1: SV performed at less than 10 minutes: 38 beams;

Group 2: SV performed between 11 and 20 minutes: 473 beams;

Group 3: SV performed at more than 21 minutes: 1140 beams.

Patient # 1: DRRs and ExacTrac X-ray Images

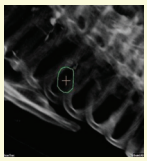

DRR 1 Image

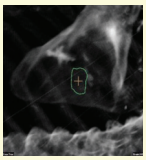

DRR 2 Image

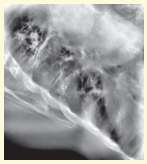

X-ray 1 Image

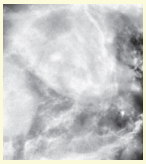

X-ray 2 Image

Results:

The mean isocenter deviation for all the beams and all the fractions was 2.10 mm.

The total mean time of one fraction was of 23 minutes [9 - 64 minutes].

The mean Snap Verification deviations were 1.65 mm [1 - 8], 2.30 mm [0 - 8] and 2,62 mm [0 - 8] for the three «SV-time» groups: 1, 2 and 3 respectively.

For these three «SV-time» groups:

- the percentages of deviation SV ≥ 3 mm were 7.89% (3/38), 13.10% (62/473) and 17.98% (205/1140);
- the percentages of deviation SV ≥ 5 mm were 5.2% (2 /36), 3.59% (17/473) and 5.17% (59/1140) respectively.

Reasons for the deviations

The table rotation

For 12/17 patients, a table rotation was necessary.

The mean isocenter deviations increased from 1.92 mm before the table rotation (178 beams) to 2.88 mm for the first beam treated after rotation (35 beams).

The patient physical condition

In some cases, deviations of the isocenter were observed for patients that:
- had pain,
- caugh or,
- talked during the irradiation treatment.

Conclusion:

Our preliminary experience on seventeen patients allows to conclude that Snap Verification is an efficient tool in detecting isocenter deviations, which increase in amplitude and frequency with the fraction duration.

It makes possible and highly suitable the intra-fraction verification for the SBRT, taking in account clinical condition and technical issues.

With high-quality images at low X-ray doses, Snap Verification gives an accurate targeting from the beginning to the end of each fraction, inducing confidence to escalate the dose.

Our department we will continue to use this technique in order to eventually reduce the PTV margins. Other types of tumors will be as well evaluated.

Snap Verification appears to be an important tool for ensuring the quality control for SBRT.

Patient # 1: Results – Fowler Adenocarcinoma

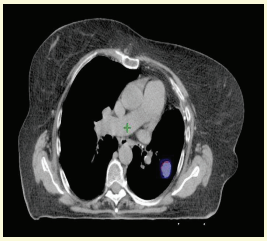

- 56 Gy in 4Gy/fraction
- 11 beams; 14 fractions
- 408 minutes (~ 30 min per fx) for 182 snaps
- End of treatment: 06/04/09

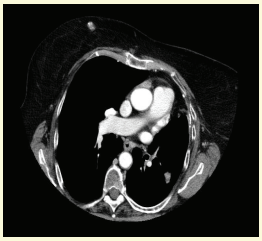

- Scanner 21/06/09:
- Diminution of the Fowler lesion size:
  20x14 mm *Vs* 25x18 mm

Appendix 7

- Abstract and poster at the SFPM meeting (5-7 June 2013) in Nice, France;

L'INFLUENCE DU NOMBRE DE CHAMPS ET DE L'ENERGIE SUR LES PLANS SBRT-RCMI POUR LES CANCERS DE LA PROSTATE
UNE EVALUATION AVEC DIFFERENTS CRITERES OBJECTIFS

Corina UDRESCU [1, 2], Olivier CHAPET [1], Ronan TANGUY [1], Benjamin PIGNATA [2], Marie-Pierre SOTTON [2],
Julien RIBOUTON [2], Amandine BENEUX [2], Patrice JALADE [2]

[1]- Service de Radiothérapie-Oncologie, [2]- Service de Physique Médicale et Radioprotection, Centre Hospitalier Lyon Sud, PIERRE BENITE, France

Introduction

Pour les irradiations stéréotaxiques il est fortement recommandé d'utiliser un grand nombre de champs pour améliorer la conformité de la dose à la cible et réduire la dose d'entrée au patient [1].

Objectifs

➡ L'objectif de cette étude a été d'évaluer l'influence du nombre de champs et de l'énergie sur un plan stéréotaxique (SBRT) de la prostate (5x6.5Gy) avec un boost-intégré (BI) dans la tumeur macroscopique (5x8Gy).

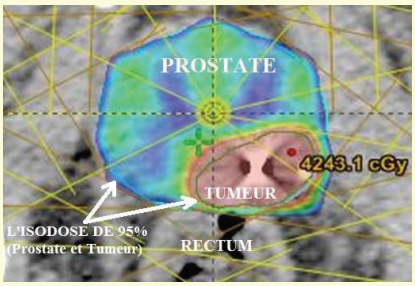

Matériel et Méthodes

La planification du traitement

1) Des simulations SBRT-RCMI ont été effectuées pour neuf patients avec trois configurations de faisceaux différentes: 7-champs (Plan1), 9-champs (Plan2) et 11-champs (Plan3). La même énergie X16, les mêmes contraintes d'optimisation et le même nombre d'itérations (300) ont été utilisés pour les 3 plans.
2) Des simulations SBRT-RCMI ont été effectuées pour cinq patients pour deux énergies différentes: X6 et X16. Le même nombre de 9 faisceaux et le même nombre d'itérations (300) ont été utilisés pour les 2 plans. Les contraintes d'optimisation ont été changées (si nécessaire) pour obtenir la même couverture du PTV dans les 2 plans.

Les paramètres d'évaluation

La comparaison des plans a été réalisée en utilisant:
a) quatre indices de conformité (CI): RTOG, van't Riet, Lomax et SALT;
b) l'indice gradient (GI) - pour le $PTV_{prostate}$;
c) l'indice d'homogénéité (HI) - pour le PTV_{tumeur}, à cause de l'influence du gradient de dose du BI;
d) les valeurs d'histogramme dose-volume pour les parois rectale et vésicale (les doses reçues par 2cc, 5cc, 10cc et 25cc).
e) la dose à l'entrée (De) - mesurée à l'axe du faisceau, à 5 mm de la peau;
f) les unités moniteurs (UM).

Résultats

L'impact du nombre de champs

Table 1. Valeurs moyennes, minimales et maximales des différentes variables.

Variable	Dose associée à une isodose	Nombre de faisceaux 7	9	11
Couverture du PTV				
V_P95% (%)	30.87 Gy	99.8 (99.5-100)	99.7 (99.3-100)	99.8 (99.3-100)
V_T95% (%)	38 Gy	100 (99.9-100)	100 (99.7-100)	100 (99.7-100)
V_P100% (%)	32.5 Gy	94.8 (91.8-96.5)	94.1 (91.4-97.1)	93.8 (88.4-97.8)
V_T100% (%)	40 Gy	95.3 (92.6-98.7)	94.1 (87.2-99)	91.3 (84.1-97.1)
3D Dmax (Gy)		42 (41.2-42.8)	42 (41.1-43.3)	41.9 (41.1-43.6)
Evaluation de la prostate				
GI_P		3.8 (3.5-4.4)	3.7 (3.6-4)	3.8 (3.5-4.1)
(P)CI_{RTOG}		1.28 (1.17-1.4)	1.26 (1.17-1.38)	1.27 (1.16-1.39)
(P)CI_{SALT}		0.99 (0.98-1)	0.99 (0.98-1)	0.99 (0.98-1)
(P)CI_{Lomax}		0.78 (0.71-0.84)	0.79 (0.73-0.85)	0.78 (0.72-0.85)
(P)$CI_{van't\ Riet}$		0.77 (0.71-0.84)	0.78 (0.72-0.83)	0.77 (0.72-0.84)
Evaluation de la tumeur				
(T)CI_{RTOG}		1.57 (1.33-1.81)	1.52 (1.33-1.7)	1.51 (1.28-1.7)
(T)CI_{SALT}		0.99 (0.99-1)	0.99 (0.99-1)	0.99 (0.98-1)
(T)CI_{Lomax}		0.64 (0.55-0.75)	0.66 (0.58-0.75)	0.66 (0.58-0.77)
(T)$CI_{van't\ Riet}$		0.63 (0.54-0.74)	0.65 (0.58-0.74)	0.65 (0.57-0.76)
$MDPD_T$		1.05 (1.03-1.07)	1.05 (1.03-1.08)	1.05 (1.03-1.09)
HI_T		0.03 (0.03-0.04)	0.03 (0.03-0.04)	0.03 (0.03-0.04)

Avec la même couverture de l'isodose de prescription, les indices d'évaluation des 3 plans sont similaires (Table 1).

Les doses moyennes reçues par *la paroi-rectale* sont de 33.7Gy, 25.8Gy, 16.7Gy et 4.8Gy pour le Plan1, 33.2Gy, 24.7Gy, 15.8Gy et 4.7Gy pour le Plan2 et 33.1Gy, 24.5Gy, 15.1Gy et 4.3Gy pour le Plan3 sur 2cc, 5cc,10cc et 25cc, respectivement.

Les doses moyennes reçues par *la paroi-vésicale* sont de 28.9Gy, 21.5Gy, 13.9Gy et 4.9Gy pour le Plan1, 28.8Gy, 21.3Gy, 13.6Gy et 5Gy pour le Plan2 et 28.7Gy, 21.1Gy, 13.5Gy et 4.8Gy pour le Plan3 sur 2cc, 5cc,10cc et 25cc, respectivement.

Les *De* moyennes reçues par faisceau pour chaque plan sont 7.8Gy, 6.3Gy et 5.8Gy pour Plan 1, 2 et 3, respectivement.

Les *UM* moyennes calculées par faisceau pour chaque plan sont 480, 386 et 323 pour Plan 1, 2 et 3, respectivement.

Le volume de l'isodose de 5 Gy a augmenté avec le nombre de faisceaux, mais le volume de l'isodose de 10 Gy a diminué (F7 *vs* F9 et F9 *vs* F11, p=0.0001 pour les 2 isodoses) (Figure 1).

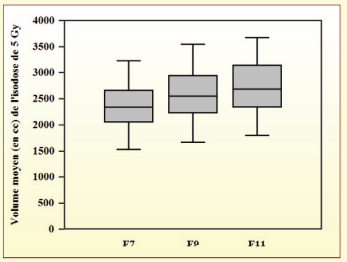

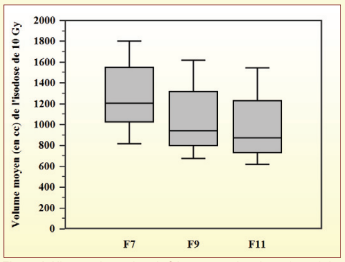

Figure 1. L'impact du nombre de faisceaux sur le volume (en cc) de l'isodose de 5 Gy et 10 Gy.

L'impact de l'énergie

Table 2. Valeurs moyennes, minimales et maximales des différentes variables.

Variable	Dose associée à une isodose	Energie X6	X16
Couverture du PTV			
V_P95% (%)	30.87 Gy	99.9 (99.8-100)	99.8 (99.5-100)
V_T95% (%)	38 Gy	100 (99.8-100)	100 (99.8-100)
V_P100% (%)	32.5 Gy	95.4 (93.5-97.6)	94 (92.6-96.7)
V_T100% (%)	40 Gy	98.5 (98.2-98.8)	93.5 (91.9-94.7)
3D Dmax (Gy)		42.1 (41.5-42.6)	41.6 (41.3-42.1)
Evaluation de la prostate			
GI_P		4 (3.8-4.3)	3.8 (3.6-4)
(P)CI_{RTOG}		1.31 (1.24-1.45)	1.27 (1.21-1.38)
(P)CI_{SALT}		0.99 (0.99-1)	0.99 (0.98-1)
(P)CI_{Lomax}		0.76 (0.69-0.8)	0.78 (0.73-0.81)
(P)$CI_{van't\ Riet}$		0.75 (0.69-0.8)	0.77 (0.72-0.8)
Evaluation de la tumeur			
(T)CI_{RTOG}		1.52 (1.42-1.61)	1.46 (1.33-1.61)
(T)CI_{SALT}		0.99 (0.99-1)	0.99 (0.99-1)
(T)CI_{Lomax}		0.65 (0.62-0.7)	0.68 (0.62-0.74)
(T)$CI_{van't\ Riet}$		0.65 (0.62-0.7)	0.67 (0.61-0.73)
$MDPD_T$		1.05 (1.04-1.06)	1.04 (1.03-1.05)
HI_T		0.02 (0.02-0.03)	0.03 (0.03-0.04)

Avec des indices d'évaluation comparables pour les deux plans (X6 vs. X16) *la couverture moyenne de l'isodose de 100% sur la tumeur est inferieure de 5% pour le PlanX16* (Table 2).

Les doses moyennes reçues par *la paroi-rectale* sont de 32.2Gy, 22.5Gy, 13.8Gy et 3.9Gy pour le PlanX6 et 32.6Gy, 23.4Gy, 14.2Gy et 3.9Gy pour le PlanX16 sur 2cc, 5cc, 10cc et 25cc, respectivement.

Les doses moyennes reçues par *la paroi-vésicale* sont de 29.3Gy, 19.4Gy, 11.4Gy et 2.2Gy pour le PlanX6 et 29Gy, 19.4Gy, 11.5Gy et 2.2Gy pour le PlanX16 sur 2cc, 5cc, 10cc et 25cc, respectivement.

Les *De* moyennes reçues par faisceau pour chaque plan sont 9.1Gy et 6.2Gy pour PlanX6 et PlanX16, respectivement.

Les *UM* moyennes calculées par faisceau pour chaque plan sont 476 et 392 pour PlanX6 et PlanX16, respectivement.

Le volume de l'isodose de 5 Gy n'a pas changé avec l'énergie, mais le volume de l'isodose de 10 Gy a diminué significativement pour l'énergie de X16 (p=0.002) (Figure 2).

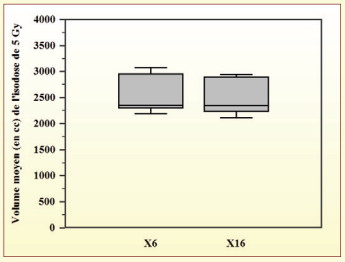

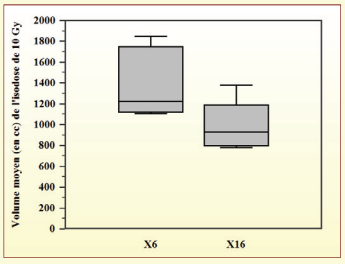

Figure 2. L'impact de l'énergie sur le volume (en cc) de l'isodose de 5 Gy et 10 Gy.

Conclusions

Pour les plans SBRT d'un cancer de la prostate avec boost-intégré:
-il n'a pas été établi d'influence du nombre de faisceaux sur les indices d'évaluation et sur les paramètres dosimétriques, mais seulement sur le volume des isodoses faibles;
- il n'a pas été établi d'influence de l'énergie sur les indices d'évaluation et sur les paramètres dosimétriques, mais sur la couverture de l'isodose de 100% dans la tumeur, sur la dose à l'entrée et sur le volume de l'isodose de 10 Gy qui diminue pour l'énergie X16.

Bibliographie

1. Benedict SH, Yenice KM, Followill D, *et al.* Stereotactic body radiation therapy: the report of AAPM Task Group 101. *Med Phys* 2010;37:4078-4101.

Appendix 8

- Abstract and poster at the 52nd Annual ASTRO Meeting (October 31 – November 4, 2010) in San Diego;

3286 A Template for Respiratory Gating in SBRT of Lung Cancer: Which Patients are to Benefit?

A. Sethi[1], D. Dave[1], C. Chollet[1], M. Hira[2], S. Nagda[1]

[1]*Loyola University Medical Center, Maywood, IL,* [2]*BrainLAB, Inc, Westchester, IL*

Purpose/Objective(s): Patients with early stage non-small cell lung cancer (NSCLC) are routinely treated using planning target volume (PTV) drawn on maximum-intensity projection 4D-CT scans. Consequently, a large volume of normal lung may be unnecessarily irradiated. In this study, we quantify benefits of respiratory gating in stereotactic body radiotherapy (SBRT) of lung patients as a function of target volume, location, extent of motion and gate parameters.

Materials/Methods: This study was based on breathing phase correlated 4D-CT scans and treatment data obtained from 79 NSCLC patients who underwent SBRT in our department. Typical PTV dose was 50 Gy in 5 fractions to at least 99% of target volume with 6MV photons and 8-12 conformal, non-opposing, non-coplanar fields. Using simulated targets in apex and middle/lower lobe of lung, the following treatment geometries were studied: target size: 1-6cm diameter, motion range (end-exhale to end-inhale) = 0.5-3 cm, and gate window: 30-40% centered on the end-exhale phase. For all cases, two conformal treatment plans were created using: (a) MIP based PTV and (b) Gated PTV. All plans were normalized to PTV dose and compared using OAR dose indices, such as lung V20, V10, D1500cc, D1000cc and heart D15cc.

Results: In general, lower lobe tumors exhibited greater range of breathing related motion (2-3 cm). For all targets, MIP based PTV ranged from 1-249 cc (mean = 67.5cc, SD = 85.9cc), whereas Gated PTV ranged from 0.5-150 cc (mean = 47.1cc, SD = 70.1cc). In MIP based plans, all targets < 4 cm diameter and up to 3 cm motion satisfied all RTOG-0813 guidelines for the OAR dose indices considered: V20 $<$ 10-15%, V10 $<$ 40%, D1500cc $<$ 12.5 Gy, and D1000cc $<$ 13.5 Gy. Therefore, these targets may not require gating. However, RTOG dose thresholds were exceeded for PTvs. > 4 cm diameter which with gating were brought to acceptable levels. Gated plans for these targets produced a decrease of up to 44% in D1000cc, 11% in V20 and 15% in V10. MIP plans for all target size and range of motion satisfied RTOG guidelines for lung D1500cc $<$12.5 Gy.

Conclusions: While all targets, regardless of size benefit from gating, the benefits of gating improve with increasing range of motion. The greatest percent improvement is seen for small targets with diameter less than 2cm. However, large targets in the lower lobe treated without gating have the greatest OAR dose burden and are most likely to benefit with gating.

Author Disclosure: A. Sethi, None; D. Dave, None; C. Chollet, None; M. Hira, None; S. Nagda, None.

3287 Dosimetric Impact of Respiration Gating on Stereotactic Body Radiation Therapy of Centrally Located Lung Tumors

A. Tai, Z. Liang, E. Gore, X. A. Li

Medical College of Wisconsin, Milwaukee, WI

Purpose/Objective(s): This study investigates dosimetric benefits of respiration gating to organs at risk (OARs) with stereotactic body radiation therapy (SBRT) treatment of centrally located lung tumors.

Materials/Methods: Data of 11 patients of early stage, medically inoperable non-small cell lung cancer (NSCLC), treated with SBRT, were retrospectively analyzed. Treatment was planned to 50 Gy and delivered in 5 fractions. Among them, 3 patients with a respiratory motion larger than 1 cm were treated with gated delivery and 8 patients were treated with free breathing (nongating). 4D-CT was acquired for each patient with a real-time position management (RPM) system. The images were sorted into 10 breathing phases with the 0% and 50% phase corresponding to the end of inhale (EI) and the end of exhale (EE), respectively. The maximum intensity projection (MIP) images were generated using either the image sets of all 10 phases (MIP10) or those of the 3 phases around EE (MIP3). The primary images were registered with the corresponding MIP images in a planning system (XiO, CMS). For a non-gated plan, the primary and MIP images are 20% phase and MIP10 images while for the gated plan they are 50% phase and MIP3 images. The internal tumor volume and OARs were delineated on the MIP images and the primary images, respectively. For this study, a new nongated plan was conducted for each of the 3 gating patients and a new gated plan was conducted for each of the 8 nongating patients. The original contours used for the actual treatment plan for each patient were populated to the new CT sets by a auto-segmentation software (ABAS, CMS Inc) based on deformable image registration. The ABAS-generated contours were carefully reviewed and manually modified if necessary by the same physician. The treatment plans followed the guidelines of RTOG lung 0813 protocols. For each patient, the gated plan and nongated plan had the same beam arrangements (gantry and couch angle), but the beam weightings may vary for achieving the same PTV coverage and the similar dose conformities.

Results: The tumor motions of these patients were 8.1 ± 4.3, 4.1 ± 1.9 and 3.0 ± 1.2 mm along superior-inferior (SR), anterior-posterior (AP) and left-right direction (LR), respectively. When gating is used, the PTV is reduced by 17% ± 10%. The V20 (volume covered by 20 Gy) and V12.5 for lung are reduced by 7% ± 8% ($p = 0.02$) and 14% ± 10% ($p = 0.001$), respectively. The V32 and V18 for heart and trachea are reduced by 39% ($p = 0.29$) and 48% ($p = 0.18$), respectively. The dose-volume reduction of lung increases as a function of the respiratory motion amplitude. The V20 and V12.5 for lung are reduced by 14% ± 12% and 26% ± 13% for the 3 gating patients and 4% ± 4% and 10% ± 4% for the rest of patients, respectively.

Conclusions: Gating ensures the safe delivery of the dose escalation in the RTOG 0813 trial.

Author Disclosure: A. Tai, None; Z. Liang, None; E. Gore, None; X.A. Li, None.

3288 Potential Interest of Developing a Focal Dose Escalation in Stereotactic Irradiation of Prostate Cancer

O. Chapet[1], C. Udrescu[1,2], M. Sotton[2], O. Rouviere[3], B. De Bari[1], J. Bouffard-Vercelli[4], P. Jalade[2]

[1]*Department of Radiation Oncology, Centre Hospitalier Lyon Sud, Lyon, France,* [2]*Department of Medical Physics, Centre Hospitalier Lyon Sud, Lyon, France,* [3]*Department of Urological Radiology, Hopital Edouard Herriot, Lyon, France,* [4]*Department of Radiology, Centre Hospitalier Lyon Sud, Lyon, France*

Purpose/Objective(s): Stereotactic irradiation is a new approach developed in low risk prostate (P) cancers. Several fractionations (≥6.5 Gy per fraction) were already evaluated with a homogenous irradiation of the whole prostate. However, the progress in

dynamic MRI often allows a visualization of the macroscopic tumors (T) in the prostate opening the way to focal therapy. The aim of the present dosimetric study was to evaluate the interest of developing an original schema of stereotactic P irradiation including a focal dose escalation into the T.

Materials/Methods: Nine patients (pts) with prostate cancer had a dosimetric CT scan/T1gadolinium MRI fusion, made on 3 implanted gold markers. The P and T were delineated by 2 radiologists on the CT/MRI fusions. Three mm were added to the P to define a PTV1 (planning target volume1), whereas 5 mm (3 mm posteriorly) were added to the T to define a PTV2. For each pts, a 9 coplanar fields IMRT plan was optimized with three different dose levels: 1°) 5 x 6.5 Gy to the PTV1 (plan1), 2°) 5 x 8 Gy to the PTV1 (plan2) and 3°) 5 x 6.5 Gy on the PTV1 combined with a focal 5 x 8 Gy on the PTV2 (plan3). Assuming an α/β ratio of 1.5 Gy, the equivalent doses are 76 Gy and 108 Gy respectively for 5 x 6.5 Gy and 5 x 8 Gy. In all the plans, at least 98% of the PTV 1 and 2 had to be covered by the 95% isodose. The doses to the rectum, bladder and femoral heads were optimized to be as low as possible. The maximum dose (MaxD), mean dose (MD) and doses received by 2% (D2), 5% (D5), 10% (D10) and 25% (D25) of the rectum and bladder walls were used to compare the 3 IMRT plans. The results below are expressed in mean values for the 9 pts.

Results: A dose escalation in the whole prostate from 5 x 6.5 Gy (plan1) to 5 x 8 Gy (plan2) increased the rectum MD, MaxD, D2, D5, D10 and D25, respectively by 3.75 Gy, 8.42 Gy, 7.88 Gy, 7.36 Gy, 6.67 Gy and 5.54 Gy. Similar results were observed for the bladder with respectively: 1.72 Gy, 8.28 Gy, 7.01 Gy, 5.69 Gy, 4.36 Gy and 2.42 Gy for the same dosimetric parameters. A focal dose escalation only in the PTV2 (plan3) reduced by about 50% the difference of doses for rectum and bladder described above with a homogenous P dose escalation. Thereby, for the rectum, the MD, D2, D5, D10 and D25 were only increased by 1.51 Gy, 4.24 Gy, 3.08 Gy, 2.84 Gy and 2.37 Gy in plan3 compared to plan1. The results for the bladder were respectively 0.43 Gy, 1.47 Gy, 1.30 Gy, 1.08 Gy and 0.76 Gy for the same parameters.

Conclusions: The present schema of focal dose escalation was created to deliver a sufficient dose to the microscopic disease into the prostate while increasing the dose to the macroscopic tumor. This approach deeply limits the doses received by the rectum and the bladder compared to a whole P dose escalation. A phase I/II trial will soon be opened in our department of radiation oncology.

Author Disclosure: O. Chapet, None; C. Udrescu, None; M. Sotton, None; O. Rouviere, None; B. De Bari, None; J. Bouffard-Vercelli, None; P. Jalade, None.

3289 Volumetric-Modulated Arc Therapy for Stereotactic Radiosurgery of Patients with Multiple, Widely-Separated Brain Metastases

H. Wagner, C. Hess, J. Sheehan, M. Ferenci

Penn State University, Hershey, PA

Purpose/Objective(s): GammaKnife (Elekta, Stockholm, Sweden) Stereotactic Radiosurgery (GKSRS), either alone or in conjunction with whole-brain irradiation, is a well-established treatment modality for brain metastases. On GKSRS models prior to the Perfexion, treatment of widely-spaced lesions potentially exposes limitations of the automated positioning system (APS) and may require trunnion-mode and/or multiple frame placements, which can significantly increase cost and treatment time. An alternate approach to treating multiple, widely-separated brain metastases using RapidArc (RA) volumetric-modulated arc therapy (Varian Medical Systems, Palo Alto, CA) was evaluated. Dosimetry and feasibility comparisons were made between RA and GKSRS.

Materials/Methods: Pairs of widely-separated, spherical, lesions were contoured onto phantom MR and CT images in extreme anterior-posterior, left-right, and superior-inferior locations. A total of 12 lesions were contoured, with diameters of 1-cm and 3-cm in each location. Treatment plans were generated for each pair of lesions of each size using GammaPlan 5.34 and Eclipse 8.6. The 1-cm lesions were planned for a dose of 20 Gy to the 50% and 80% isodose for GKSRS and RA, respectively. The 3-cm lesions were planned for a dose of 18 Gy to the same isodose lines. The RA plans included 2 planar arcs, optimized to limit normal tissue dose and normalized with 100% of the prescription dose covering 95% of the target volume. RTOG and Paddick conformity indices as well as 12 Gy volumes were compared.

Results: RTOG and Paddick conformity indices for RA plans were comparable to those of GKSRS for lesions of both sizes, with ratios (RA/GKSRS) ranging from 0.83 to 1.14. The volume receiving 12-Gy was as much as four-times larger in RA plans of 1-cm lesions, but similar for 3-cm lesions. All GKSRS plans required either trunnions or multiple frame placements.

Conclusions: Based on their similar RTOG and Paddick conformity indices alone, RA treatment plans were comparable to GKSRS plans. For smaller lesions, the potential risks from larger 12-Gy volumes need to be considered depending on the location of the lesion(s) relative to critical normal structures. RA may be considered as an alternative to GKSRS for patients with multiple, widely-separated lesions to avoid multiple frame placements, trunnion-mode treatments, or collisions.

Author Disclosure: H. Wagner, None; C. Hess, None; J. Sheehan, None; M. Ferenci, None.

3290 Treatment Time Reduction in Extracranial Radiosurgery Procedures using a New Commercially Available Software

B. E. Amendola[1,2], N. Perez[1], A. Iglesias[1], M. Amendola[1,3]

[1]Innovative Cancer Institute, South Miami, FL, [2]Wertheim College of Medicine Florida International University, Miami, FL, [3]Department of Radiology University of Miami, Miami, FL

Purpose/ Objective(s): RapidArc is a new algorithm recently developed to deliver highly focused Intensity Modulated Radiation Therapy. The purposes of this retrospective review are: 1) To determine if extracranial radiosurgery treatments could be delivered in shortened times in comparison with conventional IMRT while maintaining precision in high dose target delivery. 2) Compare the monitor units (MU) required to deliver the treatment in comparison with traditional IMRT. 3) To analyze our initial results with Stereotactic Body Radiation Therapy (SBRT) using RapidArc combined with image guided radiotherapy (IGRT).

Materials/Methods: Between October 2008 and March 2010, 45 patients were treated with Stereotactic Body Radiosurgery using RapidArc with single or multiple arcs, coplanar or non coplanar. Twenty-seven patients were treated with SBRT only and 18 patients received SBRT boost following conventional external beam fractionation. Planning was done with commercially available software using CT, MRI and PET-CT fusion depending on the diagnosis of the primary tumor. The following sites were included:

POTENTIAL INTEREST OF DEVELOPING A FOCAL DOSE ESCALATION IN STEREOTACTIC IRRADIATION OF PROSTATE CANCER

Olivier CHAPET [1], Corina UDRESCU [1-2], Marie-Pierre Sotton [2], Olivier ROUVIERE [3], Berardino DE BARI [1], Juliette Bouffard-Vercelli [4], Patrice JALADE [2],

[1] -Department of Radiation Oncology, [2] –Department of Medical Physics, EA-3738, Centre Hospitalier Lyon Sud, PIERRE BENITE, FRANCE

[3] – Department of Urological Radiology, Hôpital Edouard Herriot, LYON, FRANCE

[4] – Department of Radiology, Centre Hospitalier Lyon Sud, PIERRE BENITE, FRANCE

Background:

Stereotactic irradiation is a new approach developed in low risk prostate (P) cancers. Several fractionations (≥ 6.5Gy per fraction) were already evaluated with a homogenous irradiation of the whole prostate. The progress in dynamic MRI often allows a visualisation of a macroscopic tumors (T) in the prostate, opening a new way to focal therapy.

Purpose:

➡ To evaluate the interest of developing an original schema of stereotactic prostate irradiation including a focal dose escalation into the tumor.

Materials and Methods:

9 patients with low risk prostate cancer had 3 gold markers implanted in the prostate and :

A dosimetric CT scan (GE LightSpeed® RT16)

A T1 & T2 MRI

A fusion between the three exams was made, using the 3 markers and the General Electric Fusion ® Software

The tumor and the prostate were delineated by a radiologist on the CT/ T1 & T2 MRI fusions

Then, two PTVs (planning target volumes) were created as following:
PTV1 = 3mm margin around the prostate;
PTV2 = 5mm margin around the tumor reduced to 3mm posteriorly.

Dose prescription:

➡ For each patient, a 9 coplanar fields IMRT plan was optimized with three different dose levels:
1°) 5 x 6.5Gy to the PTV1 (plan1),
2°) 5 x 8Gy to the PTV1 (plan2) and
3°) 5 x 6.5Gy in the PTV1 combined with a focal 5 x 8Gy in the PTV2 (plan3).
➡ Assuming an α/β ratio of 1.5Gy, the equivalent doses are:
• 5 x 6.5Gy = 32.5 Gy ≈ 76Gy and
• 5 x 8Gy = 40 Gy ≈ 108Gy

Dosimetry:

➡ In all the plans, at least 98% of the PTV1 and PTV2 had to be covered by the 95% isodose line.

➡ The doses to the rectum, bladder and femoral heads were optimized to be as low as possible.

➡ The maximum dose (MaxD), mean dose (MD) and doses received by 2% (D2), 5% (D5), 10% (D10) and 25% (D25) of the rectum and bladder walls were used to compare the 3 IMRT plans.

➡ The results below are expressed in mean values for the 9 pts.

Results:

➢ ***A dose escalation in the whole prostate from 5 x 6.5Gy (plan1) to 5 x 8Gy (plan2)*** increased the rectum MD, MaxD, D2, D5, D10 and D25, respectively by 3.75Gy, 8.42Gy, 7.88Gy, 7.36Gy, 6.67Gy and 5.54Gy.

➢ Similar results were observed for the bladder with respectively: 1.72Gy, 8.28Gy, 7.01Gy, 5.69Gy, 4.36Gy and 2.42Gy for the same dosimetric parameters.

➢ ***A focal dose escalation only in the tumor visible on the MRI (plan3)*** will increase the D2, D5, D10 and D25 for the rectum respectively of 1.51Gy, 4.24Gy, 3.08Gy, 2.84Gy and 2.37Gy compared to plan1.

➢ The results for the bladder were increased respectively of 0.43Gy, 1.47Gy, 1.30Gy, 1.08Gy and 0.76Gy for the same parameters.

➢ The increased variation of doses to the rectum and bladder (excepting the Dmax) in the plan 3 (versus plan 1) was limited and reduced by about 50% compared to the plan 2 (dose escalation in the whole prostate).

Tables. Mean values (in cGy) of dosimetric parameters for the rectum and bladder, for the 9 patients and for the 3 plans.

Rectum	5 X 6.5Gy on P only	Focal irradiation	5 X 8Gy on P only
D2	3134	3558	3922
D5	2881	3190	3617
D10	2374	2658	3040
D25	1252	1489	1806
MD	971	1122	1346
MaxDose	3378	4201	4220

Bladder	5 X 6.5 Gy on P only	Focal irradiation	5 X 8 Gy on P only
D2	3003	3151	3704
D5	2509	2639	3078
D10	1947	2055	2383
D25	1018	1094	1260
MD	738	781	910
MaxDose	3367	3727	4195

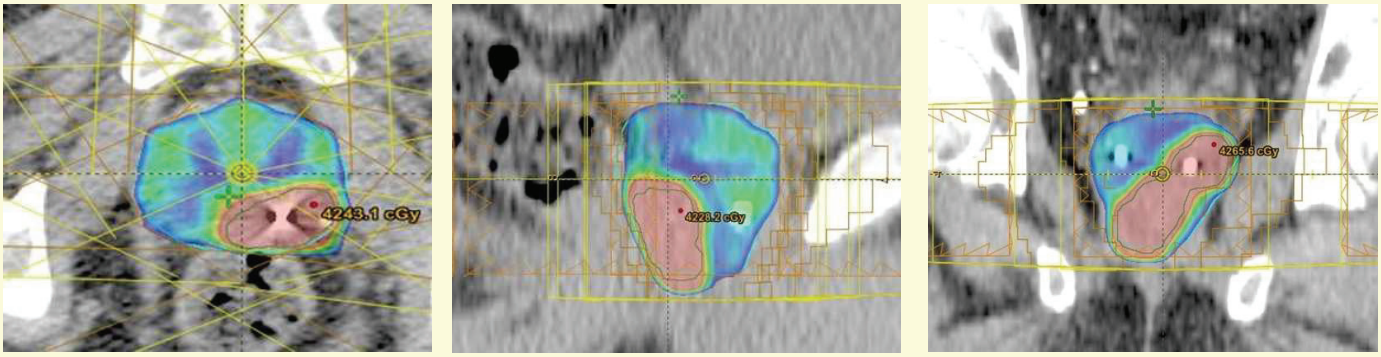

Figure. Example of a prostate irradiation at 6.5Gy with a focal dose escalation of 8Gy into the tumor.

Conclusions:

The present schema of focal dose escalation was created to deliver a sufficient dose to the microscopic disease into the prostate while increasing the dose to the macroscopic tumor.

This approach deeply limits the doses received by the rectum and the bladder compared to a whole prostate dose escalation.

In our radiation oncology department, a phase I trial is opening to evaluate 4 levels of focal dose escalation.

This project of stereotactic body radiation therapy (SBRT) in prostate cancer is supported by the Department of Clinical Research of the University Hospital in Lyon, France.

Appendix 9

- Abstract and poster at the 54th Annual ASTRO Meeting (October 28 – 31, 2012) in Boston;

- "*Digital Poster Discussion Abstract*" at ASTRO 2013

each case. This was done by making the SIB equal the prostate (CTV) contour, and then coming 5 mm off of the bladder, rectum, penile bulb, and the "anterior stripe". The anterior stripe was drawn on each prostate slice as a 0.8cm spot in the mid gland that was then extended 3cm anteriorly. The SIB did not extend outside the prostate gland and was adjusted if necessary. PTV was based on standard expansion of the prostate (CTV) contour by 5 - 6mm, 3mm posteriorly. Contouring was solely CT based, and all patients had fiducial markers. Plan was rerun with the tomotherapy Treatment Planning System (TPS), administering 1.8 Gy x 45# = 81 Gy to the PTV, and the SIB was prescribed 2.0 Gy x 45# = 90 Gy. These plans were not used for treatment, but were compared with the patients' actual treatment plans.

Results: The average treatment volumes were 28.0 cc for the SIB, 60.3 cc for the CTV, and 114.8 cc for the PTV. The mean dose to the prostate (CTV) was 82.97 Gy in the standard plan, and 89.80 Gy in the dose painting plan ($p < 0.00001$), for an 8.2% increase. This resulted in a BED that was 11.6% increased, based on an alpha-beta value of 3.0. However, the rectal median dose was only increased by 2.4%, and the bladder median dose was only increased by 3.6%. Rectal V70 dropped from 9.4% to 8.1% with the dose painting plan, and the bladder V70 dropped from 13.9% to 13.4%. Penile bulb median dose was identical at 44 Gy. All these changes in normal tissue dose were statistically non-significant. Treatment delivery times were identical at 217 seconds.

Conclusions: Dose painting a generic peripheral zone was very straightforward, allowing a simultaneous integrated boost to be prescribed. This resulted in a significantly higher BED to be administered to the prostate gland overall, yet the rectal and bladder dosages were not significantly increased. This may improve the therapeutic ratio. We plan to test this strategy for intermediate - high risk cases and also incorporate 3T MRI fusion to help improve demarcation of prostate contour, peripheral zone, urethra, and tumor nodule(s).

Author Disclosure: D.A. Kelly: None. R. Jamison: None. S. Rhoades: None. V. Woo: None.

2499

Injection of Hyaluronic Acid (HA) to Better Preserve the Rectal Wall in Prostate Hypofractionated Radiation Therapy (HFR)

O. Chapet,[1] C. Udrescu,[1] A. Ruffion,[2] M. Sotton,[3] C. Enachescu,[1] M. Devonec,[2] M. Colombel,[4] D. Azria,[5] and P. Jalade[3]; [1]*Department of Radiation Oncology, Centre Hospitalier Lyon Sud, France,* [2]*Department of Urology, Centre Hospitalier Lyon Sud, France,* [3]*Department of Medical Physics, Centre Hospitalier Lyon Sud, France,* [4]*Department of Urology, Hopital Edouard Herriot, France,* [5]*Department of Radiation Oncology, Centre Val d'Aurelle Montpellier, France*

Purpose/Objective(s): Several studies are in favor of an α/β ratio of less than 3 Gy for prostate (P) cancer, encouraging HFR. However, the development of such radiation patterns can only be done if the risk of rectal toxicity is well controlled. The objective of the present study was to evaluate the contribution of an injection of HA between the rectum and the P to reduce the risk of rectal toxicity in a HFR approach.

Materials/Methods: A phase II study of HFR at 62 Gy in 20 fractions (BED = 84 Gy; $\alpha / \beta = 1.5$ Gy) is currently conducted. A transperineal injection of 10cc of HA is systematically performed, between the rectum and the P, under local anesthesia and under ultrasound guidance. A dosimetric CT scan is performed before (CT1) and after injection (CT2). Patients are treated with a 7 beams IMRT plan, optimized on the CT2. For the first 12 patients included in the study, the same treatment plan was optimized on CT1. The rectum was empty on the 2 CTs and defined from 2cm above the seminal vesicles to 2cm below the P. The rectal wall was defined by an internal expansion of 5 mm. The volumes of rectum irradiated, with and without HA, were compared on the following dosimetric parameters: maximum dose (D max), dose to 2.5cc (D2.5), 5cc (D5) and 10cc (D10) of rectal wall and volume of rectum receiving 90% (V90), 80% (V80) and 70% (V70) of the prescribed dose of 62 Gy. To limit a potential impact of variation of rectal volume between the two CT, all results are given in cc and not in% of volume.

Results: The mean P volume was 50.2cc (30cc - 93.8cc) on the CT1 and 51cc (32.5cc - 92.7cc) on the CT2. The injection of HA reduced the mean D max value to the rectal wall of 1 Gy (61 Gy vs 62 Gy). The mean values of V90, V80, and V70 are reduced by 77.2% (1.76cc vs 7.73cc), 59.3% (4.23cc vs 10.40cc) and 47.16% (7.16cc vs 13.55cc). Same way, the average values of D2.5, D5 and D10 are reduced by 9.4 Gy (51.7 Gy vs 61 Gy), 12.9 Gy (45.4 Gy vs 58.3 Gy) and 8.3 Gy (36.9 Gy vs 45.2 Gy).

Conclusions: In this study, the injection of HA limited the doses to the rectal wall. These results suggest that late toxicities could be significantly reduced. A phase II study is underway to assess the rate of late rectal toxicities when a HFR at 62 Gy in 20 fractions is combined with an injection of HA.

Author Disclosure: O. Chapet: H. Travel Expenses; IPSEN, ASTELLAS. C. Udrescu: None. A. Ruffion: None. M. Sotton: None. C. Enachescu: None. M. Devonec: None. M. Colombel: None. D. Azria: None. P. Jalade: None.

2500

Long-term Effects on Quality of Life After Treatment of Localized Prostate Cancer: A Comparison of 4 Different Treatment Modalities

M. Hjalm-Eriksson,[1] A. Ullén,[1] J. Hugosson,[2] S. Nilsson,[1] B. Lennernäs,[3,3] and Y. Brandberg[1]; [1]*Karolinska University Hospital, Institution of Oncology and Pathology, Stockholm, Sweden,* [2]*Salgranska University Hospital, Institution of Urology, Gothenburg, Sweden,* [3]*Sahlgrenska University Hospital, Jubileums Kliniken, Department of Oncology, Gothenburg, Sweden*

Purpose/Objective: This cohort study aims to compare late effects on Health Related Quality of Life (HRQOL) of four different treatment modalities used in patients with localized prostate cancer (PC).

Materials/Methods: All men diagnosed and treated for PC at a single center during 1988 to 1997 were included. Treatment options were retro pubic prostatectomy (RPP), external beam radiation therapy (EBRT), combined EBRT and high dose rate brachytherapy (EBRT/ HDR) or cryoablation (Cryo). Between October 2000 and mars 2001 all patients still alive were asked to answer the EORTC-QLQ- C30 and EORTC QLQ-PR25 questionnaires, in average 6.9 years after diagnosis. In total 451 out of 570 (79.1%) patients completed the questionnaires.

Results: Overall, the mean scores of the HRQoL variables were high and the symptom items were low in all treatment-groups. There was a statistical significant difference in overall quality of life ($p = 0.01$, $p = 0.0065$) and physical function ($p = 0.0001$, $p = 0.0009$), between treatment groups in both univariate and multivariate regression analysis taking into account; age, prostate cancer relapse and neoadjuvant hormonal treatment, depending on lower scores in the EBRT-group. The addition of "risk group at diagnosis" or "time from diagnosis to time for questionnaire" as confounding factors, did not change the results. Both the EBRT and the EBRT/ HDR groups reported more bowel symptoms than the RPP and Cryo in both the EORTC QLQ C30 and PR 25 questionnaires ($p = 0.001$, $p \geq 0.0001$). Patients in the EBRT group also reported significantly worse fatigue and urinary problems than the other groups ($p = 0.006$, $p \geq 0.0001$). In the PR25 questionnaire, Cryo patients were less sexually active than the other groups; 15% compared to 37% in RPP, EBRT/HDR and 34% in EBRT. Among sexually active patients, there was no statistical difference between groups concerning sexual function.

Conclusions: Although the groups differed significantly regarding clinical data, the patient reported HRQoL for the RPP, EBRT/HDR and Cryo groups were quite similar. The EBRT group reported more fatigue as well as more bowel and urinary symptoms. This finding could not be explained by differences concerning risk group profiles or age distributions among the groups. Co-morbidity might be an important explanation, but was not investigated in this study.

Author Disclosure: M. Hjalm-Eriksson: None. A. Ullén: None. J. Hugosson: None. S. Nilsson: None. B. Lennernäs: None. Y. Brandberg: None.

INJECTION OF HYALURONIC ACID (HA) TO BETTER PRESERVE THE RECTAL WALL IN PROSTATE HYPOFRACTIONATED RADIOTHERAPY (HFR)

Olivier CHAPET [1], Corina UDRESCU [1-3], Alain RUFFION [2], Marie-Pierre SOTTON [3], Ciprian ENACHESCU [1], Marian DEVONEC [2], Marc COLOMBEL [4], David AZRIA [5], Patrice JALADE [3],

[1]-Department of Radiation Oncology, [2]- Department of Urology, [3] –Department of Medical Physics, EA-3738, Centre Hospitalier Lyon Sud, PIERRE BENITE, FRANCE

[4] – Department of Urology, Hôpital Edouard Herriot, LYON, FRANCE, [5]- Department of Radiation Oncology, Centre Val d'Aurelle, MONTPELLIER, FRANCE

Background:

Randomized trials demonstrated that an increased dose improves the biochemical failure free survival in external radiotherapy for low to intermediate risk prostate cancer.

Several studies are in favour of an α/β ratio of less than 3 Gy for prostate cancer, encouraging HFR. However, the development of such radiation patterns can only be done if the risk of rectal toxicity is well controlled.

The results of Phase I or II trials showed that an HFR with dose per fraction higher than 3Gy can be associated with late grade ≥ 2 rectal toxicities between 15% and 25%.

Purpose:

➡ The objective of the present study was to evaluate the dosimetric contribution of an injection of HA between the rectum and the prostate to reduce the dose to the rectum in a HFR approach.

Materials and Methods:

a.) Patient condition:

• In a phase II study, patients with low- or intermediate-risk prostate cancer are treated by exclusive IMRT technique with a total dose of 62 Gy in 20 fractions of 3.1Gy daily fraction, 5 days per week (BED = 84Gy with α/β ratio of 1.5 Gy).
• Three gold markers are implanted in the prostate, for CT/MRI fusion and daily repositioning.
• A transperineal injection of 10 cc of HA (NASHA™ Spacer gel, Q-Med AB, Uppsala, Sweden) is systematically done between the rectum and the prostate, under local anaesthesia and under ultrasound guidance (Figure 1).

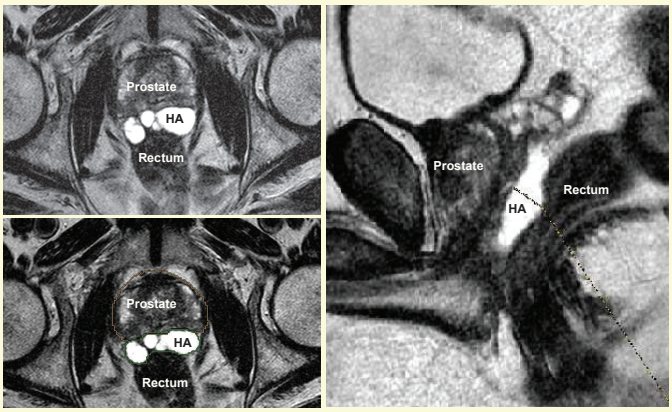

Figure 1: AH between the rectum and the prostate

b.) Treatment volumes definition:

A dosimetric CT scan is performed before (CT1) and after injection (CT2).
For each of the two CT scans, the following volumes were created:

CTV1 (Clinical Tumor Volume) = corresponding to the prostate and the first centimeter of the seminal vesicles;
CTV2 = corresponding to the prostate only;
PTV1 (Planning Target Volume) = corresponding to the CTV1 with a margin of 8 mm in all directions, excepting posterior where the margin was of 4 mm;
PTV2 = corresponding to the CTV2 with a margin of 8 mm in all directions, excepting posterior where the margin was of 4 mm;
The rectum was empty on the 2 CTs and defined from 2 cm above the seminal vesicles to 2 cm below the prostate. The rectal wall was defined by an internal expansion of 5 mm.

c.) Dosimetry:

The patients are treated with a 7-beam IMRT plan, optimized on the CT2. For the first 16 patients included in the study, the same treatment plan was optimized on the CT1 for the dosimetric comparison.

➡ The PTV1-PTV2 was covered by the 2.1 Gy isodose (95% of 2.2Gy) and 90% of this volume received at least 2.2 Gy per fraction (BED = 46 Gy with α/β = 1.5 Gy).

➡ The PTV2 was covered by the 2.95 Gy isodose (95% of 3.1Gy) and 90% of the PTV2 received at least 3.1 Gy.

d.) Data analysis:

The volumes of rectum, irradiated with and without HA, were compared on the following dosimetric parameters: maximum dose (D max), dose to 2.5cc (D2.5), 5cc (D5) and 10cc (D10) of rectal wall and volume of rectum receiving 90% (V90), 80% (V80) and 70% (V70) of the prescribed dose of 62 Gy. To limit the potential impact of the variation of the rectal volume between the two CTs, all results are given in cc and not in % of volume.

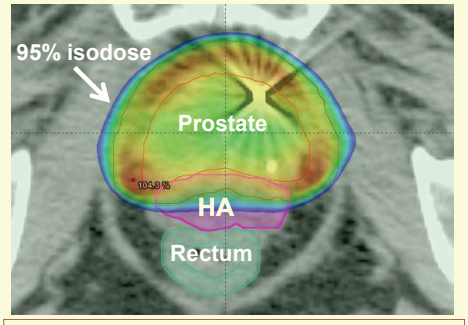

Figure 2: Example of rectal wall preservation with HA injection.

Results:

➢ The mean prostate volume was 51.7 cc (range, 28.7 - 93.9) on the CT1 and 52.7 cc (range, 31.4 - 92.7) on the CT2.

➢ The mean values of V90, V80, and V70 are reduced by 73.8% (p<0.0001), 55.7% (p=0.0003) and 43% (p=0.01), respectively.

➢ Same way, the average values of D2.5, D5 and D10 are reduced by 8.5 Gy (p<0.0001), 12.3 Gy (p<0.0001) and 8.4 Gy (p=0.005), respectively.

Table. Mean values for the rectum wall for CT1 and CT2 plans.

	Without HA		With HA
D max	62.4Gy		61.2Gy
V90	7.65cc	73.8%	2.1cc
V80	10.4cc	55.7%	4.6cc
V70	13.3cc	43%	7.6cc
D2.5	60.9Gy	8.5Gy	52.4Gy
D5	58.5Gy	12.3Gy	46.2Gy
D10	45.7Gy	8.4Gy	37.3Gy

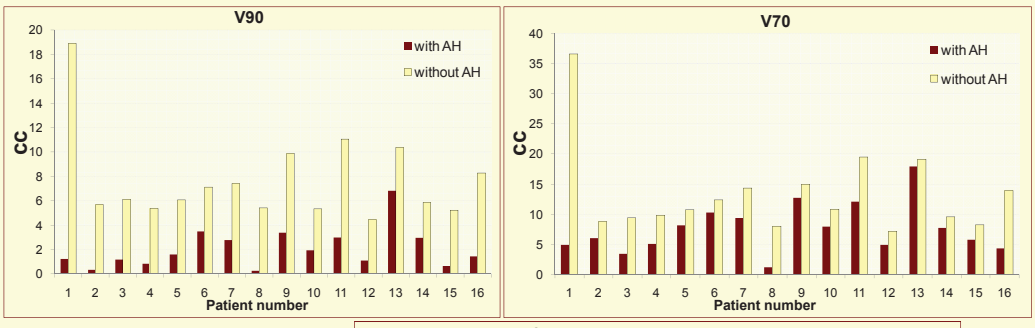

Figures. V90 and V70 for the rectum wall, by patient, with and without HA.

Conclusions:

In this study, the injection of HA limited the doses to the rectal wall. These results suggest that late toxicities could be significantly reduced. A phase II study is underway to assess the rate of late rectal toxicities when a HFR at 62 Gy in 20 fractions is combined with an injection of HA.

This project of hypofractionated irradiation in prostate cancer is supported by the Department of Clinical Research of the University Hospital in Lyon, France.

correlate with increased risk of biochemical failure and may present a potential target for focally-directed, dose-escalated radiation therapy.
Author Disclosure: G. Shukla: None. M. Rosen: None. S. Both: None. N. Vapiwala: None. J. Bekelman: None. J. Christodouleas: None. Z. Tochner: None. C. Deville: None.

1064

Acute Rectal Toxicities for 180 Prostate Carcinoma Patients Administered Spacer Material in Conjunction With Radiation Therapy

L. Barnes, K. Tokita, T. Kim, A. Mesa, M. Gazzaniga, L. Kobashi, A. Alavi, and J. Ravera; *KSK Medical, Irvine, CA*

Purpose/Objective(s): To present acute rectal toxicities for 180 patients who were administered spacer material in conjunction with prostate cancer radiation therapy.
Materials/Methods: Between January 2010 and August 2012, 180 prostate carcinoma patients were administered a spacer material in conjunction with radiation therapy. The spacer is administered transperitoneally. Injection of the spacer gel between the prostate rectal interspace creates a gap on the order of 1 cm between the prostate and rectum. This gap provides a physical dosimetric advantage for rectal dose sparing. These 180 patients underwent either a combination course of therapy consisting of external beam IMRT (5040 cGy) and HDR brachytherapy (2200 cGy) or full course external IMRT treatments. We analyzed this group for acute toxicity. Rectal symptoms were evaluated for increased stool/diarrhea over baseline and graded according to the Common Terminology Criteria for Adverse Events V.4.0 for gastrointestinal disorders.
Results: Median follow-up was 3 months. Of these 180 patients, 19 patients (10.5%) exhibited grade 1 acute diarrhea, 1 patient (0.6%) exhibited grade 2 acute diarrhea, and no patients exhibited acute diarrhea symptoms of grade 3 or greater. This is in contrast to previously published historical controls who did not receive spacer material. Historical control data from our clinic show a 29.7% incidence of grade 1, 2, and 3 acute diarrheas, while this group with injected spacer material shows an 11.1% incidence of grade 1, 2, and 3 acute diarrhea with no patients exhibiting greater than grade 2 symptoms.
Conclusions: This group of 180 patients represents one of the largest cohorts of patients to have received spacer material in conjunction with prostate carcinoma radiation therapy. The data reveal acute rectal toxicities are both rare and relatively mild for patients administered spacer material. In comparison with historical controls, the reduction in rectal symptoms is clearly significant with an almost 65% reduction in grade 1, 2 and 3 acute rectal symptoms. Our experience shows the use of a spacer material is highly effective in sparing the rectum.
Author Disclosure: L. Barnes: None. K. Tokita: None. T. Kim: None. A. Mesa: None. M. Gazzaniga: None. L. Kobashi: None. A. Alavi: None. J. Ravera: None.

1065

Hypofractionated Intensity Modulated Radiation Therapy With Injection of Hyaluronic Acid for Localized Prostate Cancer: Results of a Phase 2 study (RPAH1)

O. Chapet,[1] E. Decullier,[2] A. Faix,[3] A. Ruffion,[4] P. Jalade,[5] P. Fenoglietto,[6] C. Enachescu,[1] and D. Azria[6]; [1]*Department of Radiation Oncology, Centre Hospitalier Lyon Sud Pierre Benite, France,* [2]*Pôle Information Médicale Évaluation Recherche, Hospices Civils de Lyon, France,* [3]*Department of Urology, Clinic Beausoleil Montpellier, France,* [4]*Department of Urology, Centre Hospitalier Lyon Sud Pierre Benite, France,* [5]*Department of Medical Physics, Centre Hospitalier Lyon Sud Pierre Benite, France,* [6]*Department of Radiation Oncology and Physics, CRLC Val d'Aurelle-Paul Lamarque, Montpellier, France*

Purpose/Objective(s): Several studies are in favor of an α/β ratio of less than 3 Gy for prostate cancer, encouraging hypofractionated radiation therapy (RT). However, the development of such radiation patterns can only be done if the risk of rectal toxicity is well controlled. In a multicentric phase II trial, hypofractionated irradiation was combined with an injection of hyaluronic acid to preserve the rectum wall.
Materials/Methods: From 2010 to 2012, 36 patients with low to intermediate risk prostate cancer were included in this study (IRB and informed consent). A transperineal injection of 10 cc of HA was performed between the rectum and the prostate under local anesthesia and ultrasound guidance. Three gold markers were implanted within the prostate for CT/MRI fusion and Image Guided RT (IGRT). An intensity-modulated RT technique was used to deliver 62 Gy in 20 fractions of 3.1 Gy (BED = 84 Gy; α/β = 1.5 Gy). Acute toxicity (CTCAE v4.0) was defined as occurring during RT and up to 3 months after RT. Tolerance of HA was evaluated with a visual analog scale during injection, 30 minutes post-injection and at each visit. Preliminary results (tolerance of the injection and acute toxicity rates) on 28 patients with a follow-up of at least 3 months after RT are presented in this abstract.
Results: Injection of HA induced a mean pain score of 4.9 +/- 1.9. After 30 minutes, one patient still noted a pain score of 3 but no residual pain or discomfort persisted during treatment and follow-up. No grade $\geq$2 acute rectal toxicity occurred. Only grade 1 rectal toxicity were reported during treatment (n = 15, 53.6%). Three months after completion of RT, all rectal toxicity had completely regressed. The incidence of grade 0, 1, and 2 acute urinary toxicity was 3.6%, 42.8%, and 53.6%, respectively. At 3 months, 34.6% and 3.8% of patients had a residual urinary toxicity graded 1 and 2, respectively.
Conclusions: In the present study, the combination of IGRT with injection of HA allows the delivery of hypofractionated irradiation in 4 weeks with a dose per fraction >3 Gy without any significant acute rectal toxicity. Complete analyses of the 36 patients will be presented at the time of the meeting.
Author Disclosure: O. Chapet: None. E. Decullier: None. A. Faix: None. A. Ruffion: None. P. Jalade: None. P. Fenoglietto: None. C. Enachescu: None. D. Azria: None.

1066

Improved Geometric Performance of Diffusion-Weighted Imaging for Prostate Tumor Delineation Using a Readout-Segmented Echo-Planar-Imaging Technique

W. Foltz, T. Stanescu, J. Lee, A. Simeonov, D. Jaffray, T. Craig, P. Chung, and C. Ménard; *Princess Margaret Hospital, Toronto, ON, Canada*

Purpose/Objective(s): Geometric accuracy is fundamental for incorporation of functional imaging into radiation therapy, yet these factors are underemphasized in clinically standard diffusion-weighted imaging (DWI) using single-shot echo-planar imaging (EPI). The alternative use of readout-segmented EPI DWI has been shown to reduce distortion by significantly shortening the echo-spacing compared to single-shot EPI. An additional 2D navigator pulse corrects for motion effects between segments. This project investigates readout-segmented-EPI DWI during endorectal coil MRI for treatment planning of patients with prostate cancer enrolled on an ongoing prospective clinical trial of tumor dose escalation.
Materials/Methods: All studies used a 3 Tesla MRI system combined with a phased-array endo-rectal receiver coil (ERC). DWI was acquired with 1.4 x 1.4 x 3-mm voxels and 4 b-values of 0, 250, 800, and 1000 s/mm^2. In vitro: A prostate geometric accuracy phantom was constructed as a set of 3 concentric water-filled cylinders of 1.5, 3, and 6 cm radii consistent with the ERC diameter, anterior border of the peripheral zone, and anterior border of the prostate respectively. Segmented EPI and standard DWI were acquired, meshes for cylinder boundaries were generated, and cylinder boundaries were tracked to quantify distortion (MIPAV). In vivo: In vivo geometric performance improvement was validated in patients with prostate cancer (n = 7), by visualization of distortion relative to T2-weighted (T2w) anatomic images.
Results: In vitro: Compared to standard DWI, segmented-EPI DWI reduced the mean RMS displacement of inner and middle cylinders 3-fold (to 0.5 mm) and reduced the maximum distortion from 13 to 3 mm. In vivo: In all patients, segmented-EPI DWI provided good image quality with visible tumor. Standard DWI was not performed in the 7th patient. All

Appendix 10

- Abstract and poster at the ESTRO 31 conference (09-13 May, 2012) in Barcelona, Spain selected for "*Young scientists ESTRO Poster Session*";

There is a significant difference in the mean intra fraction motion between the standard thermoplastic mask and the Hybrid thermoplastic mask. In the group with the Hybrid thermoplastic mask the mean intra fraction motion is smaller in the LR translation: μ=-0.1 mm vs. 0.3 mm (p<0.01), and in the AP-rotation: μ=-0.1° vs. 0.2°, (p=0.015). The standard deviations of the intra fraction motion were significantly different in the translations of the LR-direction (SD=0.4 mm vs. 0.6, p=0.005) and the AP-direction (SD=0.3mm vs. 0.4 mm, p=0.046) in favor of the Hybrid thermoplastic mask.

Conclusions: The use of a Hybrid thermoplastic mask vs. a standard thermoplastic mask, in stereo tactic radiotherapy of brain metastasis, gives a small improvement in the initial patient set-up. Furthermore, the intra fraction motion can be slightly reduced with the use of a Hybrid thermoplastic mask. However, the differences in set up errors, of both masks, are very small (<0.5 mm and 1°).

POSTER DISCUSSION: YOUNG SCIENTISTS 1: STEREO-TACTIC AND PALLIATION

PD-0277

STEADY DIET AS PROPHYLAXIS OF ACUTE DIARRHEA IN PREOPERATIVE PELVIC RADIOTHERAPY OF RECTAL ADENOCARCINOMA

E. Arregui López[1], C. Bueno Serrano[1], G. Quintana Navarro[2], M. Rodríguez Liñán[1], A. Béjar Luque[1], E. Rivín del Campo[1], A. Otero Romero[1], S. García Cabezas[1], A. Palacios Eito[1]

[1]*Hospital Universitario Reina Sofía, Radiation Oncology, Córdoba, Spain*

[2]*Hospital Universitario Reina Sofía, Department of Nutrition, Córdoba, Spain*

Purpose/Objective: Concomitant preoperative radiotherapy with capecitabine is one of the choice treatments in patients with rectal adenocarcinoma. This treatment has benefits for local tumor control, however it does have its complications. The main one being radiation diarrhea greatly affecting quality of life. Change in diet is essential as prophylaxis as well as for treatment in this case. The aim of this paper is to prove the superiority of a steady diet versus a diet based on general recommendations in regards to reducing the frequency and severity of radiadion diarrhea.

Materials and Methods: A prospective, randomized, controlled trial of 29 patients with adenocarcinoma of the rectum treated with pelvic radiotherapy with concomitant preoperative capecitabine. Patients were divided into two groups: **control group**, patients on a recommendation based on exclusion diets and a **steady diet group**. Patients were evaluated at baseline, at three weeks and after radiotherapy. At each visit we evaluated the weight, toxicity (CTC v2.0 scale) and quality of life with the validated FACIT-D questionnaire.

Results: Between November 2010 and May 2011, a total of 29 patients were evaluated. The median dose received in pelvis was 45Gy. Fourteen patients were included in the control group and 15 in the steady diet group.

The control group showed a significant increase in incidence and grade of acute diarrhea (≥G2 in CTC v2.0 scale) at the end of treatment compared with the steady diet group (p=0.035).

The mean weight loss in the control group at 3 weeks was 1.02kg while there was a 1.22Kg (p=0.024) gain in the steady group. At the end of the treatment, the control group lost 2.12kg and the steady diet group gained 1.41kg (p=0.001).

At three weeks, patients in steady group showed less decreased in quality of life (FACIT-D) than control group (p=0.02). These differences remained at the end of the radiotheraphy, although it were not significant (p=0.64).

Conclusions: The steady diet reduces the incidence of acute radiation diarrhea compared to that of a diet based on general recommendations. Moreover, this diet reduces weight loss significantly and could reduce the impact of quality of life.

PD-0278

INJECTION OF HYALURONIC ACID (HA) PRESERVES THE RECTAL WALL IN PROSTATE STEREOTACTIC BODY RADIATION THERAPY (SBRT)

C. Udrescu[1], A. Ruffion[2], M.P. Sotton[3], M. Devonec[2], M. Colombel[4], P. Jalade[3], O. Chapet[1]

[1]*Centre Hospitalier Lyon Sud, Radiation-Oncology, Pierre Benite, France*

[2]*Centre Hospitalier Lyon Sud, Urology, Pierre Benite, France*

[3]*Centre Hospitalier Lyon Sud, Medical Physics, Pierre Benite, France*

[4]*Hopital Edouard Herriot, Urology, Lyon, France*

Purpose/Objective: Several publications already described the experiences of SBRT for prostate cancer. The treatment is then delivered in only 4 to 5 fractions of 6.5 Gy to 10 Gy using a technique of image-guided radiation therapy. If the interest of SBRT appears evident for the patients, the development of such radiation patterns, in any department of radiation oncology, can only be done if the risk of rectal toxicity is well controlled. The objective of the present study was to evaluate the contribution of an injection of HA between the rectum and the prostate (P) to reduce the risk of rectal toxicity in SBRT approaches.

Materials and Methods: As part of a Phase II study of hypofractionated radiotherapy (62Gy in 20 fractions), the patients had a transperineal injection of 10cc of HA (NASHA™ Spacer gel, Q-Med AB, Uppsala, Sweden) between the rectum and the P, under local anesthesia and ultrasound guidance. A dosimetric CT scan was systematically performed before (CT1) and after the injection (CT2). The present dosimetric study was performed on the two CT scans of the first 10 patients included in this study. Two 9-beam SBRT plans, using an Intensity Modulated Radiation Therapy technique, were optimized on the CT1 and CT2 according to 2 levels of dose: 5 x 6.5Gy (Plan A) and 5 x 8.5Gy (Plan B). The Planning Target Volume was defined by a 3 mm margin around the P. The rectum was empty on both CTs and the wall was defined by an internal expansion of 5 mm, from 2 cm above the P to 2 cm below. The volumes of the rectum, irradiated with and without HA, were compared on the following dosimetric parameters: maximum dose (Dmax), dose to 2.5cc (D2.5), 5cc (D5) and 10cc (D10) of the rectal wall and the volumes of the rectal wall receiving 90% (V90), 80% (V80) and 70% (V70) of the prescribed doses. To limit the potential impact of the variation of the rectal volume between the two CTs, all results are given in cc and not in % of volume

Results: The mean P volume was 52cc (30cc - 93.8cc) on the CT1 and 52.4cc (32.5 - 92.7) on the CT2. The injection of HA reduced the mean Dmax value to the rectal wall by 2.7 Gy for Plan A and 2.5 Gy for Plan B. The mean values of V90, V80, and V70 are reduced by 90%, 82% and 70% respectively for Plan A and 91%, 77% and 62% respectively for Plan B. Same way, the average values ??of D2.5, D5 and D10 are reduced by 7.9 Gy, 8 Gy and 3 Gy for Plan A and 12 Gy, 10 Gy and 4 Gy for Plan B. The injection of HA allows to increase the dose of irradiation from 5 x 6.5Gy to 5 x 8.2Gy without increasing the D2.5 and D5 values.

Rectum		Dmax (cGy)	D2.5 (Gy)	D5 (Gy)	D10 (Gy)	V90 (cc)	V80 (cc)	70 (cc)
5x6.5 Gy (PlanA)	CT1 w/o AH	3366	30.29	23.54	13.22	3.2	4.4	5.4
	CT2 w AH	3096	22.42	15.52	10.19	0.3	0.8	1.6
5x8.5 Gy (PlanB)	CT1 w/o AH	4368	40.32	32.61	19.00	3.5	4.7	5.8
	CT2 w AH	4120	27.98	22.07	14.95	0.3	1.1	2.2

Conclusions: In this study, the injection of HA limited the doses to the rectal wall. These results suggest that late toxicities could be significantly reduced. The injection of HA could secure the initiation and development of the SBRT in many centers. A phase II study is underway to assess the rate of late rectal toxicities when a SBRT (5 x 7.5Gy) is combined with an injection of HA.

PD-0279

VALUE OF 18F-FDG-PET/CT AFTER STEREOTACTIC BODY RADIATION THERAPY FOR STAGE I NON-SMALL CELL LUNG CANCER

N. Andratschke[1], J. Wantke[2], B. Mayer[2], R.A. Bundschuh[2], B. Haller[3], S.T. Astner[4], M. Molls[4], M. Essler[2]

[1]*Universität Rostock, Department of Radiation Oncology, Rostock, Germany*

[2]*Technische Universität München, Department of Nuclear Medicine, Munich, Germany*

[3]*Technische Universität München, Institut für Medizinische Statistik und Epidemiologie, Munich, Germany*

[4]*Technische Universität München, Department of Radiation Oncology, Munich, Germany*

Purpose/Objective: To evaluate the predictive value of pre- and post-therapeutic [^{18}F]-FDG-PET/CT in patients with stage I NSCLC with regard to disease specific survival, local control and distant failure after definitive SBRT.

Materials and Methods: 45 patients with histologically proven stage I NSCLC received a staging FDG-PET/CT investigation before definitive SBRT of which 29 received in addition a follow-up PET/CT investigation 12 months after SBRT. SUV_{mean} and SUV_{max} were measured as indicators of the glucose metabolism intensity. Tumor volumes were calculated through segmentation of the corresponding CT images (TrueD© Software, Siemens). The predictive value of these parameters to detect patients at high risk for local and distant recurrence as well as reduced survival was investigated for the pre- and post-treatment PET/CT investigations.

Results: *Post-treatment PET/CT*: SUV_{mean} values higher than 2.81 (p = 0.023), SUV_{max} values higher than 3.45 (p = 0.007) and a relative decrease of SUV_{mean} or SUV_{max} post-treatment of less than 32% (p= 0.015) or 52% (p = 0.013) in comparison to the pre-therapeutic PET/CT values correlated with a significantly increased risk of disease specific death. These parameters were also significantly correlated with local control: SUV_{mean} values higher than 3.44 (p = 0.001), SUV_{max} values higher than 5.48 (p = 0.009) or a relative decrease of SUV_{mean} or SUV_{max} of less than 43% (p= 0.030) or 52% (p = 0.025) correlated with a significantly increased risk for local recurrences. In addition, a relative decrease of SUV_{max} of less than 62% (p = 0.040) at the post-treatment PET significantly correlated with an increased risk for regional lymph node metastases. In contrast, none of the investigated parameters correlated with overall survival or distant failure.

Pre- treatment PET/CT: No significant correlation between SUV_{max} or SUV_{mean} and disease specific survival and local control and distant metastases could be detected.

Conclusions: Quantitative analysis of the pretherapeutic PET/CT investigation did not correlate with prognosisof patients with stage I NSCLC. In contrast, post-treatment mean SUV and SUV decrease within one year after SBRT correlated significantly with disease specific survival and local control. Post-treatment SUV 1 year after SBRT may serve as biomarker to detect patients at high risk for relapse.

PD-0280

STEREOTACTIC BODY IRRADIATION IN PATIENTS WITH SOLITARY LUNG NODULES

M. Marcenaro[1], L.B. Belgioia[2], D.A. Agnese[2], D.D. Doino[2], F.L. Lamanna[2], S.V. Vagge[1], E.M. Mantero[2], S.G. Garelli[3], M.Z. Zeverino[3], R.C. Corvò[1]

[1]*IRCCS San Martino IST National Institute for Cancer Research, radiation oncology, Genova, Italy*

[2]*Radiotherapy School University of Genoa Italy, radiation oncology, Genova, Italy*

[3]*IRCCS San Martino IST National Institute for Cancer Research Genoa Italy, Department of Medical Physics, Genova, Italy*

Purpose/Objective: To evaluate toxicity and clinical outcome in pts treated with SBRT for solitary lung nodules.

Materials and Methods: From August 2009 to July 2011, 33 pts with solitary lung nodules were treated Helical Tomotherapy (HT). Until May 2010 pts were given 60Gy/8fx thereafter we used different fx-schemes according to T stage, nodule location in the chest (peripheral/central) and presence of single metastasis (mts) from previous primary tumours. According to our protocol peripheral T1 were given 48 Gy/4 fx, peripheral T2 52Gy/4, central T1-2 50Gy/5fx and mts 60Gy/8fx. All but 2 pts had diagnostic or simulation TCPET scan.

Results: Median pts age was 73 yrs (57-88). Median follow up was 14 mo (3-24 months). 28/33 pts had NSCLC (21 primaries and 7 recurrences), the other 5 pts had 1 mts from other primaries. Of the 21 pts with primary NSCLC 18 had T1N0 and 3 T2N0. Of the 33 treated nodules, 24 were peripheral and 9 central. Medial tumour size was 20 mm (8-40). Histology was available in 14/28 of lung cancer pts (10 Adenoca, 5 SCC, 1 Adenoca/SCC and 2 NSCLC without other specifications). In 10 pts diagnosis was CT and CTPET based. Of the 5 pts with mts 2, 1, 1 ,1 had mts from bladder, kidney, gastric and colon cancer. Pts were treated as follow: 11 pts 60Gy/8fx, 3 pts 52Gy/4fx, 4 pts 50Gy/5fx and 13 pts 48Gy/4fx. 2 pts were treated with other fx-schemes. We had acute toxicity in 5 pts (3 with dyspnoea and 2 with fibrosis) and late toxicity in 4 pts (1 with dyspnoea and 3 with fibrosis). 1/27 pts was lost at follow up. 13 (40.6%), 5 (15.6%), 1(3.2%) and 13 (40.6%)pts had complete response (RC), partial response (RP), stable disease (SD) and progression (PD), respectively. Pts who had PD were as follows: local PD 3 pts, systemic PD 5 pts, local and systemic PD 5 pts. Local control (LC) was assessable in 31/33 nodules, as one pts was lost at follow up and one pts was known to be died with bone mts without further lung evaluation. 16 (10 T1, 2 mts, 4 recurrence <3 cm), 6 (4T1, 2 T2), 1 (1 mts) and 8 (3 T1, 1 T2 and 3 recurrence<3 cm) nodules had RC, RP, SD and PD, respectively. 3 pts died for non oncologic causes.

Conclusions: Data from pts treated with SBRT for solitary lung nodules show 74% of LC. RT doses are of great importance for local control and a BED>100Gy10 is recommended. Presence of single lung nodule from other previous cancers, lung recurrence from previous NSCLC and wide target size are of most importance affecting systemic progression.

PD-0281

VESTIBULAR SCHWANNOMA TREATED WITH FRACTIONATED STEREOTACTIC RADIOTHERAPY.OUR EXPERIENCE

N. Gascón[1], J.F. Pérez-Regadera[1], R. Dambrosi[1], A. Castaño[1], R. Martínez[1], M.A. Cabeza[1], A. Bartolomé[1], E. Lanzós[1]

[1]*Hospital 12 de Octubre, Radiation Oncology, Madrid, Spain*

Purpose/Objectiv: The swannomas are benign tumors of neural tissue that can be treated with surgery, radiosurgery or fractionated stereotactic radiotherapy, achieving greater preservation of hearing with the last one. We analyze the results of auditory toxicity and treatment complications of vestibular schwannomas at our institution.

Materials and Methods: Between 2004 and 2011, 95 patients have been evaluated for treatment with fractionated stereotactic radiotherapy, 49 males (51.6%) and 46 women (48.4%), with a median age of 57 years. 92.6% had no predisposing factors, while 1.1% were suffering from neurofibromatosis type 1, 3,2% neurofibromatosis type 2 and 3.2% meningiomas. Tumor size was less than 1 cm in 14,7% of patients, between 1 and 1,99 cm in 35,8%, between 2 and 2,99 cm in 33,7%, between 3 and 3,99 cm in 9,5% and greater than 4 cm in 6,3%. The hearing before treatment was normal in 4 patients (4.2%), with loss of less than 30 dB in 50 (52.6%), greater than 30 dB loss in 24 (25.3%) and deafness in 17 (17.9%). 76 patients (80.9%) they had not undergone surgery, while 14 (14.9%) they were been intervened once and 4 (4.3%) twice. Most patients (74.7%) had no facial paralysis, present in mild form in 16.8% and complete in 8.4%. Balance remained intact in 60 patients (63.2%) with mild disease in 24 (25.3%) and severe in 11 (11.6%). 47.4% had no tinnitus, compared to 52.6% who do the suffering. 81.1% of patients had no involvement of other pairs, 15.8% had involvement of the V pair, 1.1% had involvement of the IX, and 1.1% had involvement of the XII pair.According to the Matthies classification, 16 patients (23.2%) were T1, 18 (26.1%) T2, 22 (31.9%) T3 and 13 (18.8%) T4. The treatment has been performed in 72 of the

INJECTION OF HYALURONIC ACID (HA) PRESERVES THE RECTAL WALL IN PROSTATE STEREOTACTIC BODY RADIATION THERAPY (SBRT)

Corina UDRESCU [1, 3], Alain RUFFION [2], Marie-Pierre SOTTON [3], Marian DEVONEC [2], Marc COLOMBEL [4], Patrice JALADE [3], Olivier CHAPET [1]

[1]-Department of Radiation Oncology, [2]- Department of Urology, [3] –Department of Medical Physics, EA-3738, Centre Hospitalier Lyon Sud, PIERRE BENITE, FRANCE

[4] – Department of Urology, Hôpital Edouard Herriot, LYON, FRANCE

Background:

Several studies are in favour of an α/β ratio of less than 3 Gy for prostate cancer, encouraging the dose escalation.

A small number of trials already described the experiences of stereotactic body radiation therapy (SBRT) for low- to intermediate-risk prostate cancer. The treatment is delivered in only 4 to 5 fractions of 6.5 Gy to 10 Gy, using a technique of image-guided radiation therapy.

However, the development of such radiation patterns in any department of radiation oncology can only be done if the risk of rectal toxicity is well controlled.

Purpose:

➡ The objective of the present dosimetric study was to evaluate the contribution of an injection of hyaluronic acid (HA) between the rectum and the prostate to reduce the doses to the rectal wall in SBRT approaches.

Materials and Methods:

a.) Patient condition:

• In a phase II study, patients with low- or intermediate-risk prostate cancer are treated by exclusive IMRT technique with a total dose of 62 Gy in 20 fractions of 3.1 Gy daily fraction, 5 days per week (BED = 84 Gy with α/β ratio of 1.5 Gy).
• Three gold markers are implanted in the prostate, for CT/MRI fusion and daily repositioning.
• A transperineal injection of 10 cc of HA (NASHA™ Spacer gel, Q-Med AB, Uppsala, Sweden) is systematically done between the rectum and the prostate, under local anaesthesia and under ultrasound guidance (Figure 1).

b.) Treatment volumes definition:

A dosimetric CT scan is performed before (CT1) and after injection (CT2).

On the two CT scans of 10 patients included, the following volumes were created to generate the SBRT plans for comparison:

CTV (Clinical Tumor Volume) => corresponding to the prostate only;
PTV (Planning Target Volume) => corresponding to the CTV with a 3 mm uniform margin around the prostate;

The rectum was empty on both CTs and was delineated from 2 cm above the prostate to 2 cm below the prostate. The rectal wall was defined by an internal expansion of 5 mm.

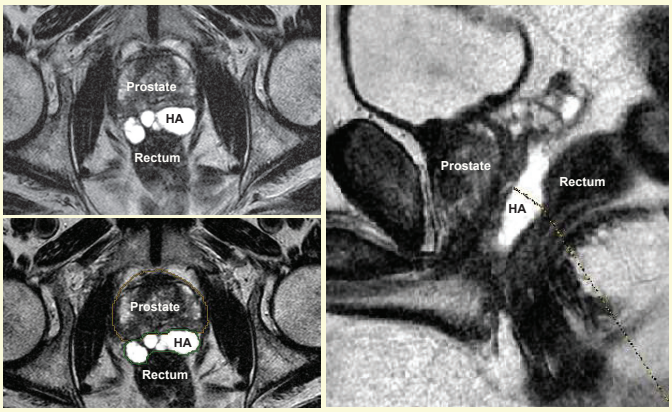

Figure 1: HA between the prostate and the rectum.

c.) Dosimetry:

The SBRT plans were simulated using a 9-beam IMRT technique and were optimized on CT1 and CT2, according to *two levels of dose*:

➡ 32.5 Gy in 5 fractions of 6.5 Gy (Plan A) (BED = 76 Gy in 38 fractions of 2 Gy with α/β = 1.5 Gy) and

➡ 42.5 Gy in 5 fractions of 8.5 Gy (Plan B) (BED ≈ 110 Gy in 55 fractions of 2 Gy with α/β = 1.5 Gy)

d.) Data analysis:

The volumes of rectum, irradiated with and without HA, were compared on the following dosimetric parameters: maximum dose (Dmax), dose to 2.5 cc (D2.5), 5 cc (D5) and 10 cc (D10) of rectal wall and volume of rectum receiving 90% (V90), 80% (V80) and 70% (V70) of the prescribed doses. To limit the potential impact of the variation of the rectal volume between the two CTs, all results are given in cc and not in % of volume.

Results:

➢ The mean prostate volume was 52 cc [range 30cc - 93.8cc] on the CT1 and 52.4 cc [range 32.5cc - 92.7cc] on the CT2.

➢ The injection of HA reduced the mean Dmax value to the rectal wall by 2.7 Gy for Plan A and 2.5 Gy for Plan B.

➢ The mean values of V90, V80, and V70 are reduced by 90%, 82% and 70% respectively for Plan A and 91%, 77% and 62% respectively for Plan B.

➢ In addition, the average values of D2.5, D5 and D10 are reduced by 7.9 Gy, 8 Gy and 3 Gy for Plan A and 12 Gy, 10 Gy and 4 Gy for Plan B.

➢ The injection of HA allows to increase the dose of irradiation from 5 x 6.5 Gy to 5 x 8.5 Gy without increasing the D2.5 and D5 values.

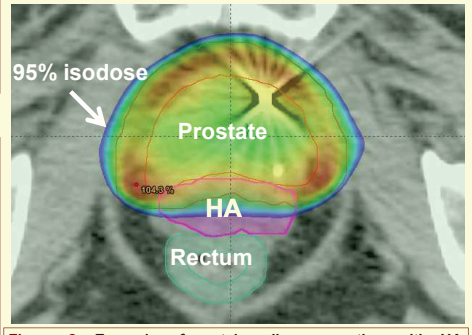

Figure 2: Example of rectal wall preservation with HA injection.

Table. Mean values for the rectum wall, for CT1 and CT2 plans.

Rectum		Dmax (Gy)	D2.5 (Gy)	D5 (Gy)	D10 (Gy)	V90 (cc)	V80 (cc)	V70 (cc)
5 x 6.5 Gy (Plan A)	CT1 w/o HA	33.66	30.29	23.54	13.22	3.2	4.4	5.4
	CT2 w HA	**30.96**	**22.42**	**15.52**	**10.19**	**0.3**	**0.8**	**1.6**
5 x 8.5 Gy (Plan B)	CT1 w/o HA	43.68	40.32	32.61	19.00	3.5	4.7	5.8
	CT2 w HA	**41.20**	**27.98**	**22.07**	**14.95**	**0.3**	**1.1**	**2.2**

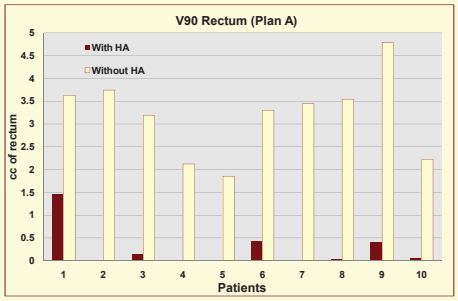

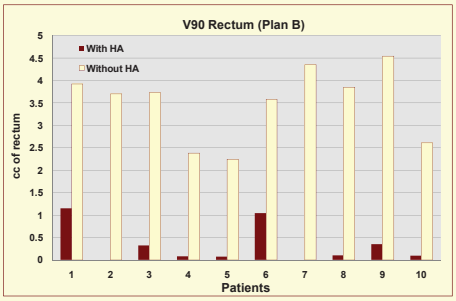

Figures. V90 for the rectum wall (Plan A and B), by patient, with and without HA.

Conclusions:

In this study, the injection of HA limited the doses to the rectal wall. These results suggest that late toxicities could be significantly reduced. The injection of HA could secure the initiation and development of the SBRT in many centers. A phase II study is underway to assess the rate of late rectal toxicities when SBRT (5 x 8.5 Gy) is combined with an injection of HA.

This project of SBRT irradiation in prostate cancer is supported by the Department of Clinical Research of the University Hospital in Lyon, France.

Appendix 11

- Posters at the SFPM meeting in 2013 (5-7 June) in Nice, France;

TEST DE SENSIBILITE D'UN SYSTEME DE DETECTION 3D A DIODES AVEC DES ERREURS DE MLC ET DE ROTATIONS DE BRAS POUR DES TRAITEMENTS RCMI

Benjamin PIGNATA [1], Corina UDRESCU [1, 2], Olivier CHAPET [2], Ronan TANGUY [2], Marie-Pierre SOTTON [1], Gaelle KERNEUR [1], Géraldine MICHEL-AMADRY [1], Julien RIBOUTON [1], Amandine BENEUX [1], Patrice JALADE [1]

[1]- Service de Physique Médicale et Radioprotection, [2]- Service de Radiothérapie-Oncologie, Centre Hospitalier Lyon Sud, PIERRE BENITE, FRANCE

Introduction

Le système Delta4® (ScandiDos) est conçu pour la vérification dosimétrique en trois-dimensions et présente de bons résultats en termes de reproductibilité, linéarité et indépendance en débit de dose.

La sensibilité de ce détecteur a déjà été analysée pour une modification de position de banc de lames (≥ 2mm), des unité moniteurs et de rotation de collimateur (≥ 2°) [1].

Objectifs

L'objectif de ce travail a été de vérifier la sensibilité du Delta4® pour des faibles erreurs du positionnement des lames (une seule lame avec des erreurs submillimétriques) et de la rotation du bras (inferieur au degré) en RCMI.

Matériel et Méthodes

La planification de traitement

Dix plans (5 prostates et 5 ORL) ont été utilisés pour cette étude.

Des erreurs systématiques de -0.2mm, -0.5mm, -0.7mm, -1mm, -2mm, -3mm, -5mm et -10mm, ont été introduites sur une lame.

Des erreurs systématiques de 0.2°, 0.5°, 0.7°, 1°, 2°, 2.5°, 3°, 4° et 5° ont été également introduites pour les rotations de bras.

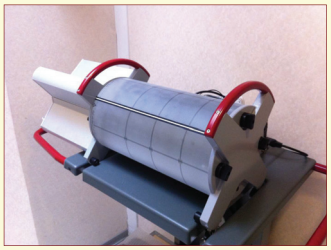

Figure 1. Le système Delta4®.

Les mesures et l'évaluation

Le système Delta4® (Figure 1) a été utilisé pour acquérir et analyser les données. Toutes les mesures ont été réalisées consécutivement pour chaque patient et nous avons tenu compte de l'influence de la répétabilité. Ainsi, 20 faisceaux identiques ont été irradiés avec le système Delta4® et l'écart-type moyen pour le gamma max (*Gmax*) est de 0.06.

Pour chaque faisceau modifié, les mesures ont été comparées au plan calculé (nommé, évaluation clinique) et à une mesure du même faisceau sans erreur (0mm ou 0°) (nommé, évaluation avec la référence).

Parce qu'il n'y a qu'une seule lame concernée avec un petit décalage, nous n'avons évalué que le Gmax et non le gamma moyen ou le pourcentage de point présentant un gamma<1.

Les valeurs de Gmax ont été relevées pour les méthodes d'évaluation gamma global (*EGG*) et local (*ELG*) avec des critères d'acceptabilité de 2%/2mm.

Résultats

Les erreurs de lames

Evaluation clinique:

Les décalages de lames ont un impact notable sur le plan de vérification clinique. Pour tous les plans, on constate des augmentations de Gmax à partir de 2 mm de décalage (de 1.6 à 3.5 pour LGE et de 1 à 2.1 pour GGE) (Figure 2, gauche).

Evaluation avec la référence:

Les décalages de lames ont un impact notable sur le plan de vérification avec la référence. Pour tous les plans, on constate des augmentations de Gmax à partir de 0.2 mm (de 0.2 à 4.3 pour LGE et de 0.1 à 2.4 pour GGE) (Figure 2, droite).

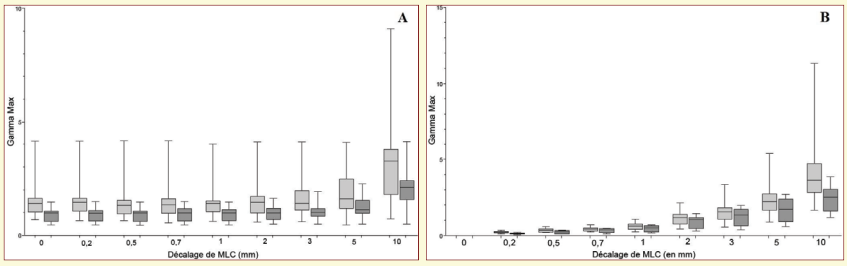

Figure 2. Evolution du gamma max avec les décalages des lames (en mm) pour le local gamma (gris clair) et pour le global gamma (gris foncé). Une évaluation clinique (A) et avec la référence (B).

Les erreurs de bras

Evaluation clinique:

Les décalages de bras ont un impact notable sur le plan de vérification clinique. Pour tous les plans, on constate des augmentations de Gmax à partir de 2° de décalage (de 1.7 à 6.9 pour LGE et de 1.4 à 3 pour GGE) (Figure 3, gauche).

Evaluation avec la référence:

Les décalages de bras ont un impact notable sur le plan de vérification avec la référence. Pour tous les plans, on constate des augmentations de Gmax à partir de 0.2° (de 0.4 à 9 pour LGE et de 0.3 à 4.8 pour GGE) (Figure 3, droite).

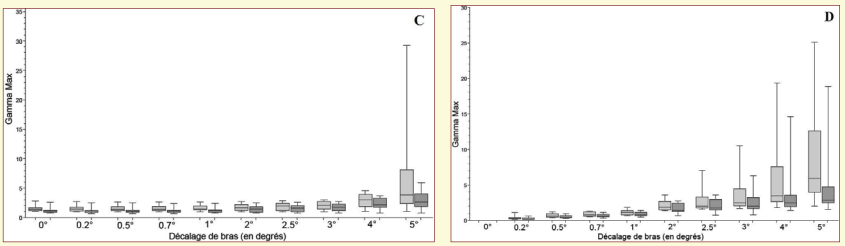

Figure 3. Evolution du gamma max avec les décalages de bras (en degré) pour le local gamma (gris clair) et pour le global gamma (gris foncé). Une évaluation clinique (C) et avec la référence (D).

Table 1. Valeurs moyennes, écart-types (SD), médianes et intervalles des gamma max pour l'évaluation avec la référence (erreurs de MLC et de bras).

	Décalage de MLC		Décalage de bras	
	Local gamma Gmax	Global gamma Gmax	Local gamma Gmax	Global gamma Gmax
0.2 mm			**0.2°**	
Moyenne ± SD	0.23 ± 0.07	0.14 ± 0.05	0.38 ± 0.28	0.26 ± 0.16
Médiane (intervalle)	0.24 [0.13- 0.36]	0.14 [0.07 – 0.23]	0.31 [0.18 – 1.12]	0.19 [0.14 – 0.63]
0.5 mm			**0.5°**	
Moyenne ± SD	0.36 ± 0.13	0.24 ± 0.09	0.7 ± 0.29	0.5 ± 0.22
Médiane (intervalle)	0.35 [0.21 - 0.59]	0.27[0.12 – 0.36]	0.63 [0.38 – 1.24]	0.43 [0.25 – 0.97]
0.7 mm			**0.7°**	
Moyenne ± SD	0.44 ± 0.14	0.35 ± 0.14	0.87 ± 0.31	0.67 ± 0.26
Médiane (intervalle)	0.45 [0.25 – 0.7]	0.39 [0.11 – 0.5]	0.81 [0.54 – 1.3]	0.64 [0.31 – 1.18]
1 mm			**1°**	
Moyenne ± SD	0.61 ± 0.24	0.48 ± 0.19	1.17 ± 0.36	0.89 ± 0.31
Médiane (intervalle)	0.63 [0.25 – 1.07]	0.53 [0.17 – 0.71]	1.17 [0.69 – 1.84]	0.81 [0.45 – 1.45]
2 mm			**2°**	
Moyenne ± SD	1.16 ± 0.48	0.91 ± 0.41	2.05 ± 0.73	1.66 ± 0.67
Médiane (intervalle)	1.19 [0.45 – 2.16]	1.05 [0.31 – 1.45]	1.87 [1.39 – 3.61]	1.46 [0.71 – 2.75]
3 mm			**2.5°**	
Moyenne ± SD	1.63 ± 0.76	1.25 ± 0.58	2.74 ± 1.67	2.04 ± 0.91
Médiane (intervalle)	1.57 [0.58 – 3.36]	1.34 [0.39 - 2]	2.03 [1.59 – 7.06]	1.75 [0.73 – 3.6]
5 mm			**3°**	
Moyenne ± SD	2.37 ± 1.22	1.68 ± 0.75	3.76 ± 3	2.55 ± 1.56
Médiane (intervalle)	2.23 [0.9 – 5.37]	1.72 [0.61 – 2.7]	2.47 [1.67 – 10.54]	2.01 [0.81 – 6.33]
10 mm			**4°**	
Moyenne ± SD	4.31 ± 2.69	2.41 ± 0.9	6.23 ± 6.52	3.82 ± 3.91
Médiane (intervalle)	3.64 [1.68 – 11.33]	2.52 [1.2 – 3.87]	3.51 [1.8 – 19.36]	2.5 [1.44 – 14.62]
NA			**5°**	
Moyenne ± SD			9.04 ± 8.03	4.79 ± 5.16
Médiane (intervalle)			5.92 [1.99 – 25.08]	2.85 [1.54 – 18.86]

Le système identifie la lame qui présente un décalage de 2 mm (voir Figure 4, gauche) ou un décalage de 3 mm (voir Figure 4, droite).

De plus sur cette lame le système identifie les détecteurs pour lesquels la mesure ne correspond pas à ce qui est désiré (points en jaune et rouge) pour un certain point de contrôle donné.

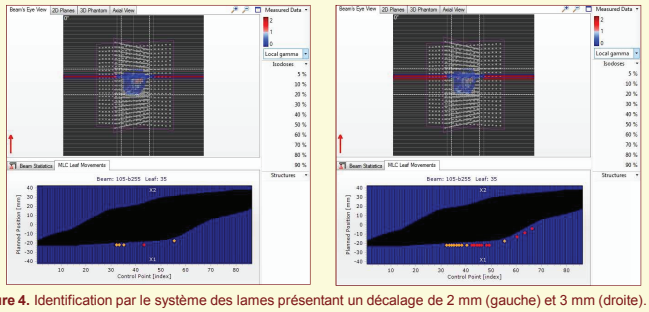

Figure 4. Identification par le système des lames présentant un décalage de 2 mm (gauche) et 3 mm (droite).

Conclusions

Le système Delta4® semble être un détecteur très sensible pour le contrôle de qualité des plans RCMI. Dans notre étude, le système a détecté de très faibles erreurs de lame et de bras. En utilisation clinique (comparaison TPS - mesures) ces faibles erreurs ne seraient pas détectées car elles demeurent en dessous des écarts existants entre les calculs du TPS et l'accélérateur.

Bibliographie:

1. Fredh A, Scherman JB, Fog LS *et al.* Patient QA systems for rotational radiation therapy: A comparative experimental study with intentional errors. *Med Phys* 2013;40: 031716-1-9;

DOIT-ON EFFECTUER LE CONTROLE DE QUALITE POUR LES PLANS STEREOTAXIQUES DU CANCER DE LA PROSTATE DANS LES CONDITIONS DE TRAITEMENT? UNE EVALUATION AVEC UN FANTOME CYLINDRIQUE A DIODES

Corina UDRESCU[1,2], Olivier CHAPET[1], Benjamin PIGNATA[2], Marie-Pierre SOTTON[2], Julien RIBOUTON[2], Géraldine MICHEL-AMADRY[2], Gaelle KERNEUR[2], Patrice JALADE[2]

[1]- Service de Radiothérapie-Oncologie, [2]- Service de Physique Médicale et Radioprotection, Centre Hospitalier Lyon Sud, PIERRE BENITE, France

Introduction

Pour les irradiations stéréotaxiques le contrôle de qualité (CQ) occupe une place d'autant plus importante a cause de fortes doses d'irradiation.

Le système Delta⁴ (ScandiDos) (Figure 1), dédié au contrôle qualité des traitements RCMI [1], est un détecteur indépendant de l'accélérateur et très stable en terme de linéarité, reproductibilité et répétabilité [2-4].

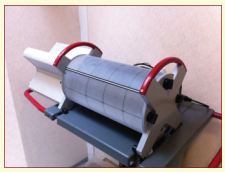

Figure 1. Le système Delta4®.

Objectifs

➡ L'objectif de ce travail a été d'évaluer l'impact de la géométrie d'irradiation sur le CQ pour des plans stéréotaxiques de prostate avec un boost intégré en utilisant un fantôme indépendant de l'accélérateur, le système Delta⁴.

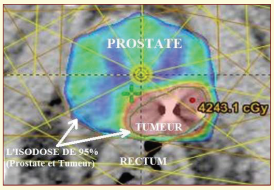

Figure 2. Schéma d'une irradiation stéréotaxique de la prostate avec un boost intégré.

Matériel et Méthodes

Le schéma du traitement

La prostate et la tumeur ont été délinéées par un radiologue à l'aide d'une fusion CT/IRM(en T1) pour 5 patients.
Dans le cadre d'un protocole, un plan RCMI à 9 faisceaux a été optimisé avec le schéma suivant:

- 5x6.5Gy dans la prostate avec un boost intégré de 5x8Gy dans la tumeur (Figure 2).

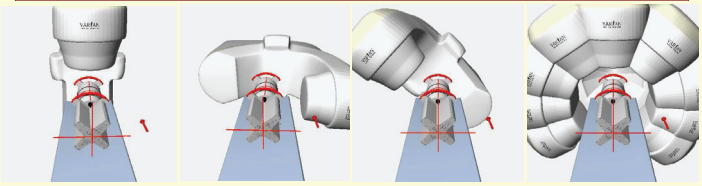

Figure 3. Illustration des 4 vérifications des plans RCMI avec le Delta⁴ et le bras à: 0°, 90°, 315° et en configuration de traitement (FparF) (de gauche a droite).

Le contrôle de qualité

Tous les faisceaux ont été consécutivement vérifiés quatre fois en utilisant le système Delta⁴ (Figure 3) avec tous les bras à:

a) 0°(Plan *B0*);
b) 90°(Plan *B90*);
c) 315°(Plan *B315*);
d) en position de traitement (242°, 270°, 297°, 328°, 0°, 38° , 76°, 101°, 127°), nommé *BFparF* (faisceau-par-faisceau).

Les plans B90, B315 et BFparF ont été comparés avec B0 en utilisant deux évaluations:

1) Global Gamma Index (GGI)
2) Local Gamma Index (LGI),

Pour chaque évaluation (GGI et LGI), deux plans ont été comparés en calculant la différence de:

- pourcentage de détecteurs présentant un gamma<1 (*%G<1*);
- gamma maximum (*Gmax*);
- gamma moyen (*Gmoy*).

Les critères d'acceptabilité sont ceux utilisés dans notre service pour un plan RCMI: 4%/3mm.
Pour la répétabilité, 20 faisceaux ont été irradiés avec le système Delta⁴ et l'écart-type moyen a été de 0.06 pour le Gmax et de 0.41% pour le %G<1.

Résultats

Evaluation global gamma

Pour GGI, les écarts moyens en %G<1 comparés à B0 sont de 0.8%±1.2%, 1.2%±1.2% et 1.2%±1.6% pour les plans B90, B315 et BFparF, respectivement. Des résultats similaires ont été obtenus pour Gmax et Gmoy (Tableau 1).

Pour GGI, il y a un écart systématique et significatif pour tous les paramètres entre le plan B0 et les plans: B90 ($p<0.0001$), B315 ($p<0.0001$) et BFparF ($p<0.0001$) mesurés avec Delta⁴ (Figure 4 et 5, gauche).

Evaluation local gamma

Pour LGI, les écarts moyens en %G<1 comparés à B0 sont de 3%, 4.4% et 2.6% pour les plans B90, B315 et BFparF, respectivement. Des résultats similaires ont été obtenus pour Gmax et Gmoy (Tableau 1).

Pour LGI, il y a un écart systématique et significatif pour tous les paramètres entre le plan B0 et les plans: B90 ($p<0.0001$), B315 ($p<0.0001$) et BFparF ($p<0.0001$) mesurés avec Delta⁴ (Figure 4 et 5, droite).

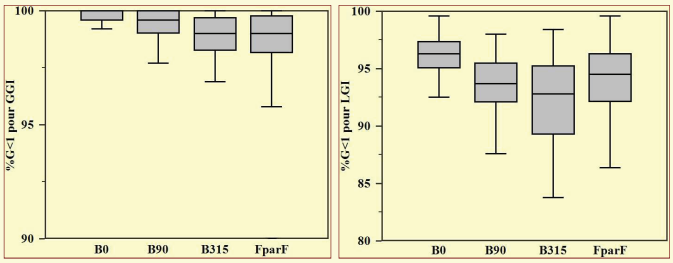

Figure 4. Pourcentage de détecteurs présentant un gamma<1 (%G<1) pour les 4 plans et pour les deux évaluations: global gamma index (GGI) (gauche) et local gamma index (LGI) (droite).

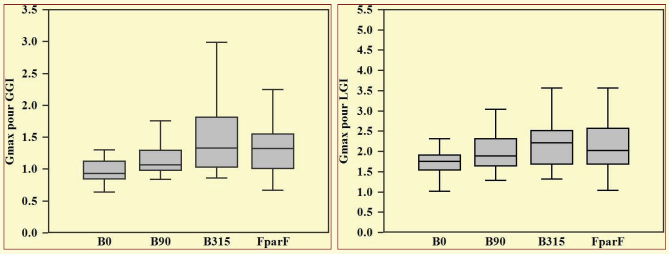

Figure 5. Le gamma maximum (Gmax) pour les 4 plans et pour les deux évaluations: global gamma index (GGI) (gauche) et local gamma index (LGI) (droite).

Tableau 1. Valeurs moyennes ± standard déviation (SD) et médianes (intervalle) pour les deux évaluations gamma, global et local.

Variable	Global Gamma Evaluation			Local Gamma Evaluation		
	G<1 (%)	Gmax	Gmoy	G<1 (%)	Gmax	Gmoy
B0						
Moyenne±SD	99.8±0.4	1±0.2	0.23±0.03	96±38.9	1.7±0.3	0.32±0.04
Mediane (intervalle)	100 (98.5-100)	0.9 (0.6-1.6)	0.23 (0.18-0.29)	96.3 (90.9-98.7)	1.8 (1-2.9)	0.31 (0.24-0.42)
B90						
Moyenne±SD	99±40.1	1.2±0.3	0.32±0.04	93.1±37.7	2±0.6	0.43±0.05
Mediane (intervalle)	99.6 (93.7-100)	1.1 (0.8-2.5)	0.32 (0.23-0.39)	93.2 (85.8-97)	1.9 (1.3-4.6)	0.43 (0.33-0.53)
B315						
Moyenne±SD	98.6±44.1	1.5±0.6	0.3±0.04	92.2±14.2	2.2±0.6	0.42±0.07
Mediane (intervalle)	98.7 (94.7-100)	1.3 (0.9-3.2)	0.29 (0.22-0.4)	92.8 (83.8-98.4)	2.2 (1.3-3.6)	0.4 (0.29-0.56)
BFparF						
Moyenne±SD	98.4±48.3	1.4±0.4	0.29±0.06	94.1±2.8	2.2±0.7	0.38±0.07
Mediane (intervalle)	98.7 (90-100)	1.3 (0.7-2.7)	0.29 (0.18-0.45)	94.5 (86.4-99.6)	2 (1-5.3)	0.38 (0.24-0.62)

Conclusions

Habituellement la vérification d'un plan RCMI est réalisée en plaçant tous les faisceaux à 0°. Cependant, il est important de vérifier le plan de traitement dans les mêmes conditions que pour le traitement.

Nous avons montré ici qu'il y a un écart important dans l'évaluation des plans RCMI stéréotaxiques car cela dépend des conditions d'irradiation. Ces écarts peuvent être expliqués par *l'impact du poids des lames* et *l'atténuation de la table*.

Il peut être recommandé que les vérifications des plans RCMI soient réalisées avec un *détecteur indépendant de l'accélérateur* et *dans la même configuration d'irradiation qu'au moment du traitement (angle de bras et position de table)*.

Bibliographie

1. Garcia R, Marguet M, Bodez V, *et al*. Validations dosimétriques et fantôme Delta⁴. SFRO 2009.
2. Sadagopan R, Bencomo JA, Martin RL, *et al*. Characterization and clinical evaluation of a novel IMRT quality assurance system. *J App Clin Med Phys* 2009;10:104-119.
3. Feygelman V, Forster K, Opp D, Nilsson G. Evaluation of a biplanar diode array for quality assurance of step-and-shoot IMRT. *J App Clin Med Phys* 2009;10:64-78.
4. Persson E, Granlund U. Validation of Delta⁴ for clinical use. ESTRO 2008.

List of publications

International Journal Publications

Publication	**Impact Factor**
1. **Udrescu C**, Jalade P, de Bari B, Michel-Amadry G, Chapet O. Evaluation of the respiratory prostate motion with four-dimensional computed tomography scan acquisitions using three implanted markers. *Radiother Oncol* 2012;103:266-9.	4.52
2. **Udrescu C**, De Bari B, Rouvière O, Ruffion A, Michel-Amadry G, Jalade P, Devonec M, Colombel M, Chapet O. Does hormone therapy modify the position of the gold markers in the prostate during irradiation? A daily evaluation with kV-images. *Cancer Radiother* 2013;17:215-20.	1.477
3. **Udrescu C**, Mornex F, Tanguy R, Chapet O. ExacTrac snap verification: a new tool for ensuring quality control for lung stereotactic body radiation therapy. *Int J Radiat Oncol Biol Phys* 2013;85:e89-e94.	4.524
4. Chapet O, **Udrescu C**, Devonec M, Tanguy R, Sotton MP, Enachescu C, Colombel M, Azria D, Jalade P, Ruffion A. Prostate hypofractionated radiation therapy: injection of hyaluronic acid to better preserve the rectal wall. *Int J Radiat Oncol Biol Phys* 2013;86:72-6.	4.524
5. **Udrescu C**, Rouvière O, Enachescu C, Sotton MP, Bouffard-Vercelli J, Jalade P, Chapet O. Potential interest of developing an integrated boost dose escalation for stereotactic irradiation of primary prostate cancer. *Phys Med* 2014;30(3):320-5.	1.167
6. Chapet O, **Udrescu C**, Tanguy R, Ruffion A, Fenoglietto P, Sotton MP, Devonec M, Colombel M, Jalade P, Azria D. Dosimetric implications of an injection of hyaluronic acid for preserving the rectal wall in prostate stereotactic body radiation therapy. *Int J Radiat Oncol Biol Phys* 2014;88(2):425-32.	4.524
Total impact factor	**20.736**

International and French Meetings

Abstract	**Meeting**
1. Chapet O, **Udrescu C**, De Bari B, *et al.* Do we really need a radiologist for the prostate delineation in radiotherapy? *Radiother Oncol* 2010;96 (Suppl. 1): S392-S419. - *Poster (12-16 September, Barcelona, Spain)*	2010, ESTRO 29
2. **Udrescu C**, Jalade P, Michel-Amadry G, De Bari B, and Chapet O. Evaluation of the respiratory prostate motion with 4D CT scans acquisitions using three implanted markers. *Radiother Oncol* 2010;96 (Suppl. 1): S392-S419. - *Poster (12-16 September, Barcelona, Spain)*	2010, ESTRO 29

3. **Udrescu C**, Jalade P, De Bari B, *et al.* Evaluation of implanted gold markers migration during irradiation of prostate cancer. *Int J Radiat Oncol Biol Phys* 2010;78(Supp): S674. 2010, ASTRO 52

- *Poster (31 October – 4 November, San Diego, USA)*

4. **Udrescu C**, Chapet O, de Bari B, Michel-Amadry G, and Mornex F. The ExacTrac Snap Verification (SV), a new tool for ensuring the quality control for stereotactic body radiation therapy (SBRT). *Int J Radiat Oncol Biol Phys* 2009;75(Suppl.):S609. 2009, ASTRO 51

- *Poster (1 – 5 November, Chicago, USA)*

5. Chapet O, **Udrescu C**, Sotton MP, *et al.* Potential interest of developing a focal dose escalation in stereotactic irradiation of prostate cancer. *Int J Radiat Oncol Biol Phys* 2010;78(Suppl.):S780-S781. 2010, ASTRO 52

- *Poster (31 October – 4 November, San Diego, USA)*

6. Chapet O, **Udrescu C**, Ruffion A, *et al.* Injection of hyaluronic acid (HA) to better preserve the rectal wall in prostate hypofractionated radiation therapy (HFR). *Int J Radiat Oncol Biol Phys* 2012 ;84(3):S406. 2012, ASTRO 54

- *Poster (28-31 October, Boston, USA)*

7. **Udrescu C**, Ruffion A, Sotton MP, *et al.* Injection of hyaluronic acid (HA) preserves the rectal wall in prostate stereotactic body radiation therapy (SBRT). *Radiother Oncol* 2012;103(Suppl.): S109-S110. 2012, ESTRO 31

- *"Young scientists ESTRO Poster Session" (9-13 May, Barcelona, Spain)*

8. **Udrescu C**, Chapet O, Tanguy R, *et al.* L'influence du nombre de champs et de l'énergie sur les plans SBRT-RCMI pour les cancers de la prostate. Une évaluation avec différents critères objectifs. 2013, SFPM

- *Poster (5-7 June, Nice, France)*

9. Pignata B, **Udrescu C**, Chapet O, *et al.* Test de sensibilité d'un système de détection 3D à diodes avec des erreurs de MLC et de rotations de bras pour des traitements RCMI. 2013, SFPM

- *Poster (5-7 June, Nice, France)*

10. **Udrescu C**, Chapet O, Pignata B, et al. Doit-on effectuer le contrôle de qualité pour les plans stéréotaxiques du cancer de la prostate dans les conditions de traitement ? Une évaluation avec un fantôme cylindrique à diodes. 2013, SFPM

- *Poster presentation (5-7 June, Nice, France)*

11. Eva A, Ribouton J, Michel-Amadry G, Pignata B, **Udrescu C**, Chapet O, Jalade P. Comparaison dosimetrique entre deux techniques d'arctherapie volumetrique pour les cancers de la prostate. 2013, SFPM

- *Poster (5-7 June, Nice, France)*

12. Shakir SI, **Udrescu C**, Enachescu C, Jalade P, Rouvière O, Chapet O. Migration evaluation of gold markers implanted in a prostate bed for salvage focal irradiation. *Int J Radiat Oncol Biol Phys* 2013;87(2):S385-S386. 2013, ASTRO 55

- *Poster (22-25 September, Atlanta, USA)*

IF=impact factor; ASTRO=American Society for Radiation Oncology; ESTRO=European Society for Radiotherapy and Oncology; SFPM=Société Française de Physique Médicale;